THE GEOLOGY OF WRECK BAY, VANCOUVER ISLAND

by

JAMES MICHAEL BREMNER

B.Sc. (Hons.),
University of Witwatersrand,
Johannesburg, 1961.

A THESIS SUBMITTED IN PARTIAL FULFILMENT OF
THE REQUIREMENTS FOR THE DEGREE OF
MASTER OF SCIENCE

in the Department
of
Geology

We accept this thesis as conforming to the
required standard

THE UNIVERSITY OF BRITISH COLUMBIA

June, 1970

In presenting this thesis in partial fulfilment of the requirements for an advanced degree at the University of British Columbia, I agree that the Library shall make it freely available for reference and study. I further agree that permission for extensive copying of this thesis for scholarly purposes may be granted by the Head of my Department or by his representatives. It is understood that copying or publication of this thesis for financial gain shall not be allowed without my written permission.

Department of GEOLOGY

The University of British Columbia
Vancouver 8, Canada

Date 15th June 1970

ABSTRACT

Wreck Bay is located on the west coast of Vancouver Island at 49°00'N, 125°38'W. It is roughly crescent shaped with a small cuspate foreland named Sand Point in the middle, and measures 2½ miles (2.17 kilometers) between the enclosing headlands of Quisitis and Wya Points.

Rocks exposed along the coast are indurated, unmetamorphosed, impure sandstones and mudstones of late Jurassic to early Cretaceous age. They were derived from the hinterland northeast of Wreck Bay, and were rapidly deposited into a trough which extended parallel to the present-day coastline. The contact between these sediments and the source rocks is thought to lie beneath a thick cover of Pleistocene material which now overlies the Estevan Coastal Plain; the southwestern edge of the paleotrough, from seismic evidence, appears to lie 5 - 6 miles (4.35 - 5.22 kilometers) seaward from the present-day coastline. Infilling of both sides of this paleotrough with Pleistocene and Recent sediments has resulted in a narrow, arcuate, present-day trough on the continental shelf adjacent to Wreck Bay. The Pleistocene sediments, consisting of cohesive grey clay and glaciofluvial outwash, were also derived from the mountainous hinterland to the northeast, and Recent sediments derived therefrom are dispersed across the bay and inner shelf. Boulders and gravel freed from the retrograding sea cliff behind the beach have settled to the base of wave erosion in the bay, and this coarse "mat" is covered by a thin veneer of very well sorted fine sand which becomes progressively finer further away

from shore. A nearshore surface current transports clay, silt and some of the sand southeastwards to Wya Point and the offshore trough.

During the summer, breaker heights in the bay vary from 0.75 - 4.00 feet (0.23 - 1.27 meters), and it is calculated that during winter storms, wave heights exceed 19 feet (5.75 meters). The foreshore in summer consists of fine, light-coloured sand, and slopes gently seaward at less than 2.6°. Profile changes on the foreshore result from three controlling factors: the breaker height, the breaker incident angle, and the position of the water table on the beach. The direction of littoral drift near the middle of the beach changes with tide level, but generally it is towards Sand Point and very strong; near Quisitis and Wya Points it is weak, and consistently away from them; elsewhere, it is weak and variable in direction. Transverse profiles were found to be most sensitive to tidal range where the breaker incident angle was small and consistent; they were virtually insensitive where the breaker incident angle was small and variable. In winter, the foreshore is generally less steep than in summer, and near Sand Point the surface material of the beach is reduced to coarse gravel as sand is carried out to the middle of the bay; northwest and southeast from here, the beach surface consists of dark-coloured medium sand; adjacent to the two headlands, the light-coloured fine sand of summer remains. Profile changes in winter are determined by breaker heights only, the other two controlling factors becoming insignificant.

Runnels, or incipient beach cusps, tend to form wherever littoral drift is not too strong, and their spacing is apparently related to the thickness of the swash wedge. The cliffbase along the northwest half of Wreck Bay very closely approximates a log-spiral curve in plan due to the angular relationship between prevailing wave fronts and the coastline; the southeast half, however, does not, because a complex wave pattern is created in the lee of islands located in the middle of the bay.

The value of gold contained in the backshore near Lost Shoe Creek is calculated to be $10,650. An offshore placer deposit at 20 fathoms (36.6 meters) depth is indicated by a great increase in the amount of magnetite and other heavy minerals there, together with the fact that a small mode of very fine sand, which contains most of the heavy minerals onshore, reappears in samples collected from this bathymetric level.

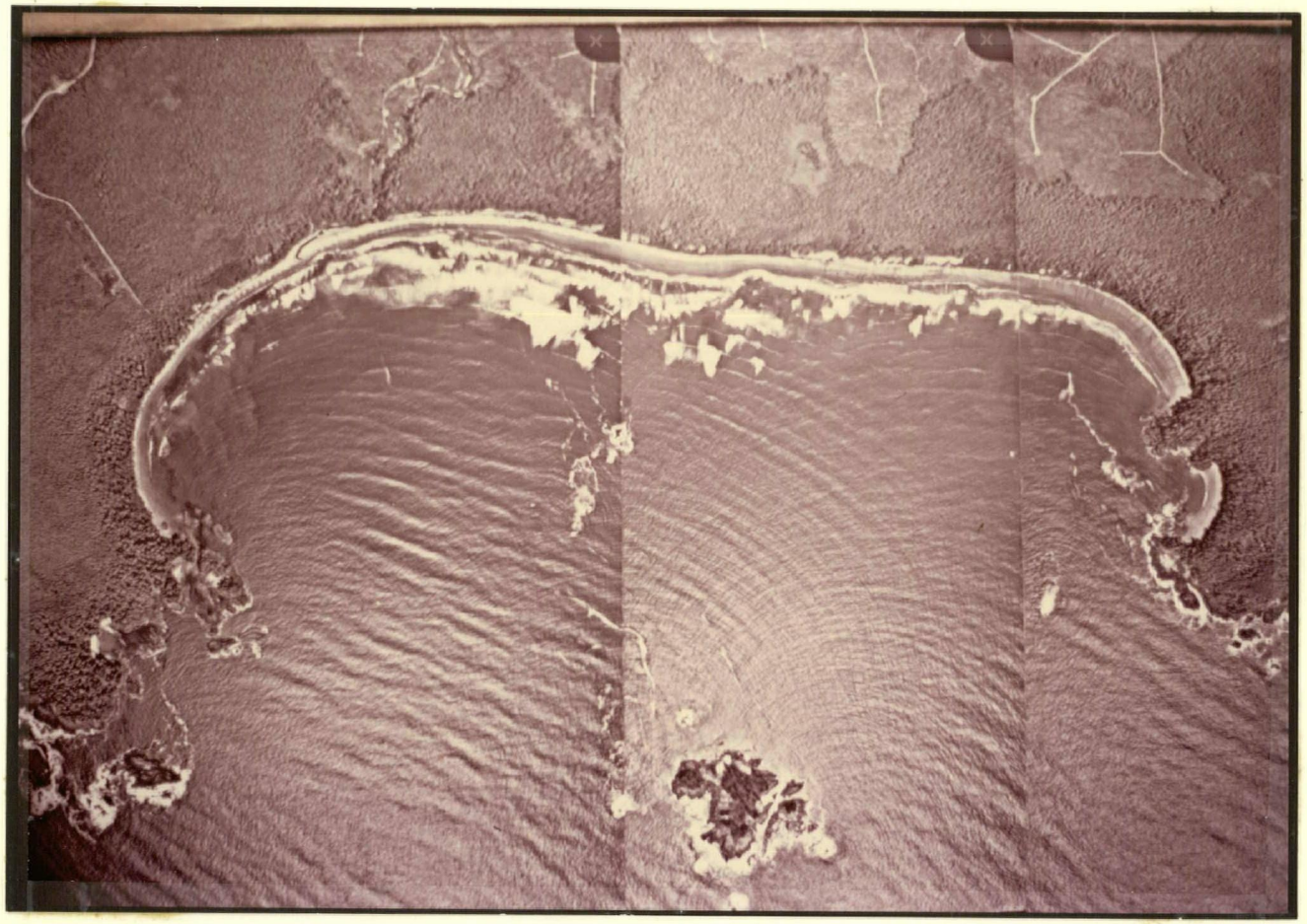

Frontispiece - Photomosaic of Wreck Bay. Approximate scale 1 inch = 2250 feet.

TABLE OF CONTENTS

LIST OF TABLES

LIST OF ILLUSTRATIONS

FIGURES AND MAPS

PLATES

ACKNOWLEDGMENTS

Many people have contributed toward the results of this work. Primarily, I wish to thank Drs. R.E.Kucera and J.W. Murray for serving as thesis advisors, and Dr. Kucera for making two informative field trips to the study area. Dr. P. LeBlond of the Institute of Oceanography, U.B.C., gave much help and advise in determining the planimetric shape of Wreck Bay, and Dr. L.E. Lavkulich of the Department of Soil Science, U.B.C., directed my efforts in X-ray diffraction analyses. I am indebted to Dr. A.J.Sinclair for guidance in trend surface analysis of the foreshore tracer experiments, and thanks are due to Drs. W.H.Mathews, W.C.Barnes and W.H.White for critically reading the chapters on Transverse Profiles, Sediment Size Analyses, and Economic Geology respectively.

Fellow U.B.C. students provided many stimulating ideas through discussion, and were directly responsible for the success of some projects. Special thanks go to M.J.L.T. Pullen, who supervised the echo sounding and sampling of Wreck Bay, and L. Carter, who collected all the offshore samples, and ran three sounding lines across the offshore trough.

Financial assistance was provided by the Department of Geology and Institute of Oceanography, U.B.C., through the kind efforts of Drs. J.W.Murray, R.E.Kucera and G.L.Pickard. This support is gratefully acknowledged.

Finally, I am deeply thankful to my wife Helen, for cheerful encouragement throughout the research period.

I. INTRODUCTION

A. HISTORICAL BACKGROUND

The name Wreck Bay derives from an incident which occurred in 1861. In January of that year, a British vessel H.M. Gunboat Foreward was despatched from Esquimalt to assist a Peruvian brigantine, the Florencia, which had become unmanageable shortly after leaving Juan de Fuca Strait, bound for Callao with lumber. The Foreward took Florencia in tow at Nootka, and while heading for Victoria experienced boiler trouble herself, and was forced to cut her charge adrift. The Florencia went aground on a small island now known as Florencia Island, where she became a total wreck (Nicholson, 1965). Since 1930, a number of maps and reports have referred to the bay leeward of the island as Florencia Bay; in this thesis the original name, Wreck Bay, has been used.

Long Beach was first known as Wickaninnish Beach after the chief of the Clayoquot indians, who over a hundred years ago reigned supreme over this part of the coast (Nicholson, 1965). Most maps still mark the nearshore region as Wickaninnish Bay.

The rocky promontories on either side of Wreck Bay, Quisitis Point and Wya Point, were apparently named after old indian villages once located there (personal communication with local indians).

The first white men to settle this coast established fur-trading posts at Clayoquat (across the bay from Tofino) and

at Ucluelet in the 1870's. Shortly before the First World War about twenty British immigrants attempted farming in the Tofino area, and by 1920 the area had been fairly thoroughly combed for its mineral deposits by migrant prospectors. Gold was discovered in a number of quartz veins along the Elk River (now known as the Kennedy River), and in the "black sands" of Wreck Bay. During the Second World War, the area underwent extensive development as part of the United States defense measures against possible Japanese attack. An airfield was built near Long Beach, and a road was constructed between Tofino and Ucluelet. Today, the principal industry of these two village municipalities is fishing, and have populations of approximately 500 and 700 respectively.

B. ACCESS

Regular ferry services exist between Vancouver and Victoria, and between Horseshoe Bay and Nanaimo. A paved highway links these two cities with Port Alberni, and from here, a rough gravel road winds over the Insular Mountains to the west coast of Vancouver Island (Figure 1). For a number of years this gravel section has been under construction, and is slated to be completely paved by mid-1970. It ends at a junction, 20 miles from Tofino, and 6 miles from Ucluelet. The Wickaninnish road leads to Wreck Bay from a turnoff 3 miles north of this junction (Map 2).

Alternatively the area may be reached by boat, as government docking facilities exist at both Tofino and

Ucluelet. Air service is provided by CP Air, with three return flights a week from Vancouver.

C. TOPOGRAPHY

Between the Pacific Ocean and the western boundary of the Insular Mountains, a narrow lowland strip known as the Estevan Coastal Plain extends along the greater part of Vancouver Island's west coast (Holland, 1964).

The area lying between Wreck Bay and the south side of Kennedy Lake is approximately 4 miles wide, and consists of unconsolidated gravels and sands below 200 feet elevation. Northwest and southeast from here, a number of isolated hills of basement project up through the unconsolidated sediment to elevations reaching 700 feet above sea level. The area is characterized by low topographic relief, but locally, a few gentle ridges and shallow depressions break the general uniformity. Some of these depressions probably reflect the course of old stream channels (see chapter on ECONOMIC GEOLOGY).

D. CLIMATE

The area has a high annual precipitation, most of which occurs during the winter as rain. For 1968, Ucluelet recorded the highest rainfall across Canada - 265.23 inches, and that winter, Tofino experienced one of the heaviest snowfalls in living memory - more than 2 feet.

In summer the days are long and warm. Early morning fog often blankets the coastal plain, and winds are generally

light from the northwest. From late autumn to winter, storm frequency and intensity increases, and the wind shifts gradually to the south. A summary of historical wind-speed averages is given in Table I (Watts and Faulkner, 1968).

SEASON \ M.P.H.	0 - 10	10 - 20	20 - 30	30 - 40	>40
April - September	42.0	41.5	12.8	2.9	0.8
October - March	20.7	40.3	26.4	8.4	4.2

TABLE I - HISTORICAL WIND-SPEED AVERAGES (%)

E. VEGETATION

Sections of the cliff behind Wreck Bay carry large straight trees of fir, cedar, hemlock and dense alder. Further north at Paradise Beach and parts of Long Beach, the cliff is less than 10 feet high, and here, the trees are scrubby and bend strongly inland (Plate I). This difference is due to the wind being deflected upwards at Wreck Bay, thus causing negligible distortion in the trees growth; elsewhere the wind drives straight inland. Another result of low cliff heights is exemplified along the southeastern part of Long Beach. Here the cliff is virtually absent, and sand from the backshore has drifted landward covering the vegetation over a 2 to 3 acre area.

Logging inland from Wreck Bay has in places progressed to within ½ mile from the cliff. The northern sector close to the road has not been logged because the ground is swampy, and trees are small and scrubby.

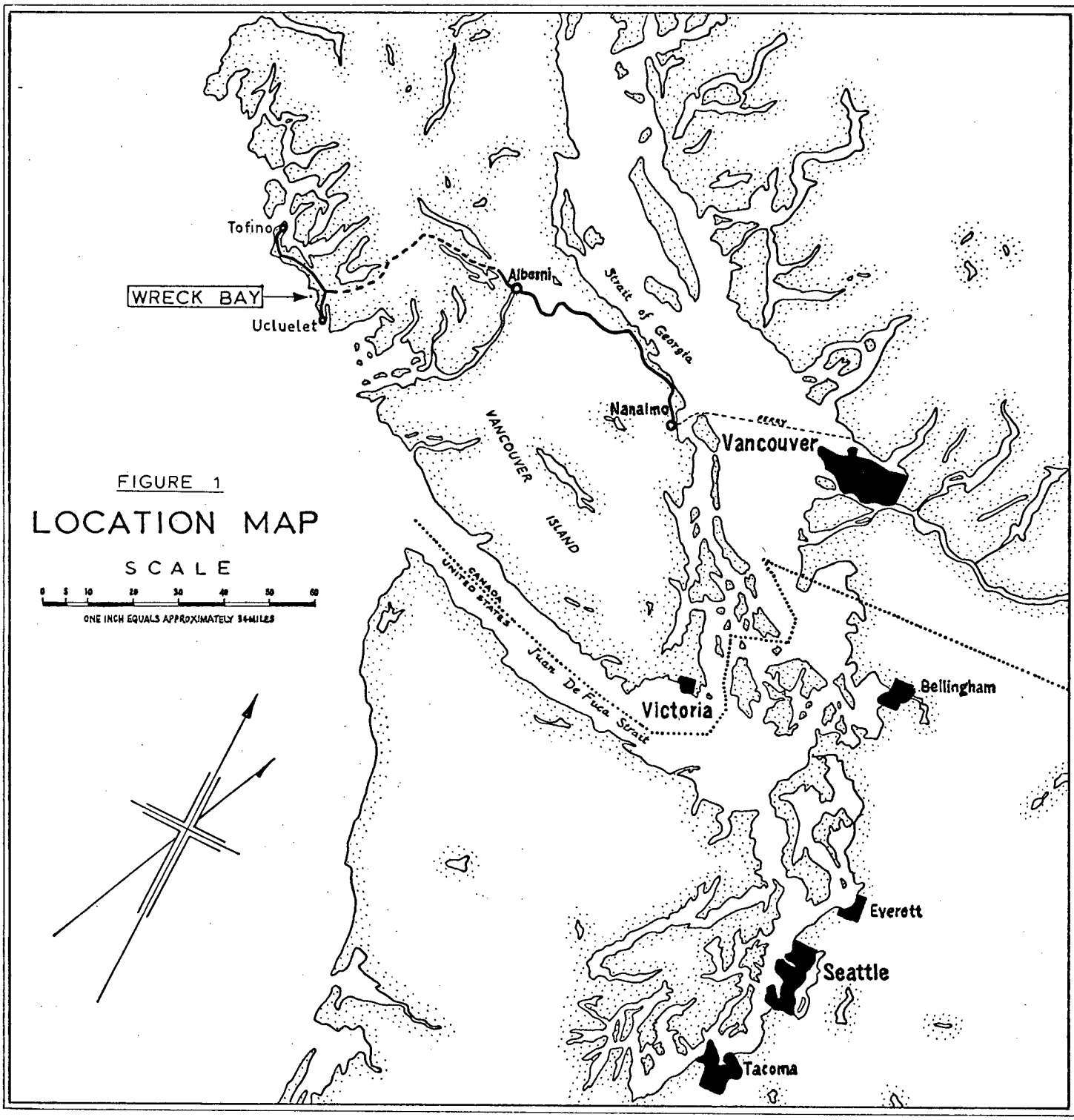

FIGURE 1

LOCATION MAP

Plate I.

Effect of strong onshore winds during the winter, on vegetation located above a low profile cliff. Paradise Beach, 2 miles southeast from Tofino.

Underbrush is commonly blueberries, salmonberries, salal and huckleberries, which occasionally form impenetrably thick growths.

II. SEA CONDITIONS

A. WAVES

A persistent groundswell approaches the west coast of Vancouver Island from the west, but during the winter months wind-blown storm waves from the south occasionally become dominant. During the summer of 1968, wave parameters measured on the beach at Wreck Bay were: significant breaker heights and period = 0.75 - 4.00 feet and 10 seconds respectively (see chapter on SAND MOVEMENT BASED ON WAVE PARAMETERS). The pattern of wave diffraction around the headlands and islands in the bay, and refraction on the shoaling bottom, is shown in Figure 2 and on the Frontispiece. The incident angle of breakers at the various profile locations were estimated from aerial photographs. This information, together with other estimated hydrodynamic and atmospheric data is given in Table III. A single storm attacked the coast during the summer, and breaker heights and periods increased to 16½ feet and 12 seconds respectively (Plate 2).

Wave measurements made aboard Shell Canada's oil-drill rig SEDCO 135-F during the winter of 1967 - 68, indicate that swell heights ranged from 6 - 10 feet, and swell periods ranged from 9 - 11 seconds (Watts and Faulkner, 1968). The

worst storm experienced by the drill rig occurred in December 1967. Winds reached 76 mph, with gusts to 92 mph from the southeast, and maximum wave heights recorded were 35 feet. The highest storm waves encountered during the winter were recorded in January 1968. Combined swell and wave height at this time reached 58 feet, after several days of 40-50mph winds. Historical averages of storms along the west coast of Vancouver Island are shown in Table II (Watts and Faulkner, 1968).

Maximum storm	Sustained 1 hour wind speed (mph)	Maximum wave height (ft)	Wave period (secs)
Annual summer storm (May-August)	40	30	15
Annual storm	70	45	15
100-year storm	100	70	15

TABLE II - Historical Averages of Storms

B. CURRENTS

An attempt was made on the 8th July 1968 to measure near-bottom current velocities and directions in Wreck Bay, with a Savonius Current Meter. Due to mechanical problems, only one successful measurement was obtained. This was located in 40 feet of water in the deep immediately northwest of Florencia Island (Map I). A seaward moving current with velocity of 0.2 knots, and azimuth 215°, was monitored 1 hour after the tide had turned to ebb.

Surface current measurements were made on the same

day using float bottles, which had been weighted to sink just beneath the sea-air interface. Five bottles were dropped along a line between Wya Point and Florencia Island, of which two were recovered five hours later approximately one mile southeast of their drop-points. Another five bottles were dropped along a line between Florencia Island and Quisitis Point. None of these were recovered, but one was sighted in the middle of the bay by a local fisherman approximately three hours later. These trends indicate a slow southeast moving surface current in the nearshore zone.

Watts and Faulkner (1968) report maximum currents on the shelf during storms, of 2.5 knots. They do not specify the current direction, but presumably it is southeastwards, conformable with the nearshore surface current.

C. TIDES

The west coast of Vancouver Island is affected by mixed semi-diurnal tides with a mean range of 8.7 feet during neap tides, and 12.9 feet during spring tides (Canadian Tide and Current Tables, 1968). The nearest reference port on which all tide elevations in this thesis were based, is Tofino, located approximately 20 miles northwest from Wreck Bay.

AIRPHOTO DATA

Date	17 June 1967	1 May 1966	15 Oct. 1954	29 Sept. 1950	29 Sept. 1930 (A-3032)	29 Sept. 1930 (A-5874)	Average*
Approx. Scale	1"=2640'	1"=1320'	1"=2640'	?	1"=980'	?	
Elevation (ft a.s.l.)	17,000	8,200	20,000	5,500	10,700	greater than 11,000	
Azimuth of deep water wave fronts	185°	170°	190°	200°	175°	160°	180°
Estimated tide height	Mid	Mid	High	Mid	Low	Low	
Azimuth of Florencia I. foam line**	75°	360°	20°	135°	320°	350°	
Estimated wind strength	Mod.	Light	Very strong	Light	Calm	Mod.	
INCIDENT ANGLE OF BREAKERS TO BEACH (degrees)***							
A	-	-5	-7	-	-5	-11	-7
B	-4	-3	-6	-	-2	3	-2
C	3	-2	-3	-	-1	3	1
D	-6	-8	0	-	-5	5	-4
E	5	-7	-13	-	2	11	3
F	-1	0	-1	-2	-3	2	-1
G	5	7	2	5	7	6	6

Table III. - Wave Parameter Estimates, and other Data, from six Sets of Aerial Photographs.

* Average of incident angle of breakers excluding storm values on 15 Oct. 1954.

** Indicates wind direction as measured from the meridian on an imaginary horizontal circle with Florencia Island as center.

*** - Sign indicates a southeast direction, no sign indicates a northwest direction.

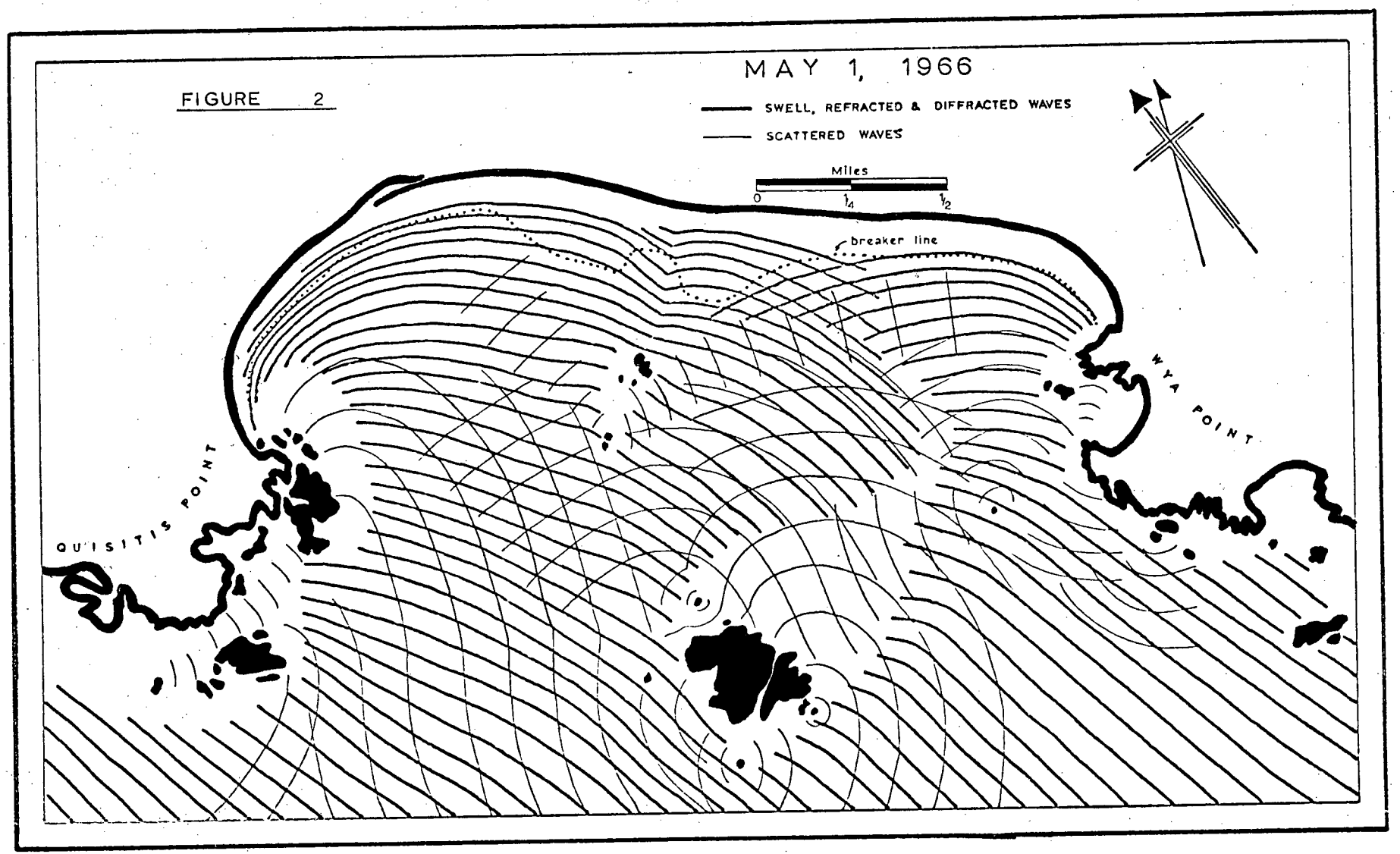

Typical wave pattern in Wreck Bay.
Drawn from aerial photographs shown on Frontispiece.

Plate 2.

Storm waves entering Wreck Bay on 18th Aug. 1968. The photograph was taken from the beach at Profile C. Five rows of breakers can be seen traversing the surf zone.

III. PHYSIOGRAPHY OF WRECK BAY AND OFFSHORE TROUGH

A. WRECK BAY

I. TOPOGRAPHY

(a) Methods

Nine days between the 5th and 20th August 1968 were spent plane tabling the three mile length of beach between Quisitis Point and Wya Point (Map I). The purpose of this undertaking was to obtain an accurate large-scale map of the principal study area of this thesis. A telescopic alidade and engineers stadia rod was used, and a local resident was temporarily employed as an assistant. A scale of 1 inch = 200 feet permitted mapping of major beach structures including berms, relict cobble cusps, etc (see chapter on BEACH STRUCTURES), and 73 rod stations at the cliffbase provided the necessary data for examining shoreline stability at Wreck Bay (see chapter on PLANIMETRIC SHAPE).

No convenient bench marks exist in the area, so elevations were based on tide heights at specific times, in areas where the sea surface was calm. On the 5th August, a lower high tide of 9.1 feet above datum occurred at 11.40 a.m., and a rock outcrop on Quisitis Point was marked with paint at this sea-level. Similarly at Wya Point, a rock outcrop was marked at sea-level on the 18th August, when a lower high tide 8.0 feet above datum occurred at 10.10 a.m. Chart datum adopted by the Canadian Hydrographic Service is based on the plane of

lowest normal tides (Canadian Tide and Current Tables, 1966).

Vertical control was maintained by first surveying the northwest half of the beach from the Quisitis Point reference elevation, to a large stationary tree-stump on Sand Point. The southeast half was then surveyed from the Wya Point reference station to the same tree-stump. A vertical error of 0.38 feet for the tree-stump elevation was obtained from the two different approaches, which was eliminated by adjusting two instrument station elevations on either side of the tree-stump.

Horizontal control was maintained by shooting a ray at a rock pinnacle on Seal Rock from each instrument station. During map compilation, instrument stations were adjusted so that their rays all coincided in a single point.

A number of points on the cliff edge were fixed by triangulation from the instrument stations, and their elevations were determined from the inclination angles. The two headlands enclosing Wreck Bay, Quisitis Point and Wya Point, were drawn onto Map I by expanding the scale of aerial photographs to that of the survey using a Saltzman Map Projector. The general outlines of Florencia Island and Seal Rock were plotted in the same way. Major faults shown on Map I were measured at the field locations, and supplemented by air-photo interpretation.

(b) Discussion

The backshore is exceptionally wide adjacent to the

two headlands, between Profiles A and B and Profiles F and G (Map I). These regions represent the more stable cliff sections behind the bay (see chapter on PLANIMETRIC SHAPE). The foreshore is exceptionally wide and flat at Sand Point, and steep and narrow at its flanks. This configuration is established by littoral currents, which are a function of tide height (see chapter on SAND MOVEMENT BASED ON TRACER DISPERSION), and wave height (see chapters on SEDIMENT SIZE ANALYSES and TRANSVERSE PROFILES). Relict gravel beach cusps exist from the mouth of Lost Shoe Creek, along the spitbar, to the area between Profiles C and D. A large number of fresh water springs emerge from the cliffbase between Profiles F and G, and 800 feet southeast of Profile E. These springs resulted in strong erosion of the summer berm, leaving it as a series of discrete sandy mounds (see Map I and chapter on BEACH STRUCTURES). The spitbar, which deflects the outlet of Lost Shoe Creek for 1250 feet northwestwards, reaches a maximum height of 23 feet above sea level along its crest. It fitted theoretical log-spiral curvature much more closely than did the cliffbase in this area (see chapter on PLANIMETRIC SHAPE).

Sea caves and blow holes are quite common along the southern part of Quisitis Point. Strong wave action has preferentially eroded the rocky coasts along fault planes, thus making their recognition fairly easy.

2. BATHYMETRY

(a) Methods

The bay was echo-sounded on the 5th and 6th July 1968, the purpose of which was to obtain an accurate bathymetric map, and to delineate exposed boulder and bedrock areas in the bay. A Furuno Model F-850 Mark II echo-sounder was used on 16 foot moter launch. It had an operating frequency of 28.5 Kc/s, and a pulse length of 1.3 ms. Initial traverses were extended from the beach profile lines out into the bay (PL lines), and subsequently, a rectangular grid was followed to obtain detail in uncovered areas (GL lines) - see Figure 3. At each of the time stations shown, a sextant was used to measure simultaneous tangential angles between three prominent topographic features on the shore.

Curves on tidal elevation for the periods spent in the field, were plotted on graph paper and then appropriate adjustments made on the echogram measurements. Pronounced 2nd and occasionally 3rd multiple reflections were interpreted as bedrock if they showed positive relief, and as boulder beds if zero or negative relief was indicated (Plate 3). Kelp beds produced strong reflections above the rock-water interface.

(b) Discussion

King (1967) found that a relatively high frequency, short pulse-length echo-sounder such as this, enabled him to delineate four distinct sedimentary types on the Scotian Shelf.

In the present study, echo reflection intensity indicated a single sediment type in the bay, and from sampling this turned out to be fine sand.

Boulder areas shown on Map I cannot represent zones of boulder concentration, since a number of them appear to exceed 1 ton in weight. Rather, they represent areas where sand has been selectively winnowed out, leaving the boulders as lag deposits. It is believed that a "mat" of boulders, derived from the glaciofluvial outwash, underlies the entire bay.

The large boulder area in the northwest corner of the bay is a result of two factors: grey cohesive clay beneath the sand effectively prohibits boulders from sinking (see chapter on TRANSVERSE PROFILES), and a persistent rip-current in this region allows only a thin cover of sand to blanket the grey clay (see Frontispiece, and chapter on PLANIMETRIC SHAPE).

The elongate boulder bed extending from Seal Rock toward the mouth of Lost Shoe Creek, occupies a distinct trough and supports no kelp (Plate 3 - lines GL2 and PL©) It probably represents an inter-longshore-bar trough, as does the small boulder area closer to shore containing sample B3, since a shoal area exists between them, and seaward of the larger boulder bed. Mothersill (1969) found that as a result of wave action, longshore bars in Lake Superior consisted of

fine sand, whereas the intervening troughs contained excess coarse material. Due to the depth of these features, they most likely developed in response to large winter storm waves, and remained unaffected by small waves in the summer. In contrast, the longshore bar in front of Profile D was definitely formed by small summer waves (see chapter on TRANSVERSE PROFILES).

The large boulder area between Profiles E and F is flat, and supports thick beds of kelp. Although it occupies a roughly equivalent position regarding bay symmetry to the elongate boulder bed described above, its exposure is due to a different set of factors. Smaller waves affect this area (see chapter on TRANSVERSE PROFILES), and it lies in shallower water. Presumably this area represents the source of sand for beach accretion and bar building during the summer, and in winter it becomes covered with sand as a result of beach degradation.

Small boulder areas on the flanks of Sand Point probably result from similar circumstances. In summer, sand is transported from these areas onto the point by converging wave trains in the lee of Seal Rock, thus supplementing the littoral drift pattern which exists in this area (see chapters on SEDIMENT SIZE ANALYSES and SAND MOVEMENT BASED ON WAVE PARAMETERS). In winter, all this sand is transported out beyond Seal Rock to build the shoal area present there.

The large bedrock and boulder area near Pocket Beach

has positive relief, and its lack of sand is due to winnowing by currents and waves.

Bedrock areas, where not exposed at the surface as small islands, are all truncated at a depth of 40 feet (Plate 3 - line GL-III). The reason for this is not known. It may be a result of glacial decapitation, or else wave erosion during a stillstand in sea level during Holocene times.

B. OFFSHORE TROUGH

Continental shelf bathymetry offshore from Wreck Bay is shown in Figure 4. Three echo-sounding lines were run across the trough, again to delineate different sedimentary facies indicated by sampling. An EDO Western Sonar Model 185 was used aboard Canadian Naval Auxillary Vessel LAYMORE.

Intensity of the 1st multiple reflection proved to be diagnostic (Figure 4), and indicated silty muds in the bottom of the trough, sand along its edges, and gravel on top of La Perouse Bank (Line 3, between time stations 2145 and 2215). Strong intensity proved to be bedrock covered with a thin veneer of relict gravels (see chapter on COASTAL ROCKS).

Maximum trough depth is at 60 fathoms located at its head (sample location OS-16), and the shallowest depth at 50 fathoms occurs over a broad sill area (sample location OS-14). The latter is thought to be the locus of maximum clay particle deposition at the present time (see chapter on RECENT SEDIMENTS).

FIGURE 3

ECHO SOUNDING — WRECK BAY — 5, 6 JULY 1968

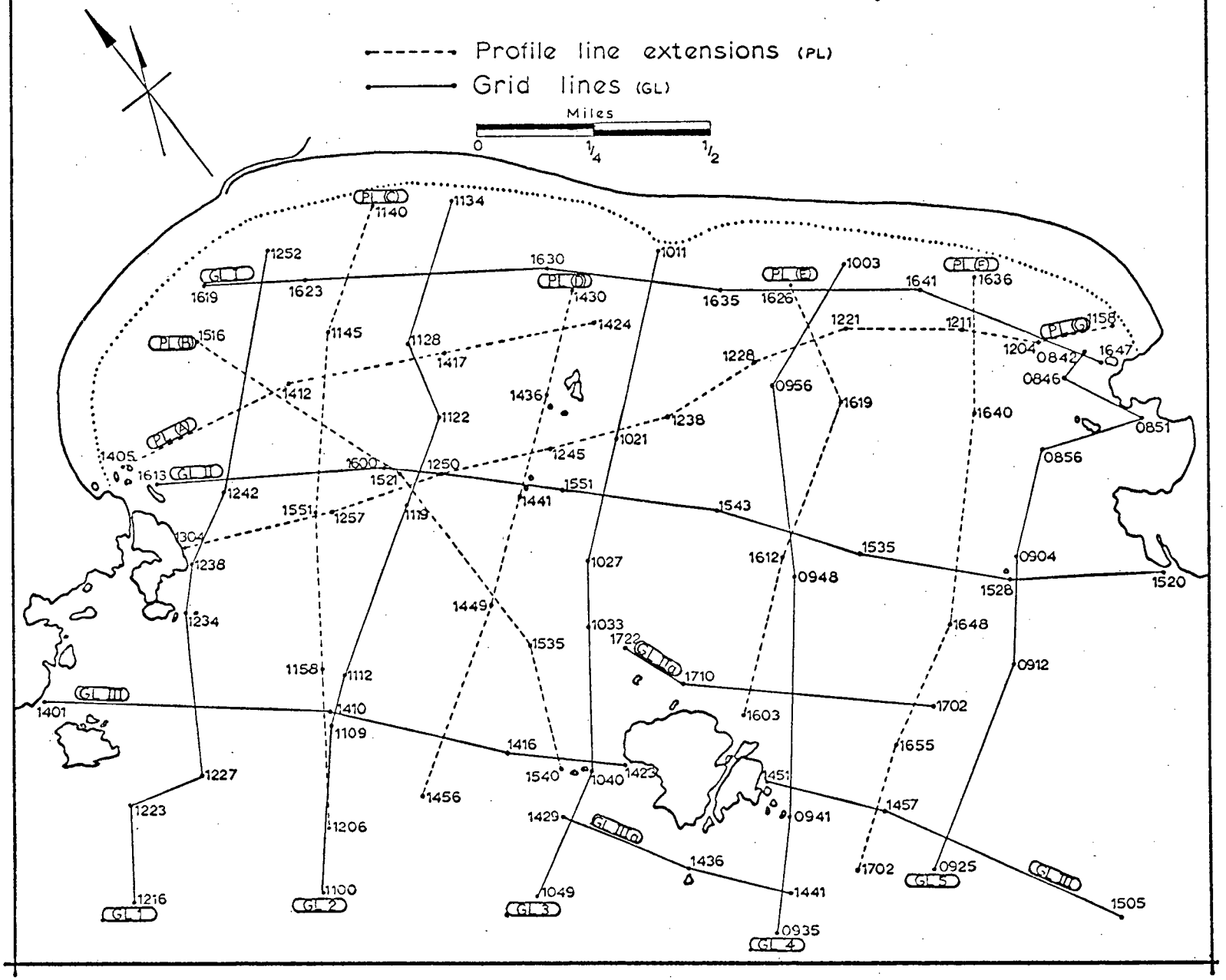

FIGURE 4

ECHO SOUNDING – OFFSHORE TROUGH – 30 MAY, 1968

FIRST MULTIPLE INTENSITY
strong
moderate
weak or absent

VERTICAL SCALE APPROX. = HORIZONTAL SCALE

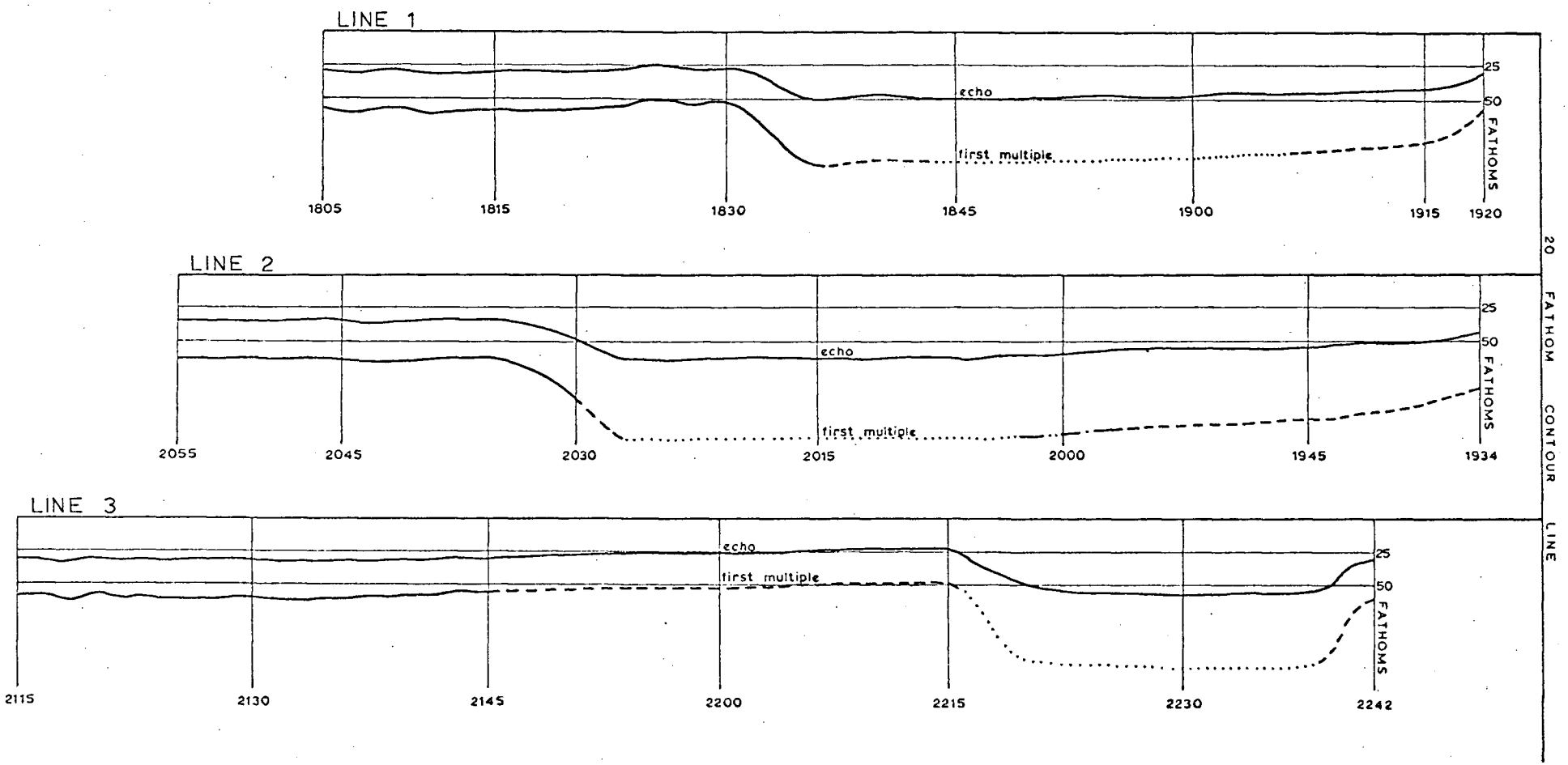

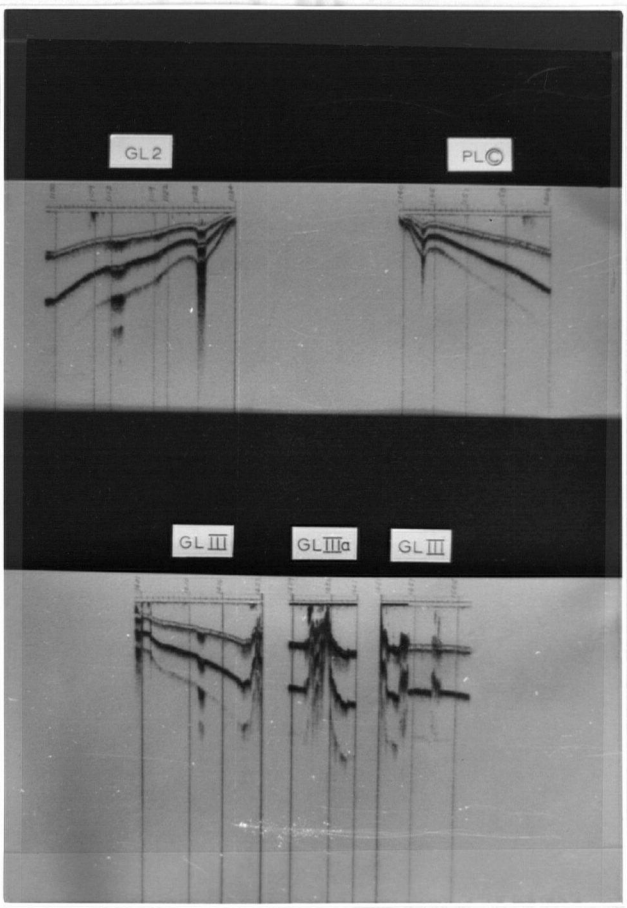

Plate 3.

Echograms of some traverses in Wreck Bay.
For location of these traverses, see Figure 3.

IV. COASTAL ROCKS

A. INTRODUCTION

Rocks exposed along the shoreline at Wreck Bay have been tentatively named by Muller and Carson (1969), as the "Tofino Greywacke Unit". They are a poorly sorted assemblage of sedimentary rocks ranging from argillites to argillaceous sandstones, and outcrop intermittently along the west coast of Vancouver Island as a discontinuous peripheral belt. At the northern end of the island, the unit is 3,000 feet thick at Kyuquot Sound, and 3,600 feet thick at Quatsino Sound (Sutherland Brown, 1966).

B. LOCAL DISTRIBUTION, LITHOLOGY AND STRUCTURE

Florencia Island and the southern part of Quisitis Point are characterized by the absence of exotic material in the sediments. The rocks are dark greyish-brown, very poorly bedded, impure sandstones, and contain numerous lenses of brownish-black mudstone (Plate 4a). Sandstones from samples FI-3, FI-8, FI-11, QP-2 and QP-3 (Figure 5) are all quite similar in composition, and from visual estimates, contain 15 -20% feldspar, 5 - 15% rock fragments, and more than 15% matrix (Plate 4c). They therefore correspond to lithic arkoses and felspathic arenites in Folk's (1968) classification. The particles are angular to sub-rounded, and consist of varying proportions of quartz, chert, K-felspar, plagioclase,biotite, muscovite, epidote, hornblende, clinopyroxene, chlorite and

opaque minerals. The quartz is predominantly of plutonic origin (straight extinction), but volcanic (rounded embayments, and no microlites) and metamorphic (undulose extinction) varieties are present as well. Felspars are highly altered, mainly to sericite, and only 10 - 20% is normally fresh. An increase in grain-size towards the northeast was noticed in these samples: QP-3 and FI-8 are very fine-grained, QP-2 is fine-grained, and FI-3 and FI-11 are medium-grained. The matrix consists of clay, chlorite and sericite.

In thin section a few micro-structures are evident. Sample FI-3 appeared to be weakly graded, and FI-8 showed a ½ inch deep erosion channel, which was filled with material identical to that below. The other samples are massive and structureless. All of them exhibit irregular shear-stringers carrying iron-oxide, and these in turn, are cut by wide tension fractures containing calcite.

Large scale folding was rarely seen except on Florencia Island (Plate 4a). Here, near sample location FI-11, an overturned anticline, with limbs showing constant thickness of competent sandstone, suggests a concentric type of folding. However, the tightness of the fold,and crushed state of mudstone in the core, indicate that it more likely represents a slump structure, developed when the sediments were still in a semi-consolidated state. No measurements on the plunge were possible, but the fold is recumbent to the east.

Faulting seems to have been much more significant than folding, in the deformation of these sediments. Most of the faults trend north-eastwards, and dip steeply towards the northwest (Map I). Locally, competent sandstones have been mylonitized by intense shearing (Plate 4b).

Samples QP-11, WP-3 and WP-13 (Figure 5) were also sandstones, but had been strongly modified from the general picture presented above. QP-11 is an intensely sheared sequence of relatively thin sandstone and black argillite bands, into which calcite and iron-oxide have apparently been deposited together along the fractures. Minute pyrite cubes and pyrrhotite nodules lie embedded in the calcite, and epidote has been formed in isolated patches, thus indicating low-grade metamorphism in this area. Sample WP-3 is also intensely sheared, and comes from a fault zone trending parallel to the coast, that has been impregnated with iron-oxide. Quartz particles exhibit crenulated borders, undulose extinction, and alignment of their longest axes parallel to the shear planes; felspars are all highly altered. Sample WP-13 typified much of Wya Point, in that chert nodules and thin chert bands constituted up to 50% of the rock volume (Plate 5a). Calcite was also present in significant amounts, as fracture fillings, and locally replacing quartz.

The southeast corner of Wreck Bay is isolated from Pocket Beach by a pillowed lava flow (Plate 5b). More commonly

it is brecciated, and contains blocky grey chert. Nowhere was it seen in contact with the sandstones, and therefore its age relationship is unknown. If the size and shape of pillows can be considered a diagnostic criterion, they were identical to pillows seen in Karmutsen basalts on the north side of Kennedy Lake. In thin-section, the rock is completely altered to fibrous amphibole (uralite), but still preserved are a few small amygdules lined with chlorite, and filled with zeolites (Sample WP-1). No magnetite is present, but the felty groundmass is criss-crossed by a great number of chlorite veins. These in turn are cut by quartz, and later by carbonate veinlets.

Seal Rock consists of a singular, unique rock type. It is very fine grained and pale green in colour, and in thin section, a cryptocrystalline felty mass completely masks its original identity (Sample SR-1). Scattered through this mass are tiny acicular crystals with preferred orientation, and a great many irregular fractures contain calcite. It is thought to be an altered tuff, and possible correlates with the Bonanza Group.

C. EXOTIC MATERIAL

Wya Point sandstones, and to a lesser extent the middle and northern parts of Quisitis Point, are characterized by exotic blocks of chert and marble. The origin of this material is unknown, but the large dimensions of some of these

blocks suggest that they were transported over a relatively short distance. Samples QP-4, WP-31, WP-25 and WP-12 were obtained from chert. QP-4 is a pale greenish-grey, mottled chert, consisting of cryptocrystalline quartz with scattered "concretions" of microcrystalline quartz, showing undulose extinction. These concretions may be recrystallized radiolarian tests, as veinlets of iron-oxide do not appear to pass through them (Plate 6b). A number of clear quartz stringers cut the iron-oxide veinlets, and elsewhere, appear to be cut by them. Sample WP-31 came from a chert outcrop which appeared to occupy most of the southern boundary of Pocket Beach. It is dark grey in colour, and contains numerous elongate "concretions" which are perhaps recrystallized sponge spicules. Both quartz and iron-oxide veinlets are present, but both are cut and locally replaced by calcite veins. Sample WP-25 came from a large block of laminated chert showing small-scale folding (Plate 6a). It is identical to sample QP-4 except that "concretions" are much more abundant, and no iron-oxide veinlets are present. Quartz-filled fractures are also somewhat wider, with small crystals oriented perpendicular to and adjacent to the edges, and large interlocking crystals with undulose extinction in the middle. Sample WP-12 is from a nodule contained in the sandstone (Plate 5a). The weathered exterior is white, but a freshly broken surface possesses a medium-grey colour. In thin section it is identical to WP-31, except that carbonate

veinlets are more abundant.

Large exotic blocks of recrystallized limestone occur at sample locations WP-9 and WP-30. WP-9 is an irregularly shaped body with bulbous protuberances extending into the sandstone (Plate 7a), whereas WP-30 is oval shaped. They are both greyish-white in colour, and consist of fine-grained interlocking calcite crystals. Irregular and intersecting shear zones have resulted in local recrystallization to large twinned lamella (Plate 7b), the latter often being bent. In sample WP-30, the crystals exhibit preferred alignment (Plate 7b), whereas WP-9 consists of a mosaic of equant grains. Furthermore, sample WP-30 is cut by several iron-oxide veinlets, whereas WP-9 is not.

Sample WP-7 is coarse grained, pale grey, and has the appearance of an intrusive rock. The sample location was separated from sandstones to the northeast by a sharp contact, whereas the other boundaries were indiscernible. Several other small occurrences of this material are exposed between this location, and the end of the promontory. In thin-section, it consists of coarse grained interlocking metamorphic quartz grains, highly altered felspar, abundant large chlorite lathes, and blotches of epidote. It is therefore a low-grade regionally metamorphosed derivative of unknown silicious parent material, that was incorporated into the Tofino Greywacke Unit similar to other exotic material.

D. INTRUSIVES

Only one intrusive body was found along the coastal section that was examined. This was an 8 foot wide diabase dyke (Map I) represented by sample WP-26. It consists of labradorite laths showing alignment (fluidal texture), and a few zoned euhedral felspar phenocrysts. Augite, partially chloritized, and magnetite are the next most common constituents, and oxidation of the latter has imparted a reddish-brown colour to the weathered surface. It probably is part of the basic Kennedy Intrusions of Cretaceous or Tertiary age, described by Eastwood (1968).

E. RELATIVE AGE

Sutherland Brown (1966) has assigned a late Jurassic-early Cretaceous age to the Tofino Greywacke Unit (Callovia-Aptian), i.e. 120-160 million years B.P. This contention is indirectly supported by a number of factors:

1. LOWER LIMIT

Its unmetamorphosed condition and high felspar content, together with the fact that it contains a number of low-grade regional metamorphic minerals like epidote, amphibole and chlorite, suggest that it was deposited after emplacement of the Kennedy Batholith, which has been dated at 167 million years B.P.

2. UPPER LIMIT

Muller and Carson (1969) report that a quartz-monzonite

stock intrudes the unit on Stubbs Island (across the inlet from Tofino), which has been dated as early Tertiary. Also, the diabase dyke found cutting the unit on Wya Point, is most likely of Cretaceous or Tertiary age.

A generalized stratigraphic column of rocks exposed along the coast, and directly inland from Wreck Bay, is given in Table IV.

PERIOD	UNIT	LITHOLOGY
Quaternary	WRECK BAY FORMATION	Glaciofluvial outwash and till
Cretaceous or Tertiary	KENNEDY INTRUSIONS	Basalt and gabbro
Late Jurassic to early Cretaceous	TOFINO GREYWACKE UNIT	Argillaceous sandstones and mudstones
Middle Jurassic	BATHOLITHIC INTRUSIONS (Kennedy Batholith)	Mainly granodiorite and quartz monzonite
Late Triassic to lower Jurassic	BONANZA GROUP	Pyroclastic andesite
Late Triassic	QUATSINO GROUP	Massive to thinly bedded limestone, argillite and tuffaceous argillite
	KARMUTSEN GROUP	Brecciated, amygdaloidal and pillowed basalts and andesite

Table IV - Generalized stratigraphic column of Rocks in the Vicinity of Wreck Bay.

F. REGIONAL DISTRIBUTION AND RELATION TO PRESENT-DAY OFFSHORE TROUGH

The depositional paleoslope of the Tofino Greywacke Unit is indicated by Sutherland Brown (1966) as being directly seaward in the vicinity of Wreck Bay, and Muller and Carson (1969) note that the sediments dip steeply towards the southwest. Apart from tuff composing Seal Rock, and the lava flow north of Pocket Beach, these coastal sediments are separated from Karmutsen, Quatsino, Bonanza and Batholithic Intrusions around Kennedy Lake, by a broad belt of unconsolidated glacio-fluvial outwash. Eastwood (1968) and Muller and Carson (1969) have proposed that a major fault underlies these gravels to explain the break in bedrock geology. Eastwood (1968) however, points out that this fault is unrelated to all other faults in the area, because of its northwest trend. The necessity for this inferred fault is questioned here, on the basis of the following argument. Sediments composing the coastal rocks are distinctly geosynclinal in character - the sandstones are flysch-type deposits, and along Wya Point, have been mixed with pre-flysch exotic blocks of chert and marble. Although Aubouin (1965) states that these consecutive sedimentary periods normally precede the advent of acid intrusions, evidence suggests that in this case the sandstones were deposited after emplacement of the Kennedy Batholith, and were in fact largely derived therefrom. The northeastern edge of this geosynclinal trough then, naturally overlies the acid intrusive in the

region now covered by glaciofluvial outwash.

Concerning the seaward extension of these sediments, two Continuous Seismic Profile records obtained by the U.B.C. Marine Geology Group were examined (Murray 1970, personal communication). Both lines extend from a point located approximately $2\frac{1}{2}$ nautical miles from Wya Point, # 67-26 oriented normal to the coastline, and #67-27 parallel to it in a southeast direction (Map 2). The latter simply shows crumpled sediment, dipping gently southeastwards along the base of the present-day offshore trough, and underlying approximately 100 feet of undisturbed recent sediment. Where the line crosses the edge of La Perouse Bank just north of time station 1930, the record is not clear; however, on the south side of the bank where it passes into Barkley Sound Trough, faulting is clearly in evidence, and based on the bathymetry, this fault continues into Barkley Sound in a northeast direction.

Line #67-26 too, shows crumpled sediment dipping gently in a southerly direction at the base of the offshore trough. The unconformity between these consolidated sediments (Tofino Greywacke Unit?) and the overlying recent sediment, is a fairly smooth plane which also dips gently southwards. It continues under the southern rim of the present-day offshore trough, with no sign of faulting, until it becomes masked by closely spaced multiple reflections. At time station 1830, indurated sediment forming the basement is again visible, and

dips moderately steeply toward the north. This region may represent the southern boundary of the paleogeosynclinal trough into which Tofino Greywacke Unit sediments were deposited.

Between time stations 1830 and 1800, a second trough is indistinctly suggested by the record. The sediments composing this trough are either an extension of the Tofino Greywacke Unit across an anticlinal arch, or else consist of Oligocene-Miocene deposits, implied by Sutherland Brown (1966) as existing in this area.

It appears therefore, that the southern rim of the present-day offshore trough is, at least in part, a result of unconsolidated detrital fill, and that its slope of 20 - 25 degrees represents the angle of repose of this material. The source of these sediments was almost certainty the glacial deposits on La Perouse Bank. As sea level rose during the Holocene Period, fine sand would be winnowed out of the glacial deposits by wave action and swept landward, to eventually spill into the present-day trough. Indirect evidence supporting this theory is furnished by:

- Irregularity of the 25 fathom bathymetric line on La Perouse Bank (Map 2) indicates abundance of glacial material in the form of eskers, whereas kame-kettle topography at the head of the present-day trough (lat. 48° 50', long. 125° 50' - Map 2) suggests relatively less glacial debris.
- Echogram Line 3 (Figure 4) has a moderate first multiple

reflection intensity between time stations 2145 and 2215, confirming the existence of a considerable thickness of unconsolidated material on La Perouse Bank. The intensity of first multiple reflection on Lines 1, 2 and 3 at the head of the present-day trough is strong, indicating a thin unconsolidated sedimentary cover above bedrock.

- Samples OS-19 and OS-20 from La Perouse Bank are relict glacial gravels consisting almost entirely of cobbles and pebbles, and appear identical in composition and shape to those found in the glaciofluvial outwash at Wreck Bay.

Although no seismic records exist across the northern rim of the present-day offshore trough, it is reasonable to assume that this 15 - 20 degree slope also represents the angle of repose of recent detritus. Considering the amount of fine grained material which has been removed from Wreck Bay and Long Beach, and assuming that the present southeast moving nearshore current has persisted since the end of the Holocene, infilling of the northern flank of the old Tofino Greywacke Unit depositional basin is readily explained.

In summary then, the depositional basin of the Tofino Greywacke Unit in the vicinity of Wreck Bay, was a narrow geosynclinal trough which extended parallel to the present-day coastline. The northern edge is exposed along the shore, and based on increasing grainsize of sandstones towards the northeast, and abundance of exotic blocks along Wya Point, the source of these sediments was probably the mountainous

hinterland northeast of Kennedy Lake. The southern edge of the geosynclinal trough, as suggested by seismic profile #67-26, may lie along La Perouse Bank at time station 1830, a distance of approximately 5½ nautical miles from Wya Point. Pleistocene continental glaciers appear to have passed right across this paleotrough, as evidenced by the gently southward dipping unconformity at the base of the present-day offshore trough, and abundance of glacial debris on top of La Perouse Bank. The present-day offshore trough occupies the middle of the paleotrough as a result of infilling from the south by sea level transgression over this glacial debris, and infilling from the north due to erosion of glaciofluvial outwash from Wreck Bay and Long Beach. The geometric shape of the present-day offshore trough reflects the contrasting abundances of glacial material on La Perouse Bank, and on the bank at its head.

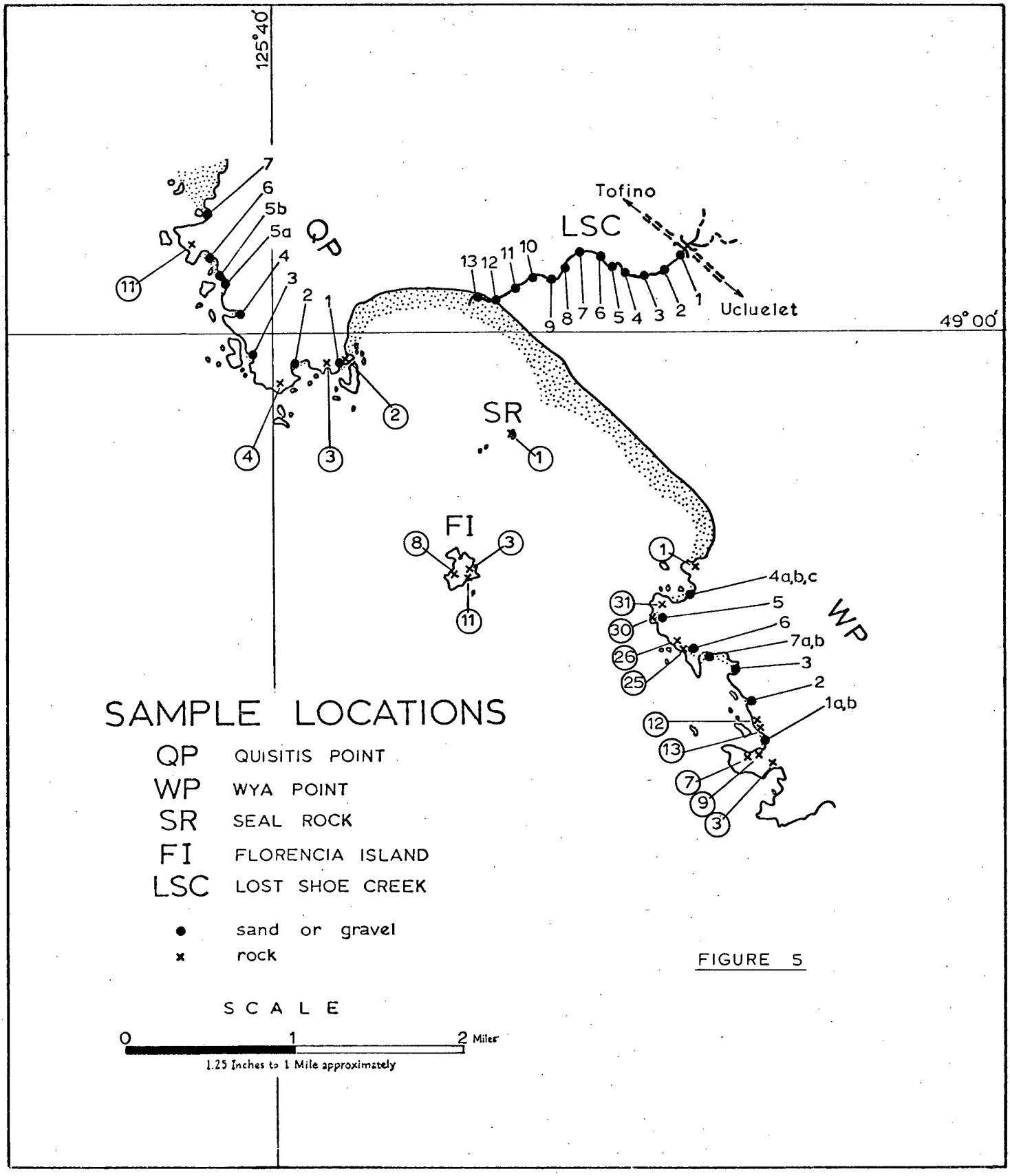
125°40'
49°00'
QP
LSC
Tofino
Ucluelet
SR
FI
WP
SAMPLE LOCATIONS
QP QUISITIS POINT
WP WYA POINT
SR SEAL ROCK
FI FLORENCIA ISLAND
LSC LOST SHOE CREEK
sand or gravel
rock
SCALE
0 1 2 Miles
1.25 Inches to 1 Mile approximately

FIGURE 5

Plate 4a. Tightly folded impure sandstone and incompetent brownish-black mudstone. Sample location FI-11.

Plate 4b. Mylonitized sandstone. Sample location FI-8.

Plate 4c. Photomicrograph of medium-grained impure sandstone. Angular to sub-rounded quartz, chert, plagioclase, altered felspar, muscovite and biotite can be identified. Sample location FI-11.

0
200 microns
400

Plate 5a. Chert nodules and bands in impure sandstone.
Sample location WP-12 and WP-13.

Plate 5b. Pillow structures in an altered lava flow, between the southeast corner of Wreck Bay, and the Pocket Beach.
Sample location WP-1.

Plate 6a. Laminated chert showing small-scale folding.
Sample location WP-25.

Plate 6b. Photomicrograph of chert showing "concretions" of undulose quartz, iron-oxide, and quartz veinlets.
Sample location QP-4.

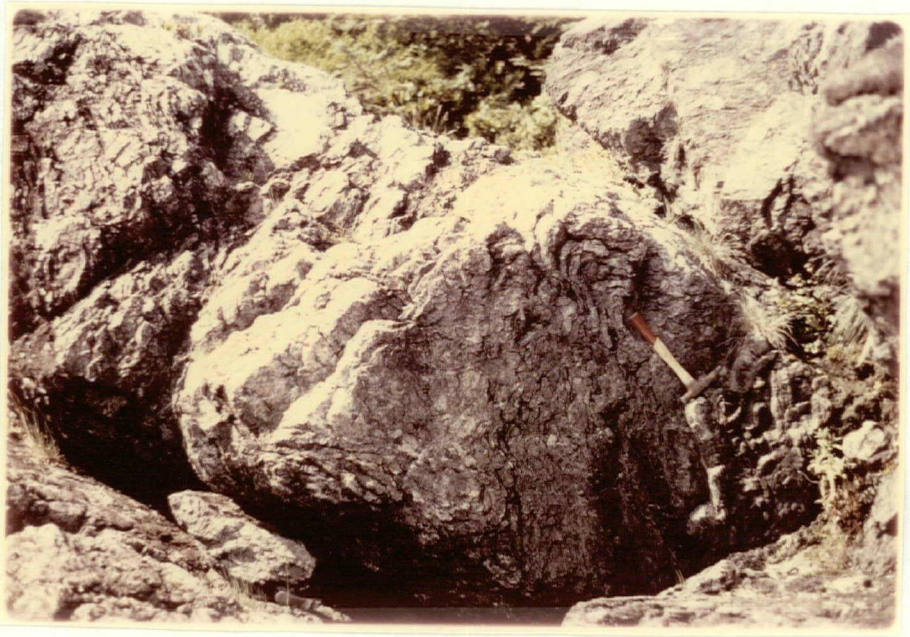

0
200 microns
400

Plate 7a. Large block of marble with bulbous protuberances projecting into the impure sandstone.
Sample location WP-9.

Plate 7b. Photomicrograph of marble showing alignment of small calcite grains, and large twinned lamella in vicinity of shear zone.
Sample location WP-30.

0
200 microns
400

V. RECENT SEDIMENTS

A. INTRODUCTION.

Glaciofluvial outwash, composing most of the coastal plain along the west coast of Vancouver Island, and best exposed at Wreck Bay, was named by Dolmage (1919) as the Wreck Bay Formation. The mineralogy of this deposit and recent sediments derived therefrom, were studied using two different techniques. The very fine sand fraction (62.5 - 125.0μ), which contained almost all the magnetite and a large percentage of other heavy minerals, was isolated for point-count analysis. Silts (2.0 - 62.5μ) and clays (<2.0μ) were separated for X-ray diffraction analysis.

Samples selected for the two investigations overlap to a degree, as shown in Table V. For point-count analysis, one sample was arbitrarily selected from fourteen environments in order to gain an impression of their association and provenance. X-ray analysis was conducted on material from two specific regions, the sea cliff and offshore trough, to examine their affinity regarding recent sediment dispersion.

Sand coarser than 125μ consisted mainly of quartz, felspar, rock fragments and shell-hash; no quantitative mineralogic study was made on this material. Gravels (>2.0 mm) too, were simply noted for their character to supplement evidence on the primary source of the sediments.

For sampling procedures and their locations, see APPENDIX.

B. POINT-COUNT ANALYSIS

1. LABORATORY PROCEDURE

Very fine sand fractions were screened from 14 selected samples to determine their weight percentages (column 1, Table VI). Magnetite was then screened from these size fractions and expressed as weight percentages (column 2, Table VI). The balance was then separated into heavy and light mineral fractions using bromoform (S.G. = 2.9) for point-count analysis.

Twenty eight thin-sections were prepared, one each for the light and heavy minerals. Approximately 300 grain counts were made on both light and heavy mineral thin-sections, and mineral proportions were calculated as percentages of total sample counts (Table VI).

2. RESULTS

Concerning Table VI, the non-magnetic opaque column contained less than 5% rutile, and the rest, though unidentified, was probably hematite. Garnet, zircon, epidote/clinozoisite, hornblende and chlorite have diagnostic optical properties, and were readily identified. The augite/diopside column consisted of equal proportions of both minerals for the Cliff sample, whereas all other samples contained roughly 75% diopside.

No attempt was made to differentiate the various types of quartz,however, glassy plutonic material made up the bulk of the column. Microcrystalline and chalcedonic quartz

varieties were grouped in the chert column. Felspars were generally highly altered to sericite and possibly kaolinite, so both K-felspar and plagioclase were determined under one column. Muscovite and biotite occurred in the light and heavy mineral thin-sections; grain-counts from both were thus added together, giving the figures shown in the column. The column headed by "U" includes unknown minerals, minerals not considered in the counting, and rock fragments; a large proportion of these grains were probably altered felspars.

3. DISCUSSION

(a) Mineralogic Associations

Grey clay and glaciofluvial outwash exposed in the cliff, provided the material for all other sedimentary environments considered in this study. It is therefore apparent that the latter sediments have been affected by at least two cycles of deposition.

First a comparison of the two "parent" cliff materials, grey clay and glaciofluvial outwash. The latter, from Table VI, contains a higher proportion of mica and heavy minerals, particularly magnetite, and somewhat less quartz, thus supporting textural evidence that the outwash transporting medium had a high competency. Brown clay, which occurs at the contact between these two materials (Plates 8a and 8b), is an alteration product of the grey clay. Contamination of its very fine sand, silt and clay fractions by the

overlying glaciofluvial outwash is readily apparent in Tables VI and VII, although its low magnetite content belies its true nature. The boulder, which is an unarmoured mudball, measured approximately 9 inches in diameter. A large number of these inclusions are contained in the glaciofluvial outwash close to the contact with brown clay, and therefore probably originated from the grey clay during initial stages of outwash deposition. Its very fine sand fraction is noticeably deficient in all mineral components except mica, which was most likely derived from the outwash while being rolled along glacial stream channels.

The sample from Lost Shoe Creek differed very little from the cliff outwash sample. Only zircon and mica concentrations were increased as a result of recent fluvial processes.

Of the three beach samples studied, one represents material affected by large waves during the winter regime (NWR-2a), and the other two represent material deposited by small waves during the summer regime (NWR-2b, NWR-2c). NWR-2a is characterized by exceedingly little very fine sand, a large proportion of which is made up of magnetite and non-magnetic opaques. It also contains a high proportion of the more resistant heavy minerals such as garnet, zircon and diopside, thus reflecting the high energy environment prevalent during winter (see chapter on ECONOMIC GEOLOGY, for gold con-

centration in this region).

The very fine sand composition of five samples collected between the upper foreshore and the offshore trough, is generally quite consistent, apart for a few significant differences. These samples include NWR-2b, NWR-2c, B-19, OS-4 and OS-16, and cover a distance of about 8 nautical miles. In comparison to cliff material, the group shows a decrease in felspar and mica content; and starting with a relatively high zircon concentration for the beach samples, the latter mineral shows progressive impoverishment further away from shore. Furthermore, the (augite + diopside)/hornblende ratio for the group shows an increase from about 0.5 to 1.0 as compared to the cliff. The most significant departures from the general group composition occur with samples NWR-2b and OS-4. The former was taken from the upper foreshore near the swash limit, where water movement is predominantly by laminar flow; the sample therefore contains a low proportion of magnetite and other heavy minerals. Sample OS-4 on the other hand has a very high magnetite content and is enriched with other heavy minerals as well, thus suggesting the presence of a relict beach placer at this 20 fathom bathymetric level (see chapter on ECONOMIC GEOLOGY).

The Long Beach sample was collected from a high energy environment similar to that represented by sample NWR-2a in Wreck Bay, i.e. from the backshore. Although it contains a high concentration of non-magnetic opaque minerals and

(augite + diopside), it is relatively sparse in magnetite. In the light mineral fraction, it contains less quartz and more felspar than the Wreck Bay marine environment. These differences perhaps reflect compositional variation in the "parent" cliff material, or else are a result of the relatively small amount of cliff material that has been eroded from Long Beach (low cliff profile).

Quisitis and Wya Point samples represent deposition by extremely high wave-energy conditions. Their mineralogic compositions are quite similar, and contain low magnetite and high non-magnetic opaque concentrations. An exception to their general uniformity occurs with their (augite + diopside)/hornblende ratios; for Quisitis Point it is <1, and for Wya Point it is >3. This suggests that sediment movement is in a southeast direction due to increased diopside concentration at Wya Point, this being the most resistant of the three minerals (Krumbein and Pettijohn, 1938).

An interesting point regarding Table VI, is the extreme variability of magnetite, and apparent uniformity of non-magnetic opaque minerals in the different samples. This may be a result of the presentation, the former being % by weight, and the latter % by counts.

(b) Provenance

In general, sediments composing the glaciofluvial outwash and grey clay are well reflected by rocks exposed

inland from Wreck Bay. Eastwood (1968) has described seven magnetite occurrences in the area, one of which was mined until recently by Brynnor Mines. No doubt these deposits were instrumental in providing the magnetite and other iron-oxides now contained in the outwash. Garnet, diopside and epidote probably came from the many skarn zones in the area. These zones have formed where argillite of the Quatsino Group and andesites of the Bonanza Group lie in contact with the Batholithic Intrusions. The latter contains roughly equivalent amounts of quartz and felspar, and other common minerals include hornblende, biotite and secondary chlorite. The felspars consist of orthoclase generally highly altered to allophane, and plagioclase somewhat altered to sericite, clinozoisite and epidote (/Eastwood, 1968).

Gravel found on the beach can usually be classified petrologically according to particle size and shape. Cobbles are invariably dioritic in composition, ellipsoidal in shape, and correlateable with the Kennedy Batholith. Coarse pebbles are generally discoidal to ellipsoidal in shape, and commonly consist of porphyritic and amygdaloidal basic volcanics, chalcedony and jasper, most likely derived from the Karmutsen Group. Fine pebbles and granules are usually irregular to spheroidal in shape, and consist of vein quartz and some volcanics, but mostly greyish-brown indurated sediment, which can be correlated with the Quatsino Group and Tofino Greywacke Unit.

Point-count Analysis	X-ray Diffraction Analysis	Environment	
LSC-6		LOST SHOE CREEK (Figure 5)	
C-1	C-1 C-2 C-3	GREY CLAY	CLIFF (Map 1)
C-6	C-2 C-3 C-4 C-5 C-6 C-7	GLACIOFLUVIAL OUTWASH	
C-2	C-2	BROWN CLAY	
BOULDER	BOULDER	BOULDER	
NWR-2a		BERM	BEACH (Map 1)
NWR-2b NWR-2c		FORESHORE	
B-19		BAY (Map 1)	
OS-4		SAND	OFFSHORE (Map 2)
OS-16	OS-11 OS-12 OS-13 OS-14 OS-16 OS-17 OS-18	MUD	
LB-4		LONG BEACH (Map 2)	
QP-4		QUISITIS POINT (Figure 5)	
WP-1b		WYA POINT (Figure 5)	

Table V. Samples considered in point-count and X-ray diffraction analyses. Sample locations are indicated by reference to maps and figures.

Environment	Sample Number	% by weight		% by counts													
				Heavy Minerals							Total	Light Minerals				Total	U
		(62.5 - 125μ) size fraction in sample	MAGNETITE in (62.5 - 125μ) size fraction	NON-MAG. OPAQUES	GARNET	ZIRCON	EPIDOTE + CLINOZO	AUGITE + DIOPS	HBLD.	CHLORITE		QUARTZ	CHERT	K-FELS + PLAGIO.	MUSCOV. + BIOTITE		
LOST SHOE CREEK	LSC-6	.04	5.17	8.4	.9	1.3	5.6	5.9	6.5	1.7	30.3	16.6	-	10.4	7.4	34.4	35.3
CLIFF: GREY CLAY	C-1	10.70	.84	5.0	.9	.1	2.7	2.7	7.2	2.5	21.1	29.0	.3	14.4	3.1	46.8	31.9
CLIFF: OUTWASH	C-6	3.75	5.47	7.7	1.3	..7	4.4	4.2	8.6	2.0	28.9	20.2	2.9	13.8	5.0	41.9	29.4
CLIFF: BROWN CLAY	C-2	13.40	.89	9.9	1.3	.9	3.1	3.7	8.4	2.4	29.7	19.2	1.3	19.3	3.1	42.9	27.0
CLIFF: BOULDER		16.85	-	7.2	.2	.2	1.6	.2	.2	2.7	12.3	14.0	-	11.7	5.4	31.1	56.6
BEACH	NWR-2a	.02	15.0	19,0	2.4	2.4	3.0	4.2	2.2	.8	34.0	15.2	.4	6.8	1.8	24.2	41.8
BEACH	NWR-2b	4.22	.94	9.0	.3	1.9	2.8	3.6	4.7	1.6	23.9	24.8	.9	8.8	1.7	36.2	39.8
BEACH	NWR-2c	8.75	2.85	8.3	1.8	1.4	3.2	3.4	5.2	2.8	26.1	26.2	1.2	7.1	.8	35.3	38.7
BAY	B-19	12.02	2.22	7.8	.8	1.1	3.0	5.7	4.6	2.1	25.1	27.9	2.1	7.4	2.8	40.2	35.0
OFFSHORE	OS-4	21.22	10.49	10.2	3.0	.2	4.7	6.7	6.3	2.0	33.1	23.8	1.0	6.9	1.2	32.9	33.5
OFFSHORE	OS-16	15.10	1.61	7.2	.6	.6	3.5	5.4	5.4	3.5	26.2	29.4	2.3	5.6	2.7	40.0	34.1
LONG BEACH	LB-4	3.98	3.82	14.8	.5	1.1	4.1	6.9	5.5	4.9	37.8	15.9	.5	10.4	1.4	28.2	33.8
QUISITIS POINT	QP-4	1.22	.67	11.2	-	.7	3.1	3.5	4.8	4.4	27.7	16.5	.9	7.9	1.8	26.1	46.1
WYA POINT	WP-1b	7.35	.91	15.3	.1	.1	4.2	6.2	2.0	2.8	30.7	17.6	.5	9.1	1.5	28.7	40.7

Table VI. Petrography of very fine Sand from Fourteen Related Environments. U equals unknown Minerals, Rock Fragments, and Mineral Species not Considered.

C. X-RAY DIFFRACTION ANALYSIS

1. LABORATORY PROCEDURE

Chemical pre-treatment on 18 cliff and offshore trough samples involved the following: Carbonates and other soluble salts were initially removed by digesting in NaOAc (pH = 5.0). Oxidizable organic matter was removed with 30% H_2O_2. Extractable iron was isolated for later analysis, by buffering the samples with sodium citrate, and slowly adding sodium dithionate.

Two clay fractions ($<0.2\mu$ and $0.2 - 2.0\mu$), and two silt fractions ($2.0 - 20.0\mu$ and $20.0 - 62.5\mu$) were isolated from each sample, except the cliff outwash samples. The latter contained little fine material, so total clay and total silt was isolated.

The clay fractions were then split in two, one half was K-saturated, and the other Mg-saturated. After X-raying oriented slides of these materials, the former was heated to 550°C, and the latter glycerated with a 1:10 glycerine:water solution, and both were X-rayed again. Silts were simply mounted in powder holders and X-rayed once.

The proportion of clay, silt and very fine sand in each sample was determined as follows: Very fine sand was removed by screening a known weight of original sample and determining its weight percent. Magnetite weight percentage in this size fraction was ascertained as described in the

point-count analysis (Table VII). 20.0 gms of the material <62.5μ was separated into the various clay and silt fractions, and these were made up into 1 litre suspensions. 50.0 ml of these suspensions were pipetted out into weighed crucibles, evaporated to dryness, and weighed again. The weight percentages were then found by simple proportion (Figure 6).

Extractable iron was determined from the lechate solutions obtained during chemical pre-treatment, on a Perkin Elmer Model 303 Atomic Absorption Spectrophotometer. The free iron-oxides include non-crystalline coatings on grains, and amorphous oxides. Very little interlayer iron or crystalline iron-oxide was included in the chemical extraction. The concentrations were found in parts per million (Table VII).

Total carbon, which includes carbonate, was determined on a Leco Induction Furnace. Each sample was run twice, and the average values are expressed as weight percentages (Table VII).

2. X-RAY ANALYSIS

Cu K_α radiation was used from 3 - 30 degrees 2θ at 1 degree/minute for the clays, and from 3 - 60 degrees 2θ at 2 degrees/minute for the silts.

The principal clay minerals and a mixed-layer derivative were identified using the following criteria:

Illite - insensitivity of its 10Å peak to all treatments.

Montmorillonoid (montmorillonite + vermiculite) - expansion

of its 14Å peak to 17 - 18Å on glyceration, and collapse to 10Å on heating.

Vermiculite - presence of a 12.2 - 12.6Å peak on the K-saturated, room-temperature diffractogram. This is due to partial collapse from loss of interlayer water (Lavkulich, 1970, personal communication).

Chlorite - insensitivity of its 14Å peak to all treatments.

Kaolinite - collapse of its 7Å peak on heating.

Montmorillonoid/chlorite mixed layer - expansion to 15.5 - 16.4Å on glyceration, and collapse to 11.0 - 11.2Å on heating.

Kaolinite is not easily distinguished from chlorite by X-ray analysis, as the latter possesses a second-order basal peak at 7Å coincident with the kaolinite 7Å peak. For this investigation, kaolinite presence was established based on the degree of 7Å peak collapse, when the K-saturated slide was heated to 550°C. Slight collapse was taken as indicating negligible kaolinite, whereas complete collapse indicated its presence. Confirmatory evidence for the existence of kaolinite in the glaciofluvial outwash was obtained by Bhoojedhur (1969), who found it in a number of samples collected from a gravel quarry at the Tofino-Alberni-Ucluelet road junction.

Semi-quantitative evaluation of clay mineral proportions was accomplished by comparing the four diffractograms obtained by the different treatments. No definite percentages

were calculated mainly because of the diversity of results obtained from different techniques (Pierce and Siegal, 1969). A priority system devised by Lavkulich (1968) was employed instead (Table VII). Silts were simply examined qualitatively for their mineralogic content.

3. RESULTS

Examination of cliff material in Figure 6 indicates that glaciofluvial outwash contains small, roughly equal amounts of clay and silt. Grey clay on the other hand is more variable in texture, being silty in samples C-2 and C-3, and clay-rich in sample C-1. This is probably a result of contamination of the former two samples by glaciofluvial outwash, since this material overlies the grey clay in these areas. Compositionally, the outwash is also more consistent than the grey clay (Table VII). Its clay fraction is typically chlorite-rich (Figure 7), with a fair amount of illite and kaolinite; the silt fraction (not shown) consists mainly of mica and amphibole, with lesser quantities of magnetite, epidote, diopside and chlorite. Clay in the grey clay is also predominantly chlorite in samples C-1 and C-3, but sample C-2 contains relatively more montmorillonoid; the silt fraction contains mica and a little magnetite. As a group, the grey clay and glaciofluvial outwash are both fairly rich in mixed-layer material, and contain no vermiculite at all; offshore samples however, show exactly the opposite relationship.

Brown clay contains more silt than the grey clay adjacent to it (Figure 6). Furthermore, its clay fraction has no montmorillonoid (Table VII), the major component of grey clay sample C-2 adjacent to it (Figure 7). As indicated in the point-count analysis, its composition corresponds more closely to the outwash, than it does to its parent material.

The boulder, although sandy in texture, possesses relatively more clay than silt (Figure 6). As was found for the very fine sand, clay and particularly silt fractions contain abundant mica.

The offshore samples all contain about twice as much silt as clay (Figure 6). However, a distinct textural trend in relation to their geographic locations is evident. Both clay and silt proportions decrease progressively from sample OS-14 out into the trough. This sample came from a broad "sill" area at 50 fathoms, and west from here, the trough axis deepens gradually to 60 fathoms at sample location OS-16 (Map 2). The clay mineralogy of these samples exhibit the same trend, OS-14 being chlorite-rich and montmorillonoid-poor, and samples west from here becoming progressively more montmorillonoid-rich and chlorite-poor (Figure 7). Other clay components are less significant, but still show the same trend (Table VII). The silts all contain garnet, epidote and calcite, and in addition, the more landward ones have diopside and the seaward ones have mica.

Clays reported above, and in Table VII, are the coarse fractions. Fine clays ($<0.2\mu$) generally showed some increase in the proportion of montmorillonoid over chlorite, except for the glaciofluvial outwash, which was analysed for total clay. Magnetite in the very fine sand characterized the different environments very well; glaciofluvial outwash is relatively rich in magnetite, grey clay is intermediate, and the offshore environment is poor in magnetite. Extractable iron and total carbon show less differentiation, but in a general way, cliff material contains more of the former, and offshore material contains more of the latter.

Finally, quartz and felspar constitute the bulk of silt-sized material, they are always present in coarse clays, and invariably occur in fine clays. This indicates that glacial rock flower has contributed significantly to the composition of these size fractions.

4. DISCUSSION

Considering the distribution of clay and silt in the offshore trough, and also the mineralogic similarity between sample OS-14 and the cliff glaciofluvial outwash, leads to the suggestion that the broad "sill" area in the trough represents the locus of maximum fine sediment deposition at the present time. Clay and silt material eroded from the cliff is initially transported southeastwards by the nearshore surface current, and presumably, it settles from suspension in the vicinity of

the sill. A near-bottom current has been found by Gross et al (1969), to move slowly westwards along the trough towards its head, which would account for the decrease in clay and silt in this direction. It also explains the increase of the montmorillonoid/ chlorite ratio in a westerly direction, since montmorillonoid particles are smaller in size to chlorite and remain in suspension longer (Lavkulich, 1968, personal communication).

Other factors supporting the proposition that the sill area represents the locus of maximum present-day sedimentation are:

- Of all the offshore samples, OS-14 is unique in that it contains some mixed-layer clay - a characteristic component of the cliff material (Table VII).
- Samples OS-14 and OS-13 have the most total carbon of offshore trough samples, suggesting introduction of carbonate from sample OS-9 (Map 2), which contained 50% shell-hash in its composition.

Although kaolinite has been found in ancient marine sediments (Grim, 1958), it is chemically unstable in seawater due to the alkalinity (pH = 7.5 - 8.4) and high cation concentration (Grim, 1968. Diagenetic alteration of this clay mineral may account for its apparent decrease in the offshore samples, and the corresponding increase of vermiculite and montmorillonoids (Table VII). Other contributing sources of

montmorillonoid to the offshore environment are the grey clay in the cliff, and possibly the basaltic lava flow between the southeast corner of Wreck Bay, and Pocket Beach.

Brown clay in the cliff is believed to originate as a result of numerous hair-line synerisis cracks in the grey clay, which would be formed by alternate expansion and collapse of its montmorillonoid clay component. Meteoric water, occasionally permeating through the overlying outwash gravels would produce these cracks, and also account for the high free iron-oxide content of the brown clay (15.6 ppm). Alteration has apparently proceded intermittently as shown by dark concentric rings of abundant free iron-oxide (Plate 8b). A number of large cracks extending sub-parallel to the contact, have locally resulted in brown clay lying stratigraphically below sections of unaltered grey clay (Plate 8a).

Clay contained in the boulder is very poorly crystallized as shown by low, broad diffractogram peaks, however, its cohesive property was almost certainly responsible for binding the unit together when it originally became incorporated into the glaciofluvial outwash. Subsequently, alteration of magnetite to free iron-oxide has resulted in its weakly cemented state.

D. GENERAL STRATIGRAPHY OF THE "PARENT" CLIFF MATERIAL

Grey clay in the cliff has been tentatively classified as glaciolacustrine in origin (Map 1), due to the

presence of ice-rafted pebbles in its composition, and also because of the limited areal extent of its exposure. Its low total carbon content, and apparent absence of sulphides, indicates low organic productivity in an oxygenated environment. Griggs and Kulm (1969) have described a pebbly clay dated at 37,000 years B.P., on the shelf off the Washington coast, and Anderson (1968) has reported on a "diamicton"* pebbly clay from the Strait of Juan de Fuca of 17,000 - 21,000 years B.P. Correlation of the grey clay with either of these units is impossible until its age is determined by C^{14} dating. Patchy occurrences of similar material have been found on the continental shelf off Vancouver Island and in Barkley Sound (Barr, Carter, 1970, personal communication). B.E.B. Cameron of the Geological Survey of Canada found that foraminifera contained in a single sample from Barkley Sound (Carter, 1970), were marine species; however, the "diamicton" pebbly clay contained foraminifera ranging from estuarine species at the base, to marine species near the top (Anderson, 1968). The grey clay therefore has a limited distribution over apparently wide areas, which suggests that it was deposited in isolated depressions where currents were weak or absent.

The glaciofluvial outwash was probably deposited during final retreat of the Vashon ice-sheet, 12,500 - 14,000 years B.P. Cross-bedding in the cliff (Plate 9a) indicates that the material was transported from the mountainous hinter-

* See GLOSSARY

land northeast of Wreck Bay, a contention supported by textural variation at different locations. Near the north end of Long Beach it is exposed in a road quarry as fine sand, at Wreck Bay it consists of approximately 50% gravel, and at the north end of Kennedy Lake it consists of sub-angular boulders and cobbles with relatively little matrix. The mode of deposition of this material was probably quite complex, as exhibited by an exposure in a quarry just nort of Ucluelet. Here, cross-bedded glaciofluvial outwash is overlain in part by a wedge-shaped sandy deposit of probable marine origin, and this in turn is covered by a 3 foot layer of till (Plate 9b).

Griggs and Kulm (1969) have indicated the maximum extent of late Pleistocene glaciers as being at the edge of the continental shelf off Vancouver Island. Retreat of these glaciers in Holocene times, accompanied by sealevel transgression across the continental shelf, has resulted in the present distribution of recent sediments along the inner shelf, and relict sediments on banks along the outer shelf. As shown in the present study, the character of recent sediments is well explained by the composition of the cliff material, and by the oceanic currents existent at the present time.

Environment		Sample Number	% by weight (62.5 - 125μ) size fraction in sample	MAGNETITE in (62.5 - 125μ) size fraction	EXTRACTABLE IRON (p.p.m.)	TOTAL CARBON %	Coarse Clay (0.2 - 2.0μ) ILLITE	MONTMORILLONOID	VERMICULITE	CHLORITE	KAOLINITE	MONTMORILLONOID/CHLORIDE
CLIFF	GREY CLAY	C-1	10.70	.84	5.2	.6	*	*	Pr	****	Pr	*
		C-2	18.10	.66	4.0	.2	*	***	Pr	**	Pr	**
		C-3	9.30	.75	4.4	.6	*	*	Pr	***	*	**
	GLACIOFLUVIAL OUTWASH	C-2	5.60	.16	10.4	.5	*	Pr	Pr	***	**	**
		C-3	2.40	1.03	6.1	.1	**	Pr	Pr	***	*	**
		C-4	1.90	2.34	3.6	-	**	Pr	Pr	***	**	*
		C-5	2.65	3.58	4.2	-	**	Pr	Pr	***	**	*
		C-6	3.75	5.47	2.7	.1	**	Pr	Pr	***	**	*
		C-7	3.00	3.18	3.8	1.6	**	*	Pr	***	**	Pr
	BROWN CLAY	C-2	13.40	.89	15.6	.1	**	Pr	Pr	***	*	**
	BOULDER		16.85	-	9.4	.2	**	Pr	Pr	**	*	**
OFFSHORE	MUD	OS-11	66.00	.26	1.2	.4	*	***	*	**	*	Pr
		OS-12	51.40	.19	2.7	.8	*	***	*	**	*	Pr
		OS-13	46.00	.46	3.9	1.3	**	**	*	***	Pr	Pr
		OS-14	24.40	.55	4.8	1.9	**	Pr	**	***	Pr	*
		OS-16	15.10	1.61	2.7	.7	**	**	**	**	*	Pr
		OS-17	63.80	.27	2.5	.7	**	**	**	**	*	Pr
		OS-18	54.90	.36	2.7	.9	**	**	**	***	Pr	Pr

LEGEND (Lavkulitch, 1968):
Pr = 0 - 10% (present)
* = 11 - 20% (trace)
** = 21 - 40% (minor)
*** = 41 - 60% (major)
**** = 61 -100% (dominent)

Table VII. Coarse Clay Mineralogy and other Properties of the Cliff and Offshore Trough Environments.

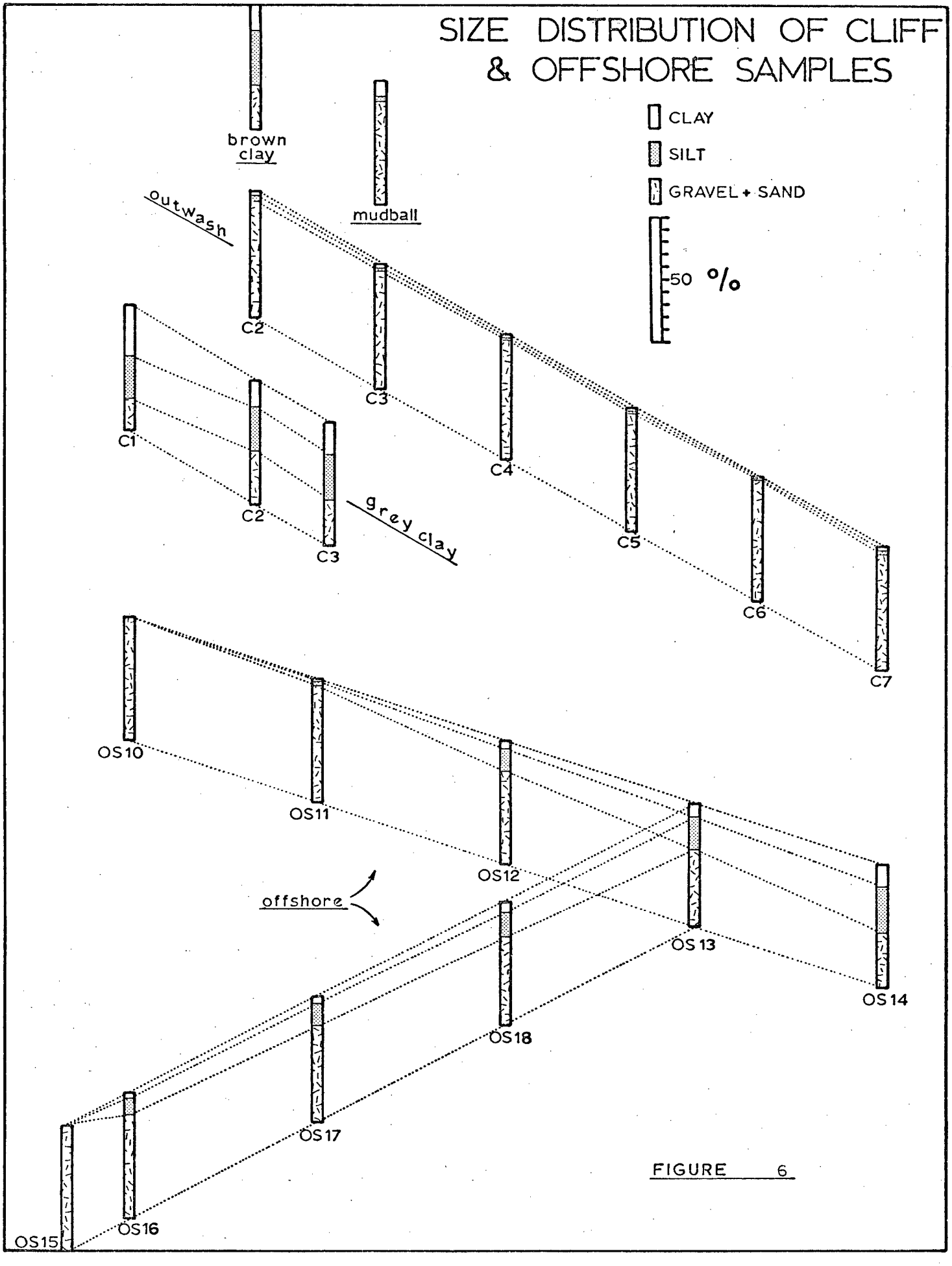
SIZE DISTRIBUTION OF CLIFF & OFFSHORE SAMPLES
CLAY
SILT
GRAVEL + SAND
50 %
brown clay
mudball
outwash
grey clay
C1
C2
C3
C4
C5
C6
C7
OS10
OS11
OS12
OS13
OS14
OS15
OS16
OS17
OS18
offshore

FIGURE 6

FIGURE 7

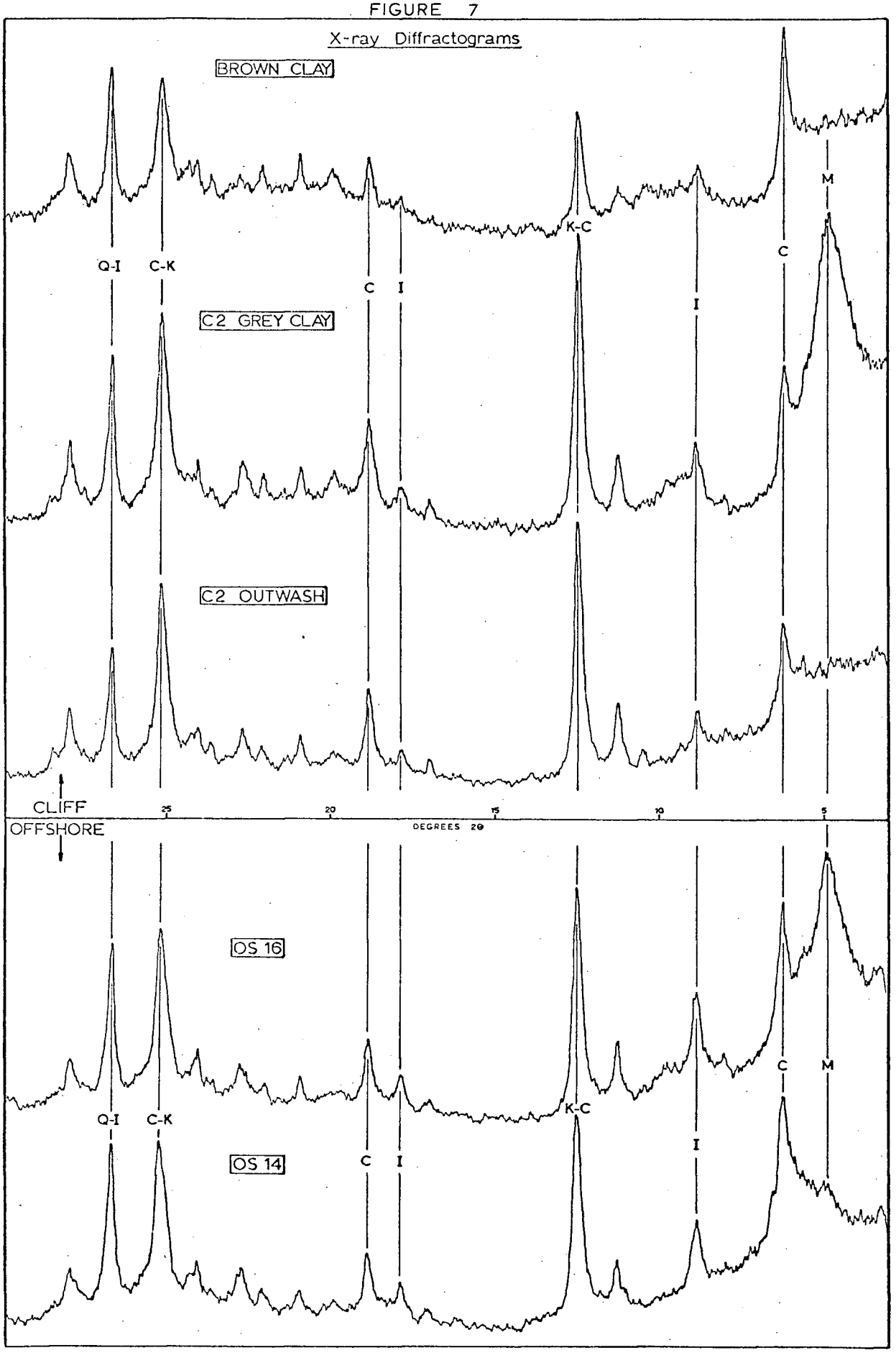

X-ray diffractograms of Mg-glycerated coarse clay (0.2 -2.0μ). M = montmorillonoid, C = chlorite, I = illite, K-C = kaolinite, chlorite, and Q-I = quartz, illite.

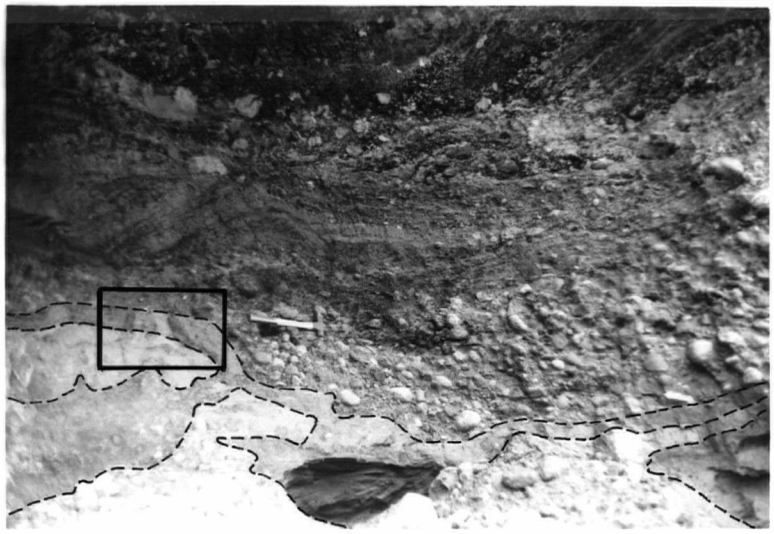

Plate 8a. Contact between grey clay and overlying glaciofluvial outwash. Brown clay occurs between these horizons, and also along cracks extending into the grey clay. Note gravel filled scour channel in the clay, and truncated cross-bedding in the glaciofluvial outwash.

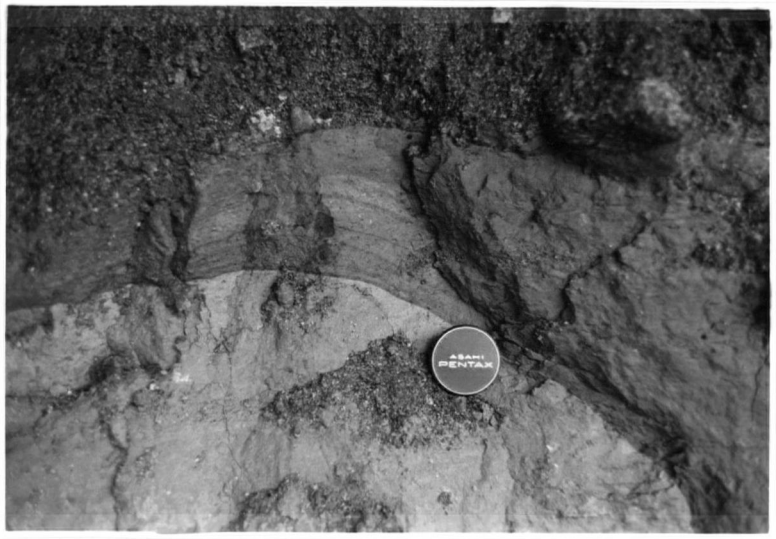

Plate 8b. Close-up view of the contact area marked by inset on Plate 8a. Concentric alteration rings can be seen in the brown clay.

Plate 9a. Poorly defined cross-bedding in glaciofluvial outwash.
Cliff view behind Profile D.

Plate 9b. Glaciofluvial outwash, partially overlain by a wedge of beach ? sand, and covered by 3 feet of till.
Exposure in road-quarry just northof Ucluelet.

VI. SEDIMENT SIZE ANALYSES

A. INTRODUCTION

Glaciofluvial outwash and grey clay in the cliff has been shown mineralogically, to have provided the material for all other sedimentary environments in the area (see heading POINT COUNT ANALYSIS). A detailed examination of the clay and silt components in the offshore trough, led to an understanding of their distribution in terms of known oceanic currents (see heading on X-RAY DIFFRACTION ANALYSIS).

The first part of the present investigation was undertaken to determine the regional pattern of recent sediment dispersal exclusive of the clay/silt environment of the offshore trough, and grey clay in the cliff. This was accomplished by characterizing the textural properties of ten related sedimentary environments in the area by means of frequency distribution curves, and two-dimensional parameter plots.

The second part of the investigation was conducted entirely on the beach environment, the principal study area of the thesis. The purpose of this work was to determine seasonal differences in the texture of surficial sediments on the beach. This was accomplished using two sets of samples (see APPENDIX):

- Large samples (also used in the regional study) were compared using their statistical parameters
- Small samples were compared using histograms.

B. METHODS

1. SAMPLE COLLECTION

A total of 123 large samples were considered in this study. In addition to these, 91 small samples were collected from the profile rod stations on the beach (See APPENDIX).

2. LABORATORY PROCEDURE

After collection the samples were laid out on clean paper to dry, so as to avoid the formation of saline crusts on top of the sample boxes.

Each sample was initially passed through a Tyler No.10 sieve (2 mm) to separate the gravel. This gravel fraction was then sieved through as many as eleven screens, the largest having a $2\frac{1}{2}$ inch mesh. The sand fraction was reduced to 100 gms on a multi-riffle splitter, and then sieved for 10 minutes on a Tyler Ro-Tap shaker. A sieve interval of quarter phi was used, with sieves ranging from 1.68 mm (-0.75 Ø) to 0.0625 mm (4.0 Ø).

Only one cliff sample had silt and clay size material in excess of 1% of the total sample weight. Consequently, analysis of this material was not undertaken, and the smaller than 4.0 Ø fraction was treated as 6.0 Ø (Friedman, 1967).

Weighings to the nearest 0.01 gm were done on a Mettler Balance.

3. STATISTICAL PARAMETERS AND COMPUTER PROGRAM

A program written by A.J. Sinclair and J. Wilson was

used on an IBM computer, to calculate the sediment parameters, both graphically (Folk, 1968) and by the method of moments (Pierce and Good, 1966). Some of the formulae defined by Pierce and Good (1966) differ from those of Friedman (1961, 1967), and are:

Mean $$\bar{x} = \frac{1}{n} \sum_{i=1}^{k} f(x_i)x_i \quad \ldots\ldots\ldots\ldots\ldots\ldots (1)$$

where n = total weight of sample

$f(x_i)$ = weight of single size class

x_i = midpoint of same size class in Ø units

k = total number of size classes

Standard Deviation $$s = \left[\frac{1}{n} \sum_{i=1}^{k} f(x_i)(x_i - \bar{x})^2\right]^{\frac{1}{2}} \ldots\ldots (2)$$

Skewness $$S_k = \frac{1}{2n} \sum_{i=1}^{k} \frac{f(x_i)(x_i - \bar{x})^3}{ns^4} \quad \ldots\ldots (3)$$

Kurtosis $$K_u = \frac{1}{2} \left[\sum_{i=1}^{k} \frac{f(x_i)(x_i - \bar{x})^4}{ns^4} - 3\right] \ldots (4)$$

In addition to these parameters, Trask's Sorting Coefficient and percentiles neccessary for determining the graphic measures (Folk, 1968) were also included in the computer print-out. Frequencey distribution curves for each sample, and two-dimensional plots between various statistical parameters were produced by a Calcomp plotter connected to the computer.

C. REGIONAL SEDIMENTARY PATTERN

1. DERIVATION OF TYPE FREQUENCY CURVES

The ten environments considered in this study are

are listed in Table VIII. A number of samples from these environments were rejected (Table VIII) since they contained an excess of 5% of the total sample weight in the first sieve fraction (coarse gravel), and the frequency curves were thus open ended. Two samples from the Long Beach environment were also rejected as one came crom a coastal dune (LB-2), and the other from the mouth of Sand Hill Creek (LB-3) (Map 2).

The statistical parameters and percentage of size fractions listed in Table VIII are the arithmetic averages for each environment. As an indication of the dispersion of sample means about the average mean, the variances of each environment were determined, and are shown at the bottom of Table VIII. It is apparent that beach (berm, MHT, MWL), bay, offshore and Long Beach environments are well represented by the average means, whereas gravel-containing environments are much more variable in mean size.

Frequency curves illustrated in Figure 8 were obtained from the Calcomp plots of individual samples. This was done by comparing the average statistical parameters of an environment (Table VIII) with the statistical parameters of individual samples within that environment. The frequency curve of the best-fitting sample was then used to represent the environment. Emphasis in sample selection was based on the moment measures of mean and standard deviation, and the size-fraction percentages.

2. MODAL ANALYSIS

Curray (1960) first developed this technique for tracing the geographic distribution of sediment masses in the highly mixed recent sediments of the Gulf of Mexico. Essentially his thesis was that individual normal components in polymodal non-normal sediments, tended to retain their own characteristics (statistical parameters). The present study differs from Curray's (1960) in that type frequency curves of ten known environments were compared for related modes, instead of individual sample frequency curves representing unknown environments. Assuming these type curves (Figure 8) to be truly representative of the ten environments, a number of deductions on the regional sedimentary pattern can be made by modal comparisons.

The type frequency curve representing glaciofluvial outwash from the cliff is characterized by five poorly defined modes, the principal one being very coarse sand (0 to -1.0 Ø). Examination of individual sample frequency curves shows that the principal mode becomes progressively finer southeastwards from the type sample location C-2 (Map 1),and at C-7 it occurs at 1.0 Ø (coarse - medium sand). This is thought to reflect sampling from consecutively higher stratigraphic horizons within the Wreck Bay Formation, and not an indication of the paleo-transport direction (See APPENDIX). Not all samples are characterized by the same five modes, however, the size

range of sediment from all the samples is consistent.

The Lost Shoe Creek environment is characterized by three poorly defined modes, the principal one in the medium sand range (1.0 to 2.0 Ø), and all of them being correlatable with the coarser cliff modes. The thirteen samples from this environment all possessed the same principal mode, but only half of them had the gravel mode (-2.0 to -3.0 Ø). The relative fineness of the principal mode, indicates a present-day fluvial transport medium of less competency than that which transported the glaciofluvial outwash. The sparsity of fine sand observed in the creek bed and reflected in the type frequency curve (Figure 8), together with the fact that the creek water during the summer appeared to be free of suspended material, indicates that maximum competency experienced during the spring thaw is capable of transporting all material finer than 2 Ø out of the environment.

The beach (berm) has a principal mode in the medium sand range (1.0 to 2.0 Ø) identical to that of Lost Shoe Creek, and a minor one close to 2.0 Ø. The absence of modes coarser than medium sand indicates that this material is unstable in the environment. The following model is proposed: The beach consists of alternating layers of gravel and sand (Plate 23b), suggesting that violent winter storm waves remove all sedimentary material except coarse gravel from the beach, which then becomes concentrated as a lag deposit. The backwash

from less violent spring storm waves is capable of removing fine sand and material finer than this from the backshore, and so a berm of medium sand becomes established above the coarse gravel. As wave size decreases even further during the summer, another berm is built, this time of fine sand, along the upper foreshore. So in effect, the coarse and heavy material is worked downward through the beach section by alternating seasonal wave conditions. The suggestion of a mode near 2 Ø almost certainly indicates rapid transfer of this material from the cliff to the foreshore.

From beach (MHT) out to the offshore environment sediments are all very similar, and correspond to the minor modes between 1.0 and 2.0 Ø already mentioned in the beach (berm) and cliff environments. They do tend to become slightly finer and more leptokurtic further from shore, thus supporting the "classical" concept of a size-graded nearshore modern sediment pattern of Johnson (1919). These unimodal, very well sorted sands extend over an extremely wide area and considering the insignificance of this mode in the type frequency curve of the cliff (and other cliff sample frequency curves), it must exist as a very thin prism on top of the coarser sediments. This contention is indirectly supported by the "outcrop" of boulder beds in areas affected by wave induced currents (see heading WRECK BAY BATHYMETRY). The small range of standard deviations of these environments (Table VIII) indicates that

extremely uniform kinetic energy conditions prevail in these hydrodynamic regions. An interesting point concerning the offshore environment is a small mode of very fine sand (3.0 to 4.0 Ø). This size fraction contains most of the heavy minerals. The type frequency curve was obtained from sample OS-1 (Figure 8), and this same minor mode exists in samples OS-2 to OS-8 (Map 2). Sample OS-4 was examined mineralogically (see heading POINT-COUNT ANALYSIS), and was found to contain an exceptionally high heavy mineral content, suggesting the presence of a relict beach placer at this bathymetric level - approximately 20 fathoms (see chapter on ECONOMIC GEOLOGY).

The Long Beach environment is typified by a frequency curve almost identical to the offshore environment. The curve, derived from sample LB-5, also reflects a small mode between 3.0 and 4.0 Ø, but this is unique to sample LB-5. Sample LB-4 contained a high proportion of non-magnetic opaque minerals, but relatively little magnetite (see heading POINT-COUNT ANALYSIS), thus suggesting that no compositional relationship between the two environments exists.

Quisitis Point has a principal mode in the coarse to very coarse sand range (~0 Ø), which has no correspondence to other environments, and therefore probably represents material derived locally from wave destruction of the headland. A very minor mode of fine sand (2.0 to 3.0 Ø) corresponds to the Long Beach principal mode because of close proximity of the

type sample location (QP-7) to this environment (Figure 8). Only samples QP-1 and QP-2 possess principal modes correlatable with the Wreck Bay beach (berm) and beach (MHT, MWL) environments.

Wya Point is characterized by a principal mode of medium sand (1.0 to 2.0 Ø) which corresponds to the beach (berm) environment. Of the eleven samples collected from this headland, only three did not possess modes typified by the Wreck Bay sediments. These were WP-2 and WP-3, which came from small pocket beaches at the head of narrow gorges, and WP-6, derived from a sand-filled rock depression on top of the headland. This supports earlier indications that a southeast moving nearshore current exists along this part of the coast (see chapter on SEA CONDITIONS, and heading on POINT-COUNT ANALYSIS). A minor mode of very coarse sand (0 to -1.0 Ø) probably reflects local destruction of the headland by high-energy waves.

		Normal to coast							Parallel to coast		
		LOST SHOE CREEK (LSC)	CLIFF GLACIOFLUVIAL OUTWASH (C)	BEACH BERM	BEACH MHT	BEACH MWL	BAY (B)	OFFSHORE (OS)	LONG BEACH (LB)	QUISITIS POINT (QP)	WYA POINT (WP)
MOMENTS	MEAN $\bar{X}$	.40	-1.10	1.36	2.45	2.60	2.71	2.84	2.72	.06	1.18
	STD.DEV. s	1.30	1.96	.71	.69	.56	.44	.34	.25	1.21	.67
	SKEWNESS S_k	-.21	0.7	-.54	-2.21	-2.46	-2.38	-1.37	-1.11	.26	-.69
	KURTOSIS K_u	.94	-.06	2.89	21.69	20.83	23.98	22.19	10.24	1.11	2.96
GRAPHIC	MEAN M_z	.47	-1.12	1.39	2.51	2.69	2.75	2.85	2.73	.01	1.20
	STD.DEV. σ_I	1.24	1.95	.65	.50	.30	.29	.27	.22	1.16	.62
	SKEWNESS Sk_I	-.13	-.02	-.09	-.19	-.19	-.19	.01	-.14	.06	.18
	KURTOSIS K_G	1.08	.90	1.11	1.26	1.55	1.63	1.51	1.03	1.17	1.17
TRASK SORTING COEFF. (mm)	So	2.18	2.70	1.34	1.13	1.12	1.13	1.10	1.11	1.99	1.39
MODE (Ø)	Mo	.05	-2.42	1.52	2.78	2.80	2.97	3.00	2.92	-.14	1.23
MEDIAN (Ø)	$Md_Ø$	.64	-1.82	1.42	2.67	2.70	2.78	2.85	2.75	.25	1.25
%	gravel	18.08	51.31	.81	3.33	.65	.61	.11	-	23.98	8.31
	Sand	81.81	48.13	99.19	96.67	99.35	99.36	99.82	99.98	76.00	91.69
	Silt & Clay	.11	.56	-	-	-	.03	.07	.02	.02	-
Number of samples collected		13	6	14	14	14	25	13	5	8	11
Samples not included in averages		LSC-3	C-4 C-7	NWR-2 SER-5 SER-7			B-1 B-3 B-8 B-18 B-23	OS-7 OS-9 OS-10 OS-15 OS-19 OS-20	LB-2 LB-3	QP-3	
Variance of means ($x_Ø$)		.81	.42	.21	.33	.01	.01	0	0	.42	.48

Table VIII. Average Statistical Parameters of Type Sediment from Ten Related Environments.

FIGURE 8

FREQUENCY CURVES OF TYPE SEDIMENTS FROM TEN RELATED ENVIRONMENTS

COLUMN 1 — NE/SW — normal to coast

COLUMN 2 — NW/SE — parallel to coast

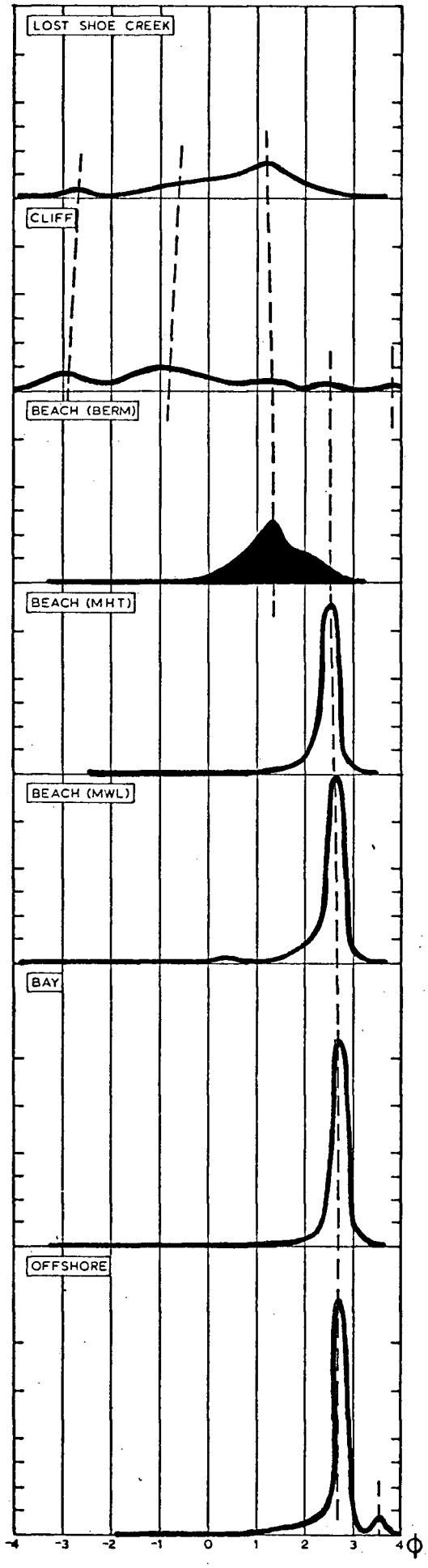

COLUMN 1

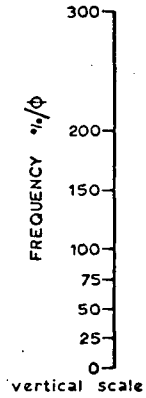

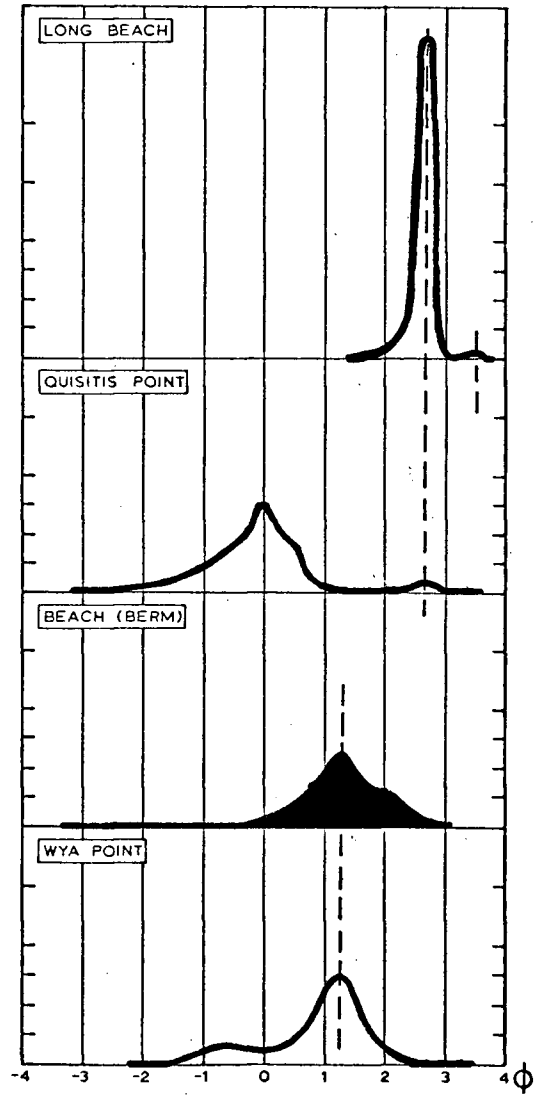

COLUMN 2

3. TWO-DIMENSIONAL PARAMETER PLOTS

(a) Moment Measures vs. Graphical Methods

For many years geologists have attempted to distinguish between different sedimentary environments by means of bivariate plots. With the recent increased availability of computers, many workers (Koldijk, 1967; Chappell, 1967; Friedman, 1961, 1967; Greenwood, 1969) have expressed a preference for moment measures over graphical procedures for determing the grain-size parameters. Moment measures require lengthy calculations, but consider the entire frequency distribution; graphical methods involve less tedium, but consider only a few specific points on the cumulative curve. Folk (1966) has highlighted some of the disadvantages of moment measures, but admits that it is "the most elegant mathematical method for obtaining parameters".

Referring to Table VIII, mean and standard deviation values obtained by both procedures are quite similar. Skewness and especially kurtosis values though, differ widely. It is generally agreed (Friedman, 1961, 1967; Folk, 1968) that beach sands are negatively skewed because fine material is winnowed from their distributions by the swash and backwash. This characteristic is illustrated by the moment skewness values for beach (MHT, MWL), bay, offshore and Long Beach environments. In contrast, the graphic procedure indicates almost equivalent negative skewness for Lost Shoe Creek and

Long Beach environments. For kurtosis, the graphic method appears to be even more erroneous, since the Lost Shoe Creek environment is indicated as being more leptokurtic than Long Beach.

On the strength of these arguments, all two-dimensional plots were constructed from statistical parameters determined by the method of moments.

(b) Environment Discrimination by Two-dimensional Plots

All the environments considered in this study involve sediment deposited by water, and furthermore, the size-range of sediment in some of these environments is very large. Geologists concerned with this type of analysis have usually compared material from different depositional environments e.g. wind blown dunes, river deposited sands, etc., and the material used generally falls within a very narrow size-range e.g. fine sand or medium sand, etc. This partially accounts for the great variability of environmental dividing lines obtained by different workers, for plots of the same parameters. There is without doubt a certain amount of intentional bias on the part of some workers though, as many of the dividing lines are drawn irregularly to include or exclude samples from a particular environment at will. For example, a commonly used plot is mean vs. standard deviation. Figure 9 is a plot of these parameters, and the tight cluster of points shown in the blown-up inset represents beach (MHT, MWL), bay,offshore and Long Beach

environments. This area corresponds to a dune environment of Friedman (1961), coastal dune or river environments of Moiola and Weiser (1968), barrier dune environment of Hails and Hoyt (1969), and to only one beach environment, that of Friedman (1967). This means that water-laid deposits cannot simply be differentiated universally from other environments by a mean vs. standard deviation plot, because of the great range of sediment sizes possible at different locations.

Four of the most common two-dimensional plots have been constructed to portray the range of individual sample parameters, and to assess their merit in defining the ten environments selected for study at Wreck Bay (Figures 9, 10, 11, 12).

(i) Mean vs. standard deviation

This plot (Figure 9) is superior to the others. The tight cluster of points representing beach (MHT, MWL), bay, offshore and Long Beach environments are all unimodal leptokurtic sediments (Figure 8), yet examination of the blown-up inset (Figure 9) reveals that environment discrimination, although vague, is still possible. Glaciofluvial outwash points fall within a relatively small area at the opposite corner of the diagram. In between these two areas, the transitional environments of Lost Shoe Creek and beach (berm) occur. The former samples are spread over the entire range of parameter values (see high variance of means - Table VIII),

whereas the latter almost all fall in the moderately well sorted, medium sand bracket. In close association with these beach (berm) points are those of Wya Point, thus indirectly confirming the existence of a southeast moving nearshore current. Quisitis Point on the other hand, showed a wide range of parameter values.

It is apparent that environment discrimination is largely determined by the mean grain size, and that a weak correlation exists between the two parameters viz. an increase in grain size generally reflects a decrease in sorting. A straight dividing line drawn along mean 2.0 Ø would successfully isolate the unimodal leptokurtic sediments from the others, but this line would fall more or less at right angles to those found by other workers. The reason for this is undoubtedly due to the much wider sediment range used here by comparison to the sediment used by other workers.

(ii) Mean vs. Skewness

Skewness has been found by most geologists (Friedman, 1961; Hails, 1967; Koldijk, 1968, Greenwood, 1969) to be the most sensitive environmental indicator. The sign of skewness depends wholly on the tails of a frequency distribution curve, and hence beach sediments are negatively skewed (lack of fine tail); inland wind-borne sands are positively skewed (lack of coarse tail); and river sediments have close to zero skewness (presence of coarse and fine tails). Moiola

and Weiser (1968) have,however, found that coastal wind-borne dunes possess negative skewness approximately 50% of the time due to fine material removal in suspension, and migration of the balance by saltation. Sample LB-2, the only one from a coastal dune, does in fact possess negative skewness (Figure 10).

Skewness range of the unimodal leptokurtic sediments is much greater than their standard deviations, and hence these points fall over a wider area than in Figure 9. It is the mean, and not skewness,which again is most effective in discriminating between these water-deposited environments. A straight line drawn at mean 2.0 Ø would likewise separate the unimodal leptokurtic sediments from the others. A weak parameter correlation is also evident with this plot viz.an increase in grain size is usually accompanied by a more positive skewness.

(iii) Standard deviation vs. Skewness

Friedman (1961) obtained an environmental dividing line, which on the scaleof Figure 11 is almost straight, and extends approximately along the middle of the well sorted catagory. This line separated a beach environment (below) from a river environment (above), and in the case of Figure 11, would separate the unimodal leptokurtic sediments (below) from the others. Further distinction between the unimodal leptokurtic environments though, is not possible.

In this plot, standard deviation is more effective

than skewness in discriminating between the water-deposited environments. Correlation between the two parameters is apparently very weak.

(iv) Skewness vs. Kurtosis

This plot (Figure 12) is the least effective in discriminating between the environments. It will be noticed that a number of samples are indicated as having negative kurtosis, which in fact is physically impossible. This is due to the formula supplied by Pierce and Good (1966), in which they subtract 1.5 from the determined value. A fairly good correlation between the two parameters is evident though, viz. increased negative skewness is generally accompanied by increased kurtosis.

4. CONCLUSIONS

The method employed in modal analysis, although approximate, allowed environment characterization and judgment on the distribution of nearshore recent sediments. Bivariate analysis was only partially effective in environment discrimination, but did illustrate the range of sediment parameters contained by any one environment. The plot of mean vs. standard deviation was the most effective in distinguishing between the different water-deposited environments. Moment measures of skewness and kurtosis were the least effcient parameters. Since mean and standard deviation values found by moment and graphic procedures are in such close agreement, values derived by the latter method may have been employed with equal merit.

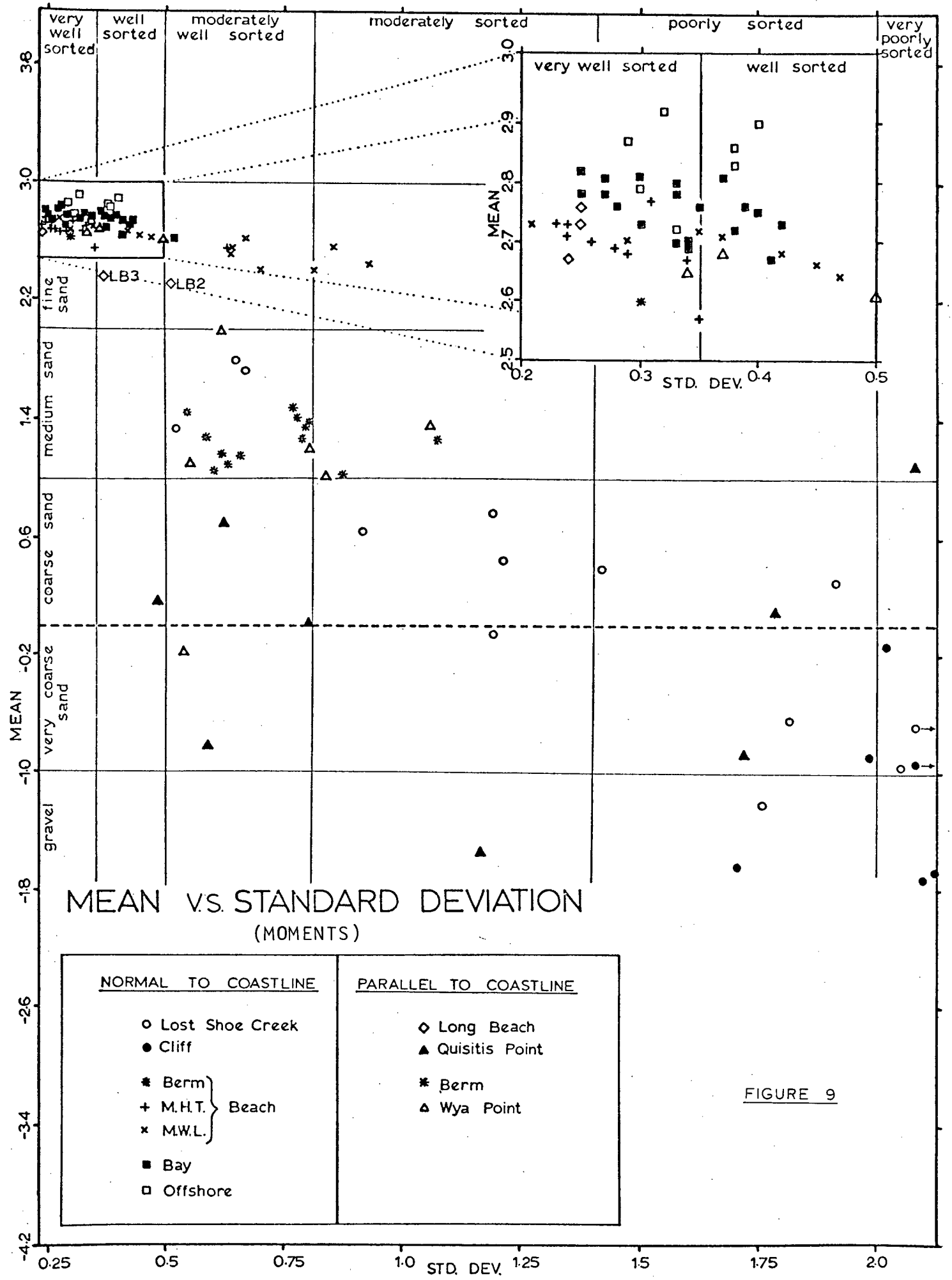
very well sorted
well sorted
moderately well sorted
moderately sorted
poorly sorted
very poorly sorted
very well sorted
well sorted
fine sand
medium sand
coarse sand
very coarse sand
gravel
LB3
LB2
MEAN
STD. DEV.
3.8
3.0
2.2
1.4
0.6
-0.2
-1.0
-1.8
-2.6
-3.4
-4.2
0.25
0.5
0.75
1.0
1.25
1.5
1.75
2.0
2.9
2.8
2.7
2.6
2.5
0.2
0.3
0.4
0.5
MEAN V.S. STANDARD DEVIATION
(MOMENTS)
NORMAL TO COASTLINE
Lost Shoe Creek
Cliff
Berm
M.H.T.
M.W.L.
Beach
Bay
Offshore
PARALLEL TO COASTLINE
Long Beach
Quisitis Point
Berm
Wya Point

FIGURE 9

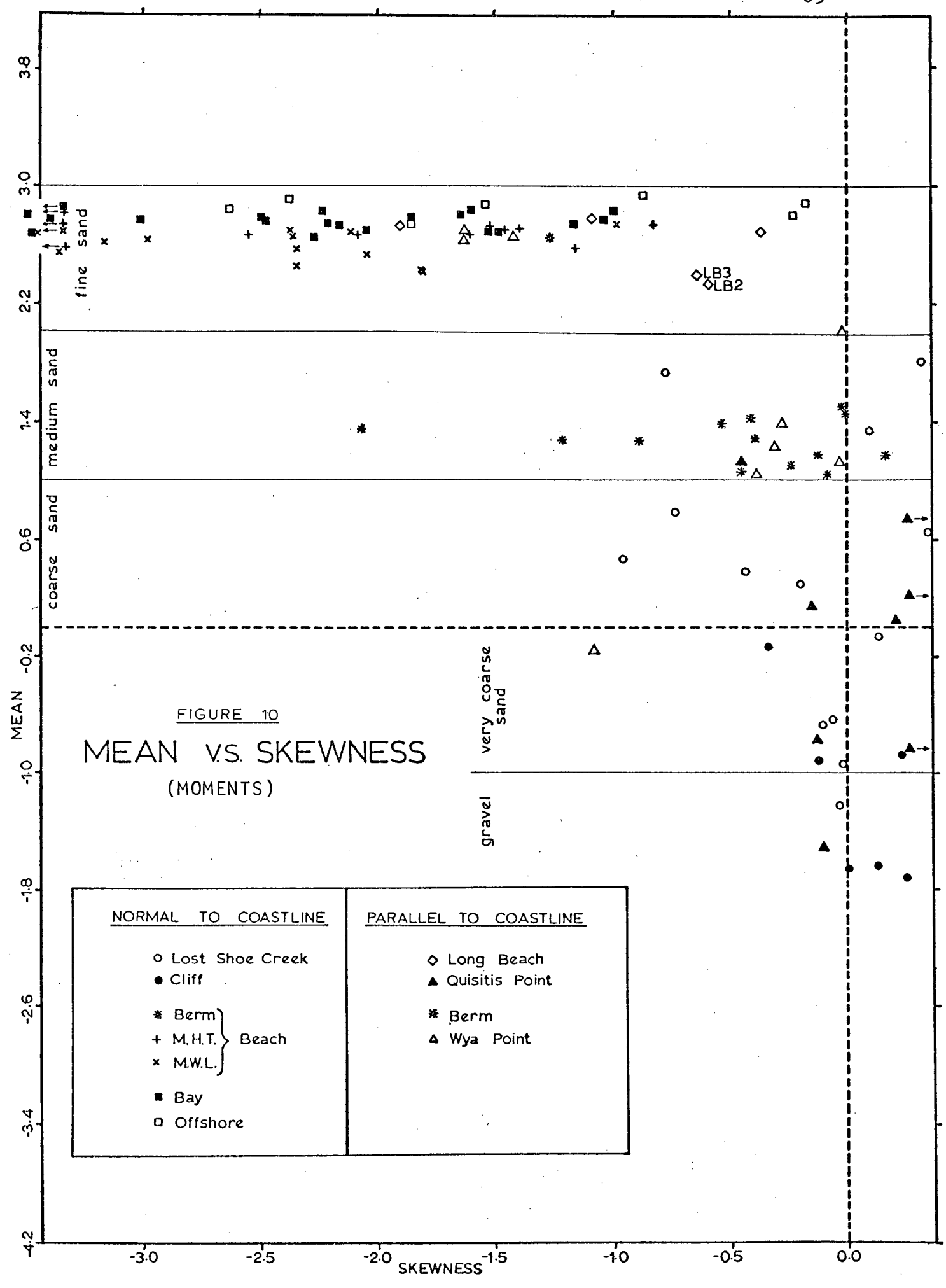

FIGURE 10

MEAN V.S. SKEWNESS

(MOMENTS)

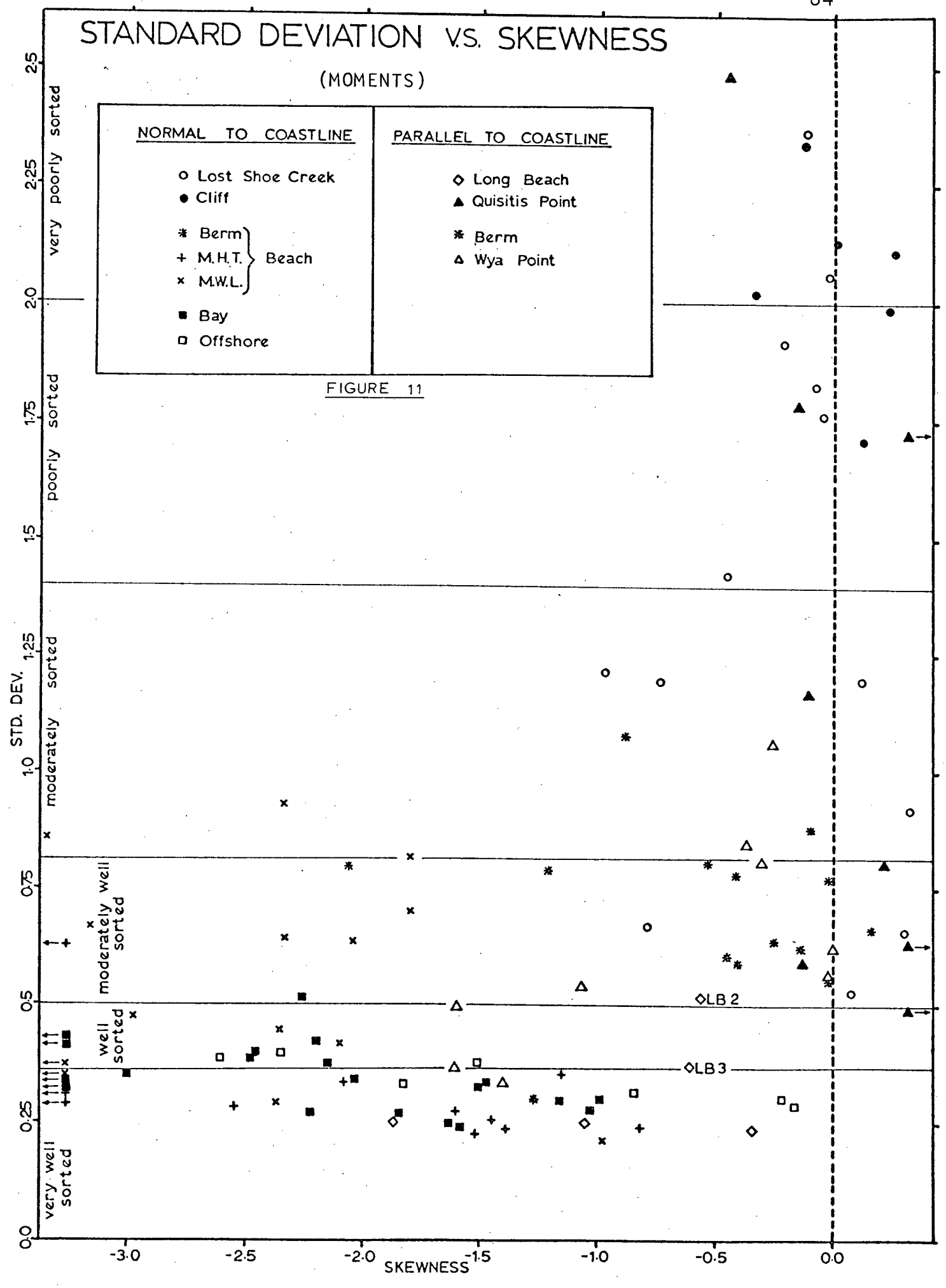
STANDARD DEVIATION V.S. SKEWNESS
(MOMENTS)
NORMAL TO COASTLINE
Lost Shoe Creek
Cliff
Berm
M.H.T.
M.W.L.
Beach
Bay
Offshore
PARALLEL TO COASTLINE
Long Beach
Quisitis Point
Berm
Wya Point
very poorly sorted
poorly sorted
moderately sorted
moderately well sorted
well sorted
very well sorted
LB 2
LB 3
STD. DEV.
SKEWNESS
2.5
2.25
2.0
1.75
1.5
1.25
1.0
0.75
0.5
0.25
0.0
-3.0
-2.5
-2.0
-1.5
-1.0
-0.5
0.0

FIGURE 11

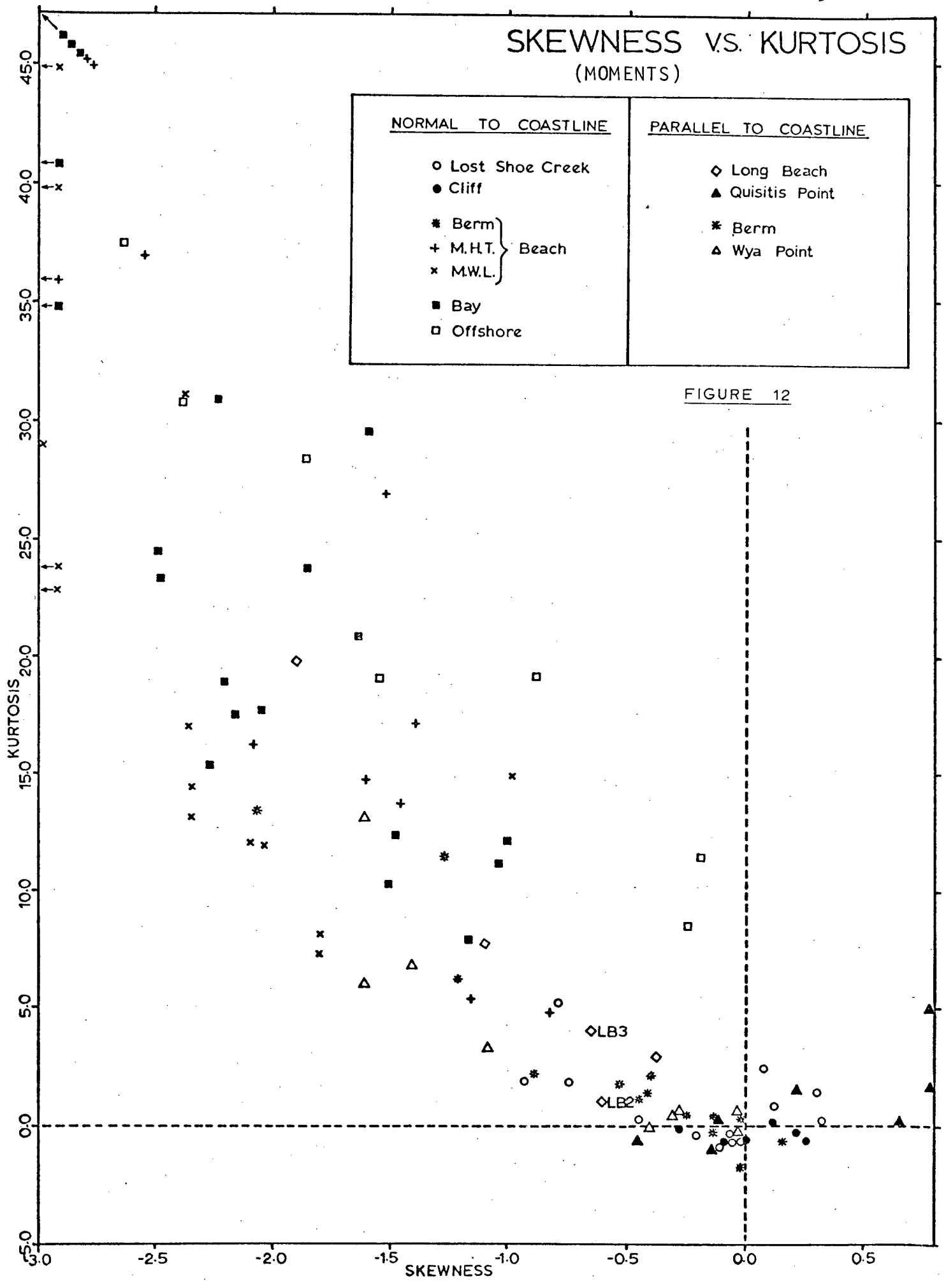
SKEWNESS V.S. KURTOSIS
(MOMENTS)
NORMAL TO COASTLINE
Lost Shoe Creek
Cliff
Berm
M.H.T.
M.W.L.
Beach
Bay
Offshore
PARALLEL TO COASTLINE
Long Beach
Quisitis Point
Berm
Wya Point
LB3
LB2
KURTOSIS
SKEWNESS
45.0
40.0
35.0
30.0
25.0
20.0
15.0
10.0
5.0
0.0
-5.0
-3.0
-2.5
-2.0
-1.5
-1.0
-0.5
0.0
0.5

FIGURE 12

D. BEACH SEDIMENTARY ENVIRONMENT

It should be stated at the onset that large samples NWR-5 (a, b, c) were probably contaminated by material foreign to the environment, due to dumping at this location by a local building contractor prior to sample collection.

1. SUMMER CHANGES

Consideration of the statistical parameters of large samples from the foreshore (Map 1, Figure 13), leads to the following observations:

- Spitbar samples SER-1(b + c) - SER-4(b +c) are slightly finer and better sorted than the samples immediately northwest of the mouth of Lost Shoe Creek, NWR-1(b + c) - (NWR-4(b + c). This suggests littoral drift towards the southeast in the vicinity of the spitbar - a direction opposite to that which would promote its "growth" (see chapter on PLANIMETRIC SHAPE). This deduction reflects the transient nature of drift directions along this part of the beach (see chapter on SAND MOVEMENT BASED ON WAVE PARAMETERS).
- Sample SER-6(b + c), located on Sand Point, is finer and better sorted than adjacent samples SER-5(b + c) and SER-7(b + c). This indicates deposition at Sand Point and erosion on either side of it (see chapter on SAND MOVEMENT BASED ON WAVE PARAMETERS).
- Sample SER-4(b + c), collected near Profile C, is more

negatively skewed and leptokurtic than any of the other foreshore samples. This means that winnowing of fine material by the swash-backwash is most efficient in this area.

Histogram plots of the small profile samples (Map I, Figures 14a, 16a, 18a, 20a, 22a, 24a, 26a) indicate the following:

- A little gravel persisted on the foreshore at a few locations even though it was then in a state of equilibrium.*
- The distribution of very fine sand (1/16 - 1/8 mm) across the profile lines is indicative of the hydrodynamic conditions at each location.

At Profiles D and E, granules and a few pebbles existed at the landward end of the two profiles, and very fine sand was concentrated at the seaward ends. This was due to high waves eroding the seaward edge of the winter berm, and transporting all but the coarsest material down the foreshores (see chapter on SAND MOVEMENT BASED ON WAVE PARAMETERS). At Profiles A and G, shell-hash existed near the middle of the profile lines, and so too did the highest concentration of very fine sand. The reason for this was because of abundant shelly material (see chapter on MARINE LIFE), and small waves affecting these areas (see chapter on SAND MOVEMENT BASED ON WAVE PARAMETERS). At Profiles B, C and F, no gravel was present, and very fine sand was spread erratically across the foreshore. This resulted from weak, variable littoral currents in these areas (see

*See GLOSSARY

chapter on SAND MOVEMENT BASED ON WAVE PARAMETERS).

2. WINTER CHANGES

Large samples collected from the backshore (which was established during the preceeding winter), indicate the following:

- Sample NWR-6a, located between Profiles A and B, was the only one with textural properties identical to the foreshore sediment deposited during the summer. This indicates persistence of a southeast moving littoral current in this region during the winter, and no addition of material from the cliff (see chapter on PLANIMETRIC SHAPE).
- Samples located along the crest of the spitbar, SER-1a - SER-4a, show no clear pattern with respect to the samples immediately northwest of the mouth of Lost Shoe Creek, NWR-1a - NWR-4a. This indicates a complex interplay of high energy waves with outflow from the river.
- Sample SER-6a, located on Sand Point, is coarser and slightly less well sorted than adjacent samples SER-5a and SER-7a, indicating more intense erosion at this location than on either side of it. It thus seems apparent that material deposited on Sand Point during the summer, is strongly eroded during the winter/spring storm period. This accounts for the bathymetric extension of Sand Point into the bay past Seal Rock (see heading on BAY BATHYMETRY).
- Sample SER-4a is also more negatively skewed and leptokurtic

than any of the other backshore samples, indicating that even during winter, the winnowing process of swash-backwash is most efficient at this location.

Small profile samples collected during the succeeding winter (Map I, Figures 14a, 16a, 18a, 22a, 24a, 26a) show the following changes: At Profiles D and E, the former consisted entirely of gravel at its landward end, and the latter possessed relatively less near the middle of the profile line, and medium sand at its landward end. This indicates that the height of waves affecting Profile E during the winter is less than at Profile D - a situation which also exists during the summer (see chapter on TRANSVERSE PROFILES). At Profiles A and G, no shell-hash was present, and the highest concentration of very fine sand occurred at the landward end of the profile lines. This means that waves affecting the two areas were only slightly higher than those measured during the summer (see chapter on SAND MOVEMENT BASED ON WAVE PARAMETERS). At Profiles B, C and F the coarsest material occurred at the landward end of the profile lines, and the very fine sand fractions increased in a seaward direction. This simply reflects beach degradation by large waves. Profile C was by far the coarsest of the three lines and comparable to Profile D in texture, thus indicating the severity of wave attack at this location (see chapter on TRANSVERSE PROFILES).

3. CONCLUSIONS

In summer, fine, light coloured sand characterizes the entire foreshore except for two small gravelly areas adjacent to Sand Point, and the two distal ends of the beach, the northwest and southeast corners, which contained some shell-hash.

In winter, the central portion of the beach is reduced to coarse gravel, almost all of the sand being transported out to the middle of the bay. At Profiles B and F, the beach becomes largely composed of medium-grained black sand,and the two distal ends remain essentially unaltered from the fine-grained, light-coloured, sandy conditions that prevail during the summer.

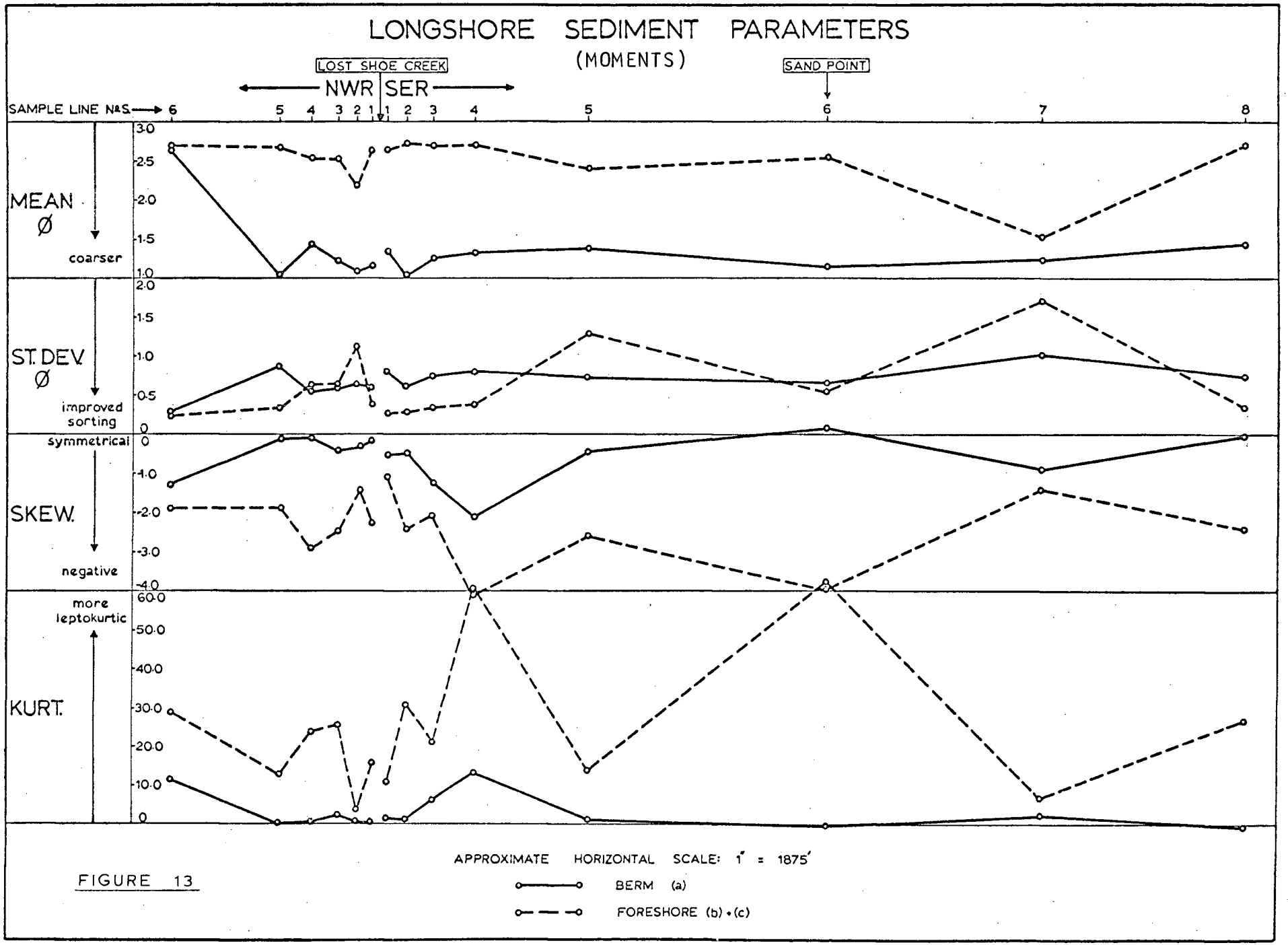
LONGSHORE SEDIMENT PARAMETERS
(MOMENTS)
LOST SHOE CREEK
SAND POINT
NWR
SER
SAMPLE LINE N&S
6 5 4 3 2 1 1 2 3 4 5 6 7 8
MEAN Ø
coarser
3.0 2.5 2.0 1.5 1.0
ST. DEV. Ø
improved sorting
2.0 1.5 1.0 0.5 0
SKEW.
symmetrical
negative
0 -1.0 -2.0 -3.0 -4.0
KURT.
more leptokurtic
60.0 50.0 40.0 30.0 20.0 10.0 0
APPROXIMATE HORIZONTAL SCALE: 1" = 1875'
BERM (a)
FORESHORE (b) + (c)

FIGURE 13

VII. TRANSVERSE PROFILES

A. INTRODUCTION

A large number of investigations have been made on the transverse changes of beaches resulting from seasonal or storm effects (Shepard and LaFond, 1940; Inman, 1953; Wiegel, Patrick and Kimberley, 1954; Johnson, 1956; Ziegler and Tuttle, 1961; Pilkey and Richter, 1964; Harrison, 1964), and laboratory investigations have been undertaken to examine the relative importance of tidal range and wave steepness in determining equilibrium* profiles (Watts and Dearduff, 1954; Rector, 1954).

The present study was conducted to determine the nature and magnitude of foreshore profile changes at Wreck Bay, during the summer regime. An attempt was made to isolate the various wave and tidal factors controlling profile development, and a summer storm in mid-August provided information on foreshore stability under violent hydrodynamic conditions. A single set of measurements obtained during the winter of 1968/1969 allowed assessment on seasonal changes that might be expected to occur on the beach.

B. FIELD TECHNIQUES

Seven transverse profiles, numbered A to G, were established across the foreshore at locations shown on Map I. Rod #1 of each profile was placed just seaward of the upper limit of swash activity during a period of spring tides in

*See GLOSSARY

June 1968. The other rods were spaced from 25 to 150 feet apart, depending on the width and character of the foreshore. This was accomplished using a Keuffel and Esser cloth tape, and no correction was made for horizontal distance.

The rods were of $\frac{1}{2}$ inch steel, cut into 4 foot lengths. They were emplaced on the foreshore so that exactly 2.00 feet protruded above the sand surface. At the cliffbase, and closely in line with each profile, a 6 inch spike was driven into the stem of a living tree. These spikes served as permanent reference points for locating the rod stations in winter, when most of them were destroyed by large waves.

The relative elevations of rod tips and reference spikes of each profile were determined by plane tabling immediately after their emplacement. These values were later tied into the regional survey of the beach, to obtain their true elevations above sea level (see heading TOPOGRAPHY OF WRECK BAY). During the summer, changes in sand level were measured to an accuracy of 0.01 of a foot with respect to the rod tips, using a graduated staff (Plate 10). In winter, a single set of foreshore elevations were measured with a dumpy level.

C. STUDY AREAS

Morphological characteristics of the seven profiles are shown in Figures 14b, 16b, 18b, 20b, 22b, 24b and 26b, and the time development of each is illustrated in Figures 15, 17, 19, 21, 23, 25 and 27.

I. SUMMER CHANGES

Profiles D and E, located adjacent to Sand Point, were affected by large waves that broke at moderately wide angles to the beach (Table X). Both areas were characterized by the same profile changes, viz. erosion of the upper and lower foreshore, and ridge-building in the mid-foreshore region. The changes which took place at Profile E were somewhat less pronounced than at Profile D, because the waves were less violent, and also because the winter berm was less extensive. Erosion of the latter provided a large portion of the material used in building the ridges. In late spring, both areas possessed wide, flat platforms just seaward of the profile lines. At Profile D, the platform was rapidly transformed into a longshore bar, which prevailed throughout the summer until a violent storm attacked the beach on the 18th August, reverting it back to its original form. A longshore bar seaward of Profile E was never directly observed, but the presence of one was suggested by the fact that waves broke in this vicinity, and then reformed closer to shore. The sensitivity of these profiles to tidal range may be described as moderate, both of them showing slight accretion on the upper foreshore during low neap - low spring tide periods (Figures 21 and 23).

The two profiles located at the distal ends of the beach, Profiles A and G, were both subjected to very small waves which impinged on the beach at wide angles (Table X).

Similar changes occurred in these areas as well, viz. erosion of the lower foreshore, and berm-building on the upper foreshore. Changes at Profile A were less pronounced than at Profile G due to relatively smaller waves affecting this area. Furthermore, grey clay was intermittently exposed along the lower foreshore here, indicating a very thin cover of sand above basement. At Profile G, a summer berm was built to such a height, that the upper foreshore was not affected by the storm on the 18th August. These profiles may be described as being moderately sensitive to tidal range as well, both showing slight accretion on the upper foreshore during low spring tide periods (Figures 15 and 27).

Profiles B, C and F were all affected by moderately large waves which impinged on the beach at very small angles (Table X). Gross profile changes were all similar in that accretion persisted across the entire foreshore. The area around Profile B displayed extreme sensitivity to tidal range, whereas the other areas were virtually insensitive. At Profile B, the upper foreshore was eroded during spring tides, and berm-building and cusp development commenced during low neap - low spring tide periods (Figure 17). At Profile C, berm building was inhibited by the presence of a relict cobble cusp on the upper foreshore (Figure 35), and at Profile F, uninterrupted foreshore accretion resulted in a well defined berm at its landward end (Figure 24b).

General foreshore accretion can be seen at the mouth of Lost Shoe Creek where stream erosion cuts through the beach sand at each low tide period (Plates IIa and IIb).

2. WINTER CHANGES

Cliff undercutting as a result of wave action was nowhere in evidence in early February 1969. The backshore however, appeared to dip uniformly seaward from the cliffbase at each profile location.

Removal of material from the backshore resulted in accretion over the foreshore, thereby creating a beach face that sloped more gently seaward than the corresponding summer profile. This general trend was evident all along the beach except in the vicinity of Profile F, where no preceeding winter berm had existed on the backshore during the summer (see chapter on BEACH STRUCTURES). There was thus no material available at this location for foreshore accretion, and the profile therefore showed a slight increase in beach slope.

Figure 14a. Histogram plots of small samples from Profile A.

- These samples represent surficial foreshore sedimentary conditions during the summer and winter regimes.

- Each histogram depicts a rod station sample screened at 1 Ø intervals.

- Rod numbers are indicated by circled numerals between the two histogram columns.

- The foreshore slope at each rod station is shown by figures adjacent to the bottom right-hand corner of the histograms, in degrees.

- The number of gravel particles in the samples is indicated on the > 4 mm histogram block; M = many.

- Figures 16a, 18a, 20a, 22a, 24a, 26a are similar presentations of Profiles B, C, D, E, F, G respectively.

Figure 14b. Morphological characteristics of Profile A at four discrete times.

- Circled numerals along the abscissa denote rod locations. Both axes of the diagram are graduated in feet, and vertical exaggeration is 20 X.

- The first curve, for 12 June 1968, represents the profile on the day of rod emplacement. The other three curves have all been plotted at equivalent times with respect to tidal range - at low spring tide. The 22 August curve, however, depicts the beach profile shortly after a summer storm, and the 3 February 1969 curve is the winter beach profile, when storm frequency was highest.

- The water table (WT) line of emergence is indicated for the two summer curves - 26 July 1968 and 22 August 1968. Mean high tide (MHT), mean water level (MWL) and mean low tide (MLT) values are shown as horizontal lines across the diagram.

- Figures 16b, 18b, 20b, 22b, 24b, 26b are similar representations of Profiles B, C, D, E, F, G respectively.

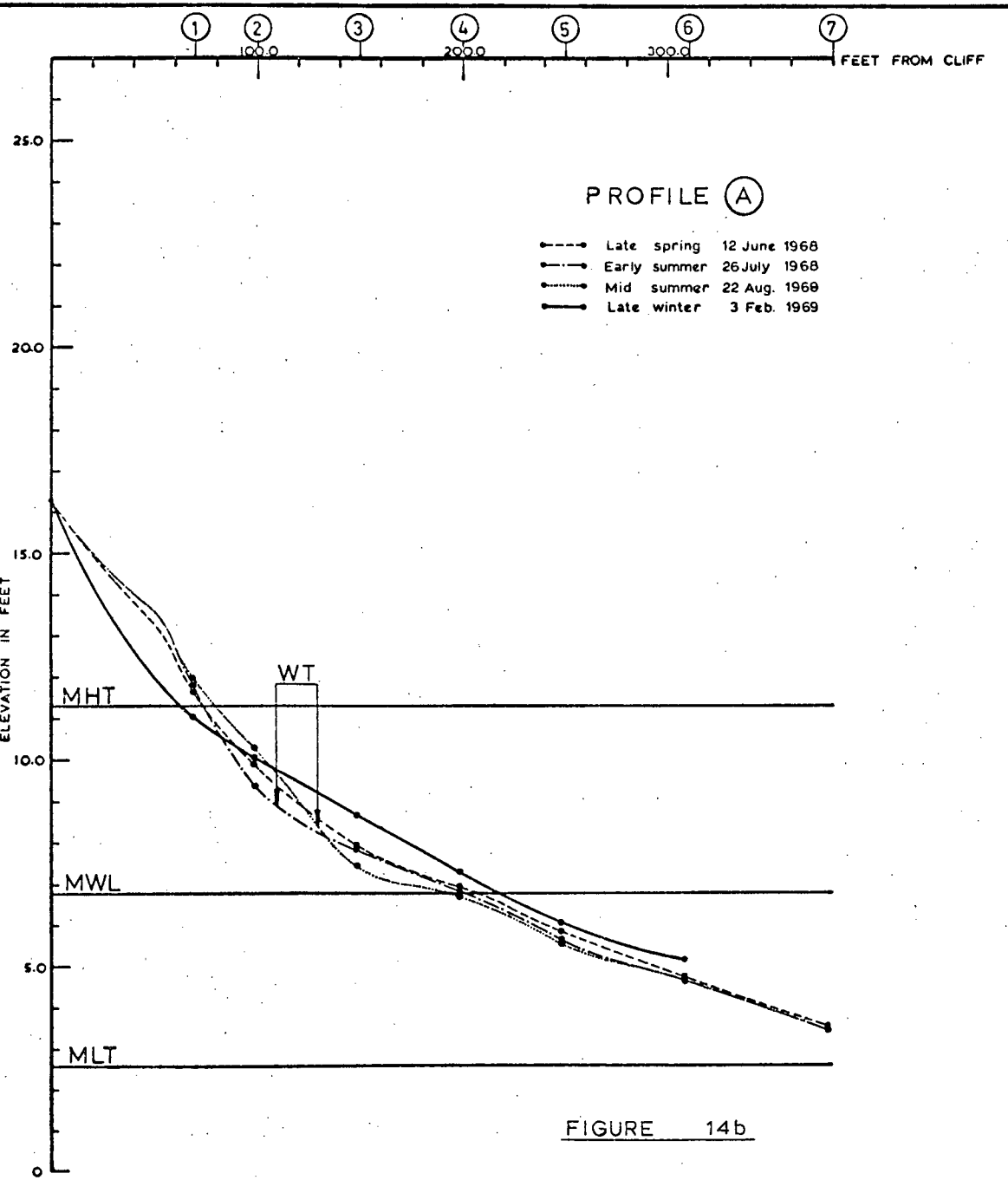

FIGURE 14b

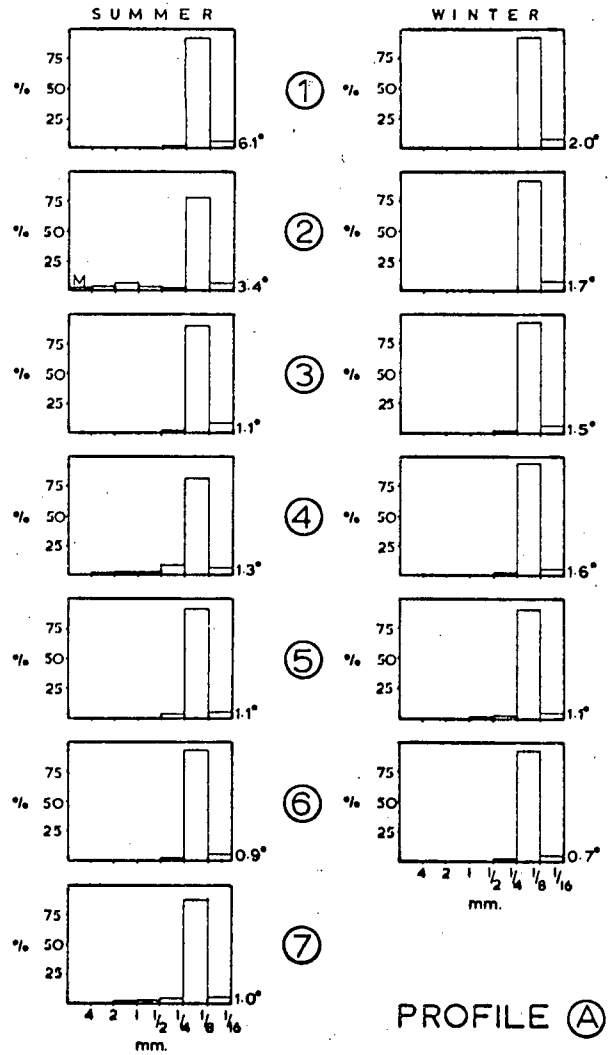

PROFILE (A)

SUMMER — 26 July 1968
WINTER — 3 Feb. 1969

FIGURE 14a

Figure 15. Foreshore modification at Profile A as a function of time.

- Circled numerals along the upper left-hand edge of the diagram denote rod numbers. Ordinate graduations are scaled in feet of accretion or erosion at any rod station.

- Foreshore elevation at each rod station was placed at zero on the day of rod emplacement; all succeeding foreshore measurements were based on this.

- In order to minimize curve distortion resulting from short-term wave effects, foreshore elevations plotted on the diagrams are averages of three consecutive field measurements: the specific one, and the preceeding and succeeding ones. These values have been joined by solid lines to form the curve. However, when either the preceeding or succeeding field measurements were spaced by four or more days from the specific one, the value of the latter was plotted directly onto the diagram, and a dotted line drawn between it and the distant field value.

- Single measurements made during the winter are shown enclosed in circles at the right-hand side of the diagram.

- The tidal range curve depicted at the bottom of the diagram, was plotted from points obtained by subtracting each day's lower low tide value from its higher high tide value.

- Figures 17, 19, 21, 23, 25, 27 are similar presentations of Profiles B, C, D, E, F, G respectively.

FIGURE 15

PROFILE Ⓐ

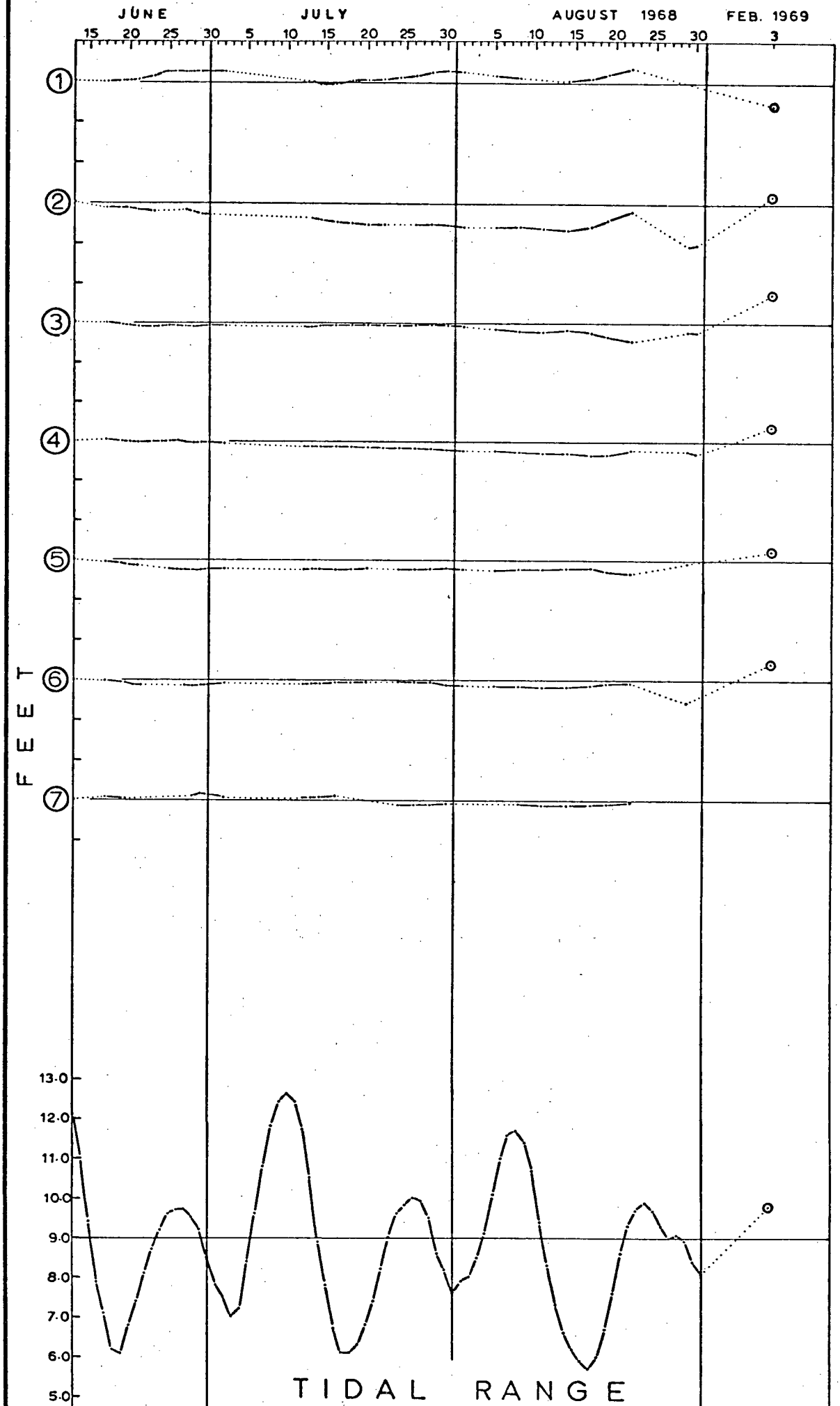

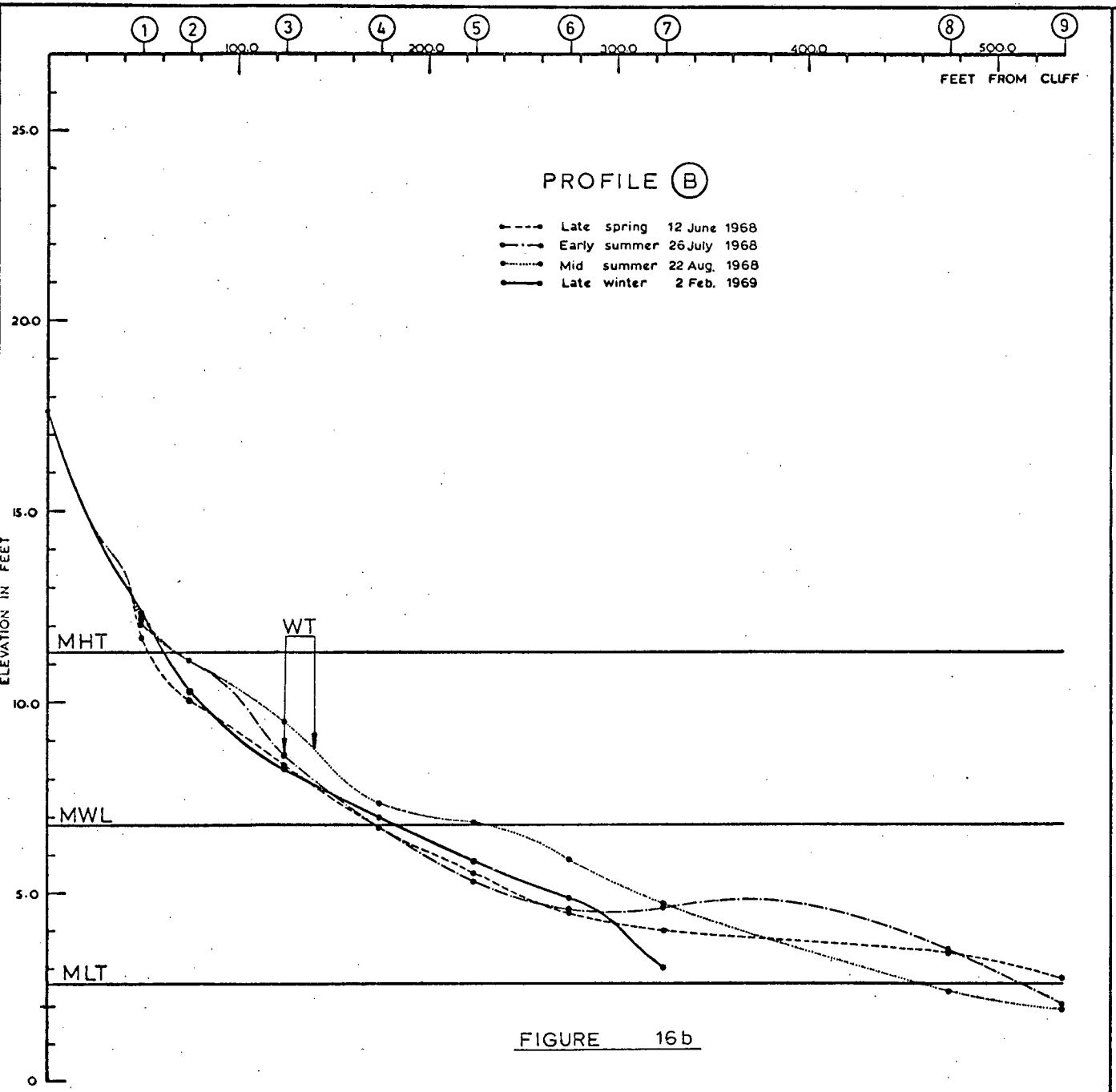

FIGURE 16b

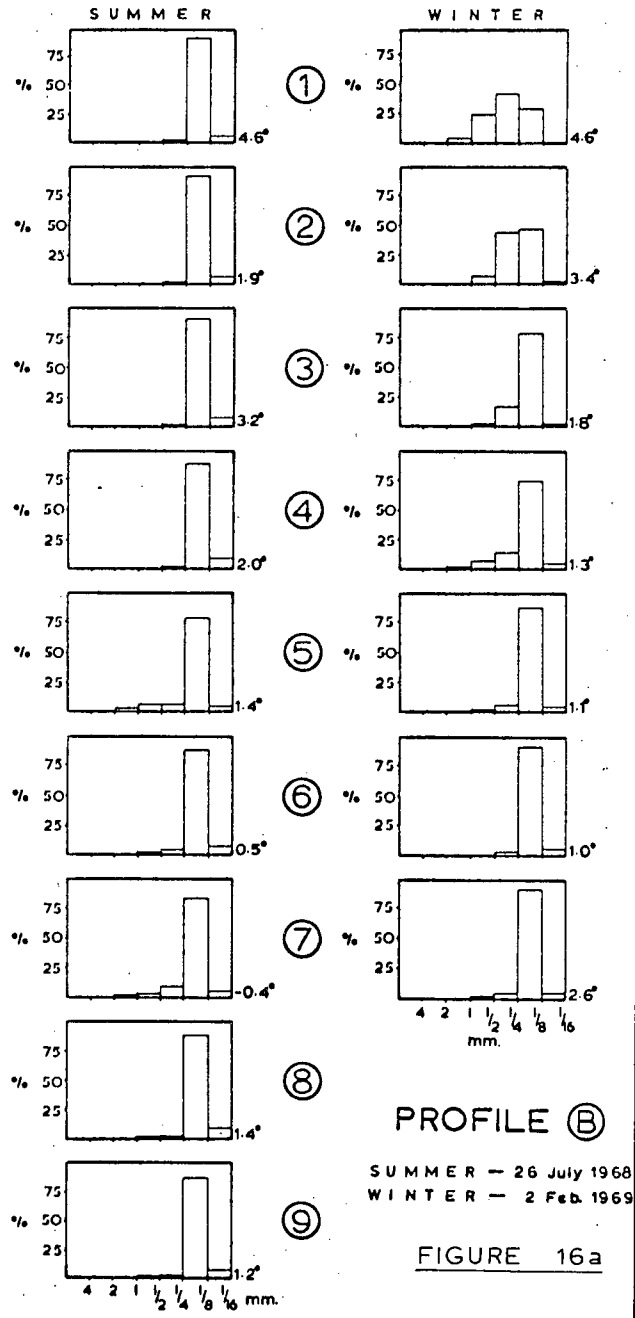

FIGURE 16a

FIGURE 17

PROFILE Ⓑ

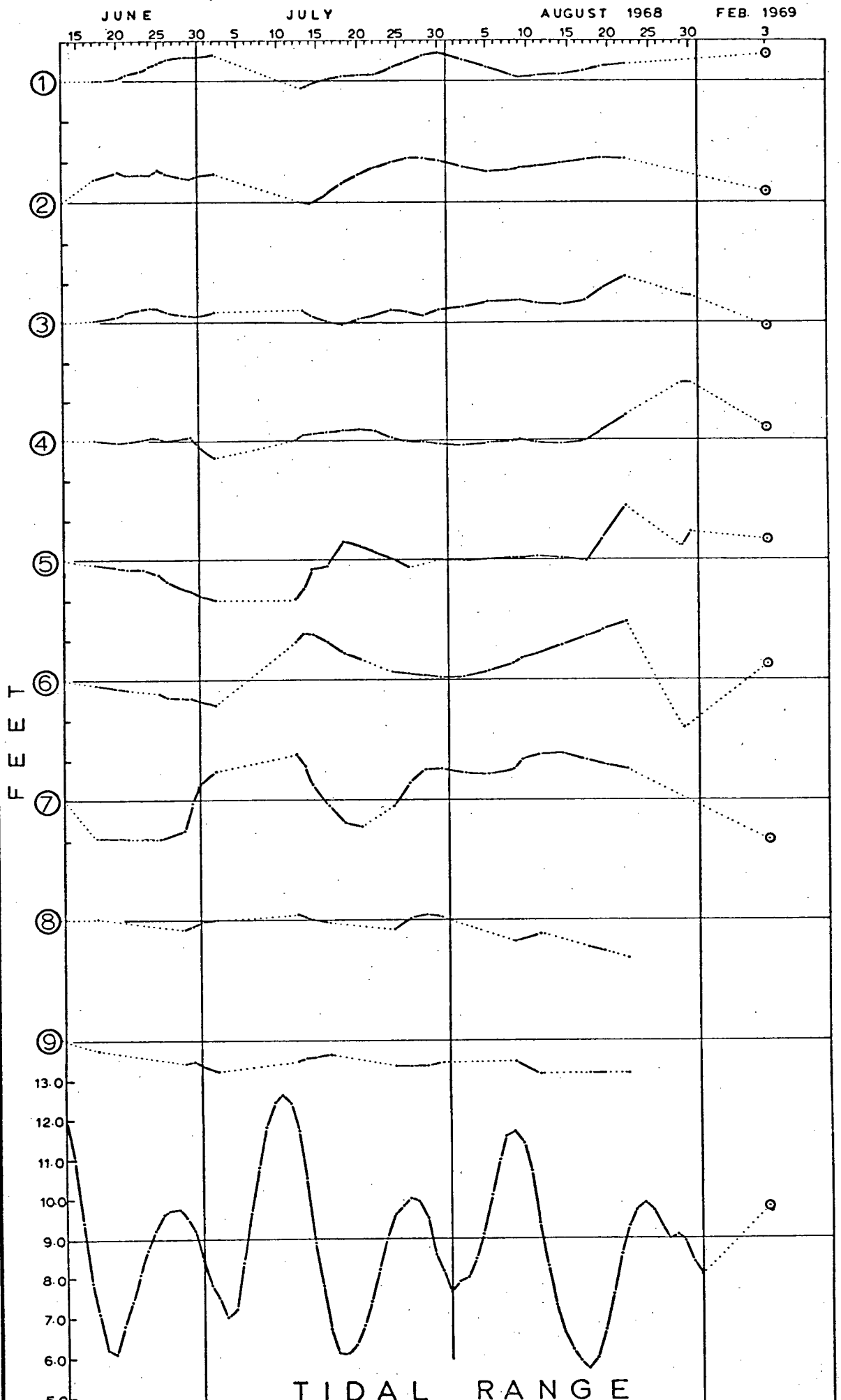

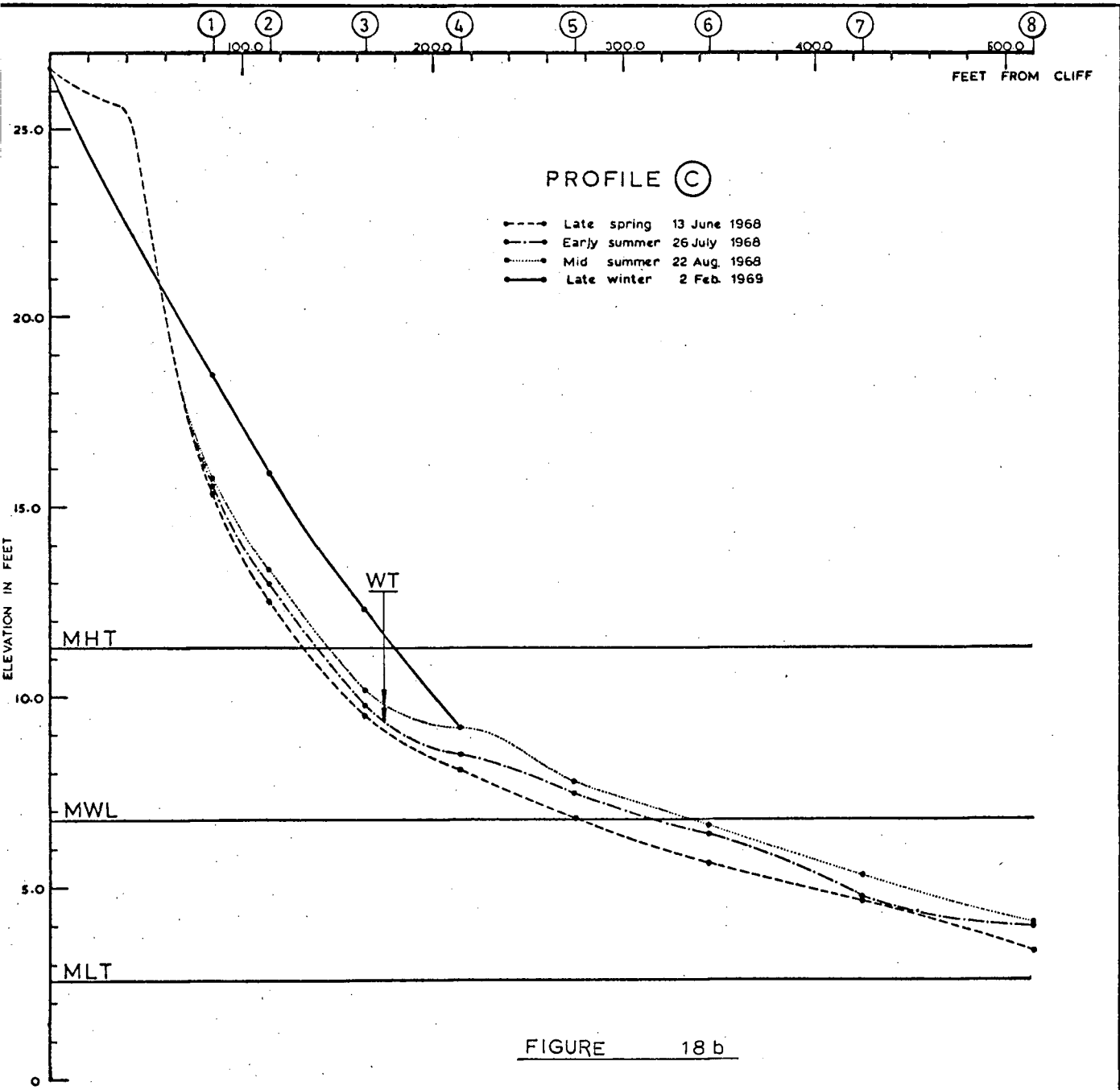

FIGURE 18 b

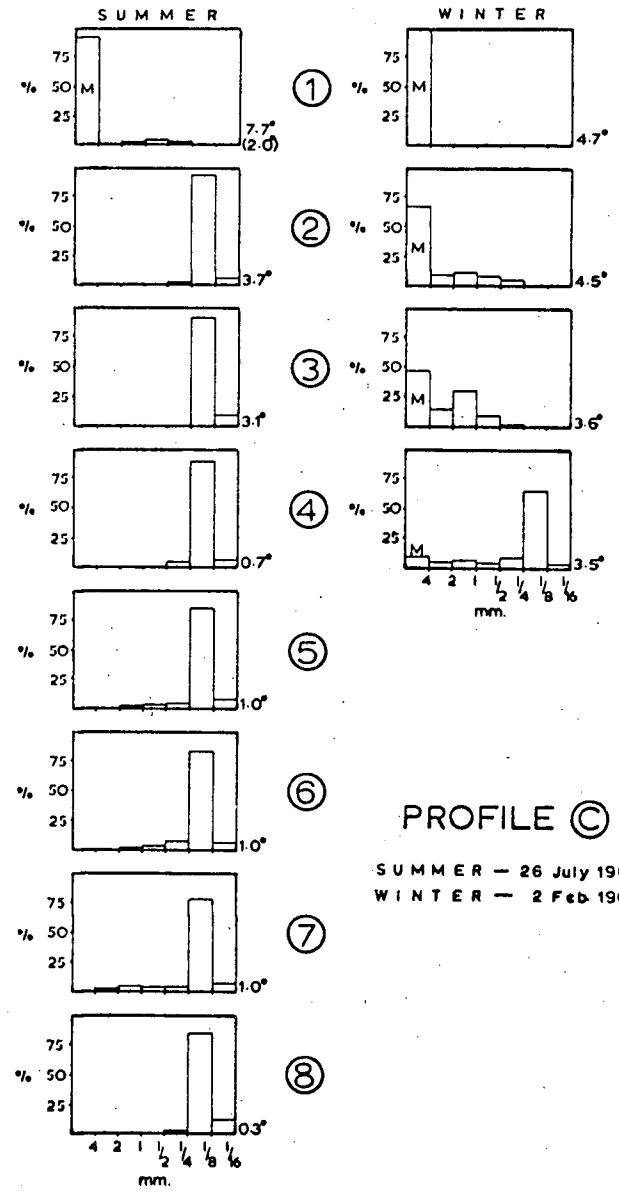

FIGURE 18 a

FIGURE 19 PROFILE ©

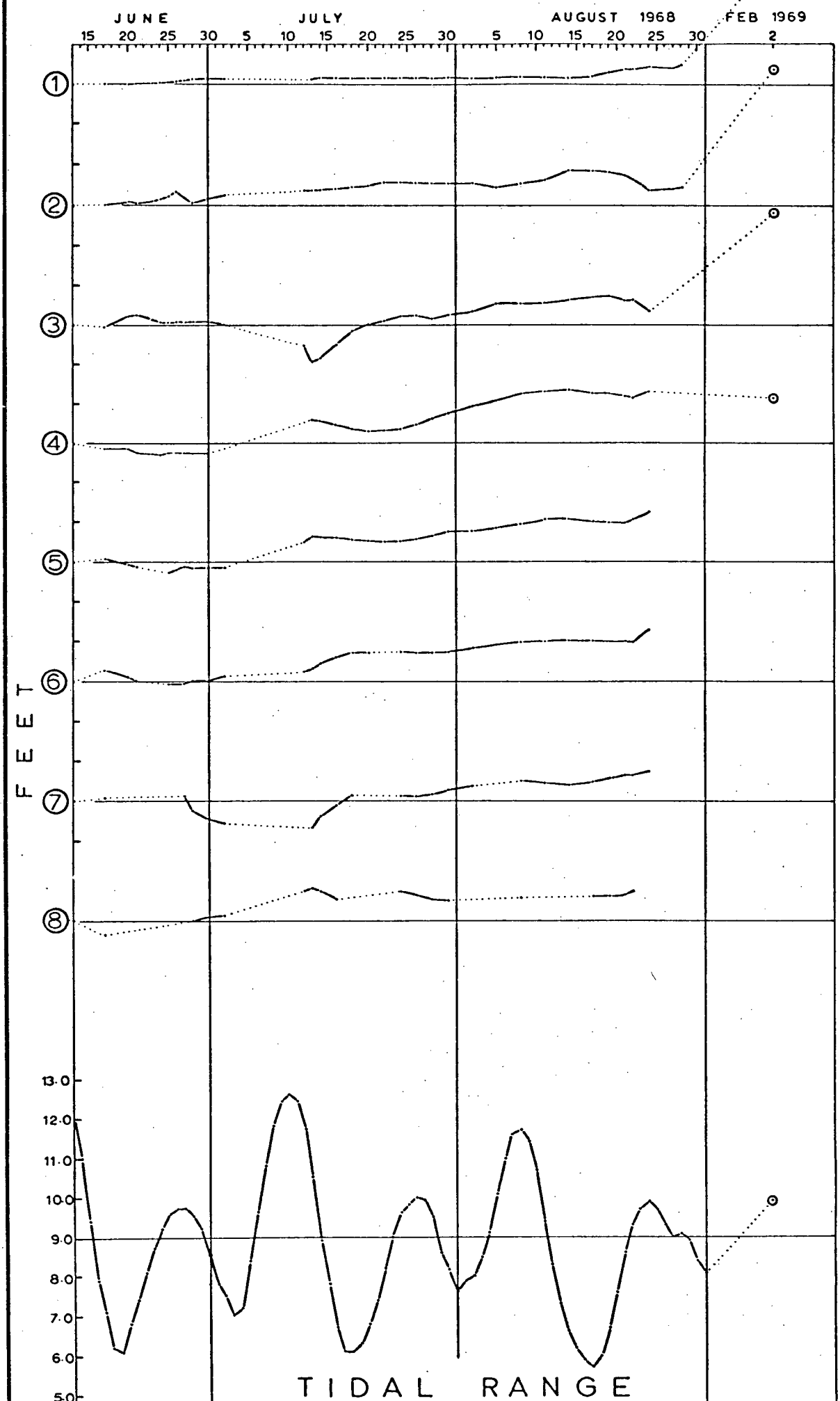

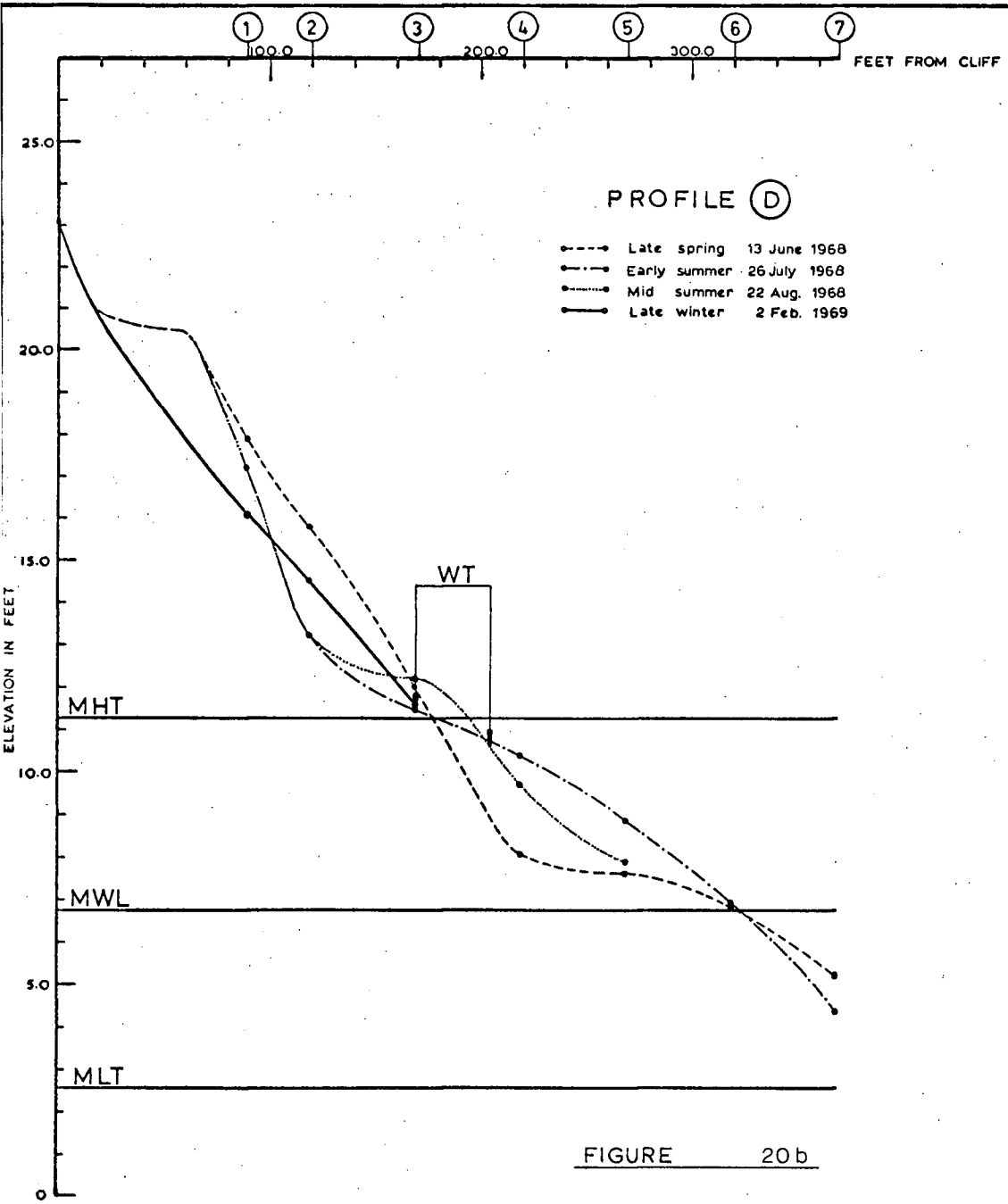

FIGURE 20b

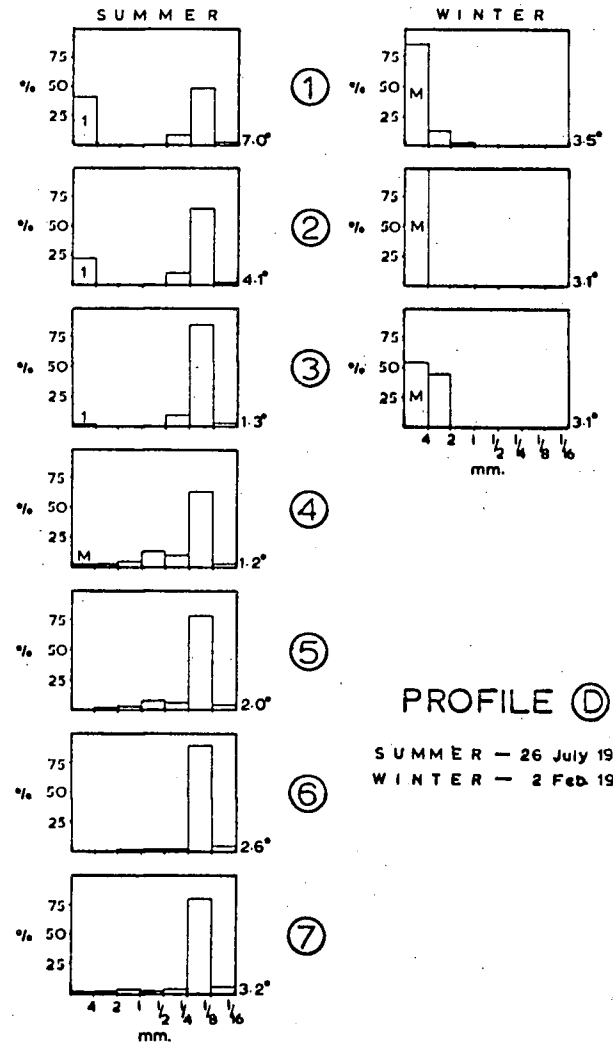

PROFILE D

SUMMER — 26 July 1968
WINTER — 2 Feb. 1969

FIGURE 20a

FIGURE 21 PROFILE Ⓓ

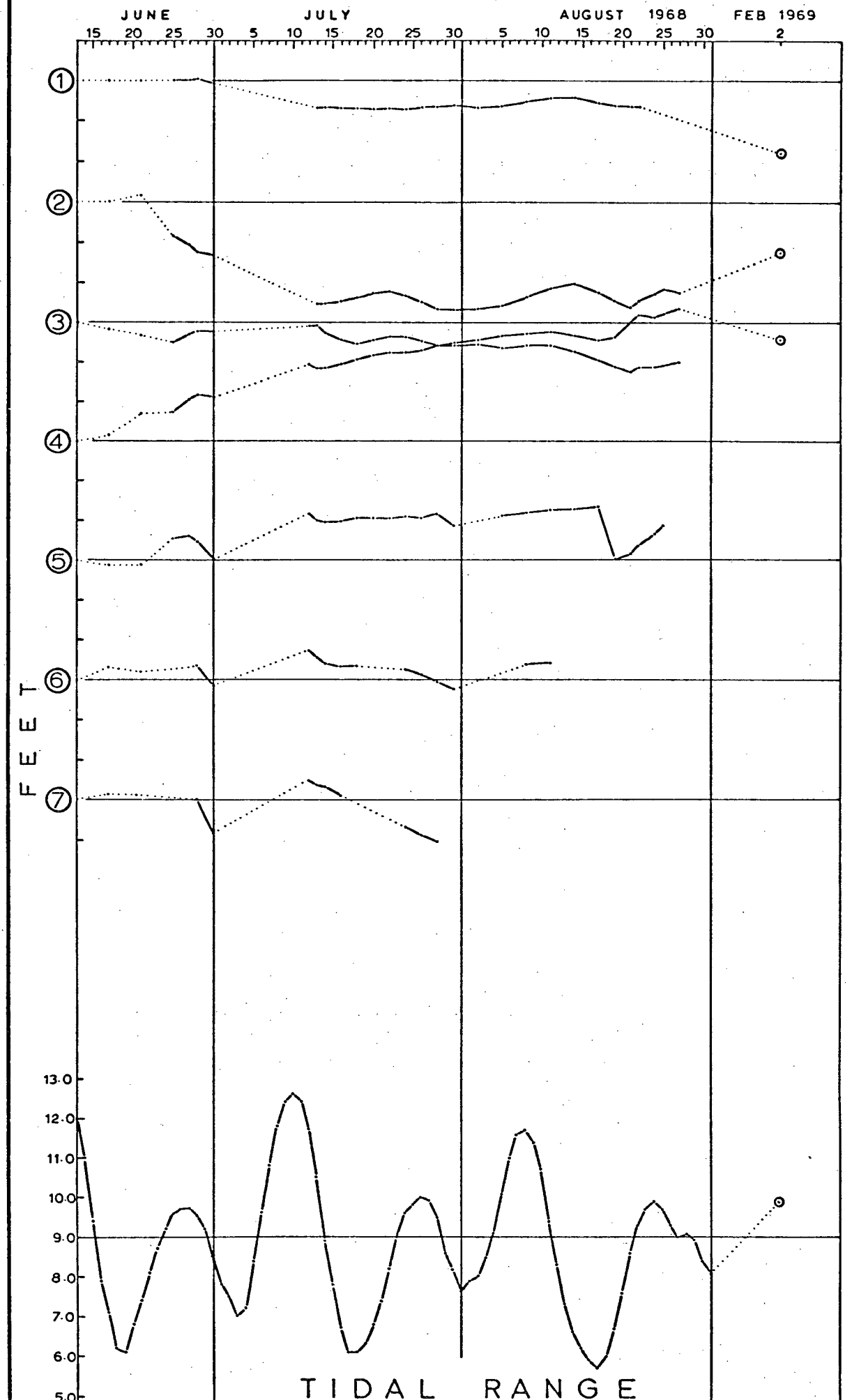

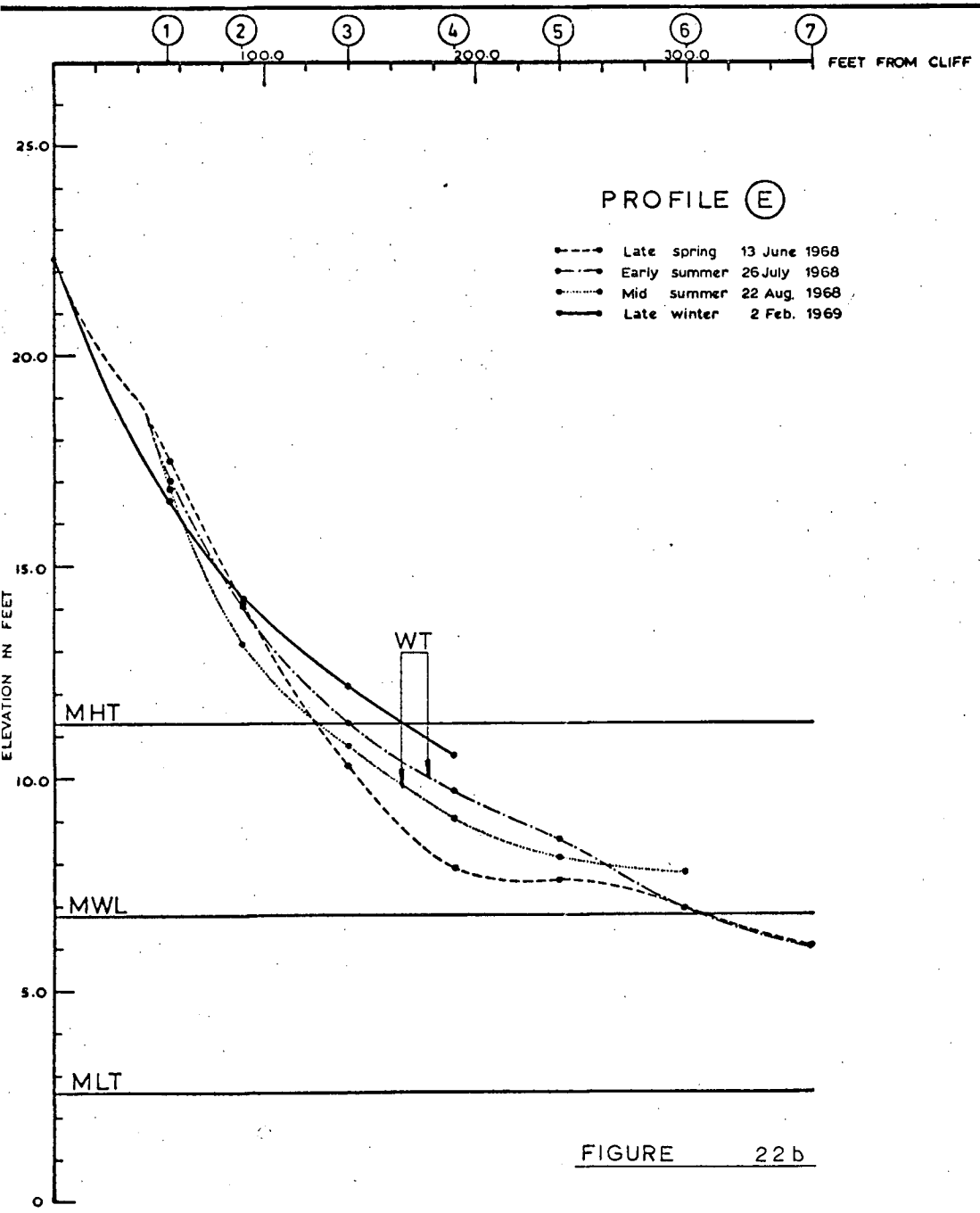

FIGURE 22b

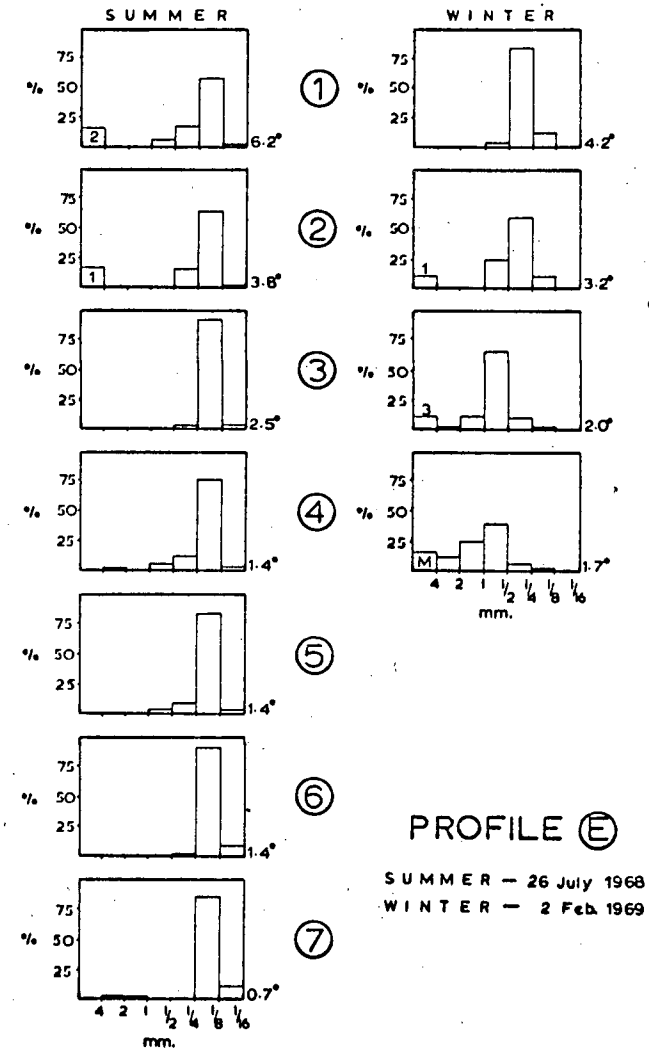

FIGURE 22a

FIGURE 23 PROFILE (E)

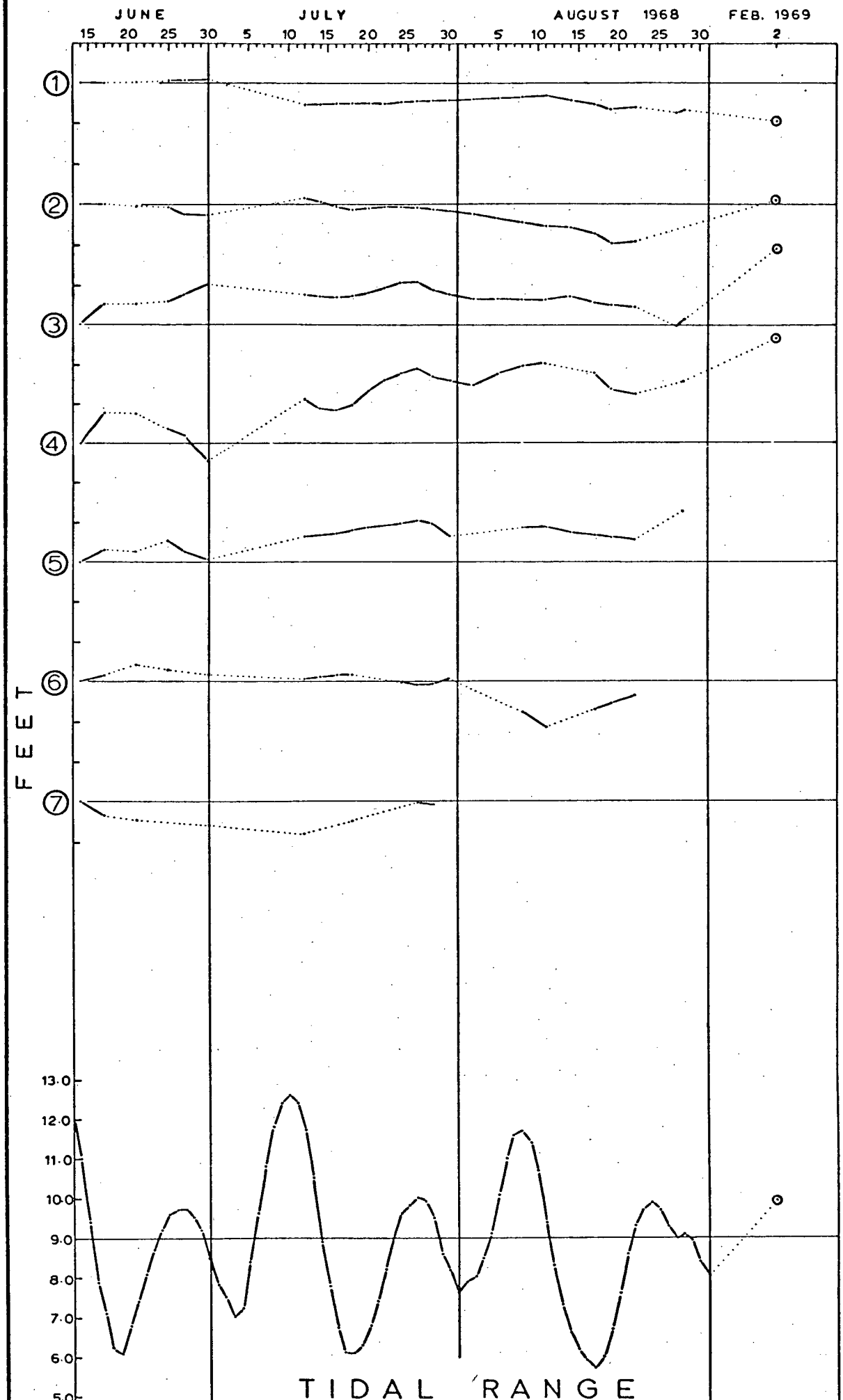

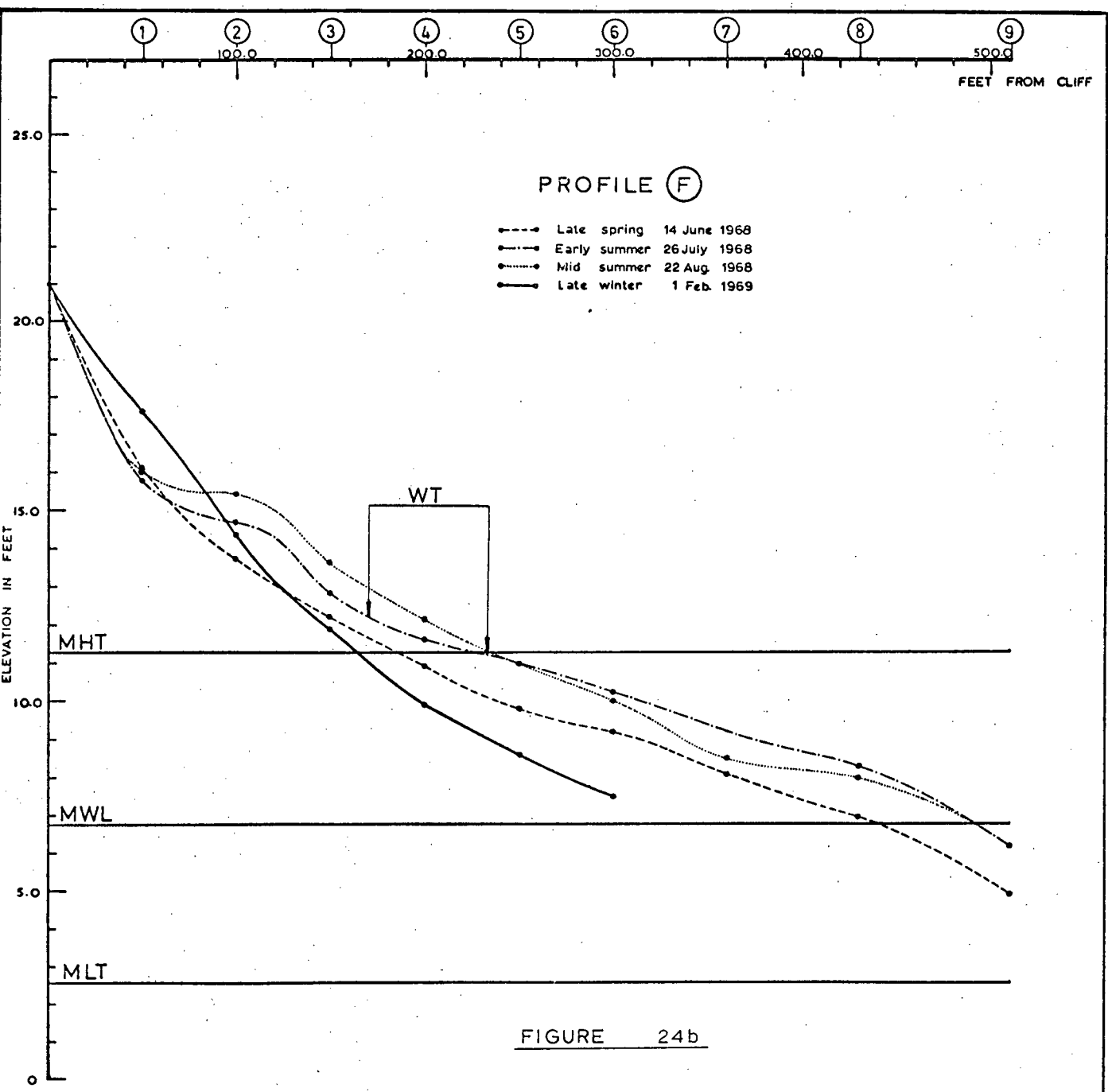

FIGURE 24b

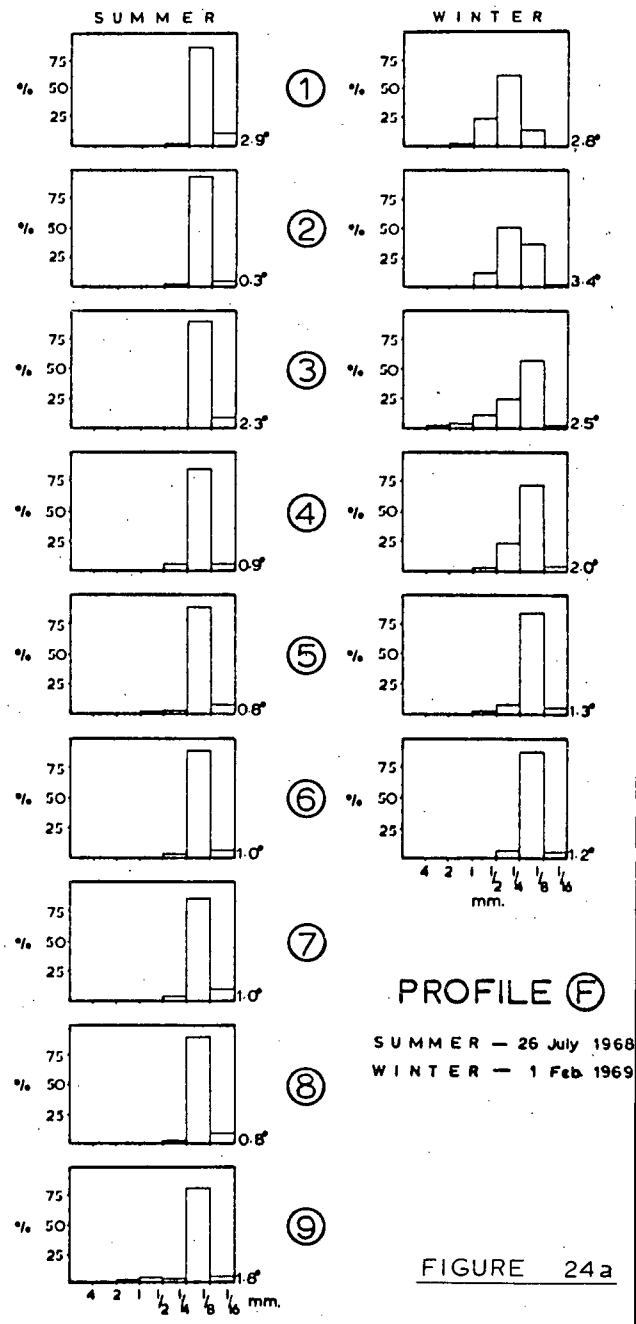

FIGURE 24a

FIGURE 25 PROFILE (F)

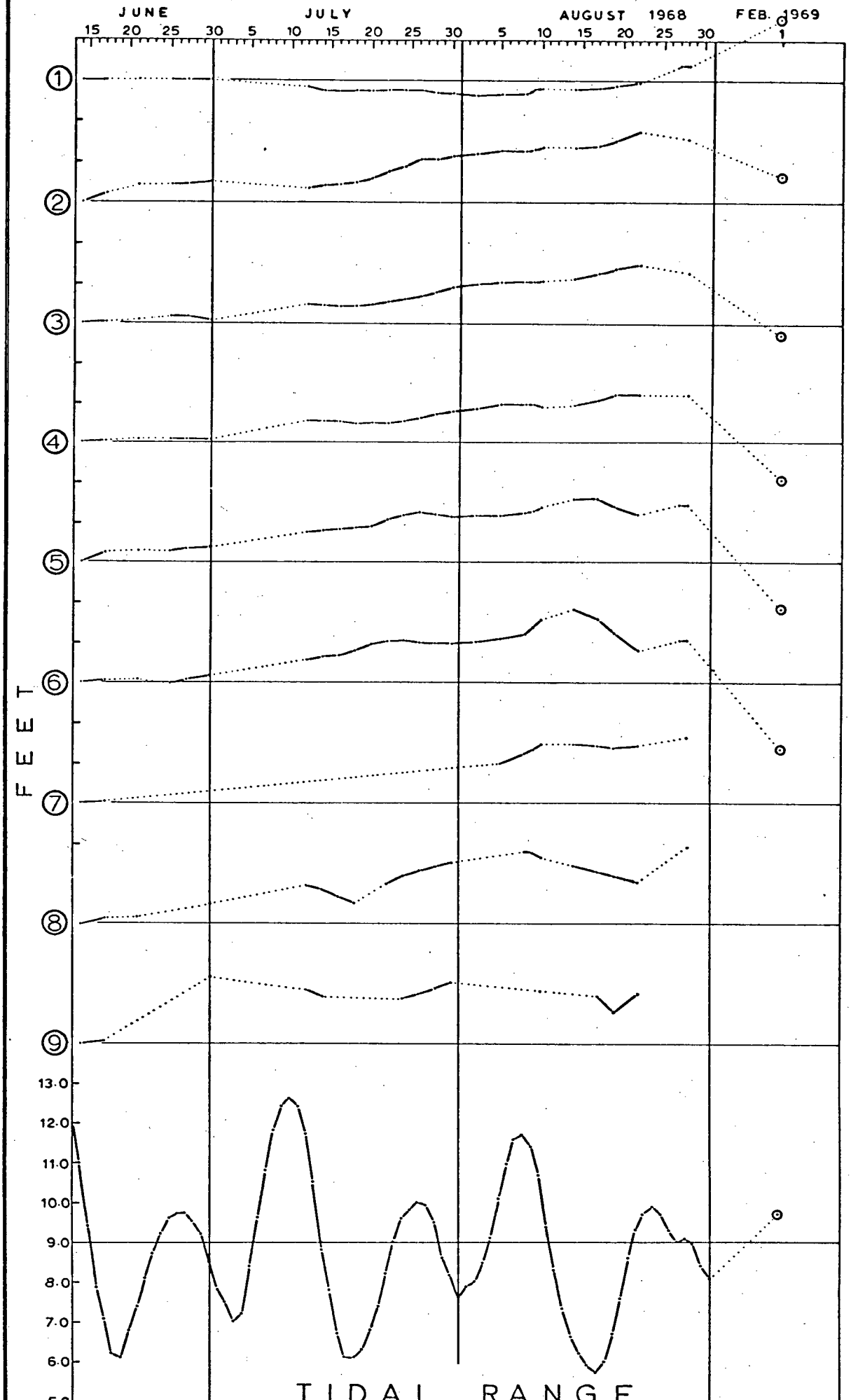

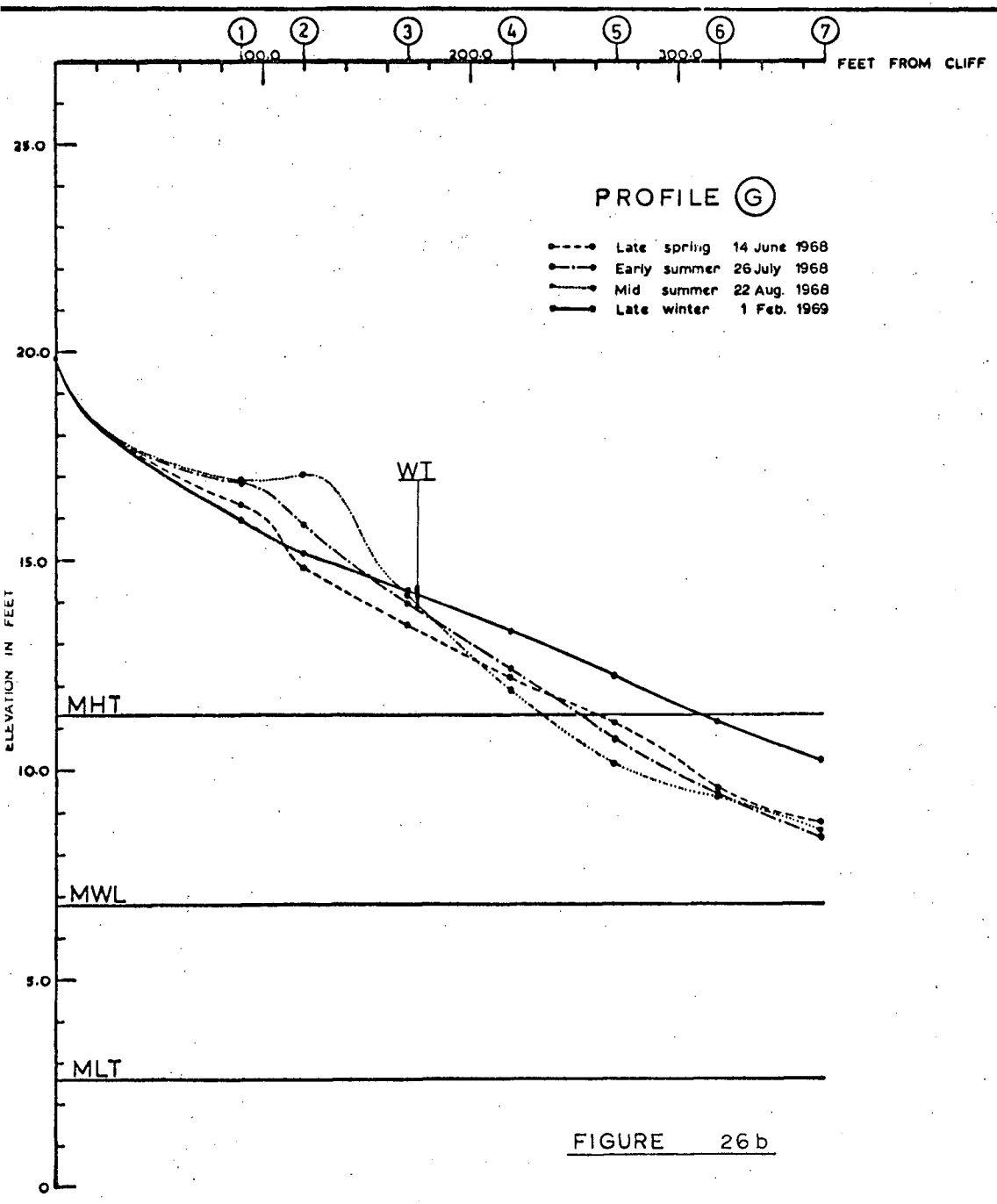

FIGURE 26 b

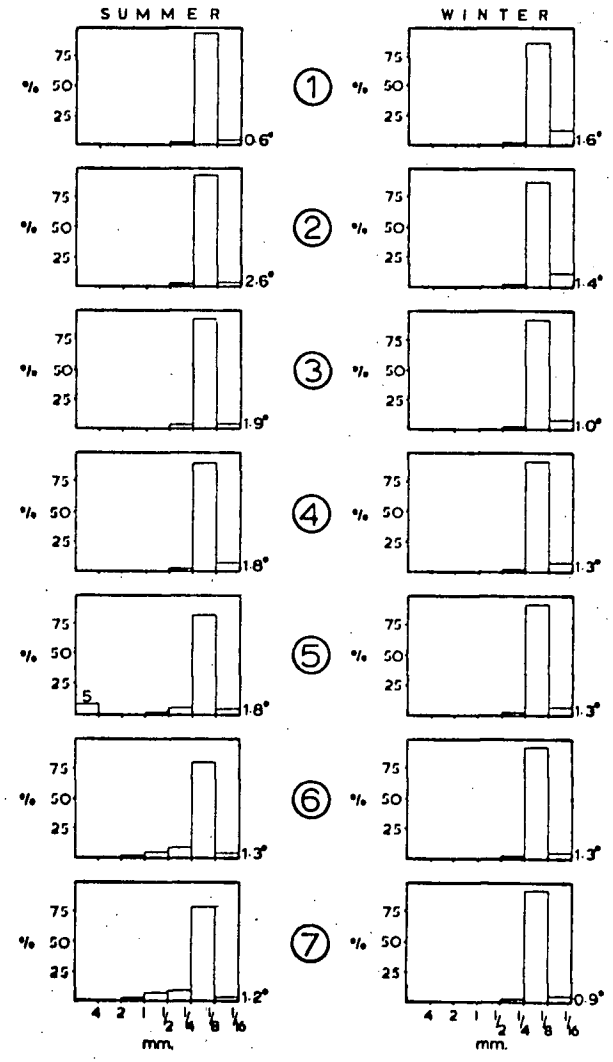

PROFILE G

SUMMER — 26 July 1968
WINTER — 1 Feb. 1969

FIGURE 26a

FIGURE 27 PROFILE Ⓖ

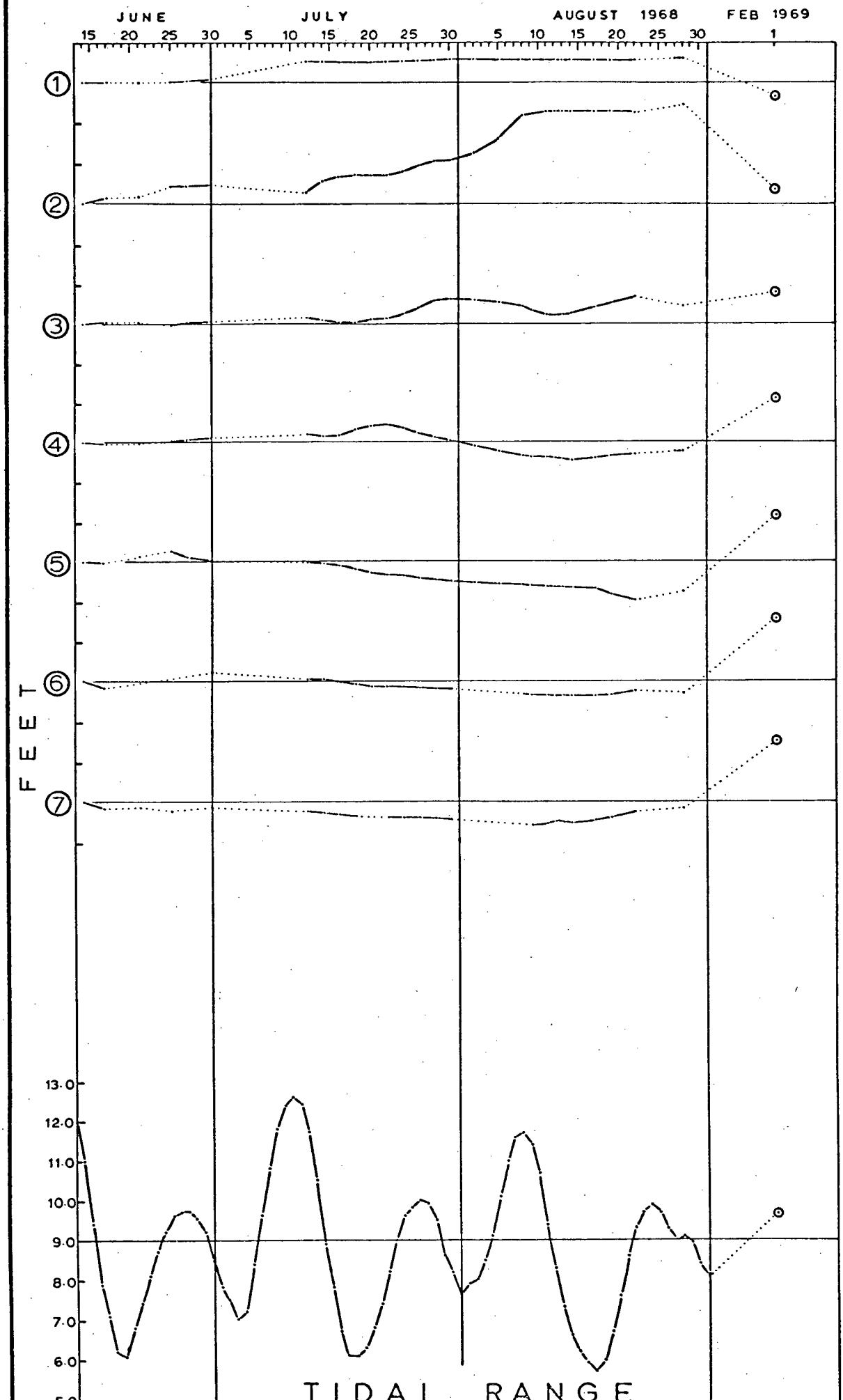

3. STORM CHANGES

A severe storm attacked the beach in the early hours of the 18th August 1968. Weather maps compiled by the Geography Department at the University of British Columbia, were examined to trace the track of the storm center, and to note its characteristics. On the 14th August, a small low-pressure area developed in the Bering Sea, which passed slowly across the Aleutian Islands, and entered the Gulf of Alaska on the 17th August. By this time it had developed into a major weather system, the front of which extended over the west coast of Vancouver Island. Winds along the coast at this time were between 15 and 20 mph from the southeast, but approximately 200 miles due west of Wreck Bay, the wind speed was 50 mph from the southeast. By the 19th August the storm had waned in intensity, and its center had moved southeastwards to the Washington coast.

On the morning of the 18th August, waves were observed breaking over the shoal area just seaward of the elongate boulder zone, and about ½ mile from the mouth of Lost Shoe Creek. Depth of the shoal is approximately 15 feet, and tide height at the time of observation was about 7 feet. Based on the premise that waves break when water depth is 4/3 the wave height (Munk, 1949; quoted in Shepard, 1963), a water depth of 22 feet gives a figure of 16½ feet for the breaker heights in this region. Up to 8 rows of breakers could be seen from the top of the cliff advancing on the beach at any one

time (Plate 2), and the breaker period was found to have increased from 10 to 12 seconds. Littoral current intensities were observed to be much greater than that encountered during the summer, and at Profiles B, C and F, the current directions were opposite to the mean summer directions (Table X). Vast piles of kelp were deposited on the beach where opposing littoral currents met (Plate 25a). The storm occurred during a period of low neap tides, when the range was only about 6 feet; had it coincided with a spring tide period, beach destruction would have been far more severe.

Effects of the storm on the beach are shown in Figure 28. The changes incurred are surprisingly similar to the overall summer changes (Figures 14b, 16b, 18b, 20b, 22b, 24b, 26b), probably as a result of the small tidal range during the storm. The scale of accretion and erosion (antinodes) however, is much greater in the southeast part of the beach (Profiles D, E, F and G) than in the northwest part (Profiles A, B, and C). The most landward antinodal zones are also much longer in the southeast part of the beach relative to the northwest part. The reason for these differences is probably due to the fact that the southeast part of the beach is directly exposed to attack from wind-blown storm waves originating in the southeast. Another departure from uniformity is exhibited by net accretion at Profiles B and G, whereas the other profiles all suffered net erosion (see tabulation below

Figure 28). Likely reasons for this are that at Profile B, more sand was transported into the environment by a reversed littoral current than could be removed by backwash erosion, and at Profile G, relatively small waves in the lee of Wya Point perhaps resulted in onshore movement of sand.

Because of increased wave lengths and breaker heights during the storm, much larger volumes of water washed up the beach face with each swash. The returning backwash had as a result, extreme erosive capacity, and the sandy foreshore between Profiles C and D, and between Profiles E and F, was reduced to coarse gravel. At times, the backwash energy was sufficiently high to stop the next incoming wave at the bottom of the backwash zone, and a hydraulic jump would form up to 2 feet high (see heading MINOR WAVES ASSOCIATED WITH BEACH STRUCTURES).

Figure 28. Profile changes as a result of the summer storm 17-19 August 1968.

- Circled letters adjacent to the ordinate are the profile numbers, and circled numerals along the profile lines are rod numbers.

- The profiles are plotted as straight lines for the 17th August, the day preceeding the storm, and the curved lines are changes incurred by the 19th August.

- Hatchuring indicates erosion; dots indicate accretion.

- Nodal points are marked with short vertical lines, and antinodal zones by numbers, the latter being the volume of material accreted or eroded in cubic feet. These volumes were determined by multiplying the antinodal areas by a profile width of 1 foot.

- Net volume changes and profile lengths are tabulated at the bottom of the diagram.

- Rods D6, D7 and E7 were washed out during the storm, and dashed curves for these profiles are hypothetical.

STORMWAVE EFFECTS

17 – 19 August, 1968

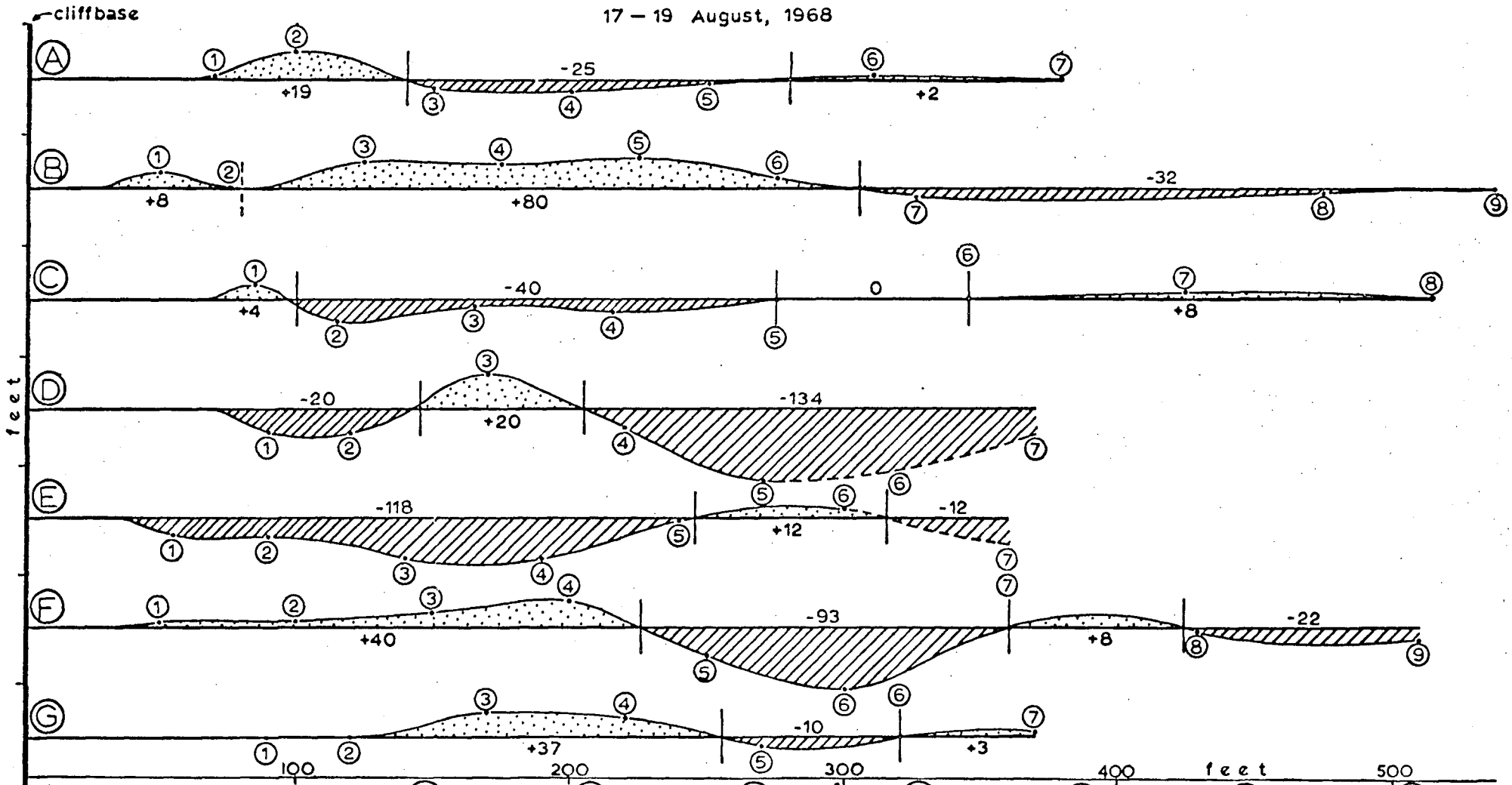

	A	B	C	D	E	F	G
Distance from cliffbase (ft)	380	535	515	370	350	510	370
Net accretion or erosion (cub. ft)	-4	+56	-28	-134	-118	-67	+30

FIGURE 28

D. DISCUSSION

Changes in transverse profiles at Wreck Bay during the summer appear to be a function of three distinct factors - the breaker angle of incidence, the breaker height, and the line of emergence of the water table on the beach. Under violent hydrodynamic conditions prevalent during winter, the water table factor becomes insignificant, and the breaker height becomes the dominant controlling influence.

The angle of breaker incidence apparently determines the availability of sand in the vicinity of the profiles, and indirectly controls their sensitivity to tidal range: At Profiles D, E and A, G, the angular approach of breakers is greater than or equal to 3° (Table X), and as a result portions of the foreshore accrete at the expense of others, and their sensitivity to tidal range is moderate. At Profiles B, C and F, the breaker angle of incidence is less than 3° (Table X), and accretion occurs across the entire foreshore. Sensitivity to tidal range is extreme at Profile B, and Profiles C and F are virtually insensitive. This apparent contradiction is explained by the fact that at Profile B, the breaker incident angle is small but consistent, whereas at Profiles C and F, the angles are very small and highly variable (see chapter on SAND MOVEMENT BASED ON WAVE PARAMETERS). To summarise then, the foreshore is most sensitive to tidal range where sand is abundant, and littoral currents are weak and uniform; it is

insensitive where littoral currents are weak and variable, and moderately sensitive where sand is scarce.

The breaker height determines whether onshore movement of sand occurs or not: At Profiles D and E, the breaker heights are greater than 3 feet (Table X), and as a result, sand is eroded from the upper foreshore and transported seawards to the ridges. At Profiles A, G and B, C, F, the breaker heights are less than 3 feet (Table X), and sand is transported landwards to the upper foreshore.

The vicinity of the water table line of emergence* behaves like a nodal zone with respect to foreshore profile changes, i.e. the magnitude of accretion or erosion is least here. At Profiles D and E, beach ridges were built immediately seaward of these zones, and erosion progressed immediately landward of them (Figures 20b and 22b). At Profiles A and G, erosion occurred seaward of the nodal zones, and berm-building progressed immediately landward of them (Figures 14b and 26b). At Profile B, sand was transported rapidly across this zone in a landward or seaward direction, depending on tidal range (Figure 17). At Profile C, the magnitude of accretion was much less landward of this zone, than it was immediately seaward of the zone (Figure 18b). At Profile F, the beach slope dipped gently seawards, and the line of water table emergence was therefore not static; continual, uniform accretion was the result (Figure 25). In summary then, foreshore changes dictated

* See GLOSSARY

by summer wave conditions are controlled by the presence and permanence of the water table line of emergence.

Implementation of Bascom's (1951) "reference level" for correlating foreshore slope with sand size, was moderately successful at Wreck Bay. A fairly wide range of foreshore slopes, 0.8° to 2.6°, is indicated for very fine sand at the mid-water level on the 26th July 1968 (Figures 14a, 16a, 18a, 20a, 22a, 24a, 26a). However, exclusion of the Profile D slope, where ridge building was in progress at the time, reduces this range to 0.8° to 14°. Incomplete profile measurements in winter prohibited similar comparisons for this period, however, the foreshore slopes were generally less steep and considerably coarser grained (Figures 14a, 16a, 18a, 20a, 22a, 24a, 26a).

Table IX is a listing of maximum profile changes witnessed during the summer, and other pertinent beach data.

Profile	Max. accretion*			Max. erosion*			Berm elevation (feet)		Water table elevation (feet) Summer
	Date	Rod No	Feet	Date	Rod No	Feet	Winter	Summer	
A	22 Aug.$	2	0.39	29 Aug.$	2	1.08	12.5	12.5	8.5
B	22 Aug.$	6	1.44	29 Aug.$	6	1.20	13.0	11.0	8.5
C	17 Aug.	4	1.38	3 July	3	1.15	25.5	-	9.0
D	11 Aug.	4	2.47	30 July	2	2.73	20.5	-	11.0
E	11 Aug.	4	2.02	11 Aug.	6	1.16	19.0	-	10.0
F	17 Aug.	6	2.00	5 Aug.	1	0.52	-	15.5	12.0
G	28 Aug.$	2	2.41	22 Aug.$	5	0.99	15.5	17.0	13.5

* Relative to the day of profile emplacement in June, until the end of August 1968.
$ After the summer storm on 18th August, 1968.

Table IX. Maximum Accretion and Erosion Values at each Profile during the Summer. Winter Berm, Summer Berm and Water Table Elevations are also shown.

It is apparent that accretion values were higher for the southeast part of the beach (Profiles D, E, F and G) relative to the northwest part (Profiles A, B and C). Conversely, erosion values were less for the southeast part of the beach, (Profiles E, F and G) relative to the northwest part (Profiles A, B, C and D). These two observations suggest that the magnitude of accretion during summer is greatest on the southeast part of the beach. Examination of aerial photographs indicate that swell entering the southeast portion of the bay has a different form to its counterpart in the northwest, this being primarily due to diffraction around Florencia Island. In the

southeast portion of the bay swell appears to have a sharp crest, and generates 2 - 3 rows of breakers on the beach; in the northwest, swell has a rounded form, and generates 4 - 5 rows of breakers on the beach (see Frontispiece and Figure 2). Waves affecting the southeast part of the beach therefore, appear to have lost a large portion of their total energy in the process of being diffracted, and are in all probability responsible for the greater magnitude of accretion there relative to the northwest part.

Profile D, located in the middle of the beach adjacent to Sand Point, is exposed to waves which have been only slightly affected by refraction across the shoaling bay. This profile experienced both the greatest amount of accretion and erosion during the summer (Table IX), indicating that it represents the most active hydrodynamic environment on the beach.

Profiles A and G, located in the lee of Quisitis Point and Wya Point respectively, experienced maximum accretion on the upper foreshore due to berm building (rods #2). Profiles D and E, on either side of Sand Point, experienced maximum accretion on the mid-foreshore due to ridge building (rods #4), and Profiles B, C and F experienced maximum accretion on the lower and mid-foreshore (rods #6 and 4).

It is interesting to note that the equilibrium profiles located in semi-protected areas of the beach, Profiles A,

B and G were all most severely affected by the summer storm. The other profiles attained their maximum accretion and erosion values prior to the storm (Table IX).

With respect to water table and summer berm elevations, it will be seen that the former is higher in the southeast part of the beach, and that summer berms are established from 2.5 - 4.0 feet above it. Winter berm elevations have no relation to the water table elevations, being dictated mainly by breaker heights in each area. Between Profile C and the spitbar (Map I), 4 distinct gravel berms existed on the backshore,the most extensive one being at 25.5 feet, which was also the highest within Wreck Bay (Table IX). Based on model tank studies (Bagnold, 1940), the height of a berm above sea level is 1.3 times the height of deep water waves which formed it, thus giving an approximate amplitude of 19 feet for the waves which formed this berm. Based on the observations made in February 1969, it is believed that violent winter storm waves are not responsible for berm building along the backshore, but actually destroy any that happen to exist there at the time. Relatively less violent spring storm waves are thought to be the agent producing these high berms (see chapter on SEDIMENT SIZE ANALYSIS), and therefore wave heights in excess of 19 feet must occur at Wreck Bay during winter storms.

E. PROFILE CHANGES THROUGH ONE TIDAL CYCLE

Profiles B, C and D were measured at half-hourly

intervals in conjunction with tracer dispersion experiments conducted at these locations (see chapter on SAND MOVEMENT BASED ON TRACER DISPERSION).

I. GROSS CHANGES

Examination of Figures 29, 30, 31, indicate that a small amount of accretion occurs as the first swashes wash over the foreshore with rising tide level - a point noticed by Strahler (1964) in a similar set of experiments. However, this accretion stage is short-lived, since close behind the swash zone, erosion becomes the dominant process in the backwash zone. As these zones advance landward with flood tide, material initially deposited by the swash, together with some original sediment, is then scoured out and transported seaward to the breaker zone step by the backwash. During ebb tide, the reverse sequence occurs, i.e. the breaker zone step is eroded by retreating backwash, and the last zone to influence the beach surface, the swash, completely restores the foreshore profile back to its equilibrium* shape.

Initial swash accretion at Profiles B and C (Figures 29 and 30) is greater above the water table line of emergence, than below it. The reason for this is that some of the swash water sinks into dry sand above the water table, and its sediment load is deposited. Below the water table line of emergence however, the swash water all returns seaward as backwash, and a portion of the sediment load is transported with it (Grant, 1948).

*See GLOSSARY

Advance and retreat of the breaker zone step through the tidal cycle is clearly evident at Profile B (Figure 29), but at Profile C (Figure 30), this phenomenon is only apparent in the vicinity of the water table. At Profile D (Figure 31), continuous half-hourly measurements at high tide were not possible, because of high waves which affected the area.

Careful examination of Figures 29, 30 and 31 indicate that a narrow zone of 15 - 25 feet, located immediately landward of the water table line of emergence, suffers more intensive backwash erosion during ebb tide than it does during flood tide. This is probably the result of a 1 - 3 hour time lag between the tide and water table periods (Emery and Foster, 1948). A higher water table during ebb tide would enhance elutriation of fine material from this zone, thereby accounting for its increased erosion.

Figure 29. Changes at Profile B through one tidal cycle.

- Circled numerals on the diagram denote primary rod numbers; small letters between them denote secondary rod numbers. The latter were emplaced at low tide on the 9th August 1968, the day tracer dispersion experiments were conducted on the foreshore, and were spaced 5 feet apart.

- The profile was measured at half-hourly intervals, and foreshore elevation changes were expressed relative to the profile at time of secondary rod emplacement.

- Figures 30 and 31 are similar presentations of Profiles C and D respectively.

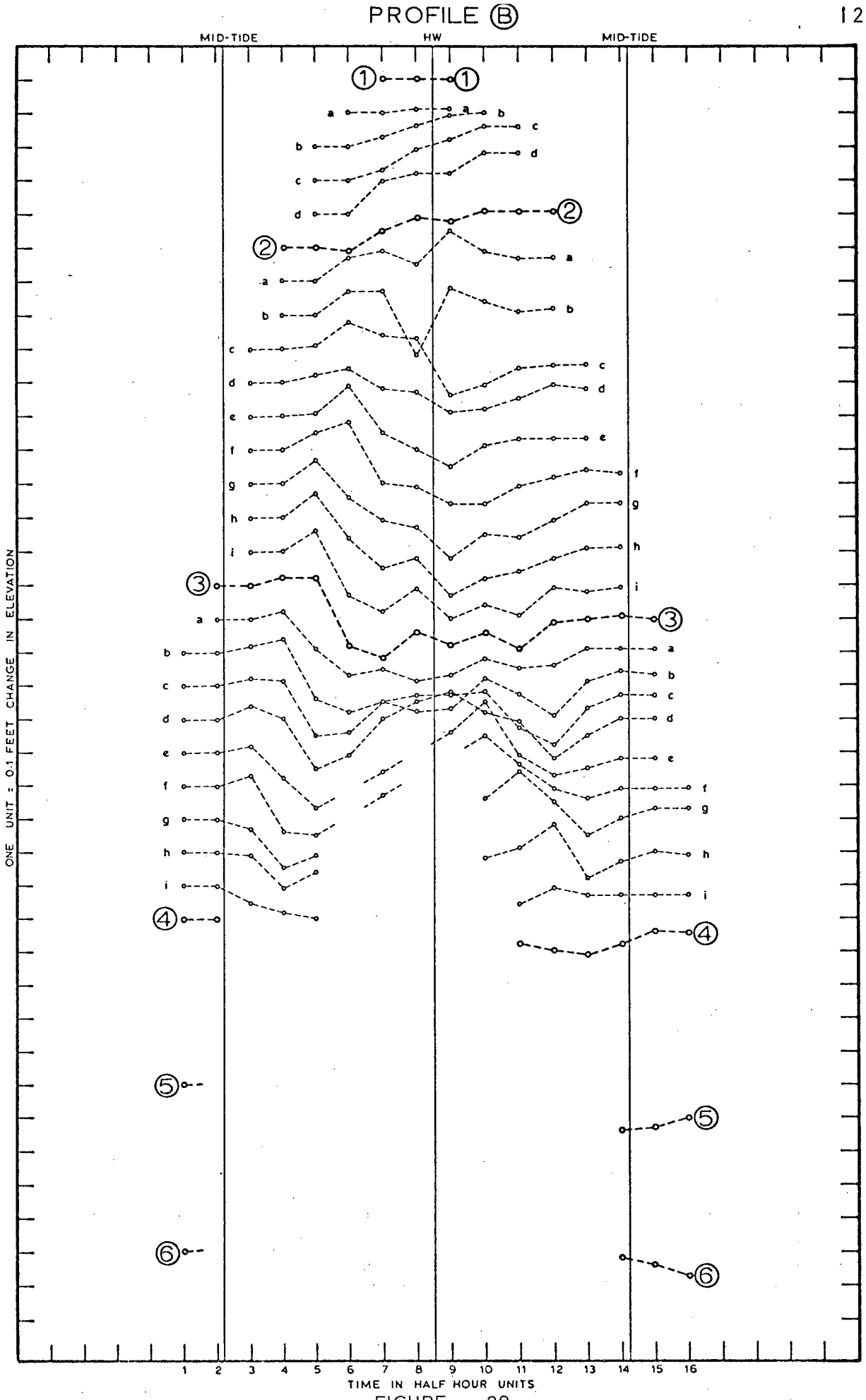

FIGURE 29

Profile changes through one tidal cycle

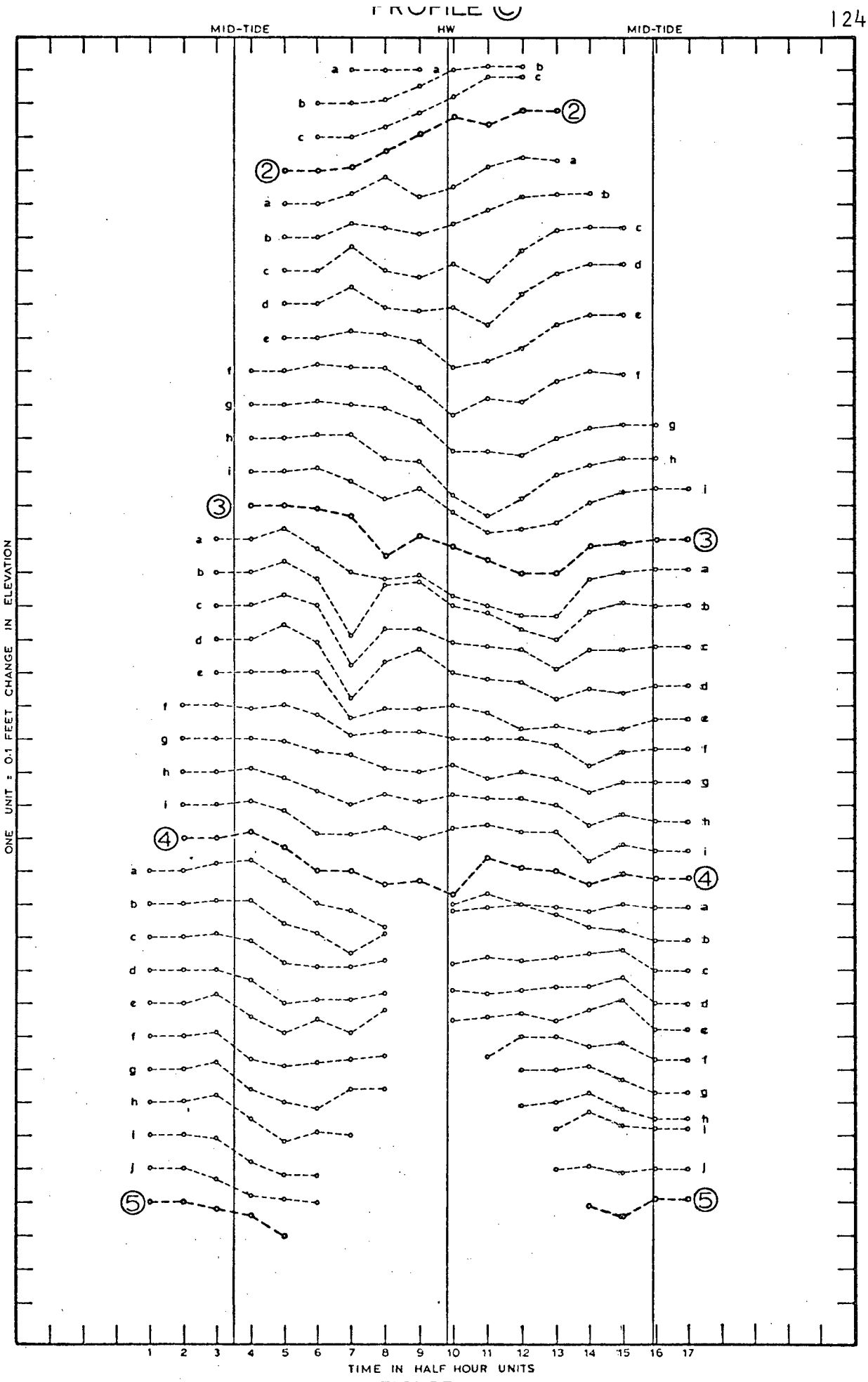

FIGURE 30

Profile changes through one tidal cycle

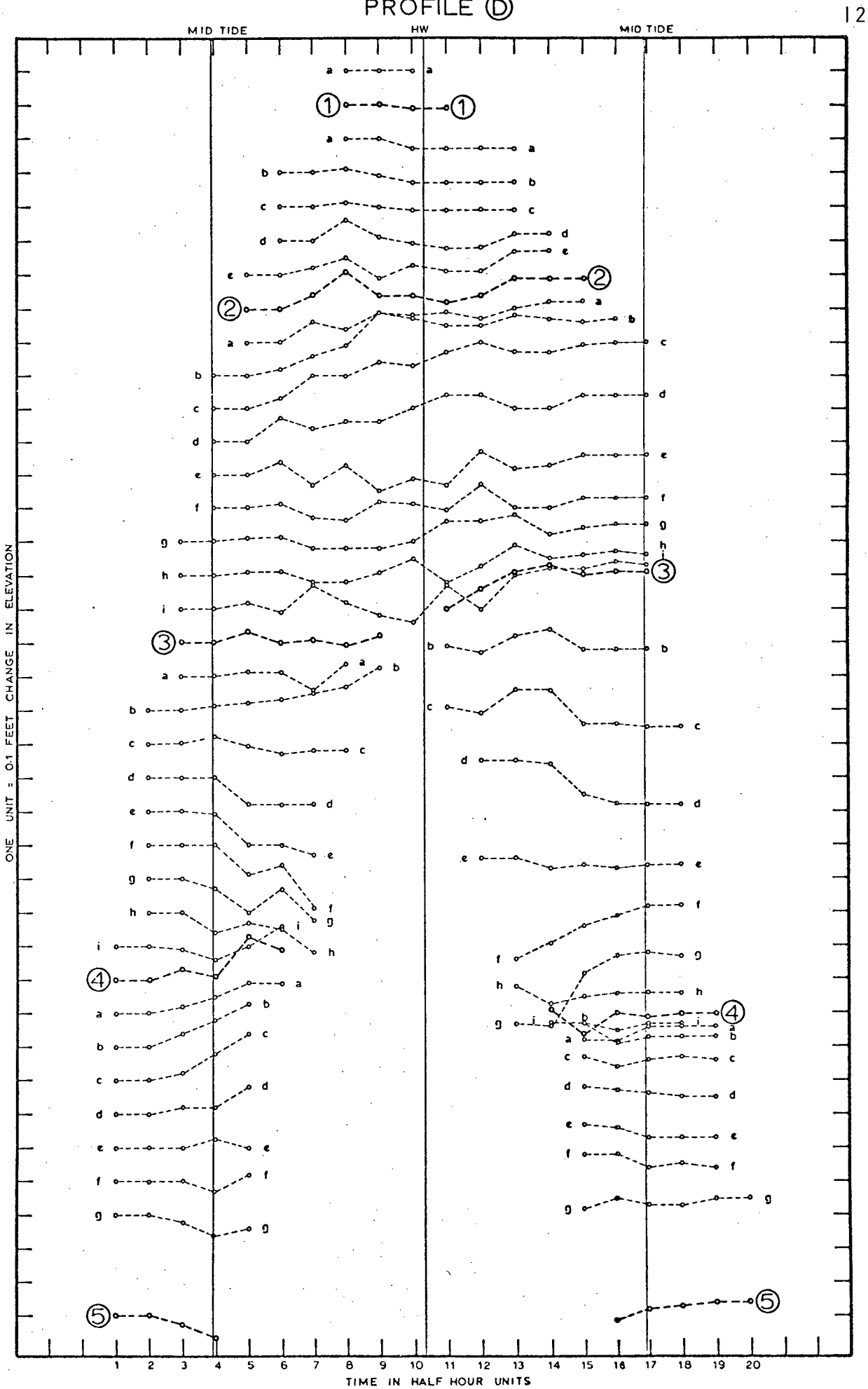

FIGURE 31

Profile changes through one tidal cycle

2. NET CHANGES

Extreme vertical exaggeration of these diagrams (100 X), and close spacing of the profile rods, illustrates that erosion does in fact occur at Profiles B and C. This was not apparent in the long-term measurements of Profile C, probably because the day-to-day changes in tidal range resulted in accretion at different places on the foreshore, thereby giving the impression of over-all accretion.

Berm building at Profiles B and C and ridge building at Profile D are, however, clearly evident. The two peaks on Profile D ridge are most likely the result of erosion on either side of the ridge - on the upper and lower foreshore.

The most dramatic event displayed by these diagrams is the apparent confinement of erosion between the water table and the high tide mark. With Profile C, it will be seen that the spatial relationship between these marks is reversed relative to Profiles B and D, and yet the same pattern occurs. This phenomenon must be a result of differential foreshore erosion above and below the water line of emergence (Grant, 1948) as seen at Profile C, and also because a higher water table elevation during ebb tide enhances erosion immediately landward of it (Emery and Foster, 1948) as seen at Profiles B and D.

Figure 32. Net changes at Profiles B, C and D after one tidal cycle.

- Circled numerals along the bottom of each profile diagram denote primary rod numbers; small letters between them denote secondary rods.

- Both axes of the diagrams are graduated in feet, and vertical exaggeration is 100 X.

- The profiles are plotted as straight lines for the foreshore elevations at low tide preceeding the tracer dispersion experiments. The curved lines represent net profile changes incurred after one tidal cycle. They were derived from Figures 29, 30 and 31 by subtracting the sand elevations at each rod station on the right-hand side of the diagrams, from those on the left-hand side.

- Position of the line of emergence of the water table, and the high tide mark are shown on top of the diagrams.

- Position of the sand tracer sampling grids are indicated for each profile, and the area of gravel tracer dispersion is shown for Profile D.

FIGURE 32

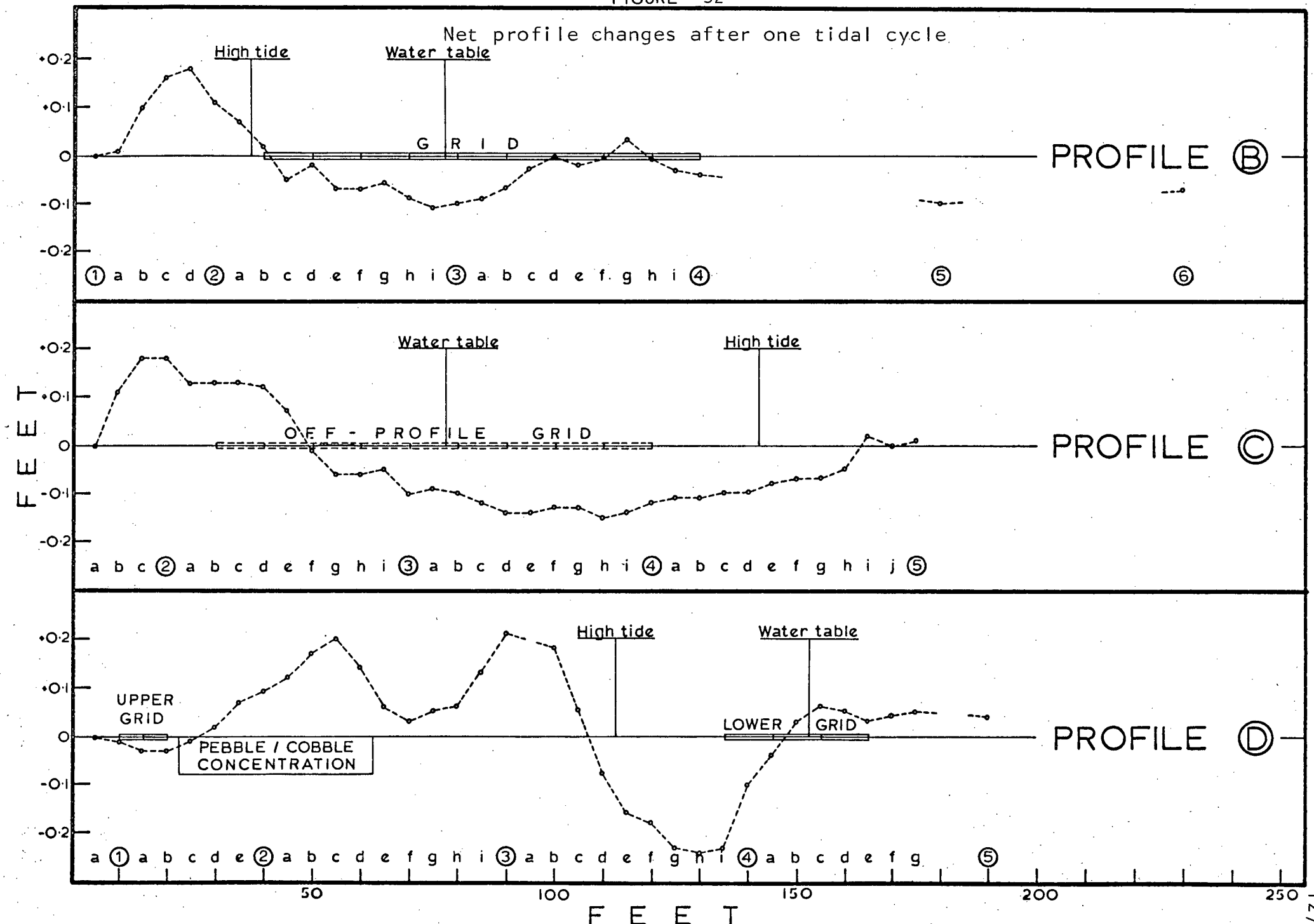
Net profile changes after one tidal cycle
High tide
Water table
G R I D
PROFILE B
① a b c d ② a b c d e f g h i ③ a b c d e f g h i ④ ⑤ ⑥
Water table
High tide
OFF - PROFILE GRID
PROFILE C
a b c ② a b c d e f g h i ③ a b c d e f g h i ④ a b c d e f g h i j ⑤
High tide
Water table
UPPER GRID
PEBBLE / COBBLE CONCENTRATION
LOWER GRID
PROFILE D
a ① a b c d e ② a b c d e f g h i ③ a b c d e f g h i ④ a b c d e f g ⑤
+0·2
+0·1
0
-0·1
-0·2
FEET
50
100
150
200
250
FEET

Plate 10. Procedure used for measuring sand elevation changes during the summer. Graduated staff, with flat base, is placed adjacent to the profile rod, and the elevation of its tip above the sand surface is measured.

Plate IIa. Mouth of Lost Shoe Creek on 30th June 1968.

Plate IIb. Mouth of Lost Shoe Creek on 31st July 1968. Note the thick layer of sand (1.1 feet) above boulders in the stream bed.

VIII. SAND MOVEMENT BASED ON WAVE PARAMETERS

A. INTRODUCTION

The wave pattern in Wreck Bay is a complex one (Figure 2), and evaluation of sand movement along the shore based on wave parameters, can only be semi-quantitative in value. However, the purpose of the investigation was simply to gain an impression of littoral drift along the beach, during a typical summer regime.

Wave generated littoral currents are usually too weak to transport beach material themselves, but turbulence created by breaking waves can set all but cobbles and boulders into a state of semi-suspension; the particles then move by rolling along the foreshore and saltation in the nearshore zone (Bascom, 1964). As a result of this,approximately 80% of littoral drift occurs within a narrow zone lying between the breaker zone and the beach (Johnson, 1956).

A method devised by Caldwell (1956) for determining littoral drift has been closely followed in this study. The technique involves wave parameter measurement close to shore, and thus takes into account the spatial variability of waves in a complex hydrodynamic environment such as at Wreck Bay.

B. WAVE PARAMETERS

Visual estimates of wave parameters were made each time the profiles were measured (see chapter on TRANSVERSE PROFILES), and included the height, approach angle, and period of breakers affecting the different locations. A number of

breaker height measurements were also made using graduated poles, which were emplaced on the lower foreshore in mid-July 1968. The average incident angle of breakers at the different profile locations were also determined by examining six sets of aerial photographs and these figures corresponded very well with the field estimates (Table III). Breaker periods were measured by counting the number to pass a profile rod in one minute.

A summary of parameters used in the calculations are shown in Table X. The significant breaker height is the average of the highest 1/3 of all breaker heights measured, and the significant breaker period is the average of periods associated with the significant breakers.

Profile	Significant breaker height (feet)	Significant breaker period (seconds)	Breaker incident angle (degrees)*
A	.75	10	-7
B	2.50	10	-2
C	2.75	10	1
D	4.00	10	-4
E	3.50	10	3
F	2.50	10	-1
G	1.00	10	6

* - sign indicates a southeast direction, no sign indicates a northwest direction.

Table X. Summary of Wave Parameters used in Littoral Drift Calculations.

C. LITTORAL ZONE

The zone in which most of the littoral drift occurs, depends on the water depth at which waves break. Emery (1960) states that this depth is approximately 4/3 the wave height; they break when water particles are unable to complete full circular orbits due to bottom friction.

To ensure that the littoral zone considered at each profile was sufficiently wide, water depths were set at twice the significant breaker height (Table XI). The zone widths thus extended from just seaward of the breaker zones to the upper limits of swash activity.

Finally, most of the field measurements on wave parameters were made at about the mid-tide level. It was therefore decided to base the calculations on a time interval of one hour. This was considered satisfactory to provide semi-quantitative estimates on the direction and intensity of littoral drift at the different locations.

D. CALCULATIONS

1. SHALLOW WATER WAVE LENGTH

The classical equation of hydrodynamics states:

$$c^2 = \frac{gL}{2\pi} \tanh \frac{2\pi d}{L} \quad \ldots\ldots\ldots\ldots\ldots\ldots\ldots\ldots\ldots\ldots (1)$$

where c = wave velocity

g = gravitational acceleration

L = wave length

d = water depth

For shallow water conditions, d becomes small compared to L, and tanh $\frac{2\pi d}{L}$ tends to $\frac{2\pi d}{L}$ (Inman, in Shepard, 1963). Therefore

$$c = \sqrt{gd} \quad \ldots\ldots (2)$$

The velocity of waves in water of any depth is given by $C = {}^{L}/_{T}$ where T is the period, and by substituting this into equation (2), the wave length can be found in terms of the period and water depth:

$$L = T\sqrt{gd} \quad \ldots\ldots (3)$$

2. TOTAL FORWARD MOVING WAVE ENERGY

The total energy per unit length of a single wave is approximately given by the following relation (Caldwell, 1956):

$$\mathcal{E} = 41T^2H^2 \tanh \frac{2\pi d}{L} \quad \ldots\ldots (4)$$

where H is the breaker height in feet, and the other quantities are also in f.p.s. units. A major portion of this total energy travels forward with the wave form. The total forward moving energy of a wave train can be found for shallow water conditions, by multiplying $\mathcal{E}$ by ${}^{t}/_{T}$ where this the selected interval of time:

$$E = 41TH^2(\tanh \frac{2\pi d}{L})t \quad \ldots\ldots (5)$$

but since tanh $\frac{2\pi d}{L}$ tends to $\frac{2\pi d}{L}$ in shallow water, the equation reduces to:

$$E = 257.7 \frac{TH^2dt}{L} \quad \ldots\ldots (6)$$

3. ALONGSHORE ENERGY COMPONENT

The angle between breaking waves and the beach

determines the direction and strength of the alongshore component of the total forward moving wave energy. This is determined from the relationship (Caldwell, 1956):

$$e = E \sin\theta\cos\theta \quad \ldots\ldots\ldots\ldots\ldots\ldots\ldots\ldots\ldots\ldots (7)$$

that is, $$= 257.7\left(\frac{TH^2dt}{L}\right)\sin\theta\cos\theta \quad \ldots\ldots\ldots\ldots\ldots\ldots\ldots (8)$$

where e = total alongshore energy in foot-pounds

θ = angle of incidence of breakers

4. LITTORAL DRIFT

Studies made by the Beach Erosion Board (1952) in Florida, and by Caldwell (1956) in California, led to an empirical relationship between the amount of littoral drift and the alongshore wave energy:

$$Q = ke^{0.8} \quad \ldots\ldots\ldots\ldots\ldots\ldots\ldots\ldots\ldots\ldots\ldots\ldots (9)$$

where Q = alongshore sand movement in cubic yards

e = alongshore wave energy in millions of foot-pounds per foot of beach per hour

k = proportionality factor (tentatively 210)

which gives the final equation used in this study:

$$Q = 210\left[257.7\left(\frac{TH^2dt}{L}\right)\sin\theta\cos\theta\right]^{0.8} \quad \ldots\ldots\ldots\ldots\ldots (10)$$

It should be pointed out that equation (9) developed by the two studies mentioned above, was determined on beach material with median diameter of about 0.4 mm. At Wreck Bay the sand is much finer with average median of 0.15 mm; the results obtained in the present study should therefore be considered as minimum values.

E. RESULTS

The results are indicated in tabular form:

Profile	Water depth (feet)	Shallow Water wave lengt (feet)	Total forward moving wave energy (foot-pounds/ hour/foot of beach)	Total alongshore energy (foot-pounds/ hour/foot of beach)*	Littoral drift (cub.yds./ hour)*
A	1.5	49	161,400	-19,530	-9.0
B	5.0	89	3,273,000	-114,100	-37.0
C	5.5	93	4,155,000	72,490	25.7
D	8.0	112	10,600,000	-737,900	-164.6
E	7.0	105	7,595,000	396,900	100.2
F	5.0	89	3,273,000	-57,120	-21.3
G	2.0	56	331,300	34,430	14.2

* - sign indicates a southeast direction, no sign indicates a northwest direction.

Table XI. Littoral Drift at Profiles A to G During the Summer Regime.

F. DISCUSSION

Adjacent to the two headlands, littoral drift at Profiles A and G was always unidirectional. The angles of wave incidence at both locations were large, but the waves themselves were small, thus resulting in very little sand movement.

Adjacent to Sand Point, Profiles D and E were affected by uniform littoral currents for most of the time, but these were always complicated by small wave trains resulting from

diffraction around Seal Rock and Florencia Island (see chapter on PLANIMETRIC SHAPE), and at Profile D, by refraction on the longshore bar at certain tide levels (see chapter on SAND MOVEMENT BASED ON TRACER DISPERSION). Furthermore, wind-blown storm waves from the south occasionally reverse the prevailing littoral current directions around the whole bay (Table III). However, although the average incident angle of waves during the summer is smaller at these two locations than at Profile A and G, the wave heights are much larger, resulting in considerable volumes of sand movement. The sand transported through Profiles D and E is deposited on the foreshore at Sand Point, resulting in significant accretion at this location.

Profile B was generally subjected to a uniform littoral current direction, but the small incident angle of waves resulted in only minor quantities of sand being transported through the profile.

Profiles C and F were characterized by negligible sand drift, this being largely due to the very small wave incident angles used in the calculations. In the field, littoral currents were observed to be fairly strong at times, but at both locations, the directions were highly variable. Sand transported one way during flood tide was often brought back again during ebb tide. There was thus an excess of material at these locations during summer, a fact supported by their continual accretion and lack of profile sensitivity to tidal range

(see chapter on TRANSVERSE PROFILES).

A persistent rip-current existed between Profiles A and B, due probably to opposed littoral and longshore current directions in this area (see chapter on PLANIMETRIC SHAPE), and similarly between Profiles F and G (from observation). Between Profiles B and D, and E and F, narrow rip-current channels frequently cut across beach ridges where they existed, and were observed to migrate up and down the length of the beach. These rip-currents developed where two opposing littoral currents converged, and a slight change in the angle of approach of deep-water waves was probably sufficient to alter the littoral current directions and intensities in these areas considerably.

IX. SAND MOVEMENT BASED ON TRACER DISPERSION

A. INTRODUCTION

This investigation was conducted to examine the manner of sediment movement across the foreshore. Three environments were selected for this purpose, each one having distinct foreshore characteristics - Profiles B, C and D (see chapter on TRANSVERSE PROFILES). The duration of each experiment was one tidal cycle, and therefore, the direction and intensity of indicated littoral drift for the three areas are not typical of the summer regime (see chapter on SAND MOVEMENT BASED ON WAVE PARAMETERS).

A space integrated technique was employed (Wright, 1962; Yasso, 1962) using sand tracers at Profiles B and C, and sand as well as gravel tracers at Profile D. Sand tracer dispersions were analysed with the aid of trend surface analysis (Boon, 1968), and gravel tracers by determining their mean vector displacements. Pebble orientation measurements were also made at Profile D, to supplement the gravel tracer information.

In conjuction with these experiments, the profiles themselves were measured at half-hour intervals, to determine the depth of foreshore disturbance during the tidal cycle (see chapter on TRANSVERSE PROFILES).

B. TECHNIQUES

1. TRACER PREPARATION

At each of the three areas studied, sand to be used

as tracer material was derived from two locations, one above and the other below the line of emergence of the water table (Figures 33, 35 and 37). At low tide on the day preceeding each experiment, the sand was collected using a cylindrical tin measuring 0.35 feet in diameter and depth. This depth was found sufficient to insure continual tracer supply so long as erosion prevailed at the source locations during the experiments (Figure 32).

A fluorescent paint with brand name "Krylon" was used for marking the tracers. It contained an acrylic ester resin which rendered it resistant to abrasion, and the colours used, red, blue and green, were brilliant in both daylight and ultraviolet light.

Sand marking was accomplished by spraying the desired paint into a plastic bag containing the dry sand. Through vigorous shaking, the sand eventually became saturated with paint. It was then spread thinly over paper to dry, and afterwards passed through a 0.25 mm screen (except D red) to remove clumps.

Before marking, approximately 50 gms of sand was retained for size analysis, the results of which are shown in Table XII:

Profile	Tracer	Mean (Ø)	Standard Deviation (Ø)	Verbal sorting scale (Friedman, 1962)
B	Red	2.63	0.28	Very well sorted
	Blue	2.64	0.30	Very well sorted
C	Red/Blue	2.67	0.29	Very well sorted
	Green	2.65	0.30	Very well sorted
D	Red	0.78	1.47	Poorly sorted
	Green	2.22	0.79	Moderately well sorted

Table XII. Textural Parameters of Sand Tracers

At low tide on the experimental days, the tracers were returned to their respective source locations.

Three gravel sizes were hand-picked along the beach for use as tracers at Profile D. They were spray painted with different colours, and then placed in circular areas on the foreshore where their sizes matched gravel exposed at the time. Blue pebbles were positioned on a narrow strip of equivalent sized material, in the middle of a coarse pebble section (see panel adjacent to profile line in Figure 37).

The properties and percentage recovery of gravel tracers are shown in Table XIII.

Colour	Mean intermediate axis (i)(mm)	General shape	Number of particles		% Recovery
			Emplaced	Recovered	
White	76	Ellipsoidal	16	4	25
Red	32	Discoidal	100	64	64
Blue	16	Irregular	300	238	79

Table XIII. Properties and Percentage Recovery of Gravel Tracers.

2. GRID DIMENSIONS AND SAMPLE RECOVERY

Rectangular grids were employed for recovering sand tracers, the dimensions and locations of which were based on hourly observations of hydrodynamic conditions at each location. At Profile D, however, grid locations were dictated by the texture of the foreshore. To insure total tracer recovery, sampling depth was designed to exceed foreshore erosion as indicated by the half-hourly profile measurements. This depth was 0.4 feet, and was accomplished using a plastic coring tube with inside diameter of 0.11 feet.

Gravel tracers were simply positioned by taping their locations from two widely spaced profile rods.

3. ENVIRONMENTAL CONDITIONS

Whereas the experiment at Profile B was conducted on a foreshore in equilibrium with the summer regime, a violent summer storm affected the foreshore prior to the experiments at Profiles C and D. Profile C was relatively little disturbed, but Profile D was reduced to a condition similar to that in late Spring (see chapter on TRANSVERSE PROFILES).

Hydrodynamic and atmospheric conditions that prevailed on the experimental days are shown in Table XIV.

Profile	Breaker		Swash		Wind
	Height(ft)	Period(secs)	Direction	Period (secs)	
B	1 - 2	10	Weak SE	13	Light NW
C	1 - 3	10	Strong NW	11	Light S
D	2 - 5	9	Strong SE/NW	10	None

Table XIV. Hydrodynamic Parameters and Atmospheric Conditions on Experimental Days.

4. SURVEY AND PHOTOGRAPHS

As soon as the tracers were emplaced, each area was plane-tabled on a scale of 1 inch = 200 feet (Figures 33, 35 and 37).

Photographs of the areas were taken at 1½-hour intervals to portray the hydrodynamic conditions with tide level (Plates 12a, b, c; 13a,b, c; 14a, b, c). The times at which they were taken, and pertinent tidal information are given in Table XV.

Profile	Day	Tidal Range (ft)	High Tide		Photograph time (hrs)		
			Time (hrs)	Height (ft)	a	b	c
B	Aug.9	6.9	1430	10.9	1500	1630	1800
C	Aug.23	5.7	1340	10.0	1430	1600	1730
D	Aug.25	7.8	1440	10.8	1500	1630	1800

Table XV. Tidal Information and Photograph Times on Experimental Days.

5. COUNTING PROCEDURES

Each sample was split four times with a microsplitter,

and the balance spread thinly over white paper for examination under ultraviolet light. The lamp used was a Mineralight M-15, which combined both long and shortwave radiation. When doubt existed as to the identity of a particle, inspection under white light was usually sufficient to decide.

C. TREND SURFACE ANALYSIS AND COMPUTER PROGRAMMING

Space integrated studies were until recently of little value in explaining foreshore sediment movement, since local variability of the raw data could not be accounted for (Wright, 1962; Yasso, 1962). By the application of trend surface analysis to the problem, Boon (1968) was the first investigator to make objective assessments on real trends.

Trend surface analysis is a procedure which dissects the raw data into two components:

$$X_n = x_n + e_n \quad \ldots\ldots\ldots\ldots\ldots\ldots\ldots\ldots\ldots\ldots (1)$$

where X_n = raw data

x_n = trend component

e_n = residual component

The trend component can be defined by a general polynomial:

$$x_n = a_o + a_1U + a_2V + a_3U^2 + a_4UV + a_5V^2 + \quad \ldots\ldots (2)$$

where x_n = is the trend component of the nth observation point

(U,V) = geographic coordinates of the nth observation on a grid

$a_0, a_1, a_2, \ldots$ = coefficients.

Both X_n and x_n may be considered to be values along a

perpendicular line with coordinates (U,V) on the 2-dimensional grid.

Polynomials of any order may be fitted to the raw data. For each of these trend surfaces (linear, quadratic, etc.), the coefficients $a_0, a_1, a_2, \ldots$ are determined by least squares procedures such that

$$\Sigma(X_n - x_n)^2 = \text{minimum} \quad \ldots\ldots\ldots\ldots\ldots\ldots\ldots (3)$$

The coefficients are then substituted into the polynomial equation, and trend components are found for each sample on the grid. As the polynomial order is increased, the smaller the deviation becomes, and the closer the trend surface approaches hand-contoured raw data.

In most geological applications of trend surface analysis e.g. regional geochemical assays, the purpose is to eliminate regional trends of systematic variation in order to allow concentration on the anomalous deviations. In this type of study the intention is just the reverse, that is, real trends in particle dispersion are sought by eliminating the local variability of each sample.

A program written by A.J. Sinclair for use on an IBM 7040/44 computer was used to calculate the coefficients for linear to sixth order polynomials. Twelve plots were thus obtained for each tracer colour - six trend surface maps, and the corresponding six residual point plots. Computer output also included the standard deviation, total variation, varia-

tion explained, and coefficient of determination for each surface.

Trend surface diagrams shown in Figures 34, 36 and 38 were selected for interpretation from 84 computer plots for the following reasons:

- Experiments at Profiles B and C show remarkably similar trend patterns, apparently related to beach cusp formation.
- The trend patterns shown for Profile D, together with gravel dispersion patterns, and petrofabric analysis of pebble orientations, successfully explain the complex hydrodynamic environment present there.
- All the trend surfaces presented, for Profiles B, C and D, show good definition and high resolution.
- Coefficients of determination for linear, quadratic and cubic surfaces shown for Profile D are all significantly non-random at the 5% level of significance (Howarth, 1967). The coefficients of determination of quartic surfaces shown for Profiles B and C are all sufficiently high to be considered as non-random.

Statistical data and other information pertaining to these surfaces, are shown in Table XVI.

Profile	Figure Number	Tracer colour	Grid size (feet)	Number of samples	Trend surface degree	Coeff. of determination	Standard deviation
B	34 - 2a	Red	40 x 90	50	4	0.647	1.43
	34 - 1a	Blue	40 x 90	50	4	0.492	2.83
C	36 - 3a	Blue	80 x 90	50	4	0.373	1.85
	36 - 2a	Red	80 x 90	50	4	0.830	2.92
	36 - 1a	Green	80 x 90	50	4	0.522	2.49
D	38 - 3a	Red	60 x 30	28	3	0.308	4.55
	38 - 2a	Red	25 x 10	15	3	0.650	15.47
	38 - 1a	Green	60 x 30	28	3	0.755	2.27
	38 - 3c	Red	60 x 30	28	1	0.195	4.91
	38 - 2c	Red	25 x 10	15	2	0.605	16.45
	38 - 1c	Green	60 x 30	28	1	p.514	3.19

Table XVI. Trend Surface Statistical Data, and Sampling Information at Profiles B,C, and D.

D. RESULTS

1. PROFILE B ENVIRONMENT

The dispersal patterns of blue and red tracer are very similar, as indicated in the trend surface diagrams (Figures 34 - 1a, 2a). This fact would have been missed had the hand-contoured raw data diagrams been considered (Figures 34 - 1b, 2b). Note that the two tracer sources were located 75 feet apart, and the edge of the sample grid coincided with the profile line (Figure 33).

From half-hourly profile measurements (Figure 29), it appears that the blue tracer source was probably affected twice by the backwash i.e. during flood tide as well as ebb tide. The red tracer however, was eroded only once viz. at high tide. For this reason, blue tracer isopleth values are higher than the red ones in the trend surface diagrams (Figures

34 - 1a, 2a). The main features of these diagrams are:

- Dispersal patterns are similar regardless of tracer source location.
- Two elongate high-concentration zones, with long axes oriented normal to the coastline, occur approximately 30 feet apart in both diagrams.
- The loci of maximum tracer concentration are located at approximately coincident points within the high zone adjacent to the profile line, and close to the water table line of emergence (Figures 33 and 34).

Residual diagrams (Figures 34 - 1c, 2c) have been included simply to illustrate the extent of deviation of the quartic trend surfaces from the hand-contoured raw data.

FIGURE 33

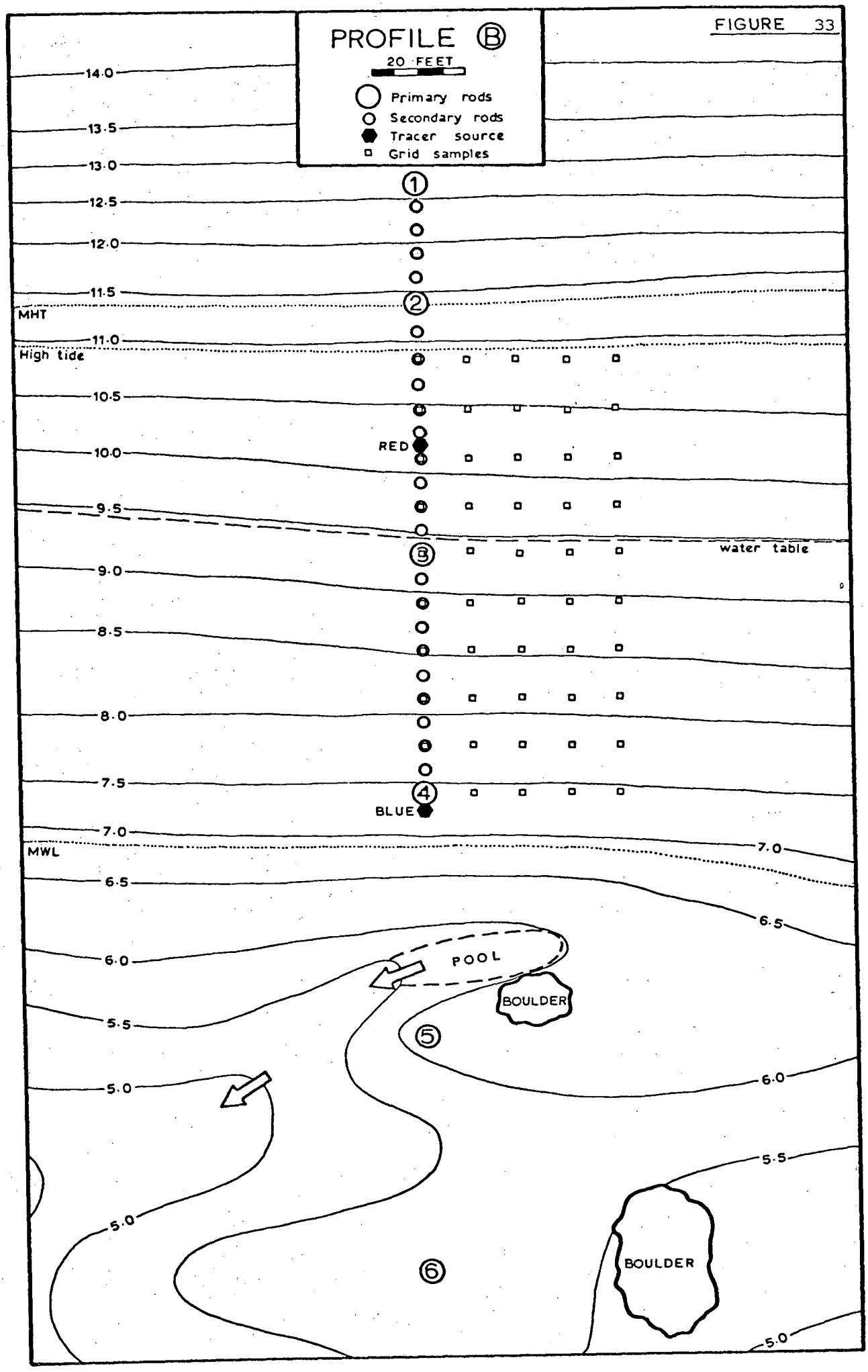
PROFILE B
20 FEET
Primary rods
Secondary rods
Tracer source
Grid samples
14.0
13.5
13.0
12.5
12.0
11.5
MHT
11.0
High tide
10.5
10.0
RED
9.5
water table
9.0
8.5
8.0
7.5
BLUE
7.0
MWL
7.0
6.5
6.5
6.0
POOL
BOULDER
5.5
5.0
6.0
5.5
5.0
BOULDER
5.0
1
2
3
4
5
6

FIGURE 34

PROFILE Ⓑ

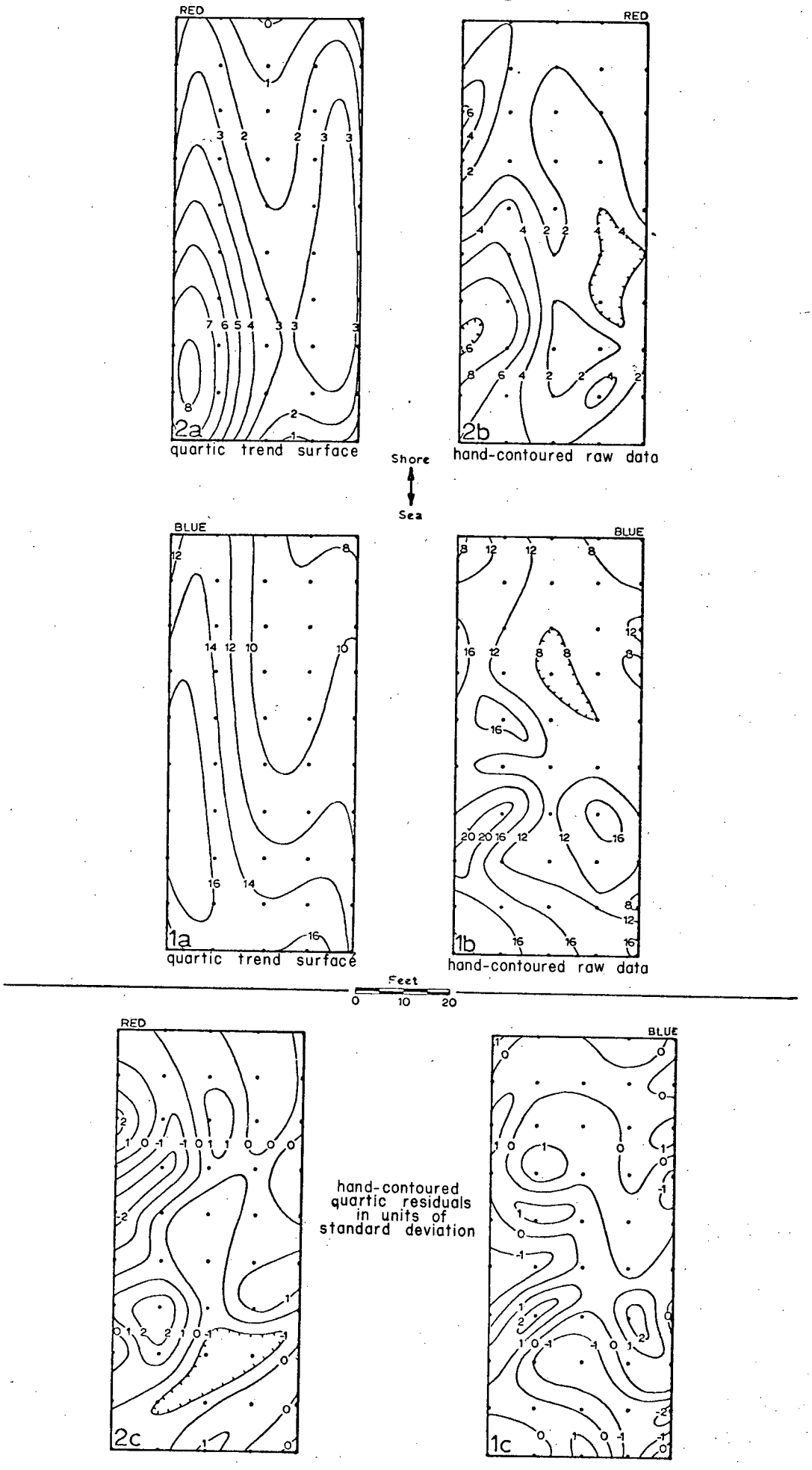

Plate 12a. Profile B shortly after peak high tide. Photograph time - 1500 hours.

Plate 12b. Profile B. Photograph time 1630 hours.

Plate 12c. Profile B. Photograph time 1800 hours.

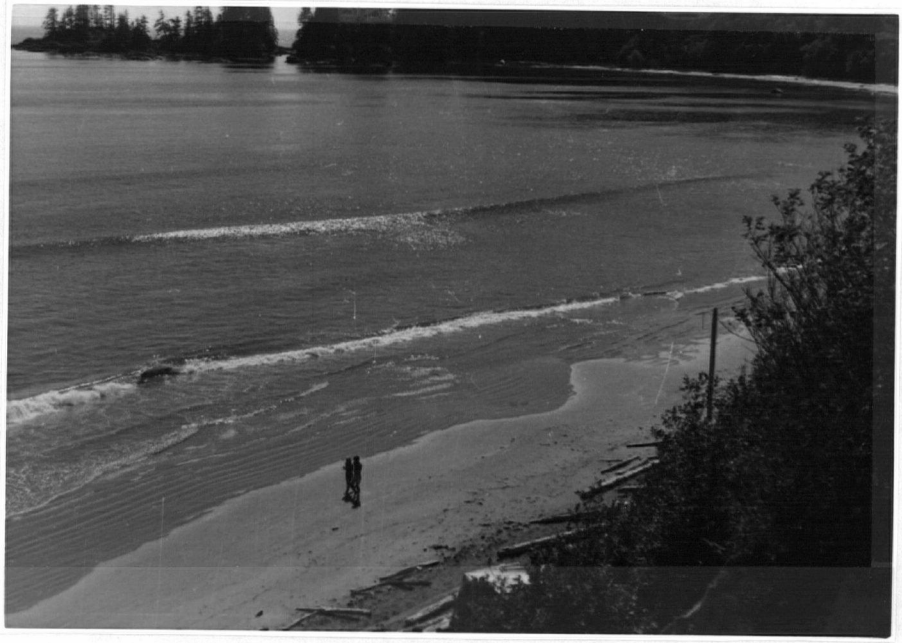

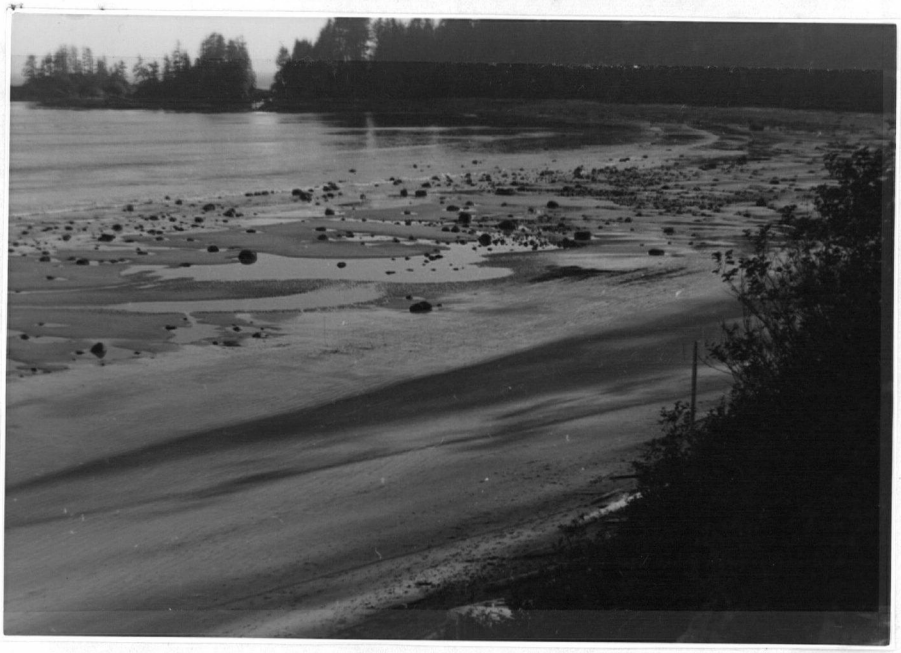

2. PROFILE C ENVIRONMENT

The three trend surfaces (Figures 36 - 1a, 2a, 3a) show that a similar dispersal pattern has again emerged, and furthermore, that they bear a remarkable resemblance to the dispersal patterns found at Profile B, although on a larger scale. Here too, a basic trend would have been obscured by local variability in the hand-countoured raw data (Figures 36 -1b, 2b, 3b). Note that the tracer sources were located 50 feet apart, and the edge of the sample grid was located 20 feet downdrift from the profile line (Figure 35).

From half-hourly profile measurements (Figure 30), it appears that the green tracer source was eroded continuously during flood tide. The red/blue tracer source however, was eroded twice, the red (top) almost totally by flood tide backwash, and the blue (bottom) only slightly by ebb tide backwash. For these reasons, green isopleth values are intermediate between high red values and low blue values in the trend surface diagrams (Figures 36 - 1a, 2a, 3a). The main features of these diagrams are:

- Dispersal patterns are similar regardless of tracer source location
- Two elongate high concentration zones, with long axes oriented normal to the coastline, occur approximately 60 feet apart for the green tracer. For red and blue tracers, these same zones are occupied by low concentrations.

- The locus of maximum green tracer concentration lies within the high zone nearest to the profile line. Maximum red and blue tracer loci occur within a high-concentration tongue in the middle of the grid. The red tracer stems from a high concentration area in the upper left-hand corner of the grid, and was transported in a direction opposed to the drift direction. Blue tracer was simply transported directly from the source in the same direction as the drift direction. Both red and blue tracer maxima lie close to the water table line of emergence (Figures 35 and 36).

FIGURE 35

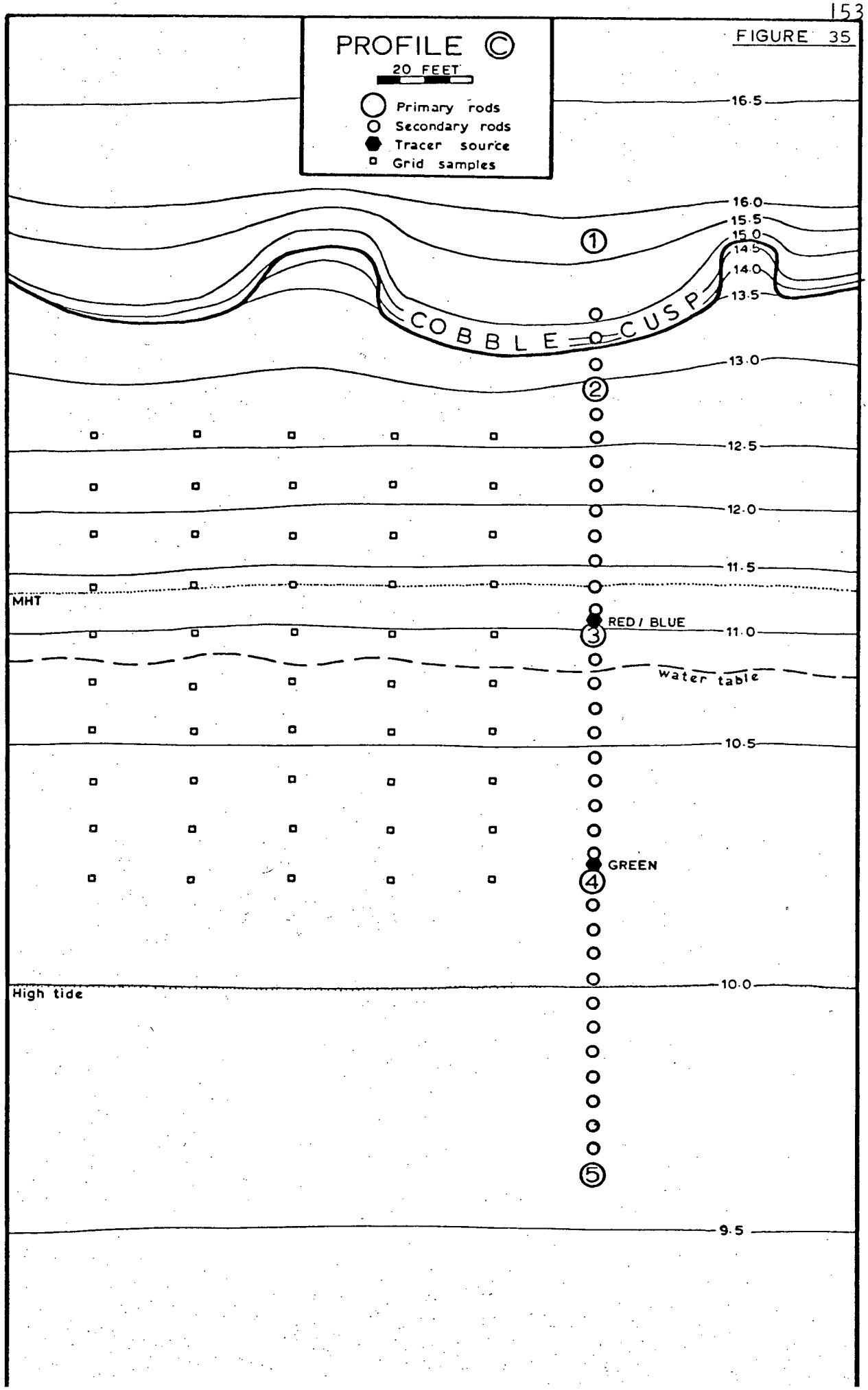
PROFILE ©
20 FEET
Primary rods
Secondary rods
Tracer source
Grid samples
16.5
16.0
15.5
15.0
14.5
14.0
13.5
13.0
12.5
12.0
11.5
11.0
10.5
10.0
9.5
COBBLE CUSP
1
2
3
4
5
MHT
RED / BLUE
water table
GREEN
High tide

FIGURE 36

PROFILE ©

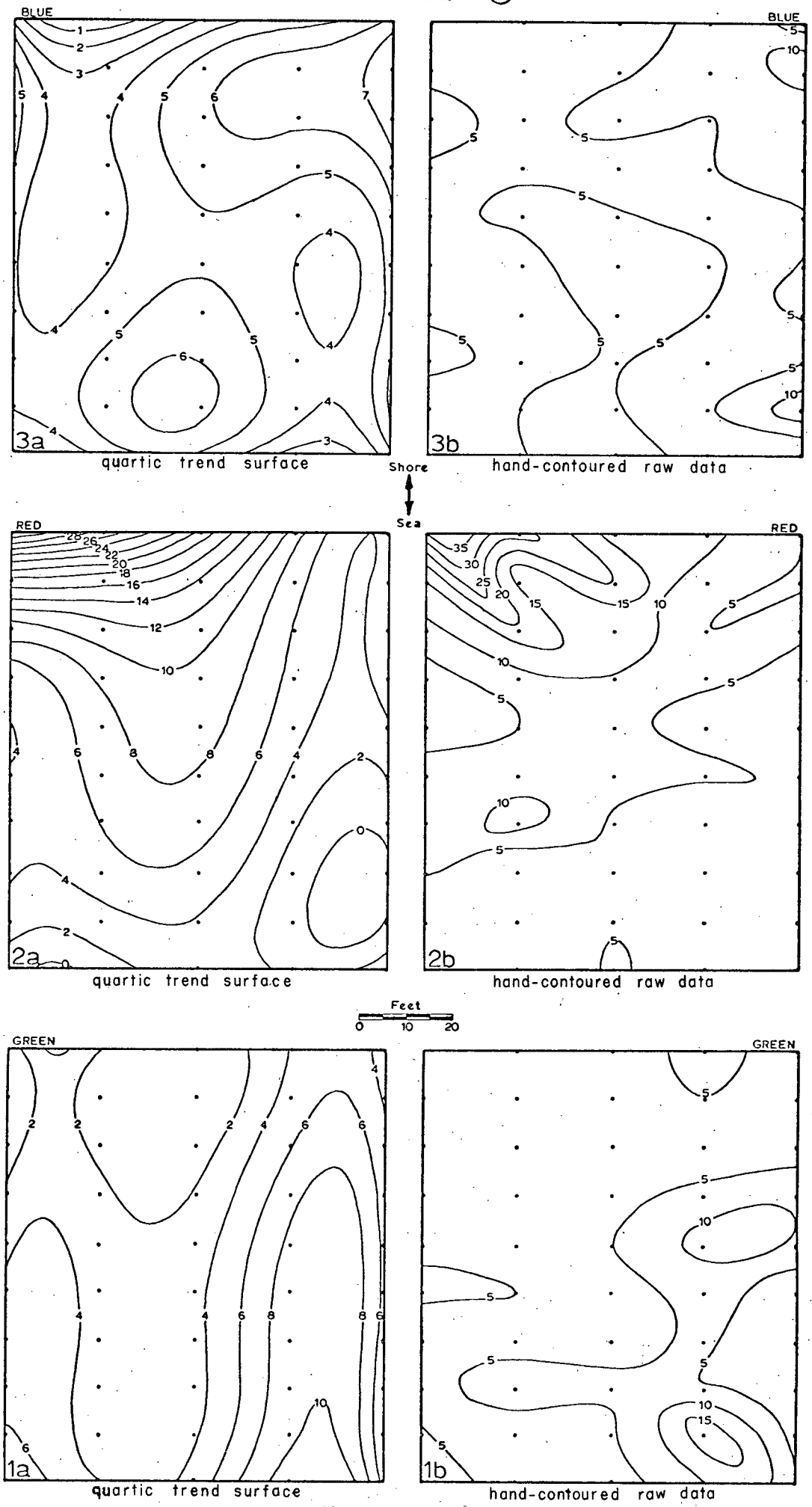

Plate 13a. Profile C shortly after peak high tide. Photograph time 1430 hours.

Plate 13b. Profile C. Photograph time 1600 hours.

Plate 13c. Profile C. Photograph time 1730 hours.

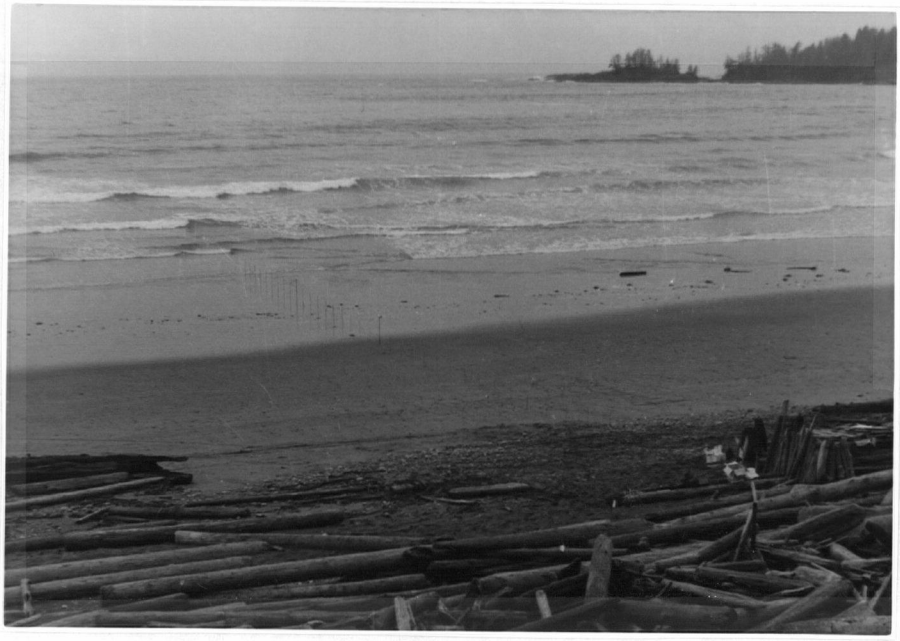

3. PROFILE D ENVIRONMENT

(a) Sand Tracers

These trend surface diagrams (Figures 38 - 1a, 2a, 3a and 1c, 2c, 3c) are completely different from those of Profiles B and C, although a distinct dispersal pattern does exist between them. This pattern is again obscured by local variability in the hand-countoured raw data diagrams (Figures 38 - 1b, 2b, 3b). Due to the prevalence of gravel in the mid-foreshore region, the two tracer sources were spaced widely apart viz. 150 feet (Figure 37). Also, two sampling grids were neccessary, both being positioned over the profile line due to uncertainty about the observed drift direction (Table XIV).

From half-hourly profile measurements (Figure 31), it is impossible to assess the frequency and intensity of erosion of the green tracer source, but it is clear that some did occur during flood tide. The red tracer source was eroded only once viz. at high tide. An insignificant amount of green tracer was transported up the foreshore across the gravel during flood tide, a total of ten particles being noted from all of the small grid samples, Conversely, a considerable amount of red tracer was carried down the foreshore with ebb tide. It was dispersed over the large grid in quantities similar to the green tracer, as shown by roughly equivalent isopleth values on the trend surface diagrams (Figures 38 - 1a, 2a, 3a and 1c, 2c, 3c). The small grid, due to close proximity

of the red tracer source, and also because of its small area, has very high red tracer isopleth values (Figures 38 - 2a, 2c). The main features of these trend surface diagrams are:

- Similarity of green and red dispersal patterns on the large grid, regardless of tracer source location.
- A high concentration zone, oriented sub-parallel to the coastline, occurs on both large and small grids (c/f Profiles B and C).
- The loci of maximum green and red tracer concentrations lie below the bottom right-hand corner of the large grid (Figure 37), resulting in slight skewness of the isopleth lines from true coastline parallelism (Figure 38 - 1a, 3a and 1c, 3c). The locus of maximum red tracer concentration on the small grid lies above the top right-hand corner of the diagrams, resulting in slight skewness of these isopleth lines as well (Figures 38 - 2a and 2c). Note that skewness directions of the large and small grids are opposite to each other, indicating that tracer material was carried southeastwards (right-hand side of the profile line - Figure 37) above and below the gravel zone. The water table line of emergence on the large grid, marks zones of minimum green and red tracer concentrations.

(b) Gravel Tracers

Particle dispersion of the three gravel fractions is shown in Figure 37. The statistically high percentage of recovery and distinctive spread of the two pebble classes,

suggests that their dispersion patterns are meaningful. Cobble recovery, contrary to expectation, was poor (Table XIII), and its dispersion pattern should be considered with reservation.

Trend surface analysis could have been applied to this data, but due to the relatively low concentration of tracer particles over a fairly large area, it was considered impractical. Instead, a point-counter was employed to assign tracer particle concentrations on a rectangular grid. These values were then hand-contoured, and are shown as insets in Figure 37. Mean vector displacement for each gravel size was calculated with tracer source as origin i.e. $(\frac{\Sigma x_c}{n}, \frac{\Sigma y_c}{n})$ where x and y are the coordinates, c is the colour, and n is the number of particles recovered. The mean vectors were then transposed back to the beach plan of Figure 37. The main features of gravel dispersion are as follows:

- All but one of the particles moved northwest from the profile line (a coarse red pebble moved to the right-hand side of the small grid).
- Based on mean vector directions, the blue pebbles migrated up the foreshore, coarse red pebbles remained on contour, and white cobbles migrated down the foreshore. This trend indicates a coarsening texture towards the lower foreshore.
- Based on mean vector lengths, it is evident that the rate of particle movement is inversely proportional to the particle size i.e. blue pebbles moved 34.5 feet, coarse red pebbles moved 23.5 feet, and white cobbles moved 12.0 feet.

FIGURE 37

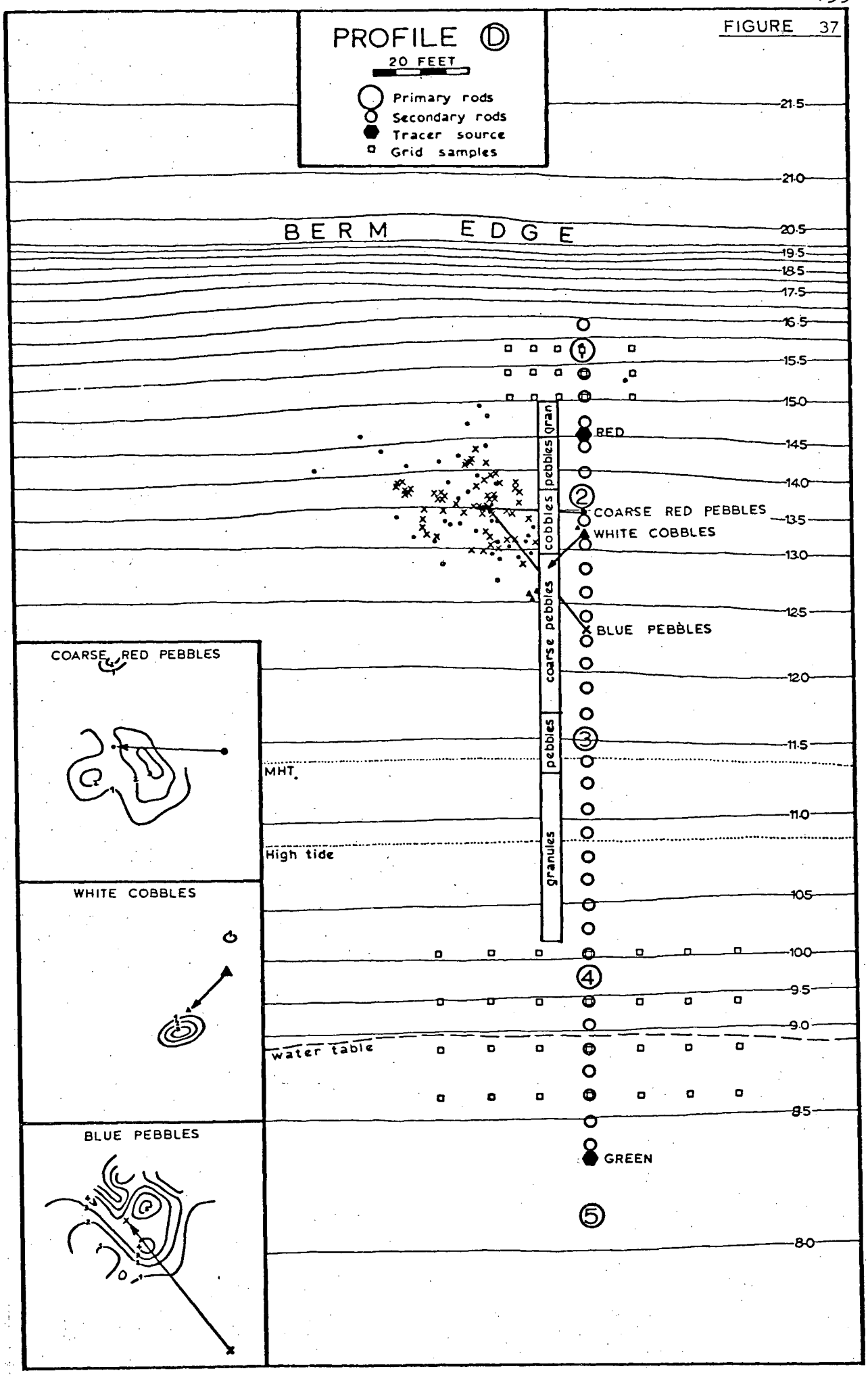
PROFILE D
20 FEET
Primary rods
Secondary rods
Tracer source
Grid samples
BERM EDGE
21.5
21.0
20.5
19.5
18.5
17.5
16.5
15.5
15.0
14.5
14.0
13.5
13.0
12.5
12.0
11.5
11.0
10.5
10.0
9.5
9.0
8.5
8.0
gran
pebbles
cobbles
coarse pebbles
pebbles
granules
RED
COARSE RED PEBBLES
WHITE COBBLES
BLUE PEBBLES
GREEN
MHT
High tide
water table
COARSE RED PEBBLES
WHITE COBBLES
BLUE PEBBLES

FIGURE 38

PROFILE D

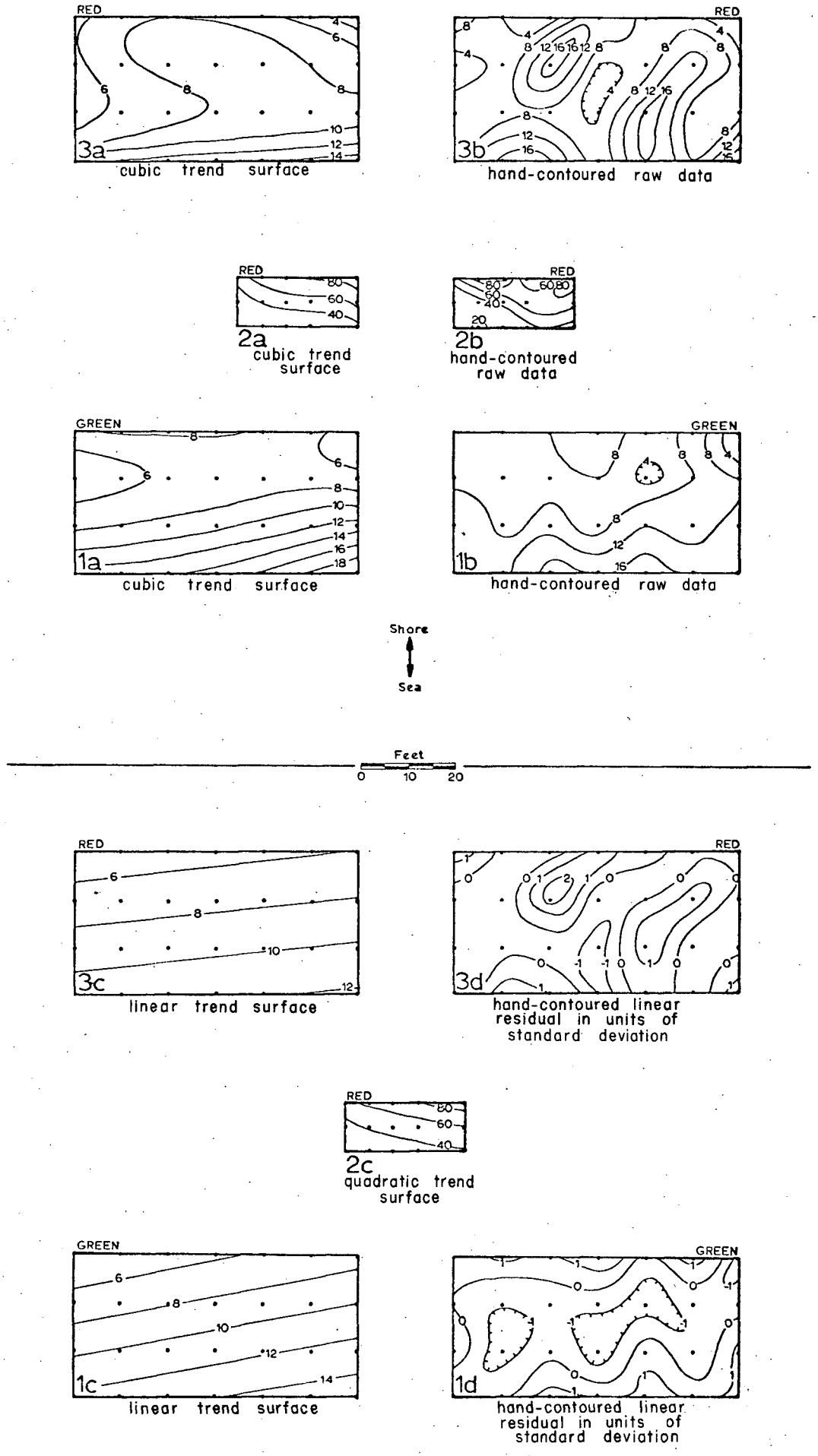

Plate 14a. Profile D shortly after peak high tide. Photograph time 1500 hours.

Plate 14b. Profile D. Photograph time 1630 hours.

Plate 14c. Profile D. Photograph time 1800 hours.

(c) Pebble Orientation and Movement

A total of 68 pebble orientation measurements were made along a one foot wide strip adjacent to the profile line when the tide had receeded. This was accomplished using a 3 foot long steel rod, which was oriented visually to align with the pebble short axes. The bearing and plunge of the rod at each pebble location was then measured and recorded.

A lower hemisphere, equal area Schmidt projection of the results is shown in Figure 39, the main feature of which are:

- The majority of pebbles lie flat on the beach face i.e. short axes are vertical.
- Some pebbles are tilted so that their short axes plunge directly landward - primary trend.
- Some pebbles are tilted so that their short axes plunge landward at an angle to the profile line - secondary trend.

From observation, pebble tilting only occurred in the upper portion of the swash-backwash zone. At the extreme top of this zone close to the swash limit, pebbles remained stationary, and were usually covered by a thin veneer of light-coloured sand by the swash. At the bottom part of the swash-backwash zone, pebbles were rolled down the foreshore by the turbulent backwash.

To check the manner in which discoidal pebbles were rolled approximately 50 of them were painted blue, and placed

on the beach face near the middle of the swash-backwash zone. It was apparent that by far the majority of them rolled edgeways like a wheel - an observation supported by differential abrasion of paint from the pebbles. The edges were scoured clean, whereas the flat sides showed only a few chips in the paint.

Tilting of pebbles in the upper portion of the swash-backwash zone was not due to wave impact, as has been postulated by Emery (1960). Rather, it was due to the force of backwash, which simply lifted the landward edges of the discs as it became deflected around the pebbles.

These three areas of pebble behaviour in the swash-backwash zone are illustrated in Plate 15.

The secondary trend exhibited by the petrofabric diagram (Figure 39) indicates that backwash moved in a northwesterly direction, and by association, so did the swash.

PETROFABRIC DIAGRAM OF PEBBLE SHORT AXES (s), AT PROFILE Ⓓ

FIGURE 39

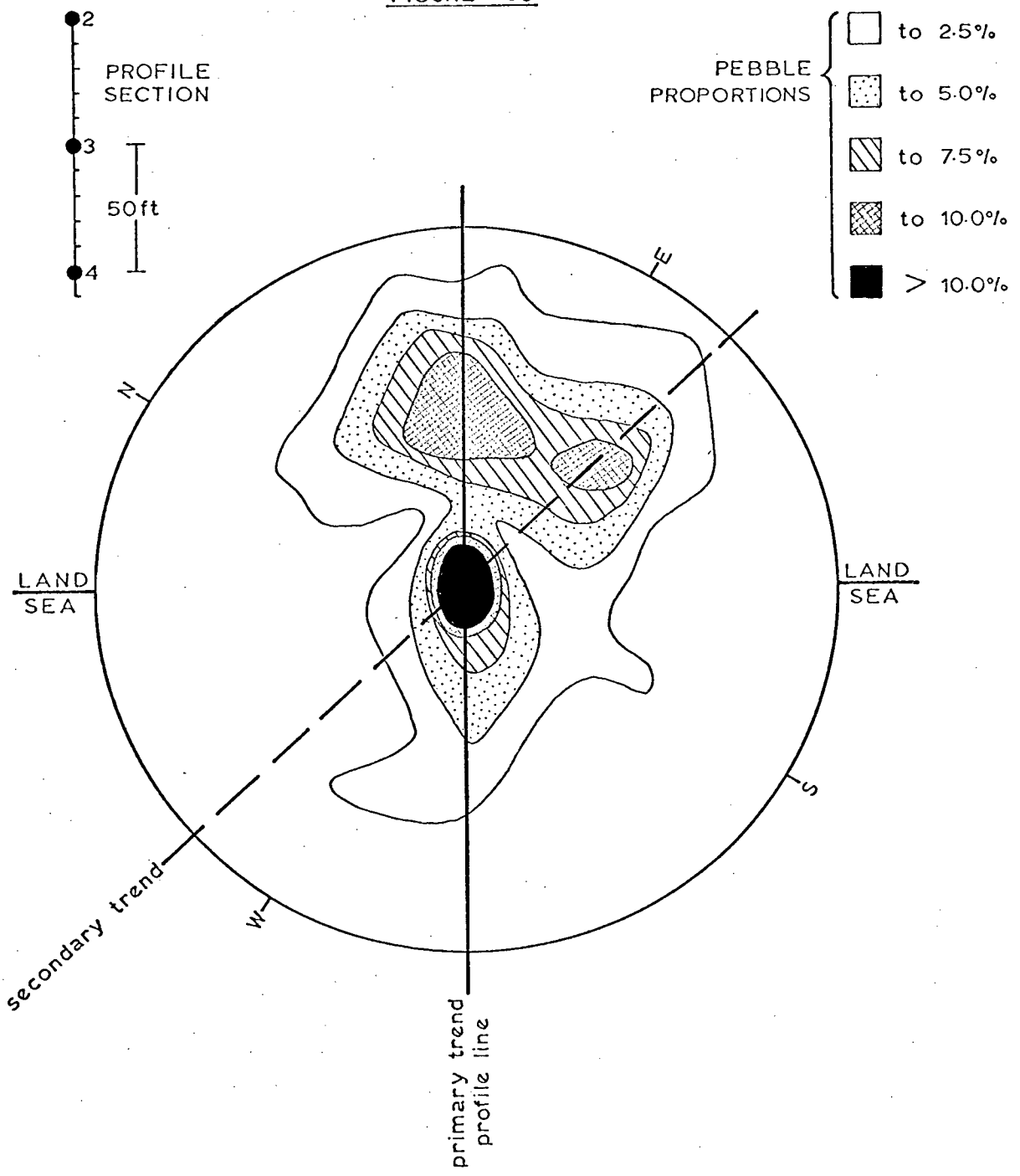

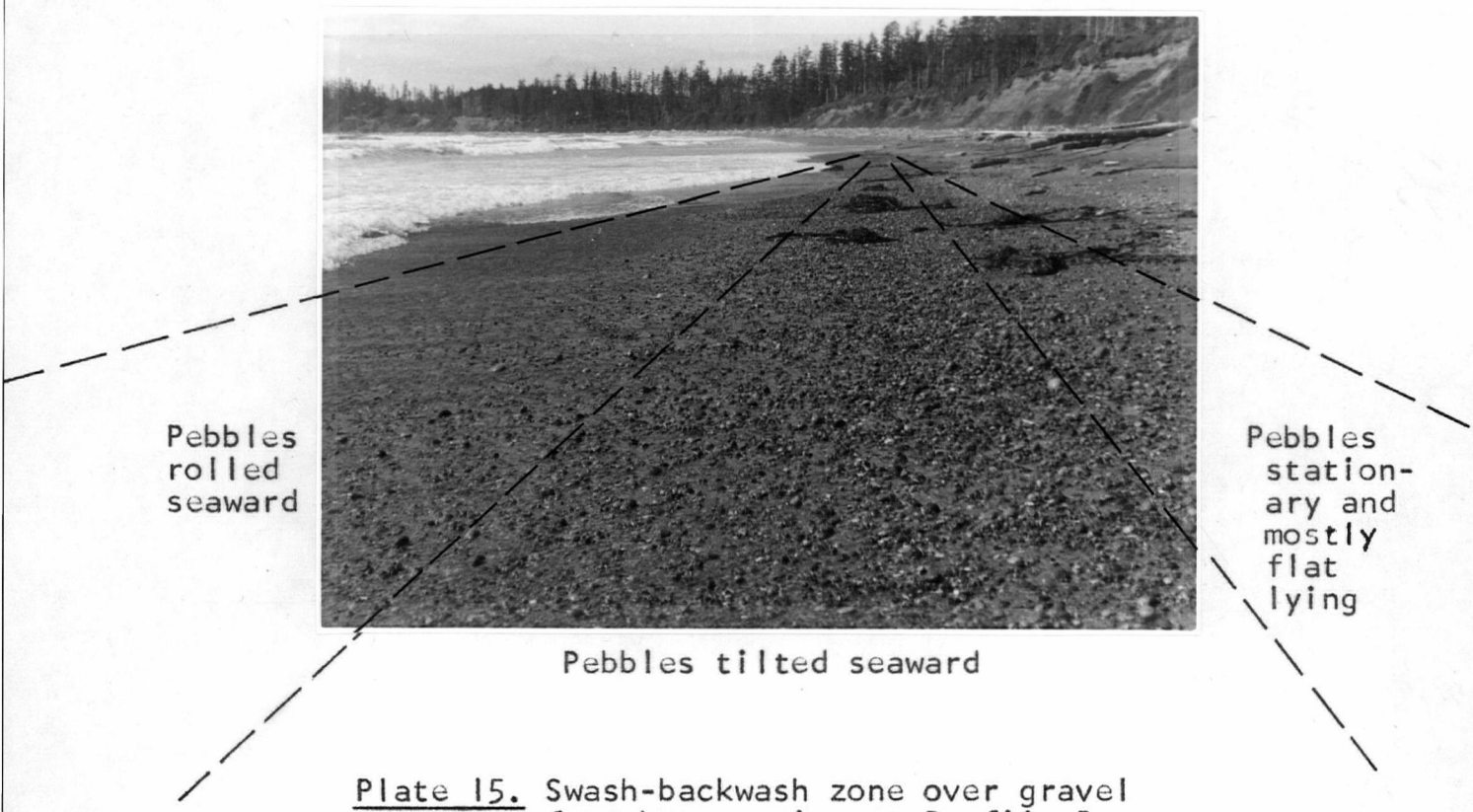

Plate 15. Swash-backwash zone over gravel foreshore region at Profile D.

E. DISCUSSION

1. BEACH CUSP FORMATION

Gravel beaches are commonly marked by the presence of runnels* where littoral currents are weak (Otvos, 1964). It is believed that these features are the precursors to beach cusps, and form in response to differential foreshore erosion by the backwash. The swash is thought to be the agent responsible for transforming these runnel forms into cusp forms, by reducing the runnel lengths through wave impact.

Due to the uniformity of texture of sandy beaches, runnel formation is less evident. However, Profiles B and C both exhibit elongate zones of tracer concentration indicative of their formation. At Profile D, the only indication of possible runnel development is from the third order trend surface of red tracer (Figure 38 - 3a). Here, a short, distorted tongue of tracer extends up the grid, suggesting that a strong northwesterly moving longshore current inhibited its proper development. At Profile C, a series of relict cobble cusps existed along the upper foreshore at the time of the experiment, with a wave length of 90 feet (Figure 35). The elongate zones of tracer concentration, however, were spaced 60 feet apart, thus negating any possibility of a genetic relationship. At Profile B, no relict cusps existed (Figure 33), and the elongate tracer concentration zones measured 30 feet apart.

The mechanism of beach cusp maintainance is fairly

* See GLOSSARY

well documented in the literature, but their origin and regular spacing remain enigmatic. Two recent theoretical explanations of this problem deserve consideration:

Cloud (1966) has analogised a breaking wave to a liquid cylinder, whose diameter equals the wave height. A physical rule exists which states that a liquid cylinder becomes unstable when its length exceeds $2\pi r$, and it then splits into subequal divisions whose lengths are proportional to the cylinder's diameter. Cloud (1966) postulated that the moment a wave collapsed, the segments would shoot forward as a regular spaced array of jets, and that if conditions were suitable for regular segmentation, beach cusps would develop.

Bowen and Inman (1969) have suggested that a formative relationship exists between beach cusps and rip-currents, and that both are dependent on the wave height. When the foreshore dips gently seaward however, they note that the wave length of cusps are generally small compared to the spacing between rip-currents. They suggest that in this case, cusps form in response to an interaction of reformed waves (associated with the bores of breaking waves), and small edge waves* travelling in the surf zone. The length of the edge waves would be determined by the distance between headlands enclosing the bay.

Practical applicability of either of these theories to the field situation is difficult, since the wave character-

* See GLOSSARY

istics which they describe are not readily apparent. The backwash as the agent responsible for cusp genesis seems to be a much more practical answer to the problem.

Consideration of a wedge of water momentarily positioned on a sloping foreshore (the instant a swash reaches its upper limit), its withdrawl down the slope (the backwash) will naturally take advantage of any minor transverse depressions that may exist there. Erosion in these depressions will be more intense than elsewhere, due to the increased volume of water there (Grant, 1948). Depending on the thickness of succeeding water wedges, amalgamation of a number of these transverse depressions into inter-runnel valleys, with distinct spacings, would naturally follow. Runnel shortening by wave impact, and valley transformation into rounded embayments by directed backwash erosion, would then create the problematic cusp forms.

In conclusion then, sediment concentration on the foreshore appears to be largely controlled by the character of the backwash. The swash simply carries sediment (and tracer material) up the beach face, and the returning backwash determines the loci of maximum transverse erosion. The fact that beach cusps apparently form best in the region of the water table line of emergence, is exemplified at Profiles B and C by maximum tracer concentrations in this vicinity. Perhaps the differential susceptibility to erosion of a dry and wet

foreshore (Grant, 1948) accentuates runnel development in this area.

2. LITTORAL DRIFT

Space integrated tracer studies, by virtue of their design, are not suitable for determining littoral drift velocities. Equally good qualitative information can be derived simply by observing swash directions across the foreshore (Table XIV). From the present tracer investigations, all that can be said is that at Profile B, the littoral drift was weak, and in a southeasterly direction; at Profile C, it was relatively stronger, and in a northwesterly direction. The Profile D environment was not so readily apparent, and will be discussed shortly.

Several attempts have been made to measure beach drift velocities from this type of investigation, none of which are really meaningful. Ingle (1966) measured the area between tracer concentration contours at different times during the tidal cycle, to calculate tracer depletion rates from his study area. Wright (1962) drew a longshore section through his study area from the tracer source, and plotted tracer particle counts on the section. Boon (1966) also drew a longshore section, but plotted the trend components instead of raw data values. Both the latter procedures assumed that a zone of high tracer concentration in a downdrift direction represented the "mode" of tracer particle movement. The present study has shown that

these "modes" are actually runnels and bear no relationship to the littoral drift.

At Profile D, sand tracers located seaward and landward of the gravel foreshore region, both migrated in a southeast direction. In the gravel area itself, gravel tracers migrated northwestwards, and pebble orientation measurements indicated that the swash-backwash also moved in a northwest direction. This change in drift direction with tide level was very likely a result of the nearshore bathymetry.

The longshore bar in front of Profile D, although reduced to a wide platform by the summer storm (see chapter on TRANSVERSE PROFILES), was separated from Sand Point by a bathymetric depression of 6 - 8 feet (Map 1). From mid-tide until just prior to high tide, waves approaching this region would undergo a shoaling transformation on the platform and Sand Point, thereby creating a divergence over the bathymetric depression. This wave divergence presumably, resulted in the northwesterly drift at Profile D, and a southeasterly drift towards Sand Point. Between low tide and the mid-tide level, waves simply broke on the seaward edge of the platform, and the effects of wave divergence over the bathymetric depression would be concentrated locally on the foreshore adjacent to Sand Point. Normal southeasterly drift would prevail because of the angular relationship between the breaking waves and the platform. Just prior to high tide, water depth over the plat-

form was probably just too great to have any shoaling effect on the incoming waves, and normal southeasterly drift would again ensue.

X. PLANIMETRIC SHAPE

A. INTRODUCTION

To date, relatively little effort has been directed towards analyzing planimetric shapes of beaches, whereas the literature is well documented with investigations into the topographic changes which occur along transverse profiles. The reason for this disparity is due to the fact that cross-sectional topographic variations result from several cyclic changes in the sea condition (e.g. seasonal, tidal); they are relatively rapid, and therefore easily followed. Planimetric configuration on the other hand, is dictated by an irreversible process which becomes progressively slower as stability is approached, thus making measurement of its time development more difficult.

An embayed coastline will develop wherever unconsolidated sediment separates two resistant headlands. The planimetric shape of the embayment depends principally on the angular approach of swell towards the coastline - when it is parallel, beaches stabilize in a circular arc plan (McLean, 1967), and when it approaches obliquely, as at Wreck Bay, a characteristic shape of different geometric dimensions is formed. Silvester (1960) has named the latter "half-heart shaped bays", and Yasso (1964) "headland-bay beaches". The latter term is preferred, and is defined by Yasso as follows:

> "... the headland-bay beach characteristically has a seaward-concave plan shape, in which the radius of plan curvature becomes greater with increasing distace from the headland."

The coastline in vicinity of Wreck Bay is oriented at approximately 130°, and deep-water swell fronts, as measured from aerial photographs, average 180° (Table III). The bay has developed in response to wave diffraction around the headlands, wave refraction along its shoaling bottom, and wave reflection from Florencia Island and Seal Rock (Fig. 40).

Examination of the shape of Wreck Bay (Map I) immediately suggests conformity between the shoreline in the northwest half of the bay, and the shape of a headland-bay beach. The southeast half appears similar though less well developed, and is oriented in the opposite direction relative to the headland (Wya Point), that is, counterclockwise. Both halves are naturally separated by Sand Point, which extends seaward from the middle of the bay. It was decided to test both halves against log-spiral curvature, and furthermore, to test a number of sections within each half, in order to examine the influence of the latter on the spiral parameters.

B. PLAN DATA ACQUISITION

Plan data was obtained from the beach survey carried out in August 1968.* Since one of the objectives of this study was to determine where cliff recession had exceeded or lagged from theoretical log-spiral curvature, the base of the cliff was used for demarcation of the coastline. A total of 73 rod

* The method employed for horizontal control, see heading TOPOGRAPHY OF WRECK BAY

stations were surveyed along the cliffbase, 49 for the northwest half, and 24 for the southeast half of the bay.

The rod stations were plotted on a cartesian grid with a scale of 1 inch = 200 feet. The grid was oriented so that the ordinate coincided with geographic north and lay tangential to the northwest corner of the bay, and the abscissa was fixed tangential to the southeast corner of Pocket Beach. Each station was then assigned (x, y) coordinates from the grid, which were accurately scaled to 5 feet, and estimated to the nearest one foot.

C. DEFINITION OF A LOGARITHMIC SPIRAL

An equiangular or logarithmic spiral is expressed by the equation:

$$\rho = e^{\theta \cot \alpha} \quad \ldots\ldots\ldots\ldots\ldots\ldots\ldots\ldots\ldots\ldots (1)$$

where ρ = length of the radius vector

e = base of natural logarithm

θ = angle between radius vector and a defined azimuth

α = spiral angle, measured between the radius vector and a tangent drawn to the curve at that point. It is a constant for any given log-spiral.

For the spiral nomenclature used here, see inset in Figure 40. Equation (1) can be rewritten as:

$$\ln \rho = \theta \cot \alpha \quad \ldots\ldots\ldots\ldots\ldots\ldots\ldots\ldots\ldots\ldots (2)$$

which allows plotting of ρ vs θ on semi-log paper as a straight line. Visual inspection of plan data deviation from this

regression line is now possible as shown in Figures 41a, b, c,

D. TEST PROCEDURE

The methods used in this study are essentially the same as those devised by Yasso (1964). The procedure involves selecting an arbitrary log-spiral center, and testing the curve generated therefrom against the plan data as follows:

- The plan data cartesian coordinates are initially converted to polar coordinates using the following transformation equations:

$$r_i = \sqrt{(x_i - X)^2 + (y_i - Y)^2} \quad \ldots\ldots\ldots\ldots\ldots\ldots\ldots (3)$$

$$\theta_i = \arctan \frac{y_i - Y}{x_i - X} \quad \ldots\ldots\ldots\ldots\ldots\ldots\ldots\ldots (4)$$

where (x_i, y_i) = cartesian coordinates of the plan data

(X, Y) = cartesion coordinates of the arbitrary log-spiral center.

- By the method of least squares, the best fitting straight line to $(\theta_i, \log r_i)$ for all i is determined. The equation of the straight line is of the form

$$\ln \rho = a\theta + b \quad \ldots\ldots\ldots\ldots\ldots\ldots\ldots\ldots\ldots\ldots (5)$$

and so by minimizing the function

$$\frac{\sum_{i=1}^{N} \left[\ln r_i - (a\theta + b)\right]^2}{N} \quad \ldots\ldots\ldots\ldots\ldots\ldots\ldots (6)$$

constants a and b are found:

$$a = \frac{N\Sigma(\theta_i . \ln r_i) - \Sigma\theta_i . \Sigma \ln r_i}{N\Sigma\theta_i^{\,2} - (\Sigma\theta_i)^2} \quad \ldots\ldots\ldots\ldots\ldots\ldots (7)$$

$$b = \frac{\Sigma\theta_i^2 \cdot \ln r_i - \Sigma\theta_i \cdot \Sigma(\theta_i \cdot \ln r_i)}{N\Sigma\theta_i^2 - (\Sigma\theta_i)^2} \quad \ldots\ldots\ldots\ldots\ldots (8)$$

(These are shown on the semi-log plots depicted in Figures 41a, b, c and 42a, b, c.)

- The mean squared error between actual radius vectors r_i, and the corresponding theoretical radius vectors ρ_i, are then calculated for each θ_i by means of:

$$\frac{\sum_{i=1}^{N}\left[r_i - e^{a\theta_i + b}\right]^2}{N} \quad \ldots\ldots\ldots\ldots\ldots\ldots\ldots\ldots (9)$$

- By employing a search square procedure, a log-spiral is eventually found whose mean squared error is a minimum. The spiral angle of this best fitting curve is determined by means of:

$$\alpha = \text{arc tan } (^1/_a) \quad \ldots\ldots\ldots\ldots\ldots\ldots\ldots\ldots\ldots (10)$$

E. COMPUTER TECHNIQUE

A program written by P. LeBlond and J.Wilson was used for evaluating plan data on an IBM 360/67 computer. The technique employed was as follows:

A single log-spiral center was arbitrarily chosen and supplied to the program, around which was created a fairly large search square - in the order of 50 sq.ft. The search square was made up of 25 centers, each of which was tested independently against the curvature of the cliffbase. Around the one with least mean squared error was created a second search

square with the same dimensions. This process continued until a center was finally located whose error was a minimum. The search square was then reduced to 1/5 of its original size, and the procedure repeated. When the search square dimensions were eventually reduced to less than 1 sq.ft. the program was terminated.

Computer printout included cartesian coordinates for the best fitting log-spiral center, root mean squared error between the actual and theoretical radius vectors, a tabulation of these radius vectors for Nθ values, and the a and b regression line constants. A sub-routine was also written to plot the regression lines shown in Figures 41a, b, c and 42a, b, c by a Calcomp Plotter attached to the computer.

As an indication of the effciency of this program, less than 3/4 hour of computer time was required to locate 6 best fitting log-spiral centers, and to plot their respective regression lines. Yasso (1964), with a similar study performed on spitbars, required 260 hours to locate 33 spiral centers, using IBM 1620 and IBM 7090 computers.

F. DESCRIPTION OF BEACH SECTIONS STUDIED

1. NORTHWEST HALF OF WRECK BAY

- Cliffbase at LSC - The cliff section extends from Quisitis Point to Sand Point. 7 Plan data points are located at the cliffbase behind Lost Shoe Creek. The best fitting log-spiral curve is shown as dashed line in Figure 40, and the

center is marked by a triangle.

- Spitcrest at LSC - This cliff section also extends from Quisitis Point to Sand Point. The 7 plan data points located at the cliffbase behind Lost Shoe Creek have been exchanged for 7 points along spitbar crest. The best fitting log-spiral center is marked by a circle in Figure 40.
- NW Corner - Extends from Quisitis Point to the mouth of Lost Shoe Creek. The best fitting log-spiral center is marked by a circle in Figure 40.

2. SOUTHEAST HALF OF WRECK BAY

- SE Pocket Beach - This cliff section extends from the southeast corner of Pocket Beach to Sand Point. The best fitting log-spiral curve is shown as dashed line in Figure 40, and the center is marked by a triangle.
- SE Corner (1) - The cliff section extends from the southeast corner of Wreck Bay to Sand Point. The best fitting log-spiral center is marked by a circle in Figure 40.
- SE Corner (2) - Same as SE Corner (1).

Parameters of the best fitting log-spiral curves to these sections are shown in Table XVII, and where available, those from Yasso (1964) have been included for comparison.

G. RESULTS

1. NORTHWEST HALF OF WRECK BAY

Examination of the plots of Figures 41a, 41b, and

41c clearly illustrate the excellent fit between plan data and theoretical log-spirals. The dashed curve shown in Figure 40 (Cliffbase at LSC) has the greatest root mean squared error of the three tests made in the northwest half of the bay, and yet the log-spiral fit is still very good.

By exchanging 7 cliffbase points for 7 spitcrest points, the root mean squared error decreased from 92.02 feet to 69.09 feet indicating improved log-spiral curvature. Furthermore, the spiral angle decreased in size (Table XVII), and the spiral center moved towards the headland and beach (northwest direction).

For the third test (NW Corner), the root mean squared error decreased still further to 31.02 feet, the spiral angle was reduced, and the spiral center moved closer towards the headland and beach. The improved fit of this cliff section is due to its shorter length. It involves fewer data points than the other two tests, and therefore incorporates fewer local distortions into the calculations.

2. SOUTHEAST HALF OF WRECK BAY

The computer program was altered here to generate log-spiral curves in a counterclockwise direction, that is, the mirror image of the spiral nomenclature diagram shown in the inset of Figure 40. It is interesting to note that the 4 beaches studied by Yasso (1964) on both the east and west coasts of the United States, the 6 beaches mentioned by

Silvester (1960) along the east coast of South Africa, and the northwest half of Wreck Bay, are all clockwise spirals. These areas are all affected by waves which approach the coastlines on the same side.

Examination of the plots of Figures 42a, 42b and 42c shows that only poor correspondence between this half of Wreck Bay and log-spiral curvature exists. The dashed curve shown in Figure 40 (SE Pocket Beach) has a very large root mean squared error, and its departure from the cliffbase is seen to be gross. A large departure is evident southeast of Sand Point where the cliff face consists of exposed glaciofluvial outwash (Figure 40). This area is marked by an incipient cuspate foreland (see chapter on BEACH STRUCTURES), and can be seen in Figure 2 as a slightly convex seaward portion of the cliffbase. The fact that the spiral angle of this curve is small, and that its spiral center is close to the headland, appears to contradict earlier observations made for the northwest half of Wreck Bay. In reality, comparison of the spiral parameters of different beaches is not a valid procedure, since the hydrodynamic environment at each location is not the same. It is believed that were the cliffbase to approach log-spiral curvature more closely for this half of the bay, the spiral angle would decrease further, and the spiral center would move closer to the headland.

The final cliff section tested (SE Corner)

unexpectedly yielded two spiral centers, thus indicating that for very poorly fitting curves there may be no unique solution. They were found by supplying the computer at different times with centers located at widely separate points. For (1) the first curve obtained, the root mean squared error is very large viz. 196.02 feet, the spiral angle is very small, and the spiral center is virtually adjacent to the headland. This log-spiral curve opens rapidly and is controlled mainly by data points located along the "elbow" of the cliff section (near Wya Point). For (2), the root mean squared error improved somewhat to 143.96 feet, the spiral angle became very large, and the spiral center is located more than a mile away from the headland and beach. This log-spiral curve thus opens slowly, probably turning about the center at least once before coinciding with the cliff section, and data points located along the "arm" (near Sand Point) bear stronger influence on the curves position. Were the cliffbase of this section to approach log-spiral curvature more closely, a unique spiral center would develop which, as noted earlier, would move towards headland and beach as the fit improved still further.

H. INFERENCES FROM GLACIOFLUVIAL OUTWASH EXPOSED CLIFF SECTIONS

With reference to Figures 40, 41a, b, c and 42a, b, c, it is apparent that approximately half of the cliff face consists of exposed glaciofluvial outwash, the rest being densely covered with underbrush and large trees. The age of these

trees, some of which grow at the cliffbase, are estimated at close to 200 years old, thus indicating the quasi-permanence of these cliff sections. Cliff sections exposing glaciofluvial outwash are generally seaward of the log-spiral curves, and timbered sections are generally landward of the curves, thus suggesting that cliff erosion is presently active in areas that would bring the two halves of Wreck Bay closer to log-spiral curvature.

Another point to notice in Figure 40, is that glaciofluvial outwash is generally exposed in cliff sections which face the open ocean. These areas are directly exposed to strong moisture-laden wind during the winter months, suggesting that this is the agent responsible for cliff erosion at the present time. In support of this contention is the fact that nowhere was cliff undercutting through wave action evident in February 1969 (see chapter on TRANSVERSE PROFILES), whereas numerous small landslides could be heard rattling down the cliff face every few minutes. Saturation of the glaciofluvial outwash by wind-driven rain would increase the pore-water pressure and decrease cohesion between the sedimentary particles, thereby promoting the small landslides.

It seems apparent therefore that the cliffbase at Wreck Bay has been stable for a relatively long time and that its planimetric shape is close to equilibrium* with the prevailing hydrodynamic environment. Limited erosion of

* See GLOSSARY

the cliff seems to occur as a result of saturation by moisture-laden wind, and this is confined to areas where retreat of the cliff would bring the planimetric shape of the two halves of Wreck Bay closer to log-spiral curvature.

I. THE EFFECT OF WAVES AND CURRENTS IN THE DEVELOPMENT OF HEADLAND-BAY BEACHES

The relative importance of refracted, diffracted and reflected waves in sculpturing the geometry of headland-bay beaches is unknown. It is apparent however, that the "arm" section of a headland-bay beach tends to align itself parallel to waves which have been simply refracted in the shoaling bay. The "elbow" section on the other hand, is subjected to the combined effects of both wave diffraction around the headland, and wave refraction on the shoaling bottom.

LeMehaute and Brebner (1961) have indicated the presence of a "diffraction current" leeward of a headland, and state that "... a current always exists from a high wave region to a low wave region". This phenomenon is similar to light diffraction around an object, resulting in a penumbra zone. The existence of such a current at Wreck Bay is indicated by two features:

- The spitbar in front of Lost Shoe Creek points northwestwards towards Quisitis Point (Map 1).
- Sand in suspension is carried from the nearshore zone in the "elbow", out towards Quisitis Point (see Frontispiece). The sand is initially put into suspension by turbulence

created by waves impinging against the boulder bed in this area (Map I).

Opposed to this nearshore diffraction current, a foreshore littoral current always moves in the opposite direction, that is, from Quisitis Point towards Lost Shoe Creek (see chapter on SAND MOVEMENT BASED ON WAVE PARAMETERS). This suggests that a circular current close to shore may be responsible for sculpturing the area leeward of Quisitis Point.

Sylvester (1960) conducted a model tank study on shoreline erosion, and assumed "equilibrium" of a half-heart shaped bay to exist when a single wave broke simultaneously around the whole length of the bay. For this assumption to be valid, bathymetric contours would have to be concentric between headlands, and each one would have to possess log-spiral curvature. These features are not apparent at Wreck Bay, but examination of the first diagram in Sylvester's (1960) paper reveals that the rate of erosion decreases significantly as the bay approaches planimetric equilibrium. This observation confirms the equilibrium status arrived at earlier for Wreck Bay.

J. GENERAL RELATIONSHIPS BETWEEN BAY GEOMETRY AND LOG-SPIRAL PARAMETERS

For the northwest half of Wreck Bay it was found that the planimetric shape approached log-spiral curvature more closely as the spiral parameters underwent the following changes:

- The root mean squared error decreased,
- The spiral angle decreased.
- The spiral center moved in towards the headland and beach.

Cliff sections examined in the southeast half of Wreck Bay deviated markedly from log-spiral curvature, and the spiral parameters were unpredictable. At the end of the Holocene Transgression, Florencia Island presumably constituted the upcoast headland for a clockwise headland-bay beach in a southeast direction and subsequently, Seal Rock became the upcoast headland. Although both are isolated from the coast today, they still have a profound effect on the morphology of the southeast portion of the bay. If they were suddenly removed, the southeast portion would prograde until Wya Point became the downcoast headland of a single headland-bay beach occupying the whole of Wreck Bay.

In conclusion, the following remarks on bay geometry and spiral parameters seem appropriate. They were derived at from logical reasoning, and their validity requires testing in a model tank:

- The equilibrium position of the spiral center, and the value of the spiral angle, depends on two factors: The distance between headlands, and the angle between prevailing deep-water wave fronts and the coastline. Knowing these two factors, calculation of an equilibrium planimetric shape for an embayed coastline should be possible. Furthermore, if

spiral parameters change sequentially as the coastline approaches planimetric equilibrium, then valid predictions on coastal mutation should be possible.

- If two headlands are separated by unconsolidated sediment, the downcoast one will limit the depth of coastal embayment since littoral drift past it will cease when the "arm" section is parallel to the refracted waves in the bay.
- If only one headland exists, downcoast embayment will progress until its log-spiral curvature "captures" the upcoast section, and the headland becomes isolated from the coast as an island.

Location	No. of plan data points	Approx. length of section (miles)	Cartesion coordinates of log-spiral center (feet) X	Y	Approx.* distance of center to head-land(ft)	Spiral angle (de-grees)	Root mean squared error (feet)
			NORTHWEST HALF OF WRECK BAY				
Cliffbase at LSC	49	1 3/4	712.0	7636.0	320	53.18	92.02
Spitcrest at LSC	49	1 3/4	624.0	7744.0	290	51.02	69.09
NW Corner	24	3/4	526.7	7919.8	280	48.77	31.02
			SOUTHEAST HALF OF WRECK BAY				
SE Pocket beach	24	1 1/2	9963.7	287.5	110	44.02	193.78
SE Corner (1)	20	1 1/4	11203.0	1358.2	10	24.53	196.02
SE Corner (2)	20	1 1/4	5294.4	-820.8	5500	81.96	143.96
			Yasso (1964)				
Spiral Beach, New Jersey	22	1/2			10	61.49	.82
Halfmoon Bay, California	57	6			250	41.26	183.7
Drakes Beach, California	20	4			3000	85.64	16.1
Limantour Spit, California	24	11			14000	82.20	234.4

* This measurement was obtained by scaling the distance between log-spiral centers and the nearest headland. Small rock islands adjacent to the headlands proper are of relatively minor importance, and were therefore not considered.

Table XVII. - Parameters of Best Fitting Log-Spiral Curves and Other Pertinent Information.

Figure 40. Planimetric shape of Wreck Bay and fitted log-spiral curves.

- The log-spiral curves shown as dashed lines, are for Cliffbase at Lost Shoe Creek and Southeast Pocket Beach, and their centers are shown by small triangles. Other spiral centers are incicated by small circles.

- The spitbar crest is shown as a dotted line, and cliff sections exposing glaciofluvial outwash, as dotted strips.

- Spiral nomenclature used in the text is shown in the inset.

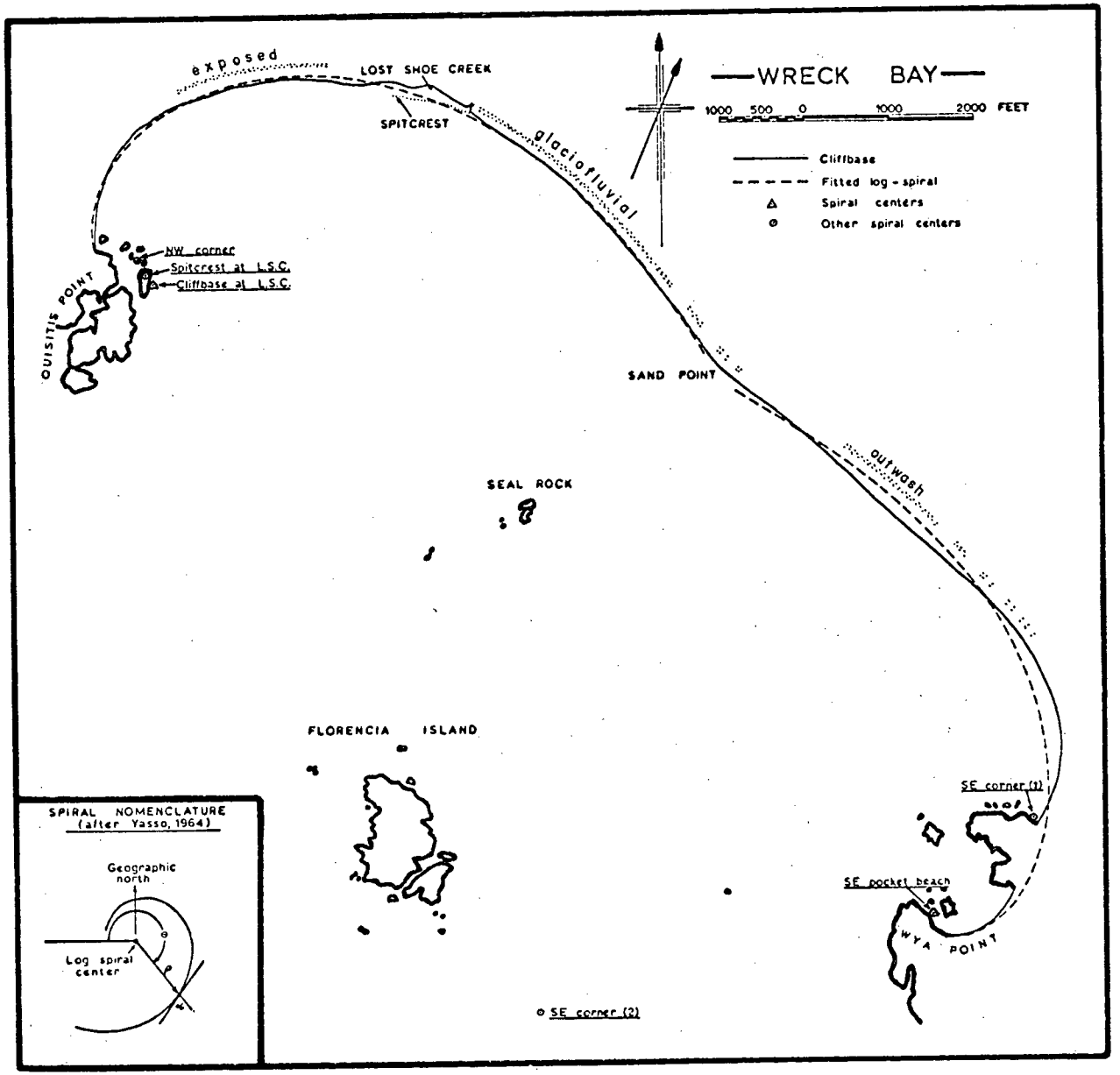
WRECK BAY
1000 500 0 1000 2000 FEET
Cliffbase
Fitted log - spiral
Spiral centers
Other spiral centers
exposed
LOST SHOE CREEK
SPITCREST
glaciofluvial
NW corner
Spitcrest at L.S.C.
Cliffbase at L.S.C.
QUISITIS POINT
SAND POINT
outwash
SEAL ROCK
FLORENCIA ISLAND
SE corner (1)
SE pocket beach
WYA POINT
SE corner (2)
SPIRAL NOMENCLATURE
(after Yasso, 1964)
Geographic north
Log spiral center

FIGURE 40

Figures 41a, b, c. Regression line plots of three log-spiral curves tested in the northwest half of Wreck Bay.

- Radius vector ρ is plotted on a logarithmic scale, and arc θ on an arithmetic scale.
- Constants a and b are indicated in the regression line equations of each diagram.
- Cliff sections exposing glaciofluvial outwash are indicated by dotted strips.

N.W. HALF OF WRECK BAY

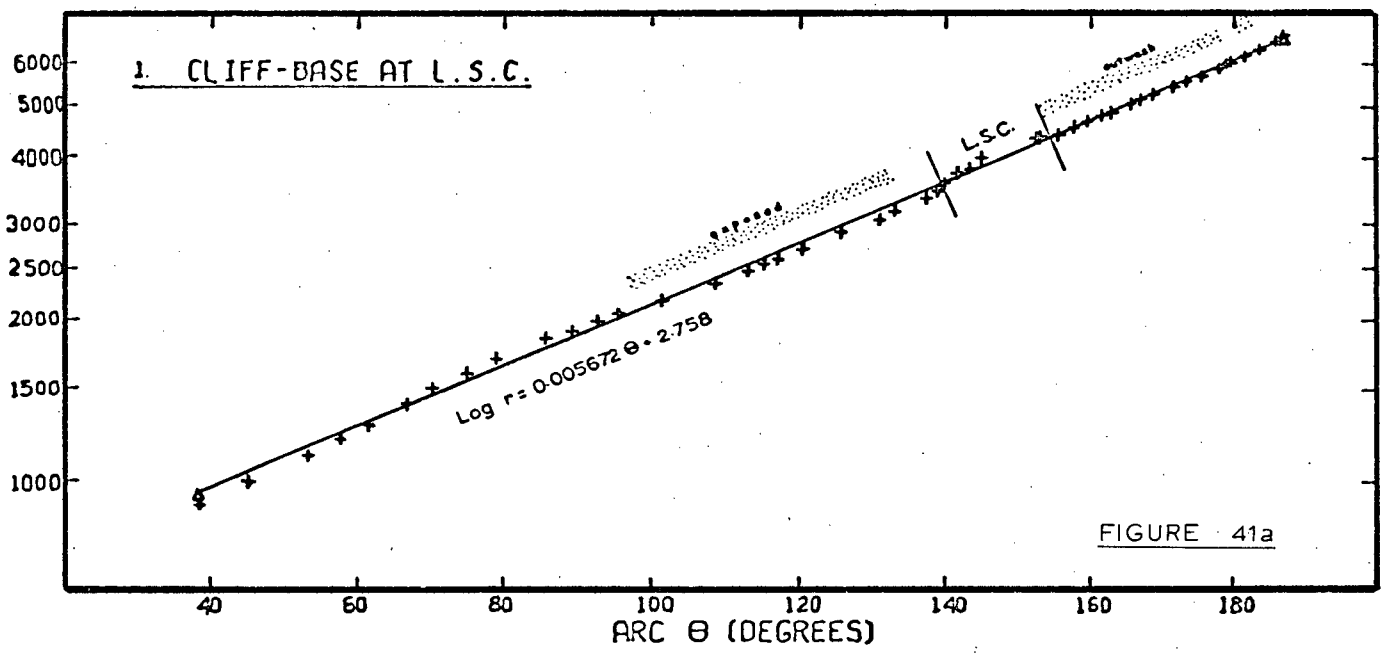

FIGURE 41a

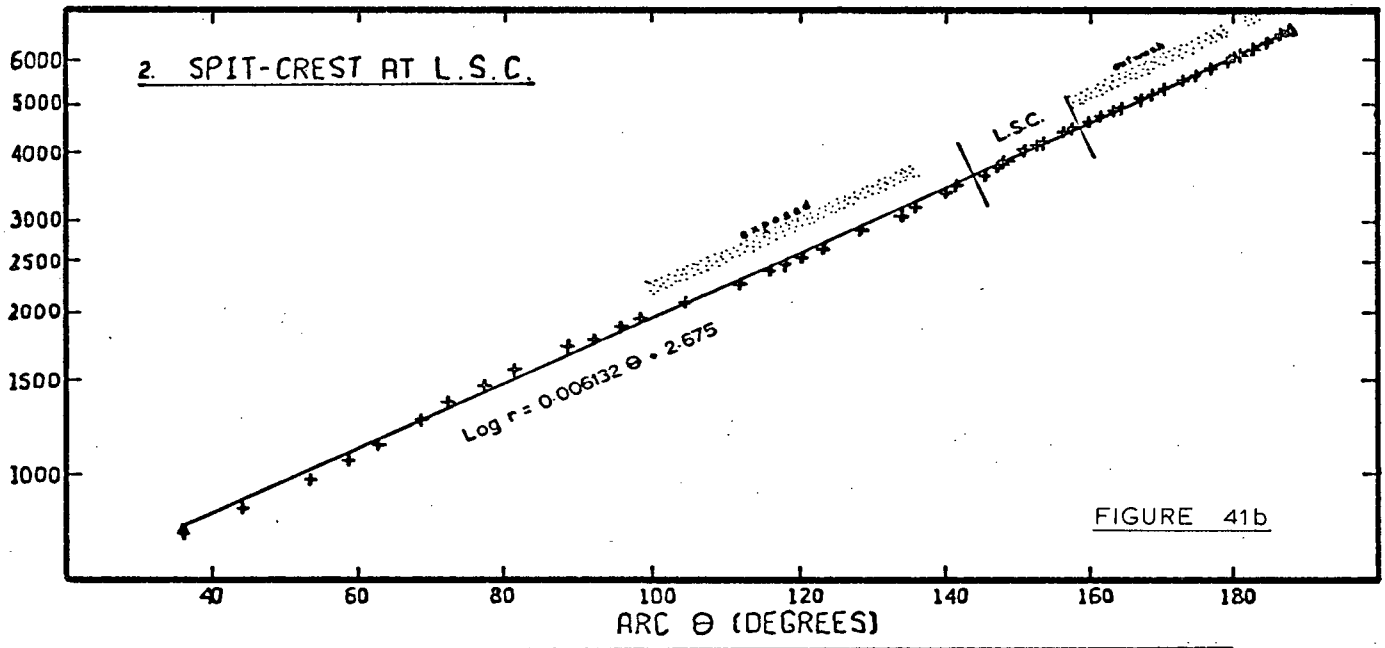

FIGURE 41b

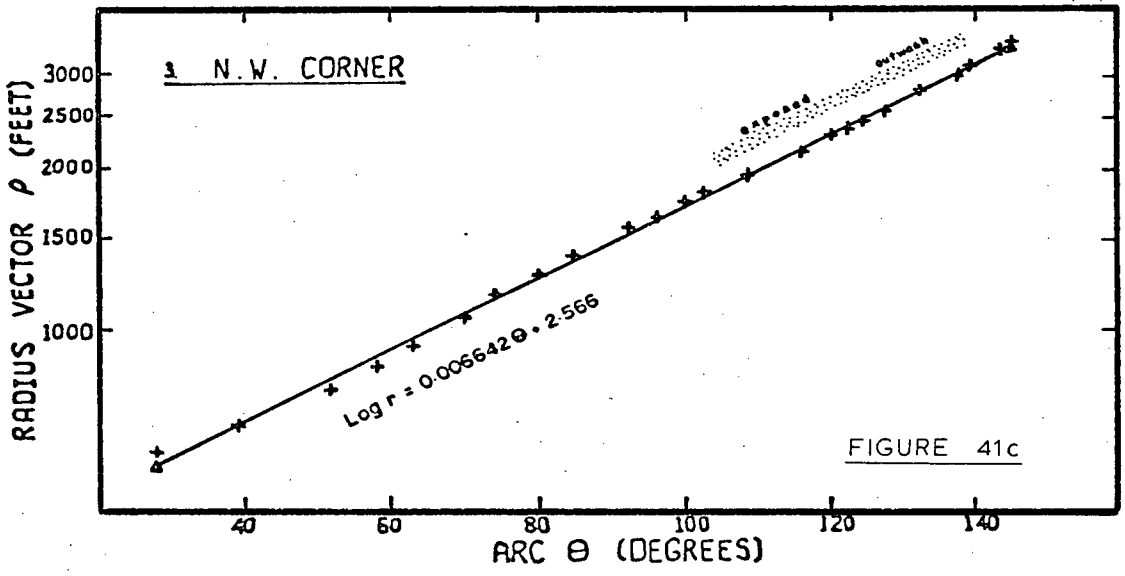

FIGURE 41c

Figures 42a, b, c. Regression line plots of three log-spiral curves tested in the southeast half of Wreck Bay.

- Information indicated is the same as Figures 41a, b, c.

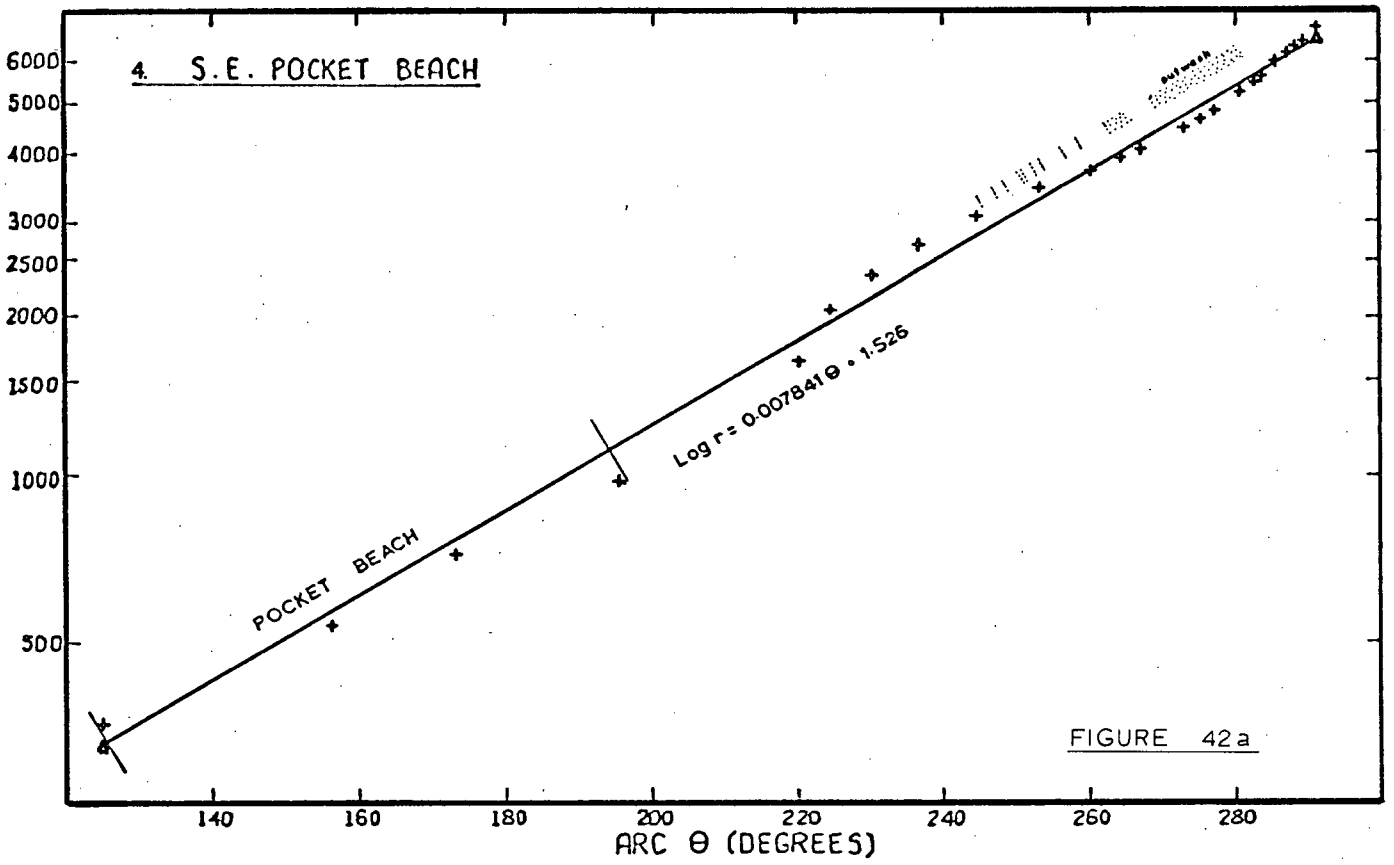

FIGURE 42a

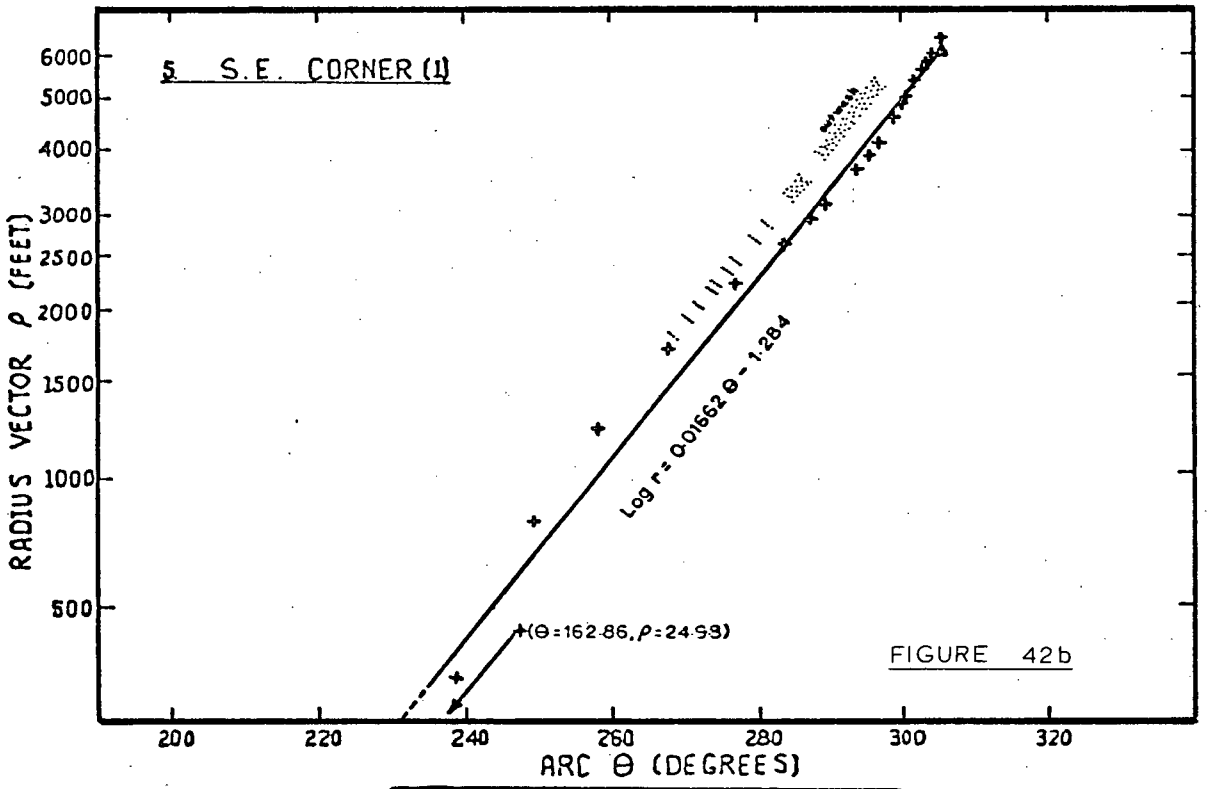

FIGURE 42b

6. S.E. CORNER (2)

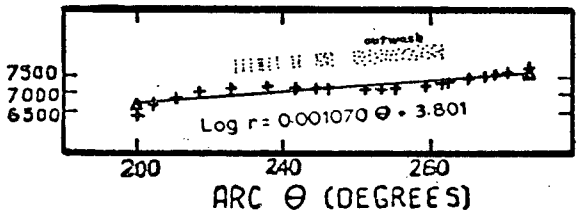

FIGURE 42c

XI. BEACH STRUCTURES

A. INTRODUCTION

A number of different beach forms exist on the beach at Wreck Bay. They can be naturally grouped according to size, into major and minor structures. The major structures are semi-permanent in that they survive for a period of a year or longer, and are of importance in many engineering problems concerned with coastal stability. The minor structures are cursory, usually being destroyed after a few hours; however when they do become preserved in the geological column, they provide valuable information on the paleo-environment.

Some of the structures listed below have been discussed in detail in other chapters. They are simply mentioned here for completeness, and reference to the pertinent chapters will be made when appropriate.

B. MAJOR STRUCTURES

1. BERMS

In places no berm exists at all, e.g. behind Profile F; whereas elsewhere, up to four berms characterize the backshore, e.g. between Profile C and the spitbar (see chapter on TRANSVERSE PROFILES, and Map 1).

2. BARS

A well defined bar extended from the foreshore between Profiles C and D southeastwards towards Sand Point during the summer of 1968 (Plate 16). Its crest was exposed at low

tide, and was separated from the foreshore by a 2 foot deep trough. A less well defined bar extended in the opposite direction, from the foreshore between Profiles E and F northwestwards towards Sand Point. This bar was never exposed, and its presence was deduced largely from the observation that waves broke in this region, and then reformed closer to shore (see chapter on TRANSVERSE PROFILES, and Map I).

3. SPITBAR

A body of sand and gravel has diverted the mouth of Lost Shoe Creek for about 1250 feet northwestwards. It does not fit the definition of a spit precisely, since the latter should terminate in deep water. The term "spitbar" has therefore been used to describe it (see chapters on SEDIMENT SIZE ANALYSES, PLANIMETRIC SHAPE, and ECONOMIC GEOLOGY; also Map I).

4. SYMMETRICAL CUSPATE FORELANDS

Sand Point, located in the middle of the beach, is a good example of a symmetrical cuspate foreland, and has formed in response to wave diffraction around Seal Rock. Swell entering the bay between Quisitis Point and Florencia Island is split by Seal Rock, and a pattern of intersecting diffracted waves extends from its lee back to Sand Point (Frontispiece and Figure 2). These diffracted waves generate littoral currents over a relatively short beach section, which converge in the vicinity of Sand Point (see chapters on SEDIMENT SIZE ANALYSES, and SAND MOVEMENT BASED ON TRACER DISPERSION; also Map I).

An incipient cuspate foreland exists approximately ½ mile southeast of Sand Point. It owes its origin to a similar but less intense wave pattern. Swell approaching the bay is split by Florencia Island, one part diffracting in between Seal Rock and the island, and the other part between Wya Point and the island. This pattern of intersecting diffracted waves extends back to an area on the beach located about 500 feet southeast of Profile E (see Frontispiece and Figure 2). Littoral drift at this profile was found to be in a northwesterly direction, thus indicating that a very short beach section is involved in nourishing the incipient cusp (see chapters on SAND MOVEMENT BASED ON WAVE PARAMETERS, and PLANIMETRIC SHAPE; also Map I).

C. MINOR STRUCTURES

I. BEACH CUSPS

During the summer of 1968 relict cobble cusps existed on the backshore behind Profile C, and along the seaward edge of the spitbar. These forms survived throughout the summer, but lost their classical shape with time (Figure 35). A series of seven photographs of the relict cobble cusp behind Profile C were taken at two day intervals, from one neap tide period through till the next. Contrary to expectations, neap tides were found to be responsible for the partial destruction of the cusp form, by dislodging cobbles and rolling them down the foreshore. Spring tides on the other hand, packed

the cobbles into a neat pile, but in so doing, the horn of the cusp became rounded. Three photographs of the series are shown in Plates 17a, b and c.

Cusps of fine sand developed periodically along the foreshore during the summer at locations where littoral currents were weakest, from Profile B to Profile C, and from Profile E to Profile F (Frontispiece and Plate 18b). Their existence correlated very well with tidal range, being best developed during neap tides, and absent during spring tides. A positive correlation appeared to exist between the cusp amplitudes, and the wave heights affecting the different areas (see chapter on SAND MOVEMENT BASED ON TRACER DISPERSION; also Map 1).

2. BEACH RIPPLES

(a). Backwash Ripples

These features commonly occurred on sandy foreshores but below the water table, they were slowly destroyed by sand creep and rills. Individual ripples were very uniform and long, usually in excess of 50 feet; they had low amplitides of about 0.1 feet, and wavelengths of approximately 2 feet (Plates 18a and 19a). In cross-section they appeared to be slightly asymmetrical, with the seaward sides being flatter than the landward sides. They formed in the turbulent zone of the backwash, and the ripple forms would remain motionless or move slowly seaward, but never opposite to the direction of backwash movement. These bedforms would actually be classified as dunes

by Simons et al (1965), and belong to their "lower flow regime". They appeared to form best during spring tides (Plates 17a, b, and c), and were commonly seen in the embayments of sandy cusps (Plate 18b).

(b) Current Ripples

These occurred in several places on the foreshore where unidirectional currents existed, e.g. in shallow channels behind beach ridges where ripples indicated water movement parallel to the shore (occasionally present in areas between Profiles C and D, and E and F); in rip-current channels, where ripples indicated water movement towards the sea (present throughout the summer between Profiles A and B); and where the lower foreshore was affected by very small waves and a weak, uniform littoral current existed (at Profile A).

Individual ripples were curved in shape, and short and irregular in length, averaging 0.5 feet; they had low amplitudes of about 0.1 feet, and short wave lengths approximately 0.4 feet (Plate 18c). In cross-section they were strongly asymmetrical, with the side from which the current came being convex, and the leeward side being short and steep. These bedforms also belong to the "lower flow regime" of Simons et al (1965), and would be classified as true ripples. They formed as a result of a weaker current velocity than that which produced the backwash ripples.

3. RHOMBOID PATTERNS

Considerable confusion exists in the literature regarding these features. For example, Emery (1960) and Hoyt and Henry (1963) refer to them as "rhomboid ripple marks", whereas Bascom (1964) calls them "backwash diamonds". Emery (1960) states that they form only on the lower saturated parts of beaches, at slope angles between 2° and 10°. Hoyt and Henry (1963) on the other hand, found at Sapelo Island, Georgia, that they formed in equal numbers in the upper and lower foreshore, at slope angles between 0.5^{o} and 2°. Both Hoyt and Henry (1963) and Bascom (1964) describe the dimensions of the rhombs, and refer to their "depth" as being between 1/16 and 1/4 inch - hence probably their description as "ripple marks". The writer considers this depth dimension insignificant in comparison to the other rhomb dimensions, and therefore the term "rhomboid pattern" is believed to be more appropriate.

Three distinct types of rhomboid pattern were observed at Wreck Bay:

- The most common type occurred on the slightly flat seaward side of backwash ripples (Plate 19a). Beach slopes varied from 0.8^{o} to 1.4^{o}, and although it formed on both upper and lower foreshores, it rapidly disintegrated below the water table due to sand creep and rills. The rhomb apices measured about 45°, shoreward pointing ones consisting of light coloured sand grains and shell-hash, and seaward

pointing ones of dark coloured heavy minerals. It appeared to form suddenly as the last thin film of backwash receded from the ripples.

- Developed only in the southeast portion of the bay between Profiles F and G, was a rhomboid pattern quite different in dimensions and mode of formation to the type described above. It developed on a smooth unrippled sand surface with beach slope of 0.8° to 1.0°. Two requirements were apparently essential for its formation: a high proportion of heavy mineral and shell-hash components in the beach sand, and a succession of thin sheets of fresh water washing over the beach surface. Ample fresh water emerges from the cliffbase as springs in this vicinity, but where it washes down the beach face as an undisturbed glassy sheet the pattern does not form. Rhomb apices measured approximately 30° and their compositions were exactly opposite to those described above viz. shoreward pointing ones consisted of dark coloured heavy minerals, and seaward pointing ones of fine shell-hash (Plate 19b). The forms were relatively unstable, and slowly mutated with time.
- The third type was similar to other rhomboid patterns except that it possessed no seaward pointing apices, and actually resembled glacial crag-and-tail structures in miniature (Plate 19c). It was a common feature on unrippled sandy beaches containing small isolated pebbles, and was particu-

larly noticeable in areas containing abundant fine shell-hash. The apices of the forms, which pointed landwards, measured approximately 70°, and were composed of dark coloured heavy minerals thus resembling the second pattern described above. All apical points were marked by small pebbles, which in every case, were oriented with their longest axes parallel to the beach. They appeared to form as the last thin film of backwash retreated down the foreshore. As soon as a pebble rolled to a stop, shell-hash and light coloured sand would momentarily continue to be transported around its edges, until it finally settled into this pseudo-rhomboid pattern as the last water dissipated. Above the water table these forms remained until the next flood tide, but below the water table, they were rapidly destroyed by sand creep.

4.RILL MARKS

These forms developed on sandy foreshore areas, below the water table, and some time after the tide had receded. Two general types were recognized, depending on the condition of the foreshore. Where the foreshore was smooth and unrippled, they would commence "growth" well below the water table as a series of tiny irregular channels. These channels would extend themselves up the beach, until a number of them united into a single large channel, which terminated growth close to the water table line of emergence. The dendritic form which

developed resembled the lower part of a river system, where the river channel opens up into a delta towards the sea.

The other type of rill mark occurred where the foreshore possessed backwash ripples (Plate 18a). Here, a similar sequence of events would commence on the seaward side of the ripples, but once the rill had crossed a ripple crest, surplus water trapped in the inter-ripple trough would be drained, and a dendritic pattern towards the land would develop. Although this form was shorter than the type described above, it resembled an entire river system from the source to the delta. Occasionally, rill "capture" resulted in doubling of the rill length, and water would be channeled across the upper delta by small levees.

The manner of growth of these features is rather complex. Ground water escaping from the beach is apparently directed towards the channels because of their slightly lower elevation. The growth point of a rill seems to extend up the beach face as very fine sand gets slumped into the channel head; the sand then moves slowly down the channel in a semi-suspended state like a slurry.

5. SWASH MARKS

These formed regularly on sandy foreshore areas, and consisted of arcuate lines of shell-hash, light coloured sand and debris. Above the water table their outlines lasted for a few hours, whereas below it, they were rapidly destroyed by sand creep.

6. SAND DOMES

These occurred on the sandy foreshore, above the water table, and close to the swash limit. They develop when water from the first swash sinks into dry beach sand, and intergranular air becomes compressed in the more porous sand layers, thus forcing the overlying wet material up like a laccolith. The second swash usually results in their decapitation, leaving a ring of dark coloured heavy minerals around the point of air escape.

7. ORGANISM MARKINGS

These were not too common at Wreck Bay, except in the lee of Quis'tis and Wya Points (see chapter on MARINE LIFE).

Plate 16. View looking northwest from Sand Point at low tide, waves can be seen breaking on the longshore bar in front of Profile D.

Plate 17a. View of a relict cobble cusp on the upper foreshore at Profile C during a period of neap tides (22 July 1968). The photograph was taken from rod C3; C1 is evident on top of the cusp, and C2 on the sandy foreshore in front of the cusp.

Plate 17b. As Plate 17a during the succeeding high tide period (25th July 1968).

Plate 17c. As Plate 17a during the succeeding neap tide period (30th July 1968).

Plate 18a. Rills actively eroding backwash ripples in the vicinity of Profile C. Note rill "capture" by some of them across two adjacent ripples.

Plate 18b. Sandy beach cusps with backwash ripples in the embayments. View from the cliff edge between Profile B and the mouth of Lost Shoe Creek. (Compare this photograph with Plate 23a, which is the same view taken in winter.

Plate 18c. Current ripples on the lower foreshore at Profile A, indicating current movement towards the land (right-hand side of photograph). Rod A7 is seen in the foreground, and Quisitis Point in the background.

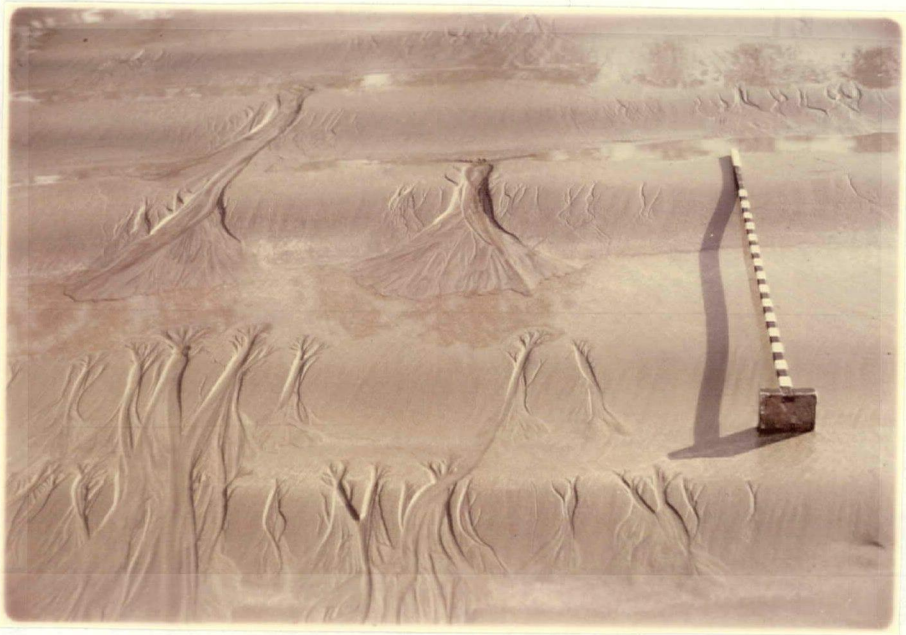

Plate 19a. Rhomboid pattern developed on the seaward side of backwash ripples. Landward pointing apices consist of light coloured minerals and shell-hash. The photograph was taken near Profile F.

Plate 19b. Rhomboid pattern developed on a gently sloping, unrippled foreshore between Profiles F and G. Landward pointing apices are of dark coloured heavy minerals.

Plate 19c. Pseudo-rhomboid pattern developed in the lee of small pebbles. Landward pointing apices are of dark coloured heavy minerals. The photograph was taken between Profiles F and G.

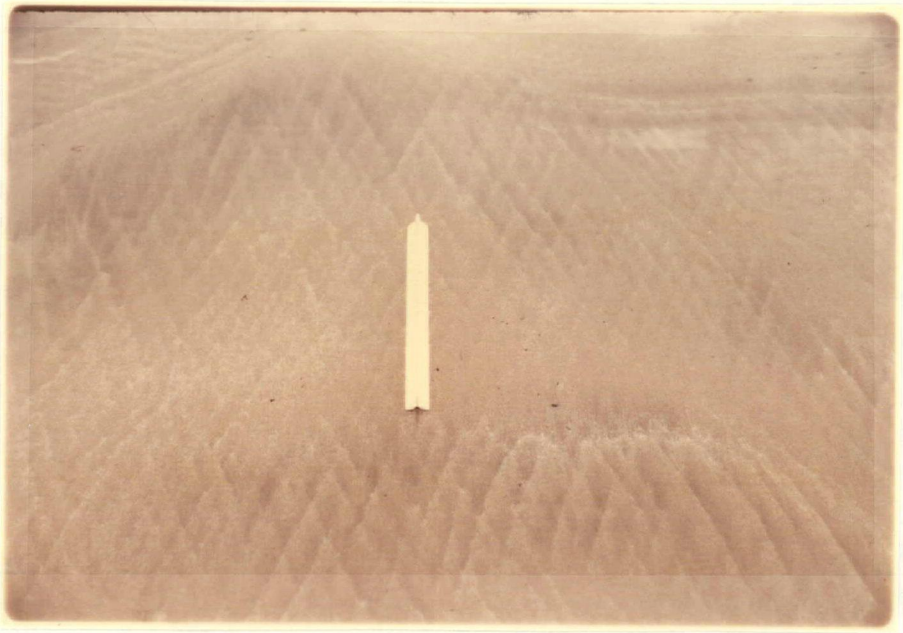

land
sea

land
sea

land
sea

D. MINOR WAVE TYPES ASSOCIATED WITH BEACH STRUCTURES

1. REFLECTED WAVES AND WATER SPOUTS

In the vicinity of Profile D, a steep gravel step existed at the base of the foreshore in early summer. Seaward from there, a shallow channel approximately 100 feet wide and 2 feet deep, isolated the longshore bar described earlier from the beach (see Map 1). With the start of flood tide, small spilling waves would wash over the bar, cross the channel, and impinge against the gravel step (Plate 20a). Part of the waves energy was dissipated as swash which permeated rapidly into the gravel, and the remaining energy was reflected as an ondular bore (P. LeBlond, 1970 , personal communication), or reflected wave (Plate 20b). This event helped to maintain the configuration of the gravel step. The reflected wave then travelled back across the channel, and collided with the next incoming spilling wave over the crest of the longshore bar. Usually these two waves approached each other at an angle resulting in a "water spout", which traversed rapidly along the bar crest (Plate 20c). This event helped to maintain the longshore bar, by preventing fine sand from being swept into the channel with each incoming spilling wave.

2. HYDRAULIC JUMP WAVES

These waves were named by Grant (1948), but are also known as ondular bores by physical oceanographers (P. LeBlond, 1970, personal communication). They commonly occurred along

sandy beach sections where incident waves were high. Their formation depended on the relative velocities of the backwash and incident waves. If the incident translatory waves velocity exceeded that of the backwash, it would break and spill over the backwash for a short distance up the foreshore. On the other hand, if the backwash velocity exceeded that of the next incoming translatory wave, the turbulent backwash heavily charged with suspended sand, would over-ride the clear water of the incident wave. In this case hydraulic jump waves or ondular bores would form, and remain essentially stationary as the two water masses moved rapidly in opposite directions, one on top of the other (Plate 21a). On occasions, when incident wave and backwash velocities were both very high, a hydraulic jump wave would momentarily rise up to about 2 feet, and then collapse. The effect of this event on the foreshore was to transport material scoured by the backwash, past the shoaling zone, and thus temporarily remove it from the beach environment.

3. SAND WAVES

The southeast corner of the beach between Profiles F and G was unique, in that a number of perennial fresh water springs emerged from the cliffbase. These springs coalesced on the backshore into small creeks, which cut through the summer berm and left it as a series of discrete sandy mounds (Map I). On the 30th July 1968, 32 of these creeks were found

cutting through the summer berm, and in so doing, behaved as natural flume channels responsible for the formation of sand waves lower down on the foreshore.

The sand waves were spaced fairly regularly at about 1.5 feet apart, and after a few seconds, would disintegrate due to some flow rate disturbance higher up in the flume. This formation-disintegration process had a periodicity of about 6 per minute. According to Inman (in: Shepard, 1963), the flow rate changed from high (sheet flow) to very high (sand waves), and Bascom (1964) states that when the flow rate is between 2.2 and 2.5 feet per second, the forms migrate against the current. They would therefore belong to the "upper flow regime" of Simons et al (1965), and correspond to the "anti-dunes" of Gilbert (1914). Migration rate of the sand waves up the foreshore was approximately 2 feet per minute, and was achieved by sheet flow of sand particles from the lee of one sand wave, to the front of the next one. Just prior to disintegration of the sand waves, they characteristically assumed the shape of a bull's horns (Plate 21b). The waves themselves had little relevance to beach structures, but as mentioned earlier, the fresh water creeks were responsible for considerable erosion of the summer berm and upper foreshore.

Plate 20a. A small spilling wave approaches the gravel step near Profile D. The photograph was taken at the start of flood tide.

Plate 20b. A few seconds after Plate 20a. A short swash traversed up the gravel foreshore, and a reflected wave travelled back across the trough towards the longshore bar.

Plate 20c. A few seconds after Plate 20b. The reflected wave (left-hand side of photograph) collided with the next incoming spilling wave (right-hand side of photograph). A water spout formed which travelled along the crest of the longshore bar. Note waves breaking in the distance on Sand Point.

Plate 21a. Hydraulic jump waves or ondular bores, developed by turbulent backwash over-riding the incoming spilling wave. The photograph was taken at Sand Point.

Plate 21b. Sand waves with characteristic "bull's horn" shape. The photograph was taken between Profile F and G, just seaward from where a fresh-water creek cut through the summer berm.

XII. ECONOMIC GEOLOGY

A. REGIONAL ASPECTS

Economic interest in the region around Wreck Bay began in 1898, at a time when lode and placer production of gold was at high level in British Columbia. Prospectors were successful in locating fine placer gold on the beach at Wreck Bay, and along Kennedy River, a number of small gold-bearing quartz veins were worked. V. Dolmage of the Geological Survey of Canada briefly described the area in 1919 and 1920, and mentioned that: "This part of the island is thinly populated, chiefly by Indians of a most primitive type." Since this time, a number of small companies and promotion groups have shown interest in the beach placers, and even today a few individuals derive some income from working beach concentrate during the winter (Plate 23a).

In the late 1950's attention was briefly directed towards the "black sands" magnetite content at Wreck Bay (Holland and Nasmith, 1958), and in 1961, Brynnor Mines commenced development of a magnetite ore-body on Draw Creek, which flows east into Barkley Sound. Since production began in April 1962 until the end of 1966, the mine produced 4,400,000 tons of ore (Eastwood, 1968). Several other small iron and copper showings in the area have been known for a long time, and occur where granodiorite or diorite of the Kennedy Batholith have intruded Quatsino Limestones.

B. SUMMARY OF GOLD PRODUCTION AND SAMPLING AT WRECK BAY

The total amount of gold extracted from the black sands is unknown, but from records that were kept in the past, it is apparent that rich pay streaks were located and mined.

From 1896 until 1901, $20,589 worth of gold was recovered ($15.20/oz.), and in 1919, when Dolmage visited the area, two samples collected at the cliffbase produced phenomenal assays: (i) concentrates from 3 pans - $416.70/cu.yd., (ii) unpanned average black sand - $115.20/cu.yd. ($20.67/oz). In 1920, the Ucluelet Placer Mining Company was formed, and during that summer, $9,400 worth of gold was recovered from 600 yards of gravel ($15.75/oz). From 1931 to 1935, a total of $1,997 was taken ($21.60/oz). In 1936, Stevenson conducted a semiquantitative investigation on the recoverability of gold from a number of different environments, the results of which are summarised in Table XVIII.

Sample locations	Number of samples	Oz's/cu.yd.		Average value/cu.yd.*
		Range	Average	
Beach black sands	5	0.048-3.488	1.086	$38.01
Gravel from cliff face	7	Tr-0.096	0.030	$1.05
Gravel from behind cliff	4	Tr-0.009	0.002	$0.08
Gravel in Lost Shoe Creek	1	0.024	0.024	$0.84

* ($35.00/oz)

Table XVIII. Summary of semi-quantitative Investigation of Gold Recoverability by Stevenson (1936).

All mining and sampling was conducted in the vicinity of Lost Shoe Creek. On the strength of this, the present investigation was designed to emphasise examination of this particular beach section.

C. PRESENT INVESTIGATION AND RESULTS

In conjunction with general field sampling of the area (see APPENDIX), a number of additional samples were panned to concentrate gold and magnetite for later evaluation in the laboratory. Approximately 10 lbs. of material was used in each case, and this was panned down to about 1 lb.

In the laboratory, magnetite was first extracted with a hand-magnet, and its proportion by weight roughly estimated. The balance of the heavy mineral concentrate was then processed on a Super Panner, and the number of "colours" counted and isolated. The results of this work are listed in Table XIX.

It should be mentioned here that during the summer of 1968, five prospect-holes were dug at various places on the beach by an unnamed exploration company. A mechanical shovel was used, and the holes measured about 6 feet across, and 6 feet deep. An attempt by the writer to sample the beach in depth with hand-auger and casing met with little success; consequently, one of the prospect holes was channel sampled in four 1.3 foot lengths. This particular hole was located 850 feet northwest of Profile D, and 90 feet from the cliffbase,

just behind the winter berm crest (Plate 23b).

D. ESTIMATED VALUE OF GOLD NEAR LOST SHOE CREEK

The diameter of gold colours was arbitrarily broken down into three catagories, as shown in Table XIX, to simplify determination of a mean particle size. Colours were examined under a petrographic microscope with a micrometer eye-piece (Plate 22).

Results in Table XIX confirm that the backshore near Lost Shoe Creek contains the highest gold values. We will therefore consider samples from NWR-5a (1,375 feet northwest of Lost Shoe Creek) to SER-5a (1,250 feet southeast of Lost Shoe Creek), for a total beach section of 2,625 feet (Map 1). These 9 samples together contained a total of 72 gold colours. Assuming the category midpoints to be: large = 300μ, medium = 150μ, and small = 50μ, multiplying these values by the number of particles in each category, and dividing the summed total by 72, we obtain the mean diameter of the colours, viz. 111.1μ.

Hite (quoted in Bateman, 1965) has estimated that 17×10^6 gold discs having an area of 0.1 sq.mm., averaged about 1 oz. troy for the Snake River, U.S.A. No specification on disc thickness was made, so this value is assumed to be constant regardless of source. These discs have a diameter of 11.28μ (from $\pi r^2 = 100\mu$). Therefore $(17 \times 10^6 \times 11.28)/111.1 =$ 1,700,000 colours (approximately), with diameter 111.1μ, would average 1 oz. troy.

Now each of the 9 samples originally consisted of about 10 lbs. of material. We can therefore say that 72/1,700,000 oz's of gold were recovered from 9/200 tons of material from the backshore. The amount of gold contained in 1 ton of backshore material is given by:

$$\frac{72}{1,700,000} \times \frac{200}{9} = 0.0009412 \text{ oz's.}$$

The value of this at \$35.00/oz = 3.289¢/ton or 5.271¢/cu.yd. (using the equivalent: 1¢/ton = 1.6¢/cu.yd., Bateman, 1965).

This figure represents the tenor of surface material derived from 2,625 feet of backshore. The average width of backshore in this region is 100 feet, and using the reported depth of 20 feet (or more) to the surface of the grey clay (Stevenson, 1936), gives dimensions for the zone in yards as follows: length 875, breadth 33, and depth 7. Therefore volume of the zone = 202,100 cu.yds. Assuming extension of the surface tenor with depth, we obtain the approximate value of gold contained in this zone:

$$\text{Value} = 0.05271 \times 202,100$$
$$= \$10,650.00.$$

E. DISCUSSION AND ECONOMIC SIGNIFICANCE

The figure derived at above should be regarded as a minimal value for the following reasons: Results from the prospect hole (Table XIX) indicate an increasing number of gold colours with depth - a situation probably valid for the rest of the beach as well. Furthermore, it is likely that a

number of very fine gold particles were lost through aeration during field-panning, or did not separate cleanly from the he heavy mineral concentrates on the Super Panner. This fact is borne out by the lack of results from either the cliff-face or Lost Shoe Creek, since Stevenson (1936) and others report that "colours can be obtained almost anywhere in the gravels" of the cliff-face.

Due to the exploratory nature of this study, the expense of fire-assaying large bulk samples was not deemed neccessary. The tenor derived at for the surface material (5.271¢/cu.yd.) is sub-marginal, however, in considering accessibility to the area, and the immediate abundance of water, re-evaluation in light of similar low-grade placer deposits elsewhere is required. Bateman (1965) reports that part of the Klamath Mountain Placers, consisting of cemented Miocene gravels, were economically hydraulicked with a tenor of $2\frac{1}{2}$ - 3¢/cu.yd. Similarly, some Tertiary Sierra Nevada Placers averaging 10¢/cu.yd., were also economically mined. It therefore appears likely, that by employing a cheap method of concentration such as the hydraulic method, the entire calculated zone could be mined at a profit during one summer season. Confirmation of this view should, however, first be sought through a detailed sampling program conducted in three dimensions. A point in favour of this type of mining, is that with the passing of winter, the beach would be naturally

restored to the satisfaction of conservationists.

The high surficial values obtained by Dolmage (1919), and in depth by early prospectors and Stevenson (1936), was a result of concentration over hundreds of years due to the continual "jigging" action of the surf. Low surficial values obtained in the present study suggest that most of the gold has already been taken, and therefore the deposit would appear to be capable of supporting only a single season's work.

Concerning magnetite estimates shown in the right-hand column of Table XIX, a positive correlation is indicated with gold in samples from Beach (berm) and the prospect hole. Furthermore, Holland and Nasmith (1958) report that the beach is most concentrated with magnetite along the backshore, between berm crest and cliffbase (approximately 100 feet). Depending on a detailed quantitative examination of the magnetite content in the calculated zone,a profitable by-product to gold mining such as this, could elevate the status of the mining proposition as a whole.

The only other mineral of possible economic significance found to be concentrated on the backshore, was zircon (Table VI). Finally, a small quantity of platinum has been reported to occur with the gold by a local mining company who recently examined the property.

F. SOURCE OF GOLD AND POSSIBLE OFFSHORE PLACER DEPOSITS

Several gold-bearing quartz veins were mined along

the Kennedy River at the turn of the century. These occurrences are unique to this part of the west coast (Dolmage, 1920), and as postulated by him, almost certainly gave rise to the beach placers at Wreck Bay. Stevenson (1936) noticed the shallow depression in clifftop elevation 1000 feet northwest of the mouth of Lost Shoe Creek (Map 1). He suggested that the continuence of this depression inland possibly represents the original stream bed of Lost Shoe Creek, prior to coastal uplift. The likelihood of this channel being the course of gold transportation from the hinterland is, however, most improbable, since the fine gold is dispersed throughout the glaciofluvial gravels. Pay-streaks may well exist in the gravels, but their search would be extremely difficult and costly.

Evidence for the existence of an offshore placer was derived at from two independent studies: (i) A minor mode in the very fine sand fraction (0.0625 mm to 0.105 mm), which contained most of the heavy minerals, was found to characterize samples collected along the 20 fathom line (see chapter on SEDIMENT SIZE ANALYSES, Table VI). (ii) Petrologic examination of this size fraction in samples B-19 (middle of Wreck Bay - Map 1), OS-4 (20 fathom line - Map 2), and OS-16 (60 fathoms - Map 2), revealed that OS-4 contained five times as much magnetite as the other two samples (Table VI). It also possessed a higher proportion of other heavy mineeals, namely non-magnetic opaques, garnet epidote, pyroxene and hornblende,

but somewhat less zircon (see heading on POINT-COUNT ANALYSIS).

Gold bearing beach placers produced during still-stands of sealevel in Holocene times, are known off the coast of Nome, Alaska, and in southern Oregon. In the latter area, three zones of black sand have been located on the continental shelf by positive magnetic response of the deposits (Chambers, 1968). They contain magnetite, ilmenite, chromite and gold, and occur at 40, 23, and 10 fathoms. The fact that the indicated Wreck Bay offshore placer corresponds closely in depth to the Oregon 23 fathom placer is probably fortuitous, since post-Pleistocene isostatic adjustments of the crust in the two regions have not been the same.

Environment	Sample Number	Gold "colours Large 400-200μ	Medium 200-100μ	Small <100μ	Total	Magnetite x
BEACH (berm) (Map 1)						
(northwest of river)	NWR-6a	-	1	1	2	**
	NWR-5a	1	2	3	6	**
	NWR-4a	-	6	12	18	***
	NWR-3a	-	6	7	13	***
	NWR-2a	1	-	3	4	***
(Lost Shoe Creek)	NWR-1a	1	1	1	3	***
(southeast of river)	SER-1a	-	5	3	8	***
	SER-2a	3	-	-	3	***
	SER-3a	-	4	4	8	***
	SER-4a	-	5	4	9	***
	SER-5a	-	1	3	4	*
(Sand Point)	SER-6a	1	-	-	1	*
	SER-7a	-	1	-	1	*
	SER-8a	-	-	-	-	*
CLIFF FACE GLACIOFLUVIAL OUTWASH (Map 1)						
	C-2	-	-	-	-	*
	C2 grey clay	-	-	-	-	*
	C-3	-	-	-	-	**
	C-4	-	-	-	-	**
(Sand Point)	C-5	-	-	-	-	***
	C-6	-	-	-	-	***
	C-7	-	-	-	-	***
LOST SHOE CREEK (Fig. 5)						
	LSC-3	-	-	-	-	***
	LSC-6	-	-	-	-	**
	LSC-9	-	-	-	-	*
	LSC-12	-	-	-	-	*
LONG BEACH (Map 2)						
	LB-1	-	-	-	-	*
	LB-3	-	-	-	-	*
	LB-4	-	-	-	-	*
	LB-5	--	-	-	-	*
PROSPECT HOLE						
	P-1	-	-	-	-	-
	P-2	-	-	-	-	-
	P-3	-	-	2	2	*
	P-4	1	1	1	3	**

x Magnetite content estimated visually from panned concentrate

* = little (<10%)
** = fair (10 - 30%)
*** = abundant (30%)

Table XIX.
Gold and Magnetie from Five Environments at Wreck Bay.

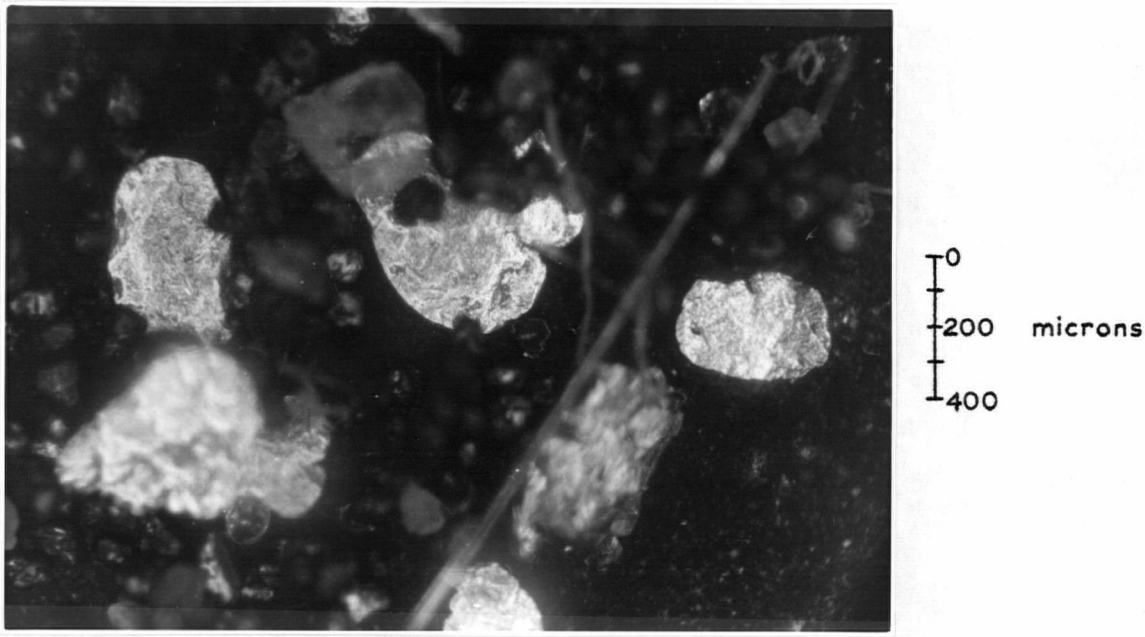

Plate 22. Photomicrograph of the largest gold "colours" obtained from Beach (berm) and Prospect Hole samples.

Plate 23a. View of the foreshore from the cliff edge between Profile B and the mouth of Lost Shoe Creek. The photograph was taken during the winter of 1968/69. Compare the dark coloured material on the foreshore (black sand) with light material present during the summer (Plate 18b).

Plate 23b. Prospect hole located near Profile D, and just landward of the winter berm crest. The measuring staff is graduated in tenths of a foot. The sampling channel is visible to the right of the measuring staff. Note alternating gravel and sand horizons in the wall of the hole.

XIII. MARINE LIFE

A. INTRODUCTION

Table XX is a list of animal marine life collected, or observed, from Wreck Bay and vicinity during the summer of 1968. The intratidal zone consisting of sandy beaches and rocky shores, provided by far the most intertebrates; a few specimens from the neritic environment were obtained during sediment sampling in the bay and offshore. The list is by no means a complete synopsis of local marine fauna, but does represent an outline of the more common species.

B. INTRATIDAL ZONE

1. SANDY BEACHES

At Wreck Bay the beach is virtually barren, except for the two distal ends, the northwest and southeast corners, The former area is most protected from waves, and shells collected there usually show little damage. The southeast corner is a more active hydrodynamic environment, and is characterized by shell-hash ranging from 0.5 to 4.0 mm in grain size. Clams and other molluscs have been reported from this area as well.

In the small beach section between Profile A and Quis'tis Point (Map I), Butter and Little-neck Clams are particularly common. Their existence there would appear to be threatened by campers, who vigorously hunt them during the summer for their food value. However, a vast pile of shells just above the cliff, at the site of an old indian village,

indicates their persistence and durability in this environment. Also present here, but less common, are Cockles, Red Turbans and Purple Olives.

Sand Fleas occur over most of the beach, except where the foreshore is gravelly. They are particularly abundant in tide-pools around boulders in the northwest corner of the beach, and are capable of inflicting painful bites which bleed profusely.

Red worms occur just beneath the sand surface. They measure up to 5 cms long, and where the foreshore is dry, they render its surface full of tiny holes (Plates 24a). Ravens eagerly seek them for food, by chopping up the beach surface with their beaks (Plate 24b). How the worms survive intense scouring of the backwash with each tidal cycle, is unknown. Presumably they migrate deeper into the sand to escape its destructive effect.

Razor Clam shells, Dead Man's Fingers (sponge), carapaces from Edible Crabs, and fragments of Mottled Stars, are occasionally washed up at various places along the beach. Sand dollars were found in only one area along the coast, at Paradise Beach, which is located a few miles south of Tofino.

2. ROCKY SHORES

The Wreck Bay environment consists of four distinct regions: Quisitis Point, Wya Point, Florencia Island, and Seal Rock.

Quisitis Point is characterized by an abundance of limpets, Blue Mussels and Acorn Barnacles; the latter two completely obscuring a few isolated boulders on the adjacent beach. Tests of animals not actually seen alive on the rocks, but found in nearby tidal pools, include: Hooked Slipper Snails, Black Top Shells (invariably housing Granular Hermit Crabs), Slender Bittium, Lirulate Margarites, Channeled Dog Whelks, and Wrinkled Purples.

Wya Point possesses abundant Blue Mussels and Acorn Barnacles, and a short distance downcoast from Wreck Bay, Goose Barnacles too become common. Northern Abalone has been reported from rocks enclosing the pocket beach, but only a few shell fragments were actually recovered.

Florencia Island supports invertebrate fauna only on the protected side facing into the bay. Three small beaches of shell-hash exist above the high-tide mark on this side of the island (Map I), and doubtless, were created by winter storm waves. Particularly common in this debris are Blue Mussel Shells (some longer than 8 inches), Weathervane Scallops, Purple-hinged Rock Scallops, Leafy Hornmouths, Purple Olives, and Carpenter Dwarf Turbans.

Seal Rock is practically barren except for a few limpets. It does, however, support a family of Hair Seals, numbering about eight, who occasionally range down to the southeast corner of the bay, and out to Florencia Island.

Worth mentioning here is a colony of Northern Sea Lion, which populate one of the small islands south of Tofino. They were never seen at Wreck Bay, but periodically a dead animal would wash up onto the northern part of Long Beach.

Ubiquitous along the rocky shores are Purple and Ochre Starfish, and the somewhat less common Sunflower Stars. Leather Chitons, Purple and Green Sea Urchins, and Green Anemones inhabit intertidal pools in rock crevices all along the coast. On Florencia Island, Sea Urchins have carved numerous round holes into the rock, some of which exceed 1 inch in depth.

C. NERITIC ZONE

1. BENTHOS

Several samples collected in the bay yielded Little Olives and baby Clams. Muds from the offshore trough contained Sea Cucumbers and Ubiquitous Brittle Stars. Between these two areas, samples OS-1 to OS-9 (Map 2) all contained some shell debris, mostly bivalves, particularly sample OS-9 which contained an excess of 50% shells. Included in the latter were Weathervane Scallops, Clams, Purple Urchin spines, Slender *Bittium*, Blue Mussel and Barnacle fragments.

2. NEKTON

On the 28th July 1968, a number of Humpback Whale were observed sounding in the bay just north of Seal Rock. While echo-sounding the bay in early July, scores of fish

(probably salmon) were seen leaping from the water at the south side of Florencia Island.

D. LAND MAMMALS, SEA BIRD AND SEA WEED

Black Bear are common along Lost Shoe Creek, where berries grow in profusion, and Raccoon were often seen there as well. Mink were frequently seen running along the shoreline at the waters edge, particularly on the southeast part of the beach.

Birds seen included the Bald Eagle, Ravens, Baird Sand Pipers, Black Oyster Catchers and Glaucous-winged Gulls. The latter two are especially common on Florencia Island, and the bare rock on the seaward side of the island serves as a nesting ground for hundreds of gulls.

Several varieties of seaweed thrive in Wreck Bay, the most impressive being Kelp, which grows in thick beds over boulder areas lying close to shore (Map I). During August 1968, a storm tore vast quantities of the weed loose from their anchors, and opposing littoral currents deposited it in huge piles on the beach (Plate 25a). Some of them still had large cobbles firmly attached to their holdfasts (Plate 25b).

Table XX. List of Animal Marine Life Collected or Observed at Wreck Bay.

MOLLUSCA	
GASTROPODA	
Acmaea instabilis (Gould)	- Unstable Limpet
A. mitra Eschscholtz	- Whitecap Limpet
A. pelta Eschscholtz	- Shield Limpet
A. persona Eschscholtz	- Mask Limpet
A. testudinalis scutum Eschscholtz	- Plate Limpet
Diodora aspera Eschscholtz	- Rough Keyhole Limpet
Crepidula adunca Sowerby	- Hooked Slipper Snail
Haliotis kamtschatkana Jonas	- Northern Abalone
Tegula funibralis (A. Adams)	- Black Top-shell
T. pulligo Gmelin	= Dusky Turban
Calliostoma ligatum Gould	- Blue Top-shell
Margarites lirulatus (Carpenter)	- Lirulate Margarite
M. helicinus Phipps	- Smooth Margarite
Astraea gibberosa Dillwyn	- Red Turban
Homalopoma carpenteri (Pilsbury)	- Carpenter Dwarf Turban
Searlesia dira Reeve	- Dire Whelk
Nassarius fossatus Gould	- Channeled Dog Whelk
Thais lamellosa Gmelin	- Wrinkled Purple
Olivella biplicata Sowerby	- Purple Olive
O. baetica Carpenter	- Little Olive
Ceratostoma foliata Gmelin	- Leafy Hornmouth
Bittium attenuatum Carpenter	- Slender Bittium
PELECYPODA	
Mytilus edulis Linnaeus	- Blue Mussel
Saxidomus giganteus (Deshayes)	- Butter Clam
Protothaca staminea (Conrad)	- Little-neck Clam
Siliqua patula (Dixon)	- Razor Clam
Clinocardium nuttalli (Conrad)	- Cockle
Pecten caurinus Gould	- Weathervane Scallop
Hinnites multirugosus (Gale)	- Purple-hinged Rock Scallop
AMPHINEURA	
Katharina tunicata Wood	- Leather Chiton
ARTHROPODA	
CRUSTACEA	
Balanus cariosus (Pellas)	- Acorn Barnacle
Lepas anatifera Linnaeus	- Goose Barnacle
Cancer magister Dana	- Edible Crab
Pagurus granosimanus (Stimson)	- Granular Hermit Crab
Orchestoidea Californiana	- Sand Flea

ECHINODERMATA	
ASTEROIDEA	
Pisaster ochraceus (Brandt)	- Purple or Ochre Starfish
Pycnopodia helianthoides (Brandt)	- Sunflower Star
Evasterias troschelii (Stimson)	- Mottled Star
Ophiopholis aculeata	- Ubiquitous Brittle Star
ECHINOIDEA	
Strongylocentrotus drobachiensis (Muller)	- Green Sea Urchin
Dendraster excentricus Eschscholtz	- Sand Dollar
HOLOTHUROIDEA	
Leptosynapta albicans	- Sea Cucumber
COELENTERATA	
ANTHOZOA	
Anthopleura xanthogrammica	- Green Anemone
PORIFERA	
DEMOSPONGIAE HADROMERINA	
Polymastia pachymastia	- Dead Man's Fingers
ANNELIDA	
POLYCHAETA	
Thoracophelia mucronata	- Red Worm
MAMMALIA	
Phoca vitulina Linnaeus	- Hair Seal
Eumetopias jubata (Schreber)	- Northern Sea Lion
Megaptera novaeangliae (Borowski)	- Humpback Whale

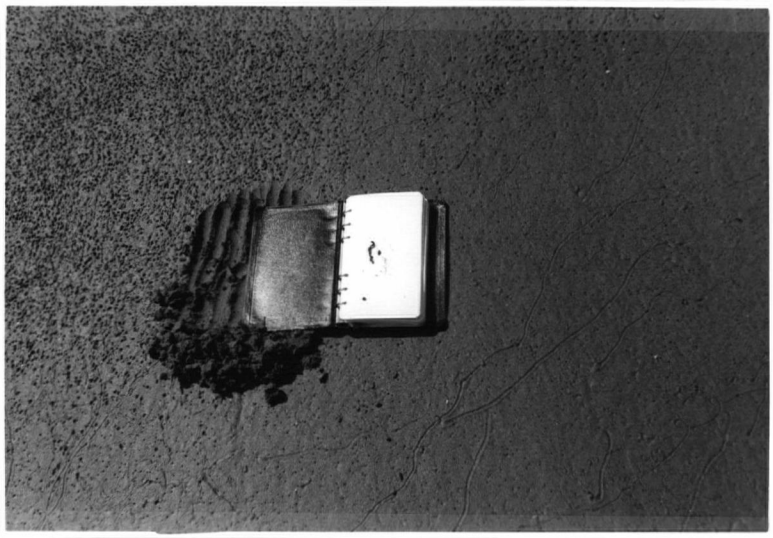

Plate 24a. A Red Worm is shown on the notebook, and the mesh of tiny holes in the beach surface is the result of their burrowing. The long tracks on the sand surface are snail markings.

Plate 24b. Raven diggings for Red Worms.

Plate 25a. Piles of delp deposited on the foreshore where opposing littoral currents converged. The photograph was takon on the 19th August 1968, just after the Summer Storm. Note the influence of the kelp piles on foreshore erosion.

Plate 25b. Kelp torn from boulder beds in the bay by large storm waves. The cobbles attached to the kelp holdfasts were similar to those in the glaciofluvial outwash.

REFERENCES

Anderson, F.E.,1968. Seaward terminus of the vashon continental glacier in the Strait of Juan de Fuca. Marine Geol., v.6, pp.419-438.

Aubouin, J., 1965. Geosynclines. Elsevier Publ.Co., New York, 288 p.

Bagnold, R.A.,1940. Beach formation by waves; some model experiments in a wave tank. J.Inst.Civ.Engrs.,v.1, Paper 5237, p.27-52.

Bascom, W.N., 1951. The relationship between sand size and beach-face slope. Trans.Amer.Geophys.Union, vol.32, p.866-874.

----------,1964. Waves and beaches. Doubleday and Co.,N.Y.267p.

Bateman, A.M.,1965. Economic mineral deposits. John Wiley & Sons Inc., 916 p.

Bhoojedhur, S.,1969. Genesis of a podzol sequence on the west coast of Vancouver Island. Unpublished M.Sc.thesis, Dept. of Soil Science, U.B.C., Vancouver.

Boon, J.D.,III,1968. Trend surface analysis of sand tracer distributions on a carbonate beach, Bimini, B.W.I. J. Geol., v.76, pp.71-87.

Bowen, A.J.,1969. Rip currents, Part I - Theoretical investigations. J.Geophys.Res., vol.74, no.23, p.5467-5478.

----------, and Inman, D.L.,1969. Rip currents, Part 2 -Laboratory and field observations. J.Geophys.Res., v.74, no.23, p.5479-5490.

Caldwell, J.M., 1956. Wave action and sand movement near Anaheim Bay, California. B.E.B. Tech.Memo.No.68, p.1-19.

Canadian Hydrographic Service, 1968. Tide and current tables, v.6.

Chambers, D.,1968. Ancient shorelines and potential economic placer deposits off Southern Oregon. Ocean,Conf., Univ.of Wash., Session IV, No.1, Feb.10,1968.

Chappell, J.,1967. Recognizing fossil strand lines from grain-size analysis. J.Sed.Petr., v.37, No.1, p.157-165.

Cloud, P.E.,Jr.,1966. Beach cusps: Response to Plateau's Rule? Science, v.154, p.890-891.

Curray, J.R., 1960. Tracing sediment masses by grain size modes. Int.Geol.Congr., 21st Session Norden, Copenhagen, p.119-130.

Dolmage, V.,1919. Barkley Sound, Vancouver Island, B.C. B.C. Minister of Mines Annual Report, p.12B-20B.

----------, 1920. West coast of Vancouver Island between Barkley and Quatsino Sounds. B.C.Minister of Mines Annual Report, p.12A-22A.

Eastwood, G.E.P.,1968. Geology of the Kennedy Lake area. B.C. Dept.of Mines and Petr.Res., Bull.No.55, 63p.

Emery,K.O., and Foster, J.F.,1948. Water tables in marine beaches. J.Mar.Res.,v.7, No.3, p.644-654.

Emery,K.O., 1960. The sea off southern California. John Wiley and Sons Inc., 366 p.

Folk, R.L.,1966. A review of grain-size parameters. Sedimentology, v.6, p.73-93.

----------, 1968. Petrology of sedimentary rocks. Hemphill's, Texas, 170 p.

Friedman, G.M.,1961. Distinction between dune, beach and river sands from their textural characteristics. J.Sed. Petr., v.31, p.514-529.

----------,1962. On sorting, sorting coefficients and lognormality of the grain-size distribution of sandstones. J.Geol., v.70, No.6, p.737-753.

----------,1967, Dynamic processess and statistical parameters compared for size frequency distribution of beach and river sands. J.Sed.Petr., v.37, p.327-354.

Gilbert, G.K.,1914. The transportation of debris by running water. U.S.Geol.Surv., Prof.Paper 86, 263 p.

Grant, U.S.,1948. Influence of the water table on beach aggradation and degradation. J.Mar.Res., v.7, p.655-660.

Greenwood, B.,1969. Sediment parameters and environment discrimination: An application of multivariate statistics. Can.J.Earth Sc., v.6, p.1347-1358.

Griggs, G.B., and Kulm, L.D., 1969. Glacial marine sediments from the northeast Pacific. J.Sed.Petr.,v.39, p.1142-1148.

Grim, R.E., 1958. Concept of diagenesis in argillaceous sediments. A.A.P.G., v.42, p.246-253.

----------, 1968. Clay mineralogy. McGraw-Hill Book Co., 596 p.

Gross,M.G., McManus, D.A., and Ling,H-Y., 1967. Continental shelf sediment, northwestern United States. J.Sed. Petr., v.37, p.790-795.

----------, Morse, B.A., and Barnes, C.A., 1969. Movement of near-bottom waters on the continental shelf off northwestern United States. Amer.Geophys.Union, p.7044-7047.

Hails, J.R., 1967. Significance of statistical parameters for distinguishing sedimentary environments in New South Wales, Australia. J.Sed.Petr., v.37, p.1059-1069.

----------, and Hoyt, J.H., 1969. The significance and limitations of statistical parameters for distinguishing ancient and modern sedimentary environments of the Lower Georgia coastal plain. J.Sed.Petr., v.39, p.559-580.

Harrison, W., 1964. Beach changes at Virginia Beach, Virginia. C.E.R.C., Misc.Paper No.6-64, p.1-25.

Hite - in Bateman, A.M., 1965. Economic mineral deposits. John Wiley and Sons Inc., 916 p.

Holland, S.S., and Nasmith, H.W., 1958. Investigation of beach sands. B.C.Dept.of Mines, March, 1958, p.3.

Holland, S.S., 1964. Landforms of British Columbia: A physiographic outline. B.C.Dept.of Mines and Petr.Res., Bull.No.48, 138 p.

Howarth, R.J., 1967. Trend surface fitting to random data - an experimental test. Amer.J.Sc., v.265, p.619-625.

Hoyt, J.H., and Henry, J.J., 1963. Rhomboid ripple mark, indicator of current direction and environment. J.Sed. Petr., v.33, p.604-608.

Ingle, J.C.,Jr., 1964. The movement of beach sand. Elsevier Publ.Co., 221 p.

Inman, D.L., 1953. Aerial and seasonal variations in beach and nearshore sediments at La Jolla, California. B.E.B. Tech.Memo. No.39, p.1-82.

----------, 1963. in: Shepard, F.P., Submarine geology. Harper and Row, 555 p.

Johnson, D.W., 1919. Shore processes and shoreline development. Hafner, New York, 584 p.

Johnson, J.W., 1956. Dynamics of nearshore sediment movement. Am.Ass.Petr.Geol.Bull., v.40, p.2211-2232.

King, L.H., 1967. Use of a conventional echo-sounder and textural analyses in delineating sedimentary facies: Scotian shelf. Can.J.Earth Sc., v.4, p.691-707.

Koldijk, W.S., 1968. On environment sensitive grain-size parameters. Sedimentology, v.10, p.57-69.

Krumbein, W.C., and Pettijohn, E.F., 1938. Manual of sedimentary petrography. Appleton-Century-Crofts, Inc., 549 p.

LeMehaute, B., and Brebner, A., 1961. An introduction to coastal morphology and littoral processes. Queens Univ. Civil Engr.Report No.14, 46 p.

McLean, R., 1967. Plan shape and orientation of beaches along the east coast, South Island. New Zealand Geographer, v.23, no.1, p.16-22.

Moiola, R.J., and Weiser, D., 1968. Textural parameters: an evaluation. J.Sed.Petr., v.38, p.45-53.

Mothersill, J.S., 1969. A grain size analysis of longshore bars and troughs, Lake Superior, Ontario. J.Sed.Petr., v.39, p.1317-1324.

Muller, J.E., and Carson, D.J.T., 1969. Geology and mineral deposits of Alberni map-area, British Columbia (92F) Geol.Surv.Canada Paper 68-50, 52 p.

Munk, W.H. - in Shepard, F.P., 1963. Submarine Geology. Harper and Row, 555 p.

Nicholson, G., 1966. Vancouver Island's west coast 1762-1962. Morris Printing Co., Victoria, 356 p.

Otvos, E.G., Jr., 1964. Observations of beach cusp and beach ridge formation on the Long Island Sound. J.Sed.Petr. v.34, p.604-609.

Pierce, J.W., and Good, D.I., 1966. Fortran II program for standard size analysis of unconsolidated sediments using an IBM 1620 computer. State Geol.Survey, Univ.of Kansas, Lawrence, Sp.Publ. 28, 19 p.

Pierce, J.W., and Siegel, F.R., 1969. Quantification of clay mineral studies of sediments and sedimentary rocks. J.Sed.Petr., v.39, p.187-193.

Pilkey, O.H., and Richter, D.M., 1964. Beach profiles of a Georgia barrier island. Univ.of Georgia Marine Inst. No. 71, p.11-19.

Rector, R.L., 1954. Laboratory study of equilibriam profiles of beaches. B.E.B., Tech.Memo.No.41, 38 p.

Shepard, F.P., and LaFond, E.C., 1940. Sand movement along the Scripps Institute pier. Amer.J.Sci., v.238, p.272-285.

Silvester, R., 1960. Stabilization of sedimentary coastlines. Nature, v.188, p.467-469.

Simons, D.B., Richardson, E.V., and Nordin, C.F., 1965. Sedimentary structures generated by flow in alluvial channels. S.E.P.M. Sp.Publ.No.12, p.34-52.

Stevenson, J.S., 1936. Wreck Bay. B.C.Minister of Mines Annual Report, Part F - Special Report.

Strahler, A.N.,1964. Tidal cycle of changes in an equilibriam beach, Sandy Hook, New Yersey. U.S.Dept.of Navy, Proj. NR 388-057, Tech.Rep.No.4, 51 p.

Sutherland Brown, A., 1966. Tectonic history of the insular belt of British Columbia. Can.Inst.Min.Met.,Spec. vol.No.8, p.83-100.

Watts,G.M., and Dearduff, R.F., 1954. Laboratory study of effect of tidal action on wave formed beach profiles. B.E.B. Tech.Memo.No.52, 21 p.

Watts, J.S., and Faulkner, R.E., 1968. Designing a drilling rig for severe seas. Ocean Industry, vol.3, no.2, p.28-37.

Wiegel, R.L., Patrick, D.A., and Kimberley, H.L., 1954. Wave longshore current, and beach profile records for Santa Margarita River beach, Oceanside, California. Trans.Amer.Geophys.Unkon, v.35, p.887-896.

Wright, F.F., 1962. The development and application of a flourescent marking technique for tracing sand movements on beaches. U.S.Dept.of Navy,Proj. NR388-057, Tech.Rep.No.2, 31 p.

Yasso, W.E., 1962. Flourescent coatings on coarse sediments: an integrated system. U.S.Dept.of Navy,Proj.NR 388-057, Tech.Rep.No.1, 48 p.

----------, 1964. Geometry and development of spitbar shorelines at Horseshoe Cove, Sandy Hook, New Yersey. U.S.Dept.of Navy, Proj. NR 388-057, Tech.Rep.No.5, 106 p.

----------, 1964. Use of flourescent tracers to determine foreshore sediment transport, Sandy Hook, New Yersey. U.S.Dept.of Navy, Proj. NR 388-057, Tech.Rep.No.6, 18 p.

APPENDIX

SEDIMENT SAMPLE COLLECTION

A total of 135 sediment samples were collected for laboratory study. They were partially used in three different investigations, and will be referred to under the appropriate headings:

- RECENT SEDIMENTS - Point-count analysis
  - X-ray diffraction analysis
- SEDIMENT SIZE ANALYSES
- ECONOMIC GEOLOGY

In addition to these samples, 91 small samples were collected from profile rod-stations specifically to examine seasonal foreshore variability - see SEDIMENT SIZE ANALYSES.

A brief description of sample procedures and locations are given. Furthermore, in order to appreciate the character of material from the different environments, a verbal range for mean and standard deviation is included, the former being Wentworth size classes (Folk, 1968), and the latter Friedman's (1962) sorting designation. The following list is for large samples, the small samples are included in the BEACH environment. For convenience, the environments have been separated into two broad catagories, one extending parallel to the coast from northwest to southeast, and the other normal to the coast passing through Wreck Bay.

PARALLEL TO COAST

LONG BEACH (LB) - Map 2, 5 samples, approximately 1000 gms each. Top one inch of beach surface scraped together. Collected behind a poorly defined winter berm, except LB-2 which came from a coastal dune, and LB-3 from the mouth of Sand Hill Creek. Fine sand; very well to moderately well sorted.

QUISITIS POINT (QP) - Figure 5, 8 samples, approximately 1000 gms each, Top one inch of beach surface scraped together. Collected from small pocket beaches in rock crevasses. Medium sand to granules; very poorly to moderately well sorted.

WYA POINT (WP) - Figure 5, 11 samples, approximately 1000 gms each. Top one inch of beach surface scraped together. Collected from small pocket beaches in rock crevasses. Fine to very coarse sand; very well to moderately well sorted.

NORMAL TO COAST

LOST SHOE CREEK (LSC) - Figure 5, 13 samples, approximately 1000 gms each. Collected from active mid-channel sediment. Samples 800 feet apart between Tofino-Ucluelet highway bridge, and river mouth (2 miles). Medium sand to granules; moderately to very poorly sorted.

CLIFF (C)

GLACIOFLUVIAL OUTWASH - Map I, 6 samples, approximately 1000 gms each. 5 foot channel samples from halfway up cliff-face, except C-2 immediately above brown clay near top of cliff. Cliff section from Profile B to Profile G ($2\frac{1}{2}$ miles). Very coarse sand to granules; poorly to very poorly sorted.

GREY CLAY - Map I, 3 samples, approximately 500 gms each. One foot channel samples just above backshore, except C-2 immediately below brown clay near top of cliff. Cliff section from Profile A to region behind spit-bar (I mile). Cohesive, silty, few pebbles.

BROWN CLAY - One sample, approximately 500 gms. One foot channel sample between glaciofluvial outwash and grey clay at C-2. Friable, silty, iron-oxide rings.

MUDBALL - One sample, approximately 1500 gms. Collected adjacent to C-3 in glaciofluvial outwash. Spheroidal, sandy, brown.

BEACH

Large samples (NWR, SER) - Map I, 42 samples, approximately 1000 gms each. Top one inch of beach surface scraped together. 6 sample lines northwest,

and 8 sampleslines southeast of Lost Shoe Creek mouth, each line containing 3 samples:

BERM (a) - Collected on backshore behind winter berm crest. Very coarse sand to granules; very well to moderately sorted.

MEAN HIGH TIDE (b) - Collected below high tide swash mark. Fine to coarse sand; very well to poorly sorted.

MEAN WATER LEVEL (c) - Collected at Bascom's (1951) "reference point", approximately the mid-tide level. Fine sand; very well to moderately sorted.

Small samples (profile rod numbers) - Map 1, 91 samples, approximately 100 gms each, 54 from summer foreshore and 37 from winter foreshore. Fine sand to pebbles; very well sorted to extremely poorly sorted.

BAY (B) - Map 1, 25 samples, approximately 500 gms each. Sampled from motor launch using Dietz-LaFond, Eckman and Van Veen grabs. Fine to coarse sand; very well to extremely poorly sorted.

OFFSHORE (OS) - Map 2, 20 samples, approximately one cu.ft. each. Sampled from C.N.A.V.LAYMORE using Pettersson and Van Veen grabs. 13 Samples sub-sampled to approximately 1000 gms each;

fine sand to cobbles; very well to poorly sorted. 7 samples sub-sampled to approximately 500 gms each; sandy green-grey silt.

GLOSSARY

The following list of terms are defined in terms of the meanings in which they have been used in this thesis:

BEACH RIDGE - An elevated body of sediment occurring on the foreshore, and oriented parallel to the shore line.

BEACH RUNNELS - Elevated bodies of coarse sediment occurring on the foreshore, and oriented at right-angles to the shore line. They are usually separated by "valleys" consisting of relatively fine material.

DIAMICTON - Non-sorted to poorly sorted clastic sediment consisting of sand and larger particles in a muddy matrix. A DIAMICTITE is a lithified diamicton. Both are non-genetically defined terms (Flint et al., 1960).

EDGE WAVE - A wave form trapped in the nearshore zone due to continual reflection off the foreshore, and relatively rapid movement of its deep water end. This results in the wave form rotating about its slower moving landward end.

EQUILIBRIUM - 1. A transverse profile on a beach, which despite minor fluctuations, maintains its form for relatively long periods of time.

2. A planimetric coastal shape which maintains constant geometric dimenstions for relatively long periods of time.

Both 1 and 2 represent a general steady state in the action of waves and currents, and the rate of sediment movement.

LITTORAL CURRENT - A current generated in the surf zone by waves breaking at an angle to the shore line.

LITTORAL DRIFT - Sediment movement along the foreshore due to littoral or longshore currents.

LONGSHORE CURRENT - A current generated in the shoaling, breaker and surf zones by wave divergence and diffraction.

WATER TABLE LINE OF EMERGENCE - The line of intersection between the foreshore and upper surface of a zone of saturation.

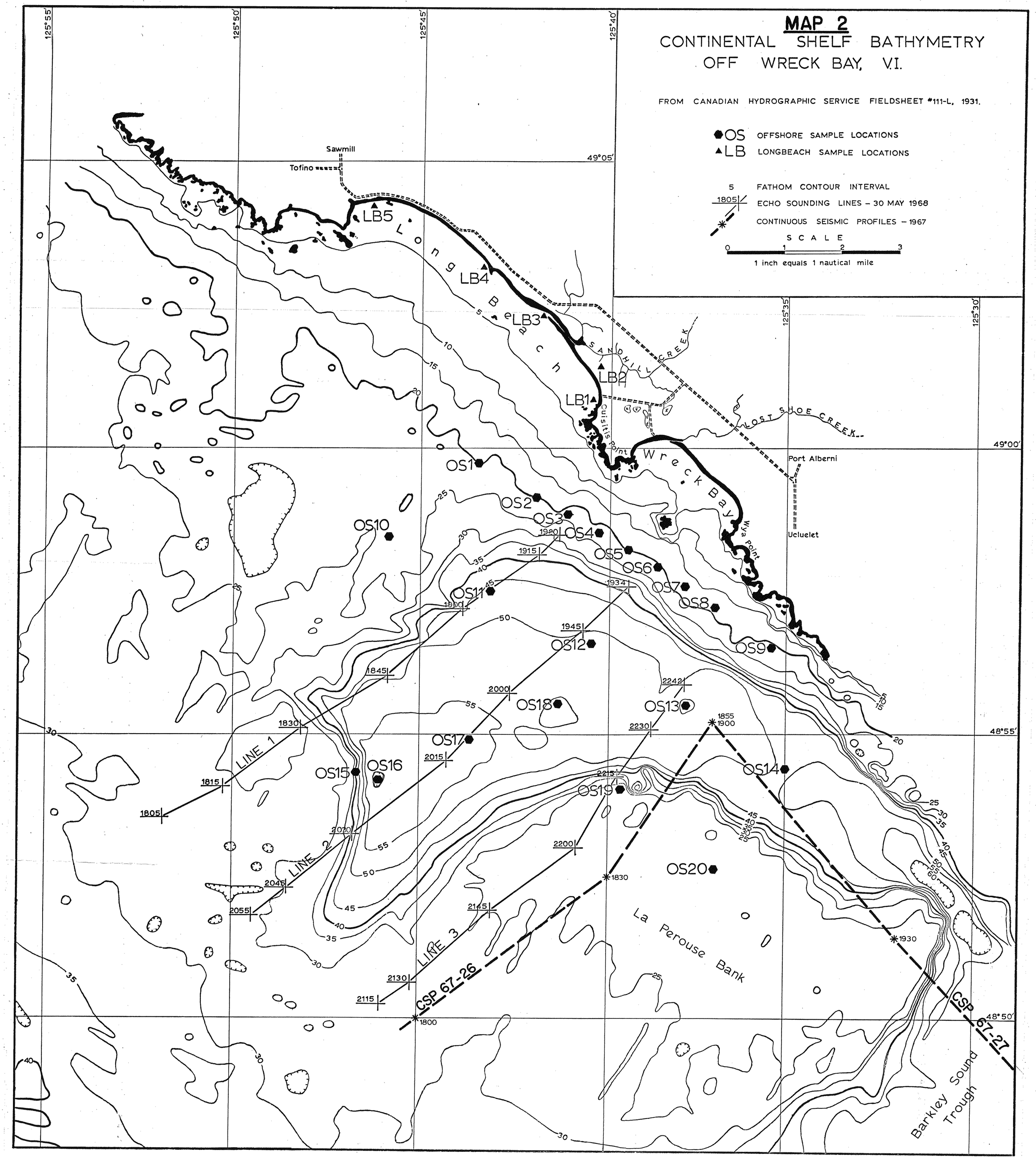
MAP 2
CONTINENTAL SHELF BATHYMETRY
OFF WRECK BAY, V.I.
FROM CANADIAN HYDROGRAPHIC SERVICE FIELDSHEET #111-L, 1931.
OS OFFSHORE SAMPLE LOCATIONS
LB LONGBEACH SAMPLE LOCATIONS
5 FATHOM CONTOUR INTERVAL
1805 ECHO SOUNDING LINES – 30 MAY 1968
CONTINUOUS SEISMIC PROFILES – 1967
SCALE
0 1 2 3
1 inch equals 1 nautical mile
125°55′
125°50′
125°45′
125°40′
125°35′
125°30′
49°05′
49°00′
48°55′
48°50′
Sawmill
Tofino
Port Alberni
Ucluelet
Long Beach
Wreck Bay
Cuisitis Point
Wya Point
SANDHILL CREEK
LOST SHOE CREEK
LB1
LB2
LB3
LB4
LB5
OS1
OS2
OS3
OS4
OS5
OS6
OS7
OS8
OS9
OS10
OS11
OS12
OS13
OS14
OS15
OS16
OS17
OS18
OS19
OS20
LINE 1
LINE 2
LINE 3
CSP 67-26
CSP 67-27
La Perouse Bank
Barkley Sound Trough